An investigation into the role of Pellino2 in lung inflammation

A thesis presented to Maynooth University, Maynooth for the degree of Doctor of Philosophy

By

Clare Finnegan, B.Sc.

Human Health Research Institute, Department of Biology,

Maynooth University

October 2018

Supervisor: Professor Paul Moynagh

Head of Department: Professor Paul Moynagh

Declaration:

This thesis has not been previously submitted to this or any other university for examination for a higher degree. The work presented here is entirely my own except where otherwise acknowledged. This thesis may be made available for consultation within the university library. It may be copied or lent to other libraries for purposes of consultation.

_____

Clare Finnegan

Table of contents:

Acknowledgements

First and foremost I would like to thank Paul for all your patience and support throughout this process. Your passion and enthusiasm for ‘anything new’ was an inspiration. I cannot thank you enough for the guidance you have given me and the many hours put in to ensure that I completed what I had started.

I would also like to thank Rebecca Ingram and Alice Dubois for their work on the flow cytometry and *in vivo* infection studies. Thanks to Helen Kennelly for teaching me the *in vivo* techniques and to Karen English for your input into the project. Thanks to Ashling Holland also who helped with proteomics work and demonstrated excellence in her work.

Thanks to everyone in Molecular Immunology: to Nezira for welcoming me into the lab and every chat we ever had that brightened up the days; to Ronan who could always be counted on for sound advice, movie reviews and a debate if I was up for it; to Bingwei for the expertise and friendship you so readily shared; to Figs for always being willing to help and offer example of what hard work looked like; to Ewa, Conor

and Linan for all your input and to Johanna for every coffee, dinner and cinema night, I will always be grateful to have had someone who shared in the experience with me.

Thanks to my family: to my father, the reason I always wanted to do a PhD, who was a coach, a counsellor and a friend throughout all of this and beyond; to my mother for the support you have always given me, I cannot begin to count how many hours you have spent listening to me through hard days and loved me through all of it; to Sarah for always having a positive note for me, to Threase of whom I am so proud, thank you for always standing by me; to Matthew, Finn and Fiachra for always letting me drop by unannounced to bend Threase's ear; to John for being my badminton partner who kept me sane at the weekends; to Harriet for all our dashboard dining through tough days and to Emma for being a little me who I wanted to keep going for. There are countless other people who have supported me through this including May and Sue, and to each I am very grateful.

Finally, I would like to thank Bryan for being everything I ever needed in the last 8 years but particularly in the last 4. You have encouraged me, supported me and loved me through everything. I don't know what I have ever done to still have you standing by my side and holding me up but I am not going to question it. Thank you for all you have given me.

Abstract

Pellino1, Pellino2 and Pellino3 form a family of E3 ubiquitin ligases that have been implicated in regulation of innate immune signalling pathways including that employed by IL-1. IL-1 signalling is an important component in the development of emphysema and COPD, for which there is no known cure. In an effort to understand the mechanisms leading to the development of emphysema, wild type and Pellino2-deficient mice were subjected to experimental models of lung injury. The studies suggest an important role for Pellino2 in mediating the early inflammatory response in elastase-induced emphysema. Interestingly whilst early inflammation was suppressed in Pellino2-deficient mice, these mice demonstrated more chronic fibrosis in response to repeated elastase challenge than wild type mice. Equivalent studies were also performed in Pellino3-deficient mice. Unlike Pellino2, Pellino3 does not appear to mediate lung inflammation or fibrosis, at least in response to elastase treatment. The studies demonstrate that these differential functions of Pellino2 and Pellino3 in lung inflammation may be associated with involvement of Pellino2 as a mediator in NLRP3 inflammasome-mediated IL-1β production whereas Pellino3 is without effect in this pathway. As Pellino2 was shown to play a role in the immune response

following lung injury, the effect of Pellino2 deficiency on the inflammatory response during respiratory infection with *Pseudomonas aeruginosa* was examined. Pellino2-deficient mice had improved survival and reduced bacterial load when compared with wild type mice in response to respiratory infection. These data are also discussed in the context of impaired activation of the NLRP3-inflammasome in Pellino2-deficient mice. In conclusion, these studies illustrate a role for Pellino2 in regulating the early immune response in the lung to bacterial infection and injury. The studies also suggest a role for Pellino2 in controlling later pathogenesis and lung fibrosis and highlight the non-redundant nature of Pellino proteins in regulation of the innate immune response.

Abbreviations

AAT	Alpha-1 antitrypsin
ADP	Adenosine diphosphate
AIM	Absent in melanoma
ALR	AIM-like receptor
ANOVA	Analysis of variance
APS	Ammonium persulphate
ASC	Apoptosis-associated speck-like protein containing a CARD
ATP	Adenosine triphosphate
BAL	Bronchoalveolar lavage
BMDM	Bone marrow-derived macrophage
BRCC	BRCA1/BRCA2-containing complex
BSA	Bovine serum albumin
ACN	Acetonitrile
CAPS	Cryopyrin Associated Periodic Syndrome
CARD	Caspase activation and recruitment domain
CD14	Cluster of differentiation 14
cDNA	Complementary DNA
CF	Cystic fibrosis
CFTR	Cystic fibrosis transmembrane conductance regulator
CFU	Colony forming units
CHAPS	3-[(3-cholamidopropyl)dimethylammonio]-1-propanesulfonate
CHRNA	Cholinergic receptor nicotinic alpha polypeptide
CID	Collision-induced dissociation
CLR	C-type lectin receptors
COPD	Chronic Obstructive Pulmonary Disease
CpG	2'-deoxyribo cytidine-phosphate-guanosine
CRD	Carbohydrate-recognition domain
CRID	Cytokine release inhibitory drugs
CS	Cigarette smoke
CT	Crossing Threshold
DAMP	Danger associated molecular pattern
DC	Dendritic cell
DC-SIGN	Dendritic-cell specific ICAM3-grabbing nonintegrin
DD	Death domain
DEPC	Diethylpyrocarbonate
DMSO	Dimethyl sulfoxide
DNA	Deoxyribonucleic acid

DNGR-1	DC NK lectin group receptor-1
dNTP	Deoxyribonucleotide triphosphate
ds	double stranded
DSS	Disuccinimydyl suberate
DTT	Dithiothreitol
dUTP	Deoxyuridine triphosphate
EDTA	Ethylenediaminetetraacetic acid
ELISA	Enzyme Linked Immunosorbent Assay
EMCV	Encephalomyocarditis virus
EMT	Epithelial-mesenchymal transition
EPS	Extracellular polymeric substances
ER	Endoplasmic Reticulum
ERK	Extracellular signal related kinase
FACS	Fluorescence activated cell sorting
FAM13A	Family with sequence similarity 13 member A
FBXL	F-box and leucine rich repeat proteins
FCS	Foetal calf serum
FD	'Function to find' domain
FOXP3	Factor forkhead box P3
g	Gravitation
GOLD	Global Initiative for COPD
GTP	Guanisine triphosphate
H&E	Haematoxylin & Eosin
HCl	Hydrochloric acid
HHIP	Hedgehog interacting protein
HPRT	Hypoxanthine-guanine phosphoribosyltransferase
ICAM	Intracellular adhesion molecule
ID	Intermediate domain
IFN	Interferon
IKK	IκB kinase
IL-	Interleukin-
IL-1R	Interleukin-1 receptor
IL-1Ra	Interleukin-1 receptor antagonist
IRAK	IL-1 receptor associated kinase
IRF	Interferon regulatory factor
IκB	Inhibitor of kappaB
JNK	c-Jun n-terminal kinase
K+	Potassium
kb	kilobase
LB	Lysogeny broth
LC	Liquid chromatography
LC-MS	Liquid chromatography-mass spectrometry
LeTx	Lethal toxin
LF	Lethal factor
LGP2	Laboratory of genetics and physiology 2 and a homolog of mouse D11lgp2
LPS	Lipopolysaccharide

LRR	Leucine rich repeats
LTA	Lipoteichoic acid
LTB	Leukotriene B
MACS	Magnetic activated cell sorting
MAL	MyD88 adaptor like
MAP	Mitogen activated protein
MAPK	Mitogen activated protein kinase
MARCH	Membrane-associated ring-CH
MBL	Mannose binding lectin
MCSF	Macrophage colony stimulating factor
MD2	Myeloid differentiation factor 2
MDA5	Melanoma differentiation-associated gene 5
MDP	Muramyl dipeptide
Mincle	Macrophage inducible C-type lectin
MKK	Mitogen-activated protein kinase kinase
MLI	Mean Linear Intercept
MLKL	Mixed lineage kinase domain like pseudokinase
MMP	Matrix metalloprotease
MMTV	Mouse mammary tumour virus
mRNA	Messenger RNA
MS	Mass Spectrometry
MyD88	Myeloid differentiation protein 88
Na3vo4	Sodium orthovanidate
NaCl	Sodium chloride
NADH	Nicotinamide adenine dinucleotide
NEMO	NFκB essential modulator
NFκB	Nuclear factor κ B
NK	Natural killer cell
NLR	NOD-like receptor
NLRC	NLR family CARD domain containing protein
NLRP	NOD, LRR and PYD-domain containing protein
NOD	Nucleotide-binding oligomerisation domain
NRF	Nuclear factor erythroid 2 like 2
OD	Optical Density
P-	Phosphorylated-
PAGE	Polyacrylamide Gel Electrophoresis
PAMP	Pathogen associated molecular pattern
PAR	Protease activated receptor
PAS	Periodic Acid Schiff
PBS	Phosphate buffered saline
PCR	Polymerase chain reaction
PFA	Paraformaldehyde
PGN	Peptidoglycan
PINK	PTEN-induced putative kinase
PMSF	Phenylmethylsulfonyl fluoride
Poly I:C	Polyinosinic-polycytidylic acid

PPE	Porcine pancreatic elastase
PRR	Pattern recognition receptor
PYD	Pyrin domain
RIG-I	Retinoic acid-inducible gene I
RIN3	Ras and Rab interactor 3
RIP	Receptor-interacting protein
RIPA	Radioimmunoprecipitation assay buffer
RLR	RIG-I like receptor
RNA	Ribonucleic acid
ROS	Reactive oxygen species
RPMI	Roswell Park Memorial Institute
RSV	Respiratory syncytial virus
SDS	Sodium dodecyl sulphate
siRNA	small interfering RNA
SMAD	Mothers against decapentaplegic homolog
SNP	Single nucleotide polymorphisms
SUMO	Small ubiquitin like modifier
TAB	TAK1 binding protein
TAK	TGFbeta-activated kinase
TBK	TANK-binding kinase
TBS	Tris-buffered saline
TdT	Terminal deoxynucleotidyl transferase
TEMED	N N N' N'-Tetramethylethylene-diamine
TGFβ	Transforming growth factor β
TIR	Toll-IL-1 receptor domain
TLR	Toll-like receptor
TMB	3 3' 5 5'-Tetramethylbenzidine
TNFR	Tumour necrosis factor alpha receptor
TNFα	Tumour necrosis factor alpha
TRAF	TNF receptor associated factor
TRAM	TRIF-related adaptor molecule
TRIF	TIR domain-containing adaptor inducing IFN-beta
TRIM	Tripartite motif containing protein
TUNEL	TdT dUTP nick-end labelling
VEGF	Vascular Endothelial Growth Factor

1 Introduction

1.1 The immune system

The immune system is multifaceted and is generally divided into two parts: the innate and adaptive immune system based on the speed and specificity of the response initiated (Kurtz, 2005). Both systems can act together and integrate with each other to mount an appropriate immune response (Lanier and Sun, 2009). The innate immune system is the first line of defence against invading pathogens and is comprised of physical barriers, soluble proteins and small bioactive molecules and receptors (membrane-bound or soluble) that can recognise patterns associated with invading pathogens (Kumar *et al*., 2009). The innate immune response controls initial infection and activates the adaptive immune response (Iwasaki and Medzhitov, 2010). The adaptive immune response is orchestrated mainly by B-cells and T-cells. These cells can recognise antigens associated with pathogens with a very high degree of specificity and work to limit infection in numerous ways: B-cells produce antibodies against antigens which neutralise pathogens, helper T-cells aid B-cells, improve the efficiency of the innate immune system and activate cytotoxic T-cells, cytotoxic T-

cells kill infected cells (Crotty, 2015). Another facet of the adaptive immune response is the role of regulatory T-cells. These cells regulate the immune response and prevent auto-immune responses that would otherwise lead to the body mounting an immune response against its own self-antigens, resulting in tissue destruction (Wu *et al*., 2009). However, regulation of the immune response occurs at various stages and is crucial as an excessive immune response can lead to damage of host tissue whilst a weak response could leave the body vulnerable to infection. This thesis will focus primarily on the regulation of the innate immune system in response to infection or acute injury of the lung. For context, a broad overview of the innate immune system is initially provided.

1.2 Innate immunity

Innate immunity is responsible for first line of defence against invading pathogens. It responds very quickly. For many years innate immunity was envisaged to act quite non-specifically but with an ability to interface with and activate the adaptive immune response. However more recently, some degree of specificity has been ascribed to the innate immune response. The response requires pattern recognition receptors (PRRs) that recognise pathogen associated molecular patterns (PAMPs) i.e. components of the invading pathogens (Janeway, 2013). Upon recognition of PAMPs extracellularly or intracellularly, PRRs initiate a signalling cascade ultimately leading to the production of inflammatory mediators that can control the infection, protect the cells and activate the adaptive immune response (Medzhitov and Janeway, 2000). Regulation of the immune response initiated by PRRs is critical for an appropriate immune response as dysregulation can lead to disease.

PRRs include 4 major groups of receptors: toll-like receptors (TLRs), nucleotide oligomerisation domain (NOD) like receptors (NLRs), retinoic acid inducible gene 1 (RIG-1)-like receptors (RLRs) and C-type lectin receptors.

1.3 Toll like receptors

1.3.1 Background to TLRs

TLRs are transmembrane PRRs that recognise a range of microbe-derived molecules. TLRs were first discovered by Hoffman and Beutler in 1998 when searching for a receptor that recognised lipopolysaccharide (LPS) during septic shock (Poltorak *et al*., 1998). It was found that mice resistant to LPS did not express a mutated version of a gene similar to the *toll* gene in *Drosophila*. In *Drosophila*, the *toll* gene is responsible for controlling dorsoventral polarity in the developing embryo. It was later found to be important for defence against fungal infections (Lemaitre *et al*., 1996). Since this initial discovery there have been 10 TLRs identified in humans and 12 identified in mice (TLR1-9 and TLR11-13) (Kawasaki and Kawai, 2014).

TLRs are differentially localised within the cell. In humans, TLR1, TLR2, TLR4 and TLR5 are expressed on the cell surface while TLR3, TLR4, TLR7, TLR8, TLR9 and TLR10 are expressed on endosomes (Akira *et al*., 2006). TLRs recognise specific microbial patterns called PAMPs and also danger associated molecular patterns (DAMPs). DAMPs are self molecules that have aberrant location or structure and have arisen as a result of cellular stress or damage (Matzinger, 2002). All TLRs are

type I transmembrane receptors and share a similar structure with a pathogen sensing leucine rich repeat (LRR) section, a transmembrane domain and an intracellular Toll-IL1 receptor (TIR) signalling domain (Reuven *et al*., 2014). LRRs are responsible for recognition of various PAMPs and DAMPs (Bell *et al*., 2003). The LRR region contains a highly conserved segment and a variable segment which has different repeat numbers and arrangements and confers the ability to recognise various ligands. This variable portion is different depending on the TLR isoform and species (Matsushima *et al*., 2007). Upon pathogen binding by the LRR extracellular domain, intracellular signalling is activated via the TIR domain. The TIR domain is responsible for binding to TIR domain containing adaptor proteins within the cell through TIR-TIR interactions. Examples of TIR domain containing adaptor proteins include MyD88 (myeloid differentiation protein 88) and MAL (My-D88-adaptor-like). TLR intracellular signalling that can be described as MyD88 dependant or independent (Akira and Takeda, 2004; O'Neill and Bowie, 2007) and culminates in the upregulation of inflammatory genes.

1.3.2 Extracellular TLRs

TLR4 was the first identified TLR in mammals. It recognises LPS, a major component of Gram-negative bacterial cell outer wall (Beutler, 2000). It requires 3 other extracellular proteins to recognise LPS: LPS-binding protein, CD14 (cluster of differentiation 14) and myeloid differentiation protein 2 (MD2) (Da Silva Correia *et al*., 2001; Kim *et al*., 2007). Studies have also shown that TLR4 can recognise viral motifs from respiratory syncytial virus and in combination with MD-2 in mice, TLR4

can recognise and respond to the anti-tumour agent taxol found in plants, although the physiological relevance of this in humans is unclear (Kawasaki *et al*., 2000).

TLR1, TLR2, TLR6 and TLR10 share a high percentage of sequence similarity and can recognise various ligands in combination with each other (Farhat *et al*., 2007). For example, TLR2 has been shown to recognise PAMPs from Gram-negative and positive bacteria, viruses, fungi and parasites. It does this by the formation of heterodimers with TLR1 and TLR6 (Oliveira-Nascimento *et al*., 2012).

TLR10 is expressed in humans but not in mice. Until recently, its role was unclear. Recent studies have shown it to have dampening effects on TLR2 signalling (Oosting *et al*., 2014). Blocking TLR10 with antagonistic antibodies enhances pro-inflammatory cytokine production particularly in response to TLR2 stimulation. TLR10 is thought to mediate this effect through production of IL-1R antagonist (IL-1Ra) and prevent IL-1 signalling (Oosting *et al*., 2014).

TLR5 recognises extracellular flagellin from Gram-negative and positive bacteria (intracellular flagellin is recognised by the NLR, Ipaf) (Miao *et al*., 2007). Flagellin is a protein that makes up the filament of bacterial flagella and is crucial for bacterial movement and invasion of host tissues (Hayashi *et al*., 2001). The mechanisms by which TLR5 recognises flagellin are as yet not certain. TLR11 is also known to bind to flagellin but this is pH dependent (Hatai *et al*., 2016).

TLR11 is not expressed in humans but is found in mouse bladder and kidney (Zhang *et al*., 2004). It recognises PAMPs from *Toxoplasma gondii* (Yarovinsky *et al*., 2008).

Specifically TLR11 recognises the *T.gondii* protein profilin (Hatai *et al*., 2016). *T.gondii* is protozoan parasite that can infect all mammals. In humans, TLR11 is a non-functional pseudogene so *T.gondii* is most likely recognized by TLR2, TLR7, TLR9 and NLRP1 inflammasome (Yarovinsky, 2014). *T.gondii* infection is controlled in healthy adults but can cause severe neurological damage in immunocompromised people or when contracted in utero (McAuley, 2014; Z.-D. Wang *et al*., 2017).

TLR12 is also not expressed in humans and like TLR11, in mice it also recognises profilin from *T.gondii* (Koblansky *et al*., 2013). Research has shown that TLR12 alone is sufficient to mount an immune response to profilin in plasmacytoid dendritic cells but TLR11 and TLR12 are required for recognition of profilin on macrophages and conventional dendritic cells (Koblansky *et al*., 2013).

TLR13 is an endosomal TLR that is expressed in mice but not expressed in humans. Although poorly characterized it has been shown to recognise unmethylated bacterial 23s ribosomal RNA (Li and Chen, 2012; Oldenburg *et al*., 2012).

1.3.3 Intracellular TLRs

Intracellular TLRs are located on the membrane of endosomes. This allows them to recognise intracellular pathogen PAMPs such as viral and bacterial nucleic acids (Akira *et al*., 2006).

TLR3 recognises double stranded RNA from viral sources (McCartney and Marco, 2008). Polyinosinic-polycytidylic acid (polyI:C) is a synthetic dsRNA which is

commonly used as a ligand to activate TLR3 in an experimental setting (Bell *et al*., 2006; Liu *et al*., 2009). TLR3 is the only TLR that does not contain a critical proline residue that is conserved in the TIR domain of all other TLRs (Oshiumi *et al*., 2003). This is why TLR3 has evolved to signal without using the adaptor protein MyD88 that binds via TIR domain interactions.

TLR7 and TLR8 are similar in sequence and recognise single stranded RNA, typical of a replicating virus (Heil *et al*., 2003; Zhang *et al*., 2016). TLR7 and TLR9 can also recognise immune complexes of mammalian DNA and RNA, which are self-antigens (Celhar *et al*., 2016). Recognition of these self-antigens by TLR7 and TLR9 leads to increased lifespan of the macrophages on which the TLRs are activated, increased phagocytic capacity and reduced antigen presentation capabilities. This may have evolved as a mechanism to prevent presentation of self antigens to T-cells (Celhar *et al*., 2016). TLR9 recognises genomic bacterial DNA (Hemmi *et al*., 2000). In an experimental setting, unmethylated cytosine phosphate guanine (CpG) motifs of single stranded DNA are often used as a ligand to activate TLR9 (Krieg, 2002) and initiate a potent inflammatory immune response.

1.3.4 MyD88 dependant signalling

MyD88-dependant signalling is common to all TLRs except TLR3 as demonstrated in Figure 1.1. Upon ligand recognition adaptor proteins are recruited to the TIR domain of the TLRs. MyD88 is an adaptor protein which contains a TIR domain, an intermediary domain (ID) and a death domain (DD) (Deguine and Barton, 2014). TLR2 and TLR4 also recruit MyD88-adaptor-like protein (MAL), which connects

TLR2 and TLR4 to MyD88 through binding at common TIR domains (Yamamoto *et al*., 2002). MyD88 recruitment in turn recruits IRAK (IL-1 receptor associated kinase) proteins which were first described in T-cells as protein kinases that co-precipitated with IL-1R1 (Martin *et al*., 1994). MyD88 specifically recruits IRAK1 and IRAK4. IRAK4 binds to MyD88 via common death domains and activates IRAK1 by phosphorylation (Dossang *et al*., 2016; Loiarro *et al*., 2009). IRAK4 then dissociates from MyD88 in complex with IRAK1 to transiently interact with TRAF6 (TNF receptor associated factor 6). TRAF6 is an E3 ubiquitin ligase and the interaction with the IRAK1/4 complex leads to ubiquitination of TRAF6. Ubiquitination of TRAF6 allows it form a complex with TAB2 (TAK1 binding protein 2)/TAB1/TAK1 (TGFβ activated kinase 1), which is already pre-formed in the cell (Kanayama *et al*., 2004). This induces activation of TAK1. TAK1 can then interact with the IKK (IκB kinase) complex composed of IKKα, IKKβ and IKKγ/NEMO. (Yamamoto and Gaynor, 2004). TAK1 phosphorylates IKKβ in this complex leading to its activation. IKKβ can then directly phosphorylate IκB, which is an inhibitor of the transcription factor NFκB, targeting it for degradation (J. Zhang *et al*., 2014). This allows NFκB to translocate to the nucleus and initiate transcription of NFκB responsive genes.

MAP (mitogen associated protein) kinase signalling can also be activated through TLR signalling. TAB1, once activated can phosphorylate MKK3/6 (mitogen activated protein kinase kinase 3/6) and TAK1 can activate MKK7, which result in downstream phosphorylation and activation of p38 and JNK respectively (Ge *et al*., 2002; Geuking *et al*., 2009; Sathyanarayana *et al*., 2003). These MAPK can then translocate to the nucleus and activate transcription of target genes.

1.3.5 MyD88 independent signalling or TRIF-dependant signalling

MyD88 independent signalling is used by TLR3 and TLR4 as demonstrated in figure 1.1. TLR4 can signal through MyD88 dependant and independent pathways (Ve *et al*., 2012). Upon ligand binding the TLRs dimerise and the adaptor protein TRIF (TIR domain containing adaptor inducing IFNβ) is recruited to the TIR domain of the TLR (Piao *et al*., 2013). For TLR4 to signal independently of MyD88, it requires an adaptor molecular TRAM (TRIF related adaptor molecule) to activate TRIF. TRIF can then form a complex with and activate TBK1 (TANK binding kinase 1)/IKKε, leading to the phosphorylation and activation of interferon regulatory factor 3 (IRF3) and IRF7 (Fitzgerald *et al*., 2003; Sharma *et al*., 2003). IRF3 and IRF7 dimerise and can then move to the nucleus and activate transcription of interferon-regulated genes.

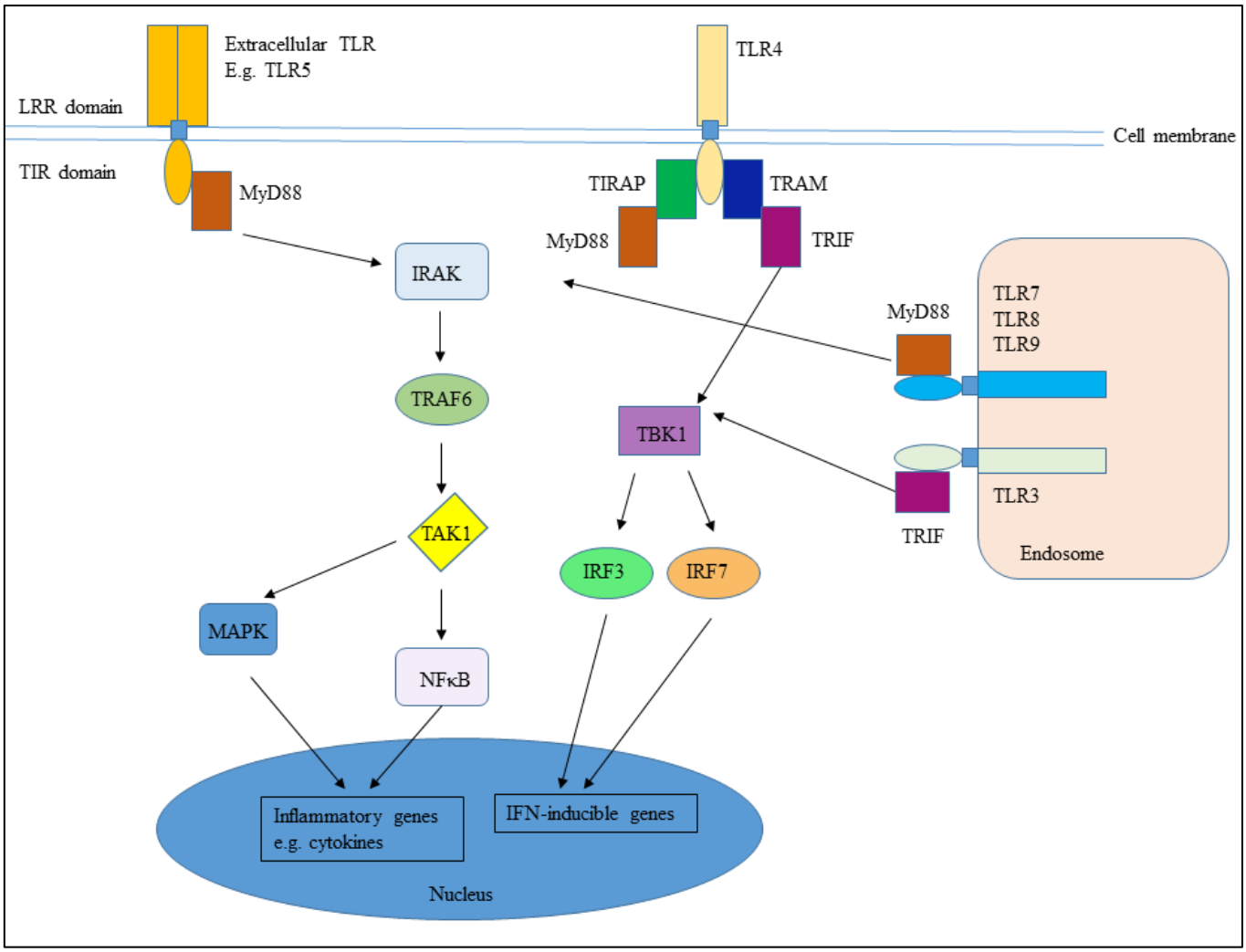

Figure 1.1 TLR signalling pathways

The above figure illustrates MyD88-dependant and MyD88-independent TLR signalling as detailed in sections 1.2.4 and 1.2.5.

1.4 Nod-like receptors

1.4.1 Background to NLRs

There are 22 members of the NLR family (Kanneganti *et al*., 2007; Proell *et al*., 2008; Ting and Davis, 2004). Unlike TLRs, NLRs are cytoplasmic receptors. NLRs are composed of a central nucleotide binding domain termed NOD (nuclear binding oligomerisation domain), a C-terminal receptor domain characterised by LRRs and an N-terminal effector domain. The C-terminal LRR is responsible for recognising and binding PAMPs (Proell *et al*., 2008). The N-terminal domain varies and defines the 4 families that NLRs are divided into: the acidic transactivation domain (NLRA), baculoviral-inhibitory repeats like domain (NLRB), caspase activation and recruitment domain ((CARD) NLRC) and the pyrin domain (NLRP) (Schroder and Tschopp, 2010). The N-terminal domain binds to other proteins and is therefore crucial for performing effector functions.

NLRs have 4 broad functions, which can be divided into autophagy, signal transduction, transcription activation and inflammasome formation. Autophagy is the destruction of cell components that have become damaged and was first described by de Duve after research into lysosomes (de Duve, 2005; de Duve *et al*., 1955). It can be induced for example by NOD2. NOD2 induces autophagy by recruiting the protein ATG16L1 (autophagy related protein 16-1) to the site of bacterial entry and hence removes the bacteria (Homer *et al*., 2010). NOD1 and NOD2 can respond to MDP (muramyl dipeptide) and signal through MAPK and NFκB to induce pro-inflammatory cytokines (Girardin *et al*., 2003; Inohara *et al*., 2003, 2001). Perhaps the

most crucial role of NLRs is in inflammasome function. The inflammasome is a complex of proteins that can cleave inactive pro-caspase-1 into active, functioning caspase-1. Caspase-1 is essential for the cleavage of pro-IL-1β into active IL-1β and IL-18. Inflammasomes can be formed by NLRP1, NLRP3. NLRC4/IPAF and AIM2 (part of ALR group, not NLR) can form inflammasomes as shown in figure 1.2.

1.4.2 Inflammasomes

A broad range of pathogenic and sterile activators trigger inflammasome formation. Some examples of pathogenic activators include various bacterial, viral, fungal and protozoan PAMPs. Sterile activators include DAMPs such as ATP, monosodium urate crystals, β-amyloid and environmental stimulus such as alum (Latz *et al*., 2013). Upon recognition of the activators, NLRs binds to ASC (apoptosis-associated speck like protein containing CARD) via a pyrin: pyrin interaction (Latz *et al*., 2013; Oroz *et al*., 2016). Pro-caspase-1 then binds to ASC via a CARD:CARD interaction to form the inflammasome complex (Srinivasula *et al*., 2002). In this complex, caspase-1 initiates autocatalysis and can then cleave IL-1β and IL-18 into their active forms (Boatright *et al*., 2003; Lamkanfi *et al*., 2007). There is debate as to how mature IL-1β is released from the cell. There is some evidence that it may be released from the cytosol via lysosomal or microvesicle exocytosis (Pizzirani *et al*., 2007) or trafficked through exosomes (Qu *et al*., 2007). Another possible route of release is via terminal secretion where pyroptosis activated by formation of the NLRP3 inflammasome leads to caspase-1 dependant pores in the plasma membrane (Fink and Cookson, 2006). Pyroptosis leads to rupture of the cell membrane causing release of cytoplasmic

contents, including active IL-1β and IL-18, into the extracellular space. Recent studies however, suggest that IL-1β can exit the cell through pores in the cell membrane that are independent to the non-specific protein leakage that occurs during cell death (Martín-Sánchez *et al*., 2016). Studies have also shown that the protein Gasdermin D can form pores in the membrane large enough for IL-1β to exit through and can form these pores in living macrophage (Evavold *et al*., 2018; Heilig *et al*., 2017). This challenges the traditional view that inflammasome activation leads to cell death.

1.4.3 NLRP1 inflammasome

NLRP1 has a slightly different structure to other NLRP family proteins. NLRP1 also contains a 'function to find' domain (FD) (Martinon *et al*., 2009). The FD domain is thought to be involved with spontaneous self-processing which is required for NLRP1 to be able to respond to stimuli (Finger *et al*., 2012; Frew *et al*., 2012). NLRP1 was also the first NLR shown to form an inflammasome that cleaved caspase-1 into its active form (Martinon *et al*., 2002).

It has been shown that anthrax lethal toxin (LeTx), produced by *Bacillus anthracis*, which leads to development of the disease anthrax, activates the NLRP1 inflammasome. LeTx is composed of a protective antigen (PA) and a lethal factor (LF). It is unclear whether the LF can cleave NLRP1 directly or its presence in the cytosol indirectly leads to cleavage of NLRP1 (Chavarría-Smith and Vance, 2015). NLRP1 inflammasome can also be activated by a reduction in adenosine triphosphate (ATP) production via chemical inhibition of glycolysis and oxidative phosphorylation in fibroblasts (Liao and Mogridge, 2013)

Conflicting evidence has been shown for the role of MDP in activation of the NLRP1 inflammasome (Chavarría-Smith and Vance, 2015) and also for *Toxoplasma gondii* (Ewald *et al*., 2014; Gorfu *et al*., 2014). For *Toxoplasma gondii* mediated activation of the NLRP1 inflammasome, only Gorfu *et al*. (2014) have shown that enough IL-1β is present following *Toxoplasma gondii* infection in *Nlrp3*$^{-/-}$ mice to suggest a role for the NLRP1 inflammasome in responding to *Toxoplasma gondii* infection. However, human susceptibility to congenital toxoplasmosis caused by *Toxoplasma gondii* infection has been linked to NLRP1 polymorphisms using knockdown studies in human macrophage cell lines (Witola *et al*., 2011). Single nucleotide polymorphisms (SNPs) in the *Nlrp1* gene are associated with autoimmune disease, auto-inflammatory disease, rheumatoid arthritis, systemic sclerosis, Crohns disease and melanoma (Finger *et al*., 2012). The SNPs typically associated with this disease usually affect transcription of NLRP1 (Jin *et al*., 2007).

1.4.4 NLRP3 inflammasome

The NLRP3 inflammasome is activated by a wide range of pathogens including bacterial, viral and fungal pathogens, pore-forming toxins, crystals and DAMPs such as ATP (Lamkanfi and Dixit, 2012). Given the range of activators it is generally agreed that NLRP3 does not directly detect each pathogen and rather detects a host factor that is changed upon detection of these pathogens. The host factor which NLRP3 detects is hypothesised to be K^+ efflux (Muñoz-Planillo *et al*., 2013), mitochondrial ROS production (Zhou *et al*., 2011), release of cytosolic cathepsin (Hornung *et al*., 2008), or mitochondrial changes such as NLRP3 translation (Subramanian *et al*., 2013) or release of mitochondrial DNA (Nakahira *et al*., 2011).

NLRP3 requires two signals for activation. The first signal is an NFκB activating signal which leads to pro-IL-1β and NLRP3 upregulation (Bauernfeind *et al*., 2009). The second signal typically used in an experimental setting is ATP (Lamkanfi and Dixit, 2012). For NLRP3 inflammasome assembly, NLRP3 must first be deubiquitinated. This has been shown extensively although it is not clear which E3 ubiquitin ligase controls basal NLRP3 ubiquitination (Juliana *et al*., 2012; Lopez-Castejon *et al*., 2013; Py *et al*., 2013). An E3 ubiquitin ligase, Pellino2, has been shown to regulate NLRP3 inflammasome mediated IL-1β production and will be discussed in further detail below (Humphries *et al*., 2018).

1.4.5 NLRC4 inflammasome

The NLRC4 or IPAF inflammasome is activated by bacterial flagellin or Gram-negative bacteria with a type III or IV secretion system (Franchi *et al*., 2006; Lamkanfi and Dixit, 2012). Examples of bacteria that can activate the NLRC4 inflammasome include *Salmonella typhimurium, Legionella pneumophilia* and *Pseudomonas aeruginosa* (Schroder and Tschopp, 2010). Maximal caspase-1 cleavage by the NLRC4 inflammasome requires ASC but in an unknown capacity since NLRC4 does not have a PYD (pyrin) domain and hence cannot interact with ASC (Suzuki *et al*., 2007). NLRC4 inflammasome mediated caspase-1 cleavage is followed by rapid cell death.

1.4.6 AIM2 inflammasome

Absent in melanoma-2 (AIM2) is part of the AIM2-like receptor (ALR) family of proteins that can recruit ASC to cleave caspase-1 into its active form (Lugrin and Martinon, 2017). AIM2 inflammasome assembly occurs when the DNA-binding domain of AIM2 senses intracellular pathogens such as cytomegalovirus and Vaccinia virus (Alnemri, 2010). AIM2 inflammasome is also of crucial importance in responding to *Fransicella tularensis* infection, which *Aim2*$^{-/-}$ mice cannot clear. The AIM2 inflammasome has also been implicated in the response to *Listeria moncytogenes* infection (Sauer *et al*., 2010).

1.4.7 RLRs

The family of RLRs consists of RIG-I (retinoic acid inducible gene-1), MDA5 (melanoma differentiation associate factor 5) and LGP2 (laboratory of genetics and physiology 2 and a homolog of mouse D11lgp2). These receptors detect viral or self-processed RNA in the cytosol and initiate an immune response (Loo and Gale, 2011). The immune response initiated involves production of type I interferons (IFN) and upregulation of other antiviral genes to control infection (Yoneyama *et al*., 2005). RLRs are expressed on most cell types with increased expression after detection of type I IFNs or viral infection (Imaizumi *et al*., 2005; Kang *et al*., 2004). This group of receptors recognises a wide range of viruses including Sendai virus, measles, Influenza A and B, Ebola, Vaccinia virus, dengue virus and West Nile virus

(Fredericksen *et al*., 2008; Kato *et al*., 2006; Loo and Gale, 2011; Pichlmair *et al*., 2009; Plumet *et al*., 2007).

1.4.8 CLRs

CLRs bind carbohydrates. CLRs are divided into 3 groups depending on their cellular location and the number of conserved carbohydrate recognition domains (CRDs) present. There are two membrane bound groups and a soluble group. Type I transmembrane CLRs contain several CRDs and include DEC-205 (Shrimpton *et al*., 2009) and macrophage mannose receptor (MMR) (Brown *et al*., 2018). Type II transmembrane receptors contain a single CRD. Transmembrane CLRs are important in sensing and activating an immune response to fungal pathogens. Soluble CRDs include mannose-binding lectin (MBL). MBL is important in detecting and responding to yeast infection (Choteau *et al*., 2016).

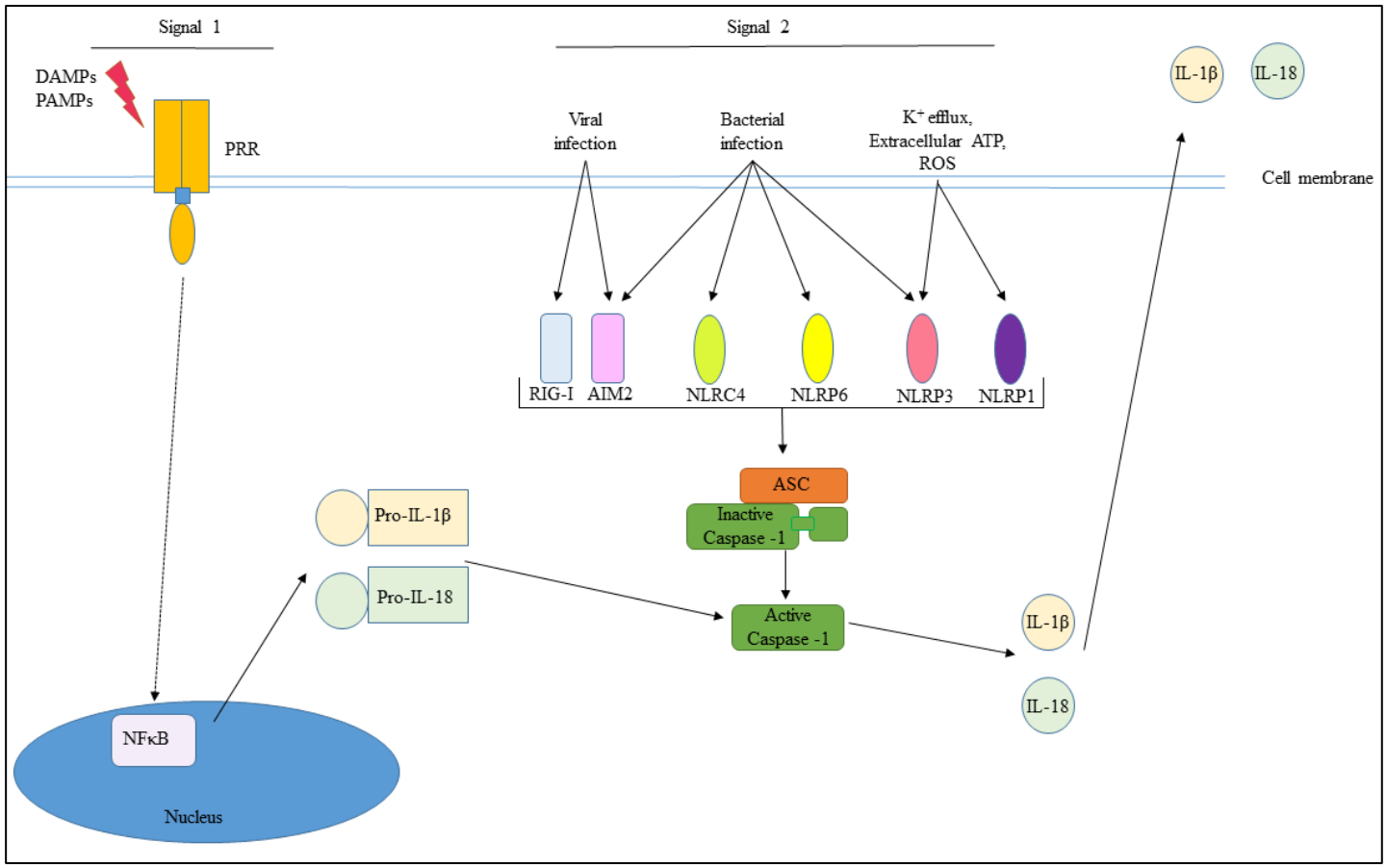

Figure 1.2 Mechanisms and action of inflammasomes

The above figure illustrates inflammasome activation and effects as described in section 1.4.2-1.4.6.

1.5 Interleukin-1

1.5.1 Background to IL-1

The PRRs described above induce a broad inflammatory response following detection of pathogens. This response includes the induction of pro-inflammatory cytokines. An important and relevant cytokine to our studies is IL-1. IL-1 comprises a family of cytokines, the best characterised of which is interluekin-1β. IL-1β is a crucial pro-inflammatory that can bind to cells and signal through IL-1R to induce production of other pro-inflammatory cytokines, growth factors, tissue remodelling components, extracellular matrix components, cytokine receptors and adhesion molecules (Dinarello, 2009). Perhaps most importantly it can induce IL-1β production in a self-positive feedback loop (Weber *et al*., 2010).

1.5.2 IL-1R signalling

IL-1β signals through the IL-1R. Similar to TLR signalling, IL-1R signals through a MyD88-dependant pathway. Once the primary receptor and subunit are bound, MyD88 and Tollip are recruited to the receptor (Acuner Ozbabacan *et al*., 2014). IRAK1 can homodimerise and bind to Tollip and the adaptors MyD88 and IRAK4 via death domains, leading to phosphorylation of IRAK1 (Neumann *et al*., 2007). Following this, TRAF6 is recruited and the signalling pathways proceeds as described for MyD88-dependant TLR signalling (Weber *et al*., 2010). As mentioned in the previous section, IL-1β signalling through IL-1R can lead to the production of more IL-1β in a positive feedback loop. As IL-1β has potent pro-inflammatory properties,

the need for tight control of its production is of crucial importance. For example, where IL-1β is produced in excessive amounts it can lead to conditions such as rheumatoid arthritis and smouldering myeloma (Dinarello, 2011).

1.6 Pellino

1.6.1 Discovery

In an effort to understand how the IL-1 pathway is regulated, our research group is especially interested in a family of E3 ubiquitin ligases called Pellino. Pellino is a family of proteins, which are highly conserved throughout evolution. They were discovered in *Drosophila melanogaster* as an interactor of the IRAK-1 orthologue *Pelle* (Grobans *et al*., 1999). The family consists of Pellino1, Pellino2 and Pellino3. The family share a high percentage sequence homology yet they have been shown to play non-redundant roles in immune regulation. Pellino proteins are E3 ubiquitin ligases (Butler *et al*., 2007; Schauvliege *et al*., 2006). This means they catalyse the attachment of polyubiquitin chains to proteins that alter the fate or function of the target proteins. Pellino proteins can attach K63 linked ubiquitin chains to proteins, which allows the target protein to become activated. The attachment of K48 linked polyubiquitin chains targets the protein for degradation in the lysosome (Malynn and Ma, 2010). Through protein modification, Pellino regulates the activity of innate immune signalling molecules such as the NFκB, to either switch on or switch off the immune response (Moynagh, 2014). To date, Pellino1 and Pellino3 have been the focus of multiple primary studies to characterise their function however, only one

study of Pellino2 characterisation exists that demonstrates physiologically relevant data.

1.6.2 Pellino1

Pellino1 has been implicated in regulation or mediation of the inflammatory response in a broad range of settings. For example, Pellino1 has been shown to regulate IL-1R and TLR signalling through interaction with IRAK1 (Jiang *et al*., 2003). Initial studies demonstrated the E3 ubiquitin ligase activity of Pellino proteins by showing that bidirectional signalling occurred between IRAK and Pellino1 (Butler *et al*., 2007). Upon TLR signalling, IRAK1 and IRAK4 became polyubiquitinated with K63-linked ubiquitin residues. Following ubiquitination, Pellino1 becomes phosphorylated by IRAK1 (Butler *et al*., 2007; Jiang *et al*., 2003). This targets Pellino1 for polyubiquitination and subsequent degradation. Pellino1 therefore serves a crucial function in IL-1R/TLR signalling and in self-regulation of the signal. Further to Pellino1 regulating TLR pathways, it has been shown that mice deficient in Pellino1 are resistant to septic shock induced by TLR3 or TLR4 ligands. It was demonstrated that this occurred because Pellino1 binds to and ubiquitinates RIP1 (receptor interacting serine/threonine protein kinase 1) which is an important signalling mediator in IKK activation during TLR3 and TLR4 signalling (Chang *et al*., 2009).

However, this role for Pellino1 in TLR3 signalling has been challenged by studies in knock-in mice that express a mutated form of Pellino1 lacking E3 ligase activity (Enesa *et al.,* 2012). These Pellino1 knock-in mice express lower levels of IFNβ but have no deficiency in activation of NFκB or MAPK downstream of TLR3 (Enesa *et*

al., 2012). The opposing roles for Pellino1 described in TLR3 signalling (Chang *et al*., 2009; Enesa *et al.,* 2012) may be a result of functional compensation in Pellino1-deficient mice by other members of the Pellino family. It is also possible that Pellino1 regulates TLR3 mediated activation of NFκB independently of its E3 ligase activity. These studies highlight the limitations of genetic knock-out animals and demonstrate that observed phenotypes should be cautiously interpreted and verified by different experimental approaches.

Pellino1 has also been implicated in suppressing the activation of T-cells (Chang *et al*., 2011). A genetic deficiency in Pellino1 leads to hyperactivation of T-cells and Pellino1-deficient mice develop autoimmunity. Pellino1 negatively regulates the activation of T-cells by negatively regulating c-Rel, an important transcription factor for T-cell activation. It mediates this regulation through attachment of K48-linked polyubiquitin chains to c-Rel (Chang *et al*., 2011).

Pellino1 also plays a role in regulation of neuroinflammation (Xiao *et al*., 2013). It has been shown that Pellino1 is highly expressed in microglia and promotes microglial activation during experimental autoimmune encephalitis (EAE) by mediating the induction of cytokines and chemokines and hence T-cell infiltration into the central nervous system through regulation of TLR signalling (Xiao *et al*., 2013).

Pellino1 also plays a role in mediating lung tumorigenesis. It was found that Pellino1 expression is higher in human lung adenocarcinoma cell lines than in non-neoplastic bronchial epithelial cell lines which prompted examination into lung tumorigenesis

(Jeon *et al*., 2017). Studies in transgenic mice overexpressing Pellino1 led to the discovery that Pellino1 induces Slug and Snail overexpression which promotes epithelial-mesenchymal transition (EMT) thereby contributing to lung tumorigenesis (Jeon *et al*., 2017; Medici *et al*., 2008).

Pellino1 has also been implicated in the regulation of the immune response to rhinovirus using *in vitro* siRNA knockdown studies (Bennett *et al*. 2012). When Pellino1 was knocked down, epithelial cells demonstrated impaired production of CXCL8 but no impairment of type I interferon production and therefore control of viral replication, in response to rhinovirus infection. As CXCL8 is an important chemokine for neutrophil infiltration, this suggests that neutralisation of Pellino1 may inhibit potentially damaging neutrophilic inflammation without loss of control of viral replication (Bennett *et al*. 2012).

1.6.3 Pellino2

Most of the studies carried out for Pellino2 have involved *in vitro* over expression or knockdown approaches. These studies have implicated Pellino2 in MAP kinase activation, particularly JNK (janus activated kinase) activation (Kim *et al*., 2012; Liselotte and Whitehead, 2003). Recently our research group has demonstrated the first physiological role for Pellino2. Using Pellino2-deficient animals, Pellino2 was shown to mediate NLRP3 inflammasome activation (Humphries *et al*. (2018). Briefly, upon stimulation with the priming signal, NLRP3 is ubiquitinated with K63-linked polyubiquitin chains, which is promoted by Pellino2. Pellino2 mediates NLRP3 ubiquitination by interacting with IRAK1 and preventing the negative regulation of

NLRP3 signalling by IRAK1. This work was on-going in the laboratory where this thesis was carried out and as such, this thesis was initially developed around the unpublished findings of Humphries *et al.* (2018). This thesis aimed to build on the work carried out by Humphries *et al*. (2018) and explore any pathophysiological roles for Pellino2, especially in the context of acute lung injury and infection.

1.6.4 Pellino3

Our group has also shown Pellino3 to negatively regulate TLR3 signalling through interaction with and ubiquitination of TRAF6 (Siednienko *et al*., 2012a). This prevents TRAF6 binding to and activating IRF7, which results in reduced type I IFN production. *In vivo* it was demonstrated that Pellino3-deficient mice were resistant to encephalomyocarditis virus (EMCV) infection (Siednienko *et al*., 2012b). Pellino3 also negatively regulates tumour necrosis factor (TNF) induced cell killing by targeting RIP1 and preventing formation of complex II formation in response to TNFR (TNF receptor) stimulation (Yang *et al*. 2013).

Our group has also implicated Pellino3 in production of IL-1β in contrast to Pellino2, the former supresses the expression of IL-1. Briefly, reduced Pellino3 expression was observed in adipose tissue of obese humans and mice (Yang *et al*., 2014). Obesity causes systemic low-level inflammation (Gregor and Hotamisligil, 2011). This inflammation involves IL-1β production that contributes to insulin resistance and the development of diabetes (Tack *et al*., 2012). Pellino3 suppresses IL-1β production by negatively regulating the stabilisation of hypoxia inducible factor 1 α (HIF1α) which

induces IL-1β expression. The reduced levels of Pellino3 in obesity may contribute to increased systemic levels of IL-1β (Yang *et al*., 2014).

Pellino3 has been implicated in regulation of the gut epithelial immune response. NOD2 is an innate immune receptor that is responsible for detection of Gram-positive bacteria in the gut through recognition of the PAMP MDP (Grimes *et al*., 2012). It has been shown that Pellino3 is involved in the positive regulation of the NOD2 response through ubiquitination of RIP2 (Yang *et al*., 2013a). Impairment of NOD2 signalling has been linked to inflammatory bowel disease and Crohns disease (Cleynen *et al*., 2016). Pellino3 is expressed at a lower level in patients who suffer from both of these diseases.

1.7 COPD

1.7.1 Pathology of COPD

Considering our group has shown important regulatory roles for Pellino proteins in mucosal immunity in the gut (Yang *et al*., 2013a), we were also keen to explore the potential physiological and pathophysiological roles of Pellino proteins at other mucosal sites and especially the lung. Chronic obstructive pulmonary disease (COPD) is an umbrella term for diseases of the lung affecting airflow including chronic bronchitis, chronic airflow limitation and emphysema (Vogelmeier *et al.*, 2017). It is characterised by airflow obstruction, fibrosis of the airways and destruction of the alveoli which leads to emphysema (Chung and Adcock, 2008). COPD affects mainly smokers and has also been linked to biomass smoke inhalation (Hurd, 2000; Ko *et al*.,

2008). Regarding epidemiology, studies have shown that risk for developing COPD is associated with poor socioeconomic status (Burney *et al*., 2014). In developing countries, the risk of developing COPD in a lifetime is estimated at 25-45% in patients who have never smoked (Salvi and Barnes, 2009). This may be a direct result of the use of biomass stoves. Studies from rural Mexico and China have shown that improved biomass stoves or ventilation reduces the risk of COPD significantly (Romieu *et al*., 2009; Zhou *et al*., 2014). A study of 13 million people in Canada suggested the risk of developing COPD in a lifetime is approximately 25% (Gershon *et al*., 2011). This study also highlighted the higher risk of COPD development in men and large studies have replicated this (Buist *et al*., 2007).

Tobacco smoke remains the major risk factor for development of COPD. Tobacco smoke has been shown to activate airway neutrophils and lead to IL-8 expression, which is a potent chemotactic factor (Lee *et al*., 2016). Increased levels of IL-8 lead to increased neutrophil infiltration (Russo *et al*., 2014). Neutrophils are innate immune cells that produce proteases and in conditions showing disproportionate levels of infiltrating neutrophils, an imbalance between protease and anti-proteases will occur leading to the destruction of alveolar walls and development of COPD (Stockley, 2002). However, not all people exposed to smoke will develop COPD (Celli and Macnee, 2004). This suggests there is some genetic element controlling the immune response to smoke in the lungs. For those who do develop COPD, it is generally agreed that it is caused by an imbalance of proteases and anti-proteases in the lung (Sinden *et al*., 2014). This idea has come from observations in individuals with alpha-1 antitrypsin (AAT) deficiency.

AAT is a serum serine protease inhibitor that regulates the effects of neutrophil elastase in the lungs. Primary studies identified AAT deficiency as a cause of pulmonary function abnormalities (Rawlings *et al*., 1976). Studies have found high variability in the development of pulmonary abnormalities in patients with inherited AAT deficiency (DeMeo *et al*., 2007). Many patients with AAT deficiency have normal lung function and would likely not develop lung abnormalities if they do not smoke (Tanash *et al*., 2017). Patients with AAT deficiency who develop COPD will often require lung transplantation.

There have also been other genetic mutations identified that predispose an individual to higher risk of development of pulmonary function abnormalities. Recent genome-wide association analysis from 6633 individuals compared SNPs from moderate and severe COPD patients to healthy individuals (Cho *et al*., 2014). Genetic loci that were significantly altered during COPD include matrix metalloproteases 12 (MMP12) and transforming growth factor β2 (TGFB2) (Cho *et al*., 2014). The extensive studies that have been carried out on pulmonary abnormality, emphysema and COPD development have identified the following aspects as important in predicting probability of COPD development: smoking, asthma, history of respiratory infections and various genetic mutations (de Marco *et al*., 2011).

Excessive inflammation is a key player in the development of COPD (Groenewegen *et al*., 2008). Destruction of alveolar architecture is preceded by sustained inflammation which includes immune cell infiltration, particularly neutrophils, and pro-inflammatory cytokine production (Noguera *et al*., 2001; Stockley, 2002). Pro-inflammatory cytokines such as IL-1β, IL-6 and TNFα are significantly increased in

patients with COPD (Bhowmik *et al*., 2000). Numerous early studies have shown that stimulation of epithelial cells with cigarette smoke extract leads to the production of neutrophil recruitment factors *in vitro* (Masubuchi *et al*., 1998; Mio *et al*., 1997; Shoji *et al*., 1995) It has long been known that neutrophil retention in the lungs is increased with smoking and COPD (MacNee *et al*., 1989; Selby *et al*., 1991). Once activated, neutrophils secrete a number of proteases such as cathepsin G, elastase and proteinase-3 that can break down collagen and may contribute to the development of emphysema in COPD (Overbeek *et al*., 2013). Therefore, control of neutrophil infiltration and the inflammatory response may represent an important mechanism in the treatment or prevention of COPD development.

1.7.2 Treatment and outlook for COPD

The GOLD (Global initiative for Chronic Obstructive Pulmonary Disease) initiative has stated that correct diagnosis must involve spirometry and should take symptoms, severity of airflow limitation, history of exacerbation and comorbidities into consideration (Vestbo *et al*., 2013). Once diagnosed, there are various options for treatment of the symptoms of COPD and exacerbations. The first and most important step taken in treatment is smoking cessation (Celli and Macnee, 2004). Nicotine replacements, pharmacological products and smoking cessation programmes are all used to help patients to stop smoking (Van Eerd *et al*., 2016). Other methods of managing stable COPD are also required (Vogelmeier *et al*., 2017). Pharmacologic interventions include bronchodilators, β2-agonists, anti-muscarinic antagonists, methyxanthines, anti-inflammatory agents, inhaled corticosteroids (ICS), oral glucocorticoids, phosphodiesterase-4 inhibitors and mucolytic and antioxidant agents

(Vogelmeier *et al*., 2017). However, long-term treatment with some of these agents can cause severe side effects. For example, long-term use of inhaled corticosteroids while reducing inflammation, can increase the risk of patients developing pneumonia, osteoporosis, diabetes and cataracts (Price *et al*., 2012). As such, there is much research being carried out on COPD in an effort to increase understanding of the disease and develop new therapies. An element of COPD, emphysema, can be easily modelled in mice and therefore is a useful tool for examination of the molecule mechanisms involved in inflammation and lung destruction seen in COPD. Emphysema involves breakdown of the alveolar walls, increased airspace in the lungs and a strong inflammatory response.

1.7.3 Elastase model of emphysema

Emphysema was first modelled in rats by administration of the protease papain into the lungs (Gross *et al*., 1965). Emphysema has since been modelled extensively in mice through the intranasal administration of elastase. This elicits an immune response similar to that seen in emphysema in humans (Limjunyawong *et al*., 2017). The response includes an inflammatory component and also destruction of alveolar walls. This model has been used extensively to study emphysema and hence it is well characterised. The model has some limitations. For example, mice have less extensive airway branching than humans, with no respiratory bronchioles. This is an issue because as humans have various membranous and respiratory bronchioles, different areas will have different responses to lung injury which is not seen in mice (Pinkerton *et al*., 2015). Therefore, any work on identification of pathways involved

in emphysema development or progression should be translated to humans to some degree in order to establish relevance.

There are many variations in the methods used for elastase-induced emphysema in mice. Many studies examining the effect of inflammatory mediators often use a single dose of elastase, with the animals being culled 14 to 21 days afterwards to examine the disease pathology. This has been used to examine the involvement of Nrf2 (Ishii *et al*., 2005), TNFα and IL-1β receptor (Lucey *et al*., 2002) and NLRP3 inflammasome (Couillin *et al*., 2015) on emphysema development. However, it has been shown that repeated doses of elastase instillation produce a more relevant pre-clinical model because it is more representative of smoke induced human disease (Cruz *et al*., 2012; Kennelly *et al*., 2016). Studies using a repeated dose model have shown not only local effects in the lungs but also systemic manifestations of the disease in the case of reduced exercise tolerance (Lüthje *et al*., 2009) and effects on cardiorespiratory function (Oliveira *et al*., 2016). For this reason the non-invasive method of repeated intranasal elastase instillation was used for the purposes of the study in this thesis as previously described by Kennelly *et al*. (2016). This provides potential for closer human relevance in relation to the role of Pellino2 in emphysema and COPD.

1.7.4 LPS model of emphysema

LPS is a component of Gram-negative bacterial cell walls. It is a common air contaminant and is found in its bioactive form in cigarette smoke (Sebastian *et al*., 2006). LPS can also be used to mimic COPD exacerbations in mice with emphysema

(Kobayashi *et al*., 2013). Chronic exposure to LPS in the lungs can lead to symptoms of emphysema in rodents. These include structural changes, airway hyper-responsiveness and inflammation (Brass *et al*., 2008; Toward and Broadley, 2000; Vernooy *et al*., 2002). There are some variations on the protocols for this model, for example, mice can be treated with LPS once a week for 4 weeks (Sohn *et al*., 2013) or daily for 4 weeks (Brass *et al*., 2008) or twice a week for 12 weeks (Vernooy *et al*., 2002). This creates some issues with comparison of methods and reliability of data.

1.7.5 Cigarette-smoke (CS) model of emphysema

Tobacco smoke is the main risk factor for development of COPD and hence, emphysema (Pauwels *et al*. 2001) and as such it has been used to model emphysema in mice. For best practise, standardised cigarettes from the University of Kentucky can be used where there is a known dose of total suspended particles and total particulate matter present however for investigations there has been no standardisation of protocols. Different mouse strains will also have different sensitivities to the procedure (Bartalesi *et al*., 2005). There is also variation in the apparatus used to expose the mice to cigarette-smoke. Cigarette-smoke exposure in mice can be achieved using a smoking apparatus, nose-only exposure or whole-body exposure. This model will lead to infiltration of macrophages and neutrophils into the lungs, fibrosis and emphysema development (Vandivier and Ghosh, 2017).

1.8 Pseudomonas aeruginosa

1.8.1 Background to *P. aeruginosa*

In addition to looking at Pellino proteins in inflammation in response to lung injury, we were also interested in their role in lung inflammation in response to respiratory infection. An important respiratory pathogen of particular interest is *Pseudomonas aeruginosa*. *P. aeruginosa* is a Gram-negative opportunistic bacterial pathogen that is present in the environment and infects immunocompromised patients and has been associated with exacerbations of COPD (Murphy *et al*., 2008). It is one of the most common causes of nosocomial infection. It is commonly resistant to many classes of antibiotic including aminoglycosides, cephalosporins, fluoroquinolones and carbapenens (Ventola, 2015). Treatment for multi-drug resistance cannot be solely through bacteriostatic/bactericidal compounds. Many reviews have highlighted the need to include a hygiene regime in healthcare setting to minimise the spread of the multi-drug resistant pathogen (Cerceo *et al*., 2016; Kaye and Pogue, 2015; Labarca *et al*., 2016). Control of *P. aeruginosa* is crucial for sensitive patients such as those with COPD or cystic fibrosis. One study estimates that 29% of infants with cystic fibrosis will acquire *P. aeruginosa* infection by 6 months of age and by age 16, 92% of cystic fibrosis patients will have *P. aeruginosa* infection (Li *et al*., 2017).

1.8.2 *P. aeruginosa* infection in cystic fibrosis

Cystic fibrosis is an autosomal recessive inherited, chronic and incurable disease that starts in childhood and significantly shortens the lifespan of patients (Cutting, 2015).

It is caused by variations in the CFTR (cystic fibrosis transmembrane conductance regulator) gene leading to excessive mucus production in the gastrointestinal and respiratory system (Donaldson and Boucher, 2007). Excessive mucus production leads to respiratory obstruction and causes inflammation and tissue damage (Cutting, 2015). It was initially thought that mutation in the CFTR gene was associated with abnormal immune function and this lead to inflammation without infection (Chmiel *et al*., 2002). However, it has been shown that inflammation does not precede infection as previously thought. Infants with cystic fibrosis without infection will have lower neutrophil numbers, lower levels of free neutrophil elastase and lower levels of inflammatory mediators in BAL (David *et al*., 2005; Douglas *et al*., 2009; Sly *et al*., 2009).

The source of infection is most commonly *P. aeruginosa.* Chronic infection with *P. aeruginosa* is associated with a worse prognosis for cystic fibrosis patients (Michael *et al*., 2003; Nixon *et al*., 2001). Respiratory infection in cystic fibrosis is one of the major contributors to morbidity and mortality in patients (Douglas *et al*. 2009). It is estimated that cystic fibrosis patients with a *P. aeruginosa* infection have a 2.6 times higher risk of death (Emerson *et al*., 2002). As such, early diagnosis and treatment is essential.

Vaccination against *P. aeruginosa* infection is not considered a viable option yet as trials have produced variable results (Johansen and Gøtzsche, 2015). In a review produced by Johansen and Gotzsche in 2015, they found only 3 trials suitable for analysis. One of the trials did not publish data but the company stated in a press release that the trial was a failure. In the other two trials, there were adverse side effects and the vaccine did not significantly lower the risk of infection. This highlights

the importance of understanding the molecular mechanisms of respiratory infection with *P. aeruginosa.* A better understanding of the pathology of *P. aeruginosa* infection may allow for better vaccine development or treatment options for cystic fibrosis patients with chronic infection.

1.8.3 *P. aeruginosa* infection in COPD

Acute *P. aeruginosa* infection has also been well documented in patients with chronic respiratory diseases such as COPD (Lyczak *et al*., 2000). It is estimated that 15% of patients with COPD will suffer from acute or chronic *P. aeruginosa* infection (Murphy, 2009). Studies have shown that the immune response to *P. aeruginosa* infection requires professional phagocytic cells such as macrophages and neutrophils and MyD88-dependant signalling is also important (Andrews and Sullivan, 2003; Koh *et al*., 2009; Mijares *et al*., 2011). This highlights the importance of an appropriate innate immune response to control *P. aeruginosa* infection.

1.9 Project aims

Our group has recently demonstrated roles for Pellino3 in regulation of mucosal immunology in the gut (Yang *et al*., 2013a). This thesis aims to build on this work by defining a role for Pellino proteins in mucosal immunology in the lung. We are particularly interested in investigating a role for Pellino2 in lung immunology, as until recently there had been no physiologically relevant role assigned to Pellino2 due to the lack of a Pellino2 knockout mouse. Recently, a Pellino2-deficient mouse was generated and research has implicated Pellino2 in mediating activation of the NLRP3

inflammasome and hence, IL-1β production. IL-1β has been previously implicated in emphysema and respiratory infection with *P. aeruginosa*. Using mouse models, it has been shown that IL-1β is important in the development of emphysema (Couillin *et al*., 2009) and a diminished IL-1β response following respiratory infection with *P. aeruginosa* can have protective effects (Iannitti *et al*., 2016). In light of this, we hypothesised that Pellino2 is involved in regulation of the immune response in the lung, specifically following acute lung injury and infection. The aims developed to test this hypothesis were;

- To explore role of Pellino2 in elastase induced emphysema
- To explore role of Pellino2 in responding *to P. aeruginosa* infection
- To examine the specificity of the role for Pellino2 in lung inflammation by characterising the role of Pellino3 in elastase induced emphysema
- To provide insights into the molecular basis for the role of Pellino2 in lung inflammation.

2 Materials and methods

2.1 Materials

2.1.1 Reagents

Reagent	Supplier
10% Neutral buffered formalin	CellPath
Acetic acid	Fisher-Scientific
Acetonitrile	Amersham Biosciences
Agar	Sigma-Aldrich
Ammonium bicarbonate	Sigma-Aldrich
Analine blue	Sigma-Aldrich
APS	Sigma-Aldrich
ATP	Sigma-Aldrich
Bouins solution	Sigma-Aldrich
Bradford reagent	Bio-rad
Bromophenol blue	Sigma-Aldrich
BSA	Sigma-Aldrich
BV6	Selleckchem
CHAPS	Sigma-Aldrich
Chloroform	Sigma-Aldrich
Collagenase	Sigma-Aldrich
CXCL2	Biolegend
DEPC water	Invitrogen
Dithiothreitol (DTT)	Sigma-Aldrich
DMSO	Sigma-Aldrich
DNAase	Roche
dNTPs	Promega
DSS	Sigma-Aldrich

EDTA	Sigma-Aldrich
Eosin Y	Sigma-Aldrich
Ethanol	Sigma-Aldrich
FCS	Invitrogen
Glycerol	Sigma-Aldrich
Hanks balanced salt solution	Sigma-Aldrich
Harris haematoxylin	Sigma-Aldrich
HCl	Merck
IFNγ	Peprotech
Igepal	Sigma-Aldrich
IL-17	R&D
Iodoacetamide	Sigma-Aldrich
Isopropanol	Sigma-Aldrich
LB broth	Sigma-Aldrich
LPS	Enzo Life Science
Lymphoprep	Stem Cell Tech
Lys-C	Promega
Mayers haematoxylin	Sigma-Aldrich
Methanol	The British Drug Houses (BDH)
Milk powder	Tesco
Mountant	Fisher-Scientific
NaCl	Sigma-Aldrich
Nitrocellulose membrane	Fisher-Scientific
Paraffin wax	VWR
PBS	Oxoid
Penicillin/Streptomycin	Invitrogen
Periodic acid	Sigma-Aldrich
Phosphomolybdic acid	Sigma-Aldrich
Phosphotungstic acid	Sigma-Aldrich
PMSF	Sigma-Aldrich
Porcine pancreatic elastase	Sigma-Aldrich
Prestained molecular weight marker	Invitrogen
Protease inhibitor cocktail	Roche Diagnostics
Protogel	National Diagnostics
Random primers	Invitrogen
Red blood cell lysis buffer	eBiosciences
RPMI	Gibco
Scarlet acid fuschin	Sigma-Aldrich
Schiff reagent	Sigma-Aldrich
SDS	Sigma-Aldrich
Sodium deoxycholate	Sigma-Aldrich
Sodium orthovanidate	Sigma-Aldrich
Sulphuric acid	Sigma-Aldrich
TEMED	Sigma-Aldrich
TGFβ	eBiosciences

Thiourea	Sigma-Aldrich
TMB	Sigma-Aldrich
TNFα	R&D
Trifluoroacetic acid	Sigma-Aldrich
Tris-base	Sigma-Aldrich
Tris-Cl	Sigma-Aldrich
Tris-HCl	Sigma-Aldrich
Trizol	Ambion
Trypan blue	Thermofisher
Trypsin	Promega
Tween-20	Sigma-Aldrich
Urea	Sigma
Xylene	Sigma-Aldrich
ZVAD	Selleckchem
Zymosan	Invivogen
β-mercaptoethanol	Gibco

2.1.2 Kits

Kit	**Supplier**
MACS Neutrophil Isolation kit	Miltneyi Biotec
In Situ Cell Death Detection kit	Roche
Fox P3 staining kit	ThermoFisher
Ready2Prep CleanUp kit	Bio-Rad
SensiMix SYBR No-ROX kit	Bioline
Murine IL-1β Duoset ELISA kit	R&D
Murine IL-6 Duoset ELISA kit	R&D
Murine TNFα Duoset ELISA kit	R&D
Murine CXCL1/KC Duoset ELISA kit	R&D
Murine CXCL2/MIP-2 Duoset ELISA kit	R&D
Murine IL-4 Duoset ELISA kit	R&D
Murine IL-33 Duoset ELISA kit	R&D
Murine IL-13 Duoset ELISA kit	R&D
Murine IL-17 Duoset ELISA kit	R&D
Murine IFNγ Duoset ELISA kit	R&D
Murine TGFβ Duoset ELISA kit	R&D

2.1.3 Antibodies

2.1.3.1 Antibodies for immunoblotting

Primary Antibody	Supplier	Dilution	Secondary*
ASC	Santa Cruz	1:200	Mouse
Caspase-1 p20	Adipogen	1:1000	Mouse
IL-1β	Adipogen	1:1000	Goat
NLRP3	Adipogen	1:1000	Mouse
P-MLKL	Abcam	1:1000	Rabbit
RIP3	Cell Signalling	1:1000	Rabbit
Vimentin	Cell Signalling	1:1000	Rabbit
βactin	Sigma-Aldrich	1:5000	Mouse

* All secondary antibodies used at dilution of 1:5000.

2.1.3.2 Flow cytometry antibodies

All flow cytometry antibodies were purchased from eBiosciences except for FoxP3 which was part of a kit from ThermoFisher. Fc block was purchased from BD Biosciences.

2.1.4 Real-time PCR primer sequences

Target gene	Sense primer sequence 5'-3' Anti-sense primer sequence 5'-3'
HPRT	AGGGATTTGAATCACGTTG TTTACTGGCAACATCAACAG
IL-1β	GGATGATGATGATAACCTGC CATGGAGAATATCACTTGTTGG
TNFα	TGCCTATGTCTCAGCCTCTT GAGGCCATTTGGGAACTTCT
CXCL1/KC	ATGATCCCAGCCACCCGCTC TTACTTGGGGACACCTTTTAGC
MMP-9	GTCTTCCTGGGCAAGCAGTA CTGGACAGAAACCCCACTTC

2.1.5 Buffers

Buffer	Composition
Blocking buffer	TBS, 0.1% (v/v) Tween-20, 5% (w/v) dried milk powder
Laemmeli sample buffer	62.5 mM Tris-HCl, pH 6.8, 10% (w/v) glycerol, 2% (w/v) SDS, 0.7 M β-mercaptoethanol, 0.001% (w/v) bromophenol blue
Ponceau Stain	0.1% (w/v) Ponceau S in 5% (v/v) acetic acid
RIPA Lysis Buffer	50 mM Tris-HCl pH 7.4, 1% (v/v) Igepal, 150 mM NaCl, 0.5% (w/v) Sodium Deoxycholate, 1 mM EDTA, 0.1% (w/v) SDS, 1 mM Na3VO4, 1 mM PMSF and protease inhibitor cocktail
TBS	25mM Tris, pH 7.4, 0.14M NaCl
SDS running buffer	25mM Tris, 192mM glycine, 0.1% SDS
FACS buffer	PBS, 2% FCS
TBST	TBS, 0.1% (v/v) Tween-20

2.2 Methods

2.2.1 Mice

Pellino2-deficient mice and Pellino3-deficient mice were generated by Taconic Artemis using proprietary technology as described previously by Humphries *et al.,* (2018) and Siednienko *et al.* (2012) respectivey.

To generate constitutive Pellino2-deficient mice, mice that were heterozygous for the targeted allele were bred with mice containing a Flpe transgene (C57BL/6J-Tg(CAC-Flpe)2Arte). This resulted in deletion of exon 2-6 and loss of function of the *Peli2* gene. The *Flpe* transgene was removed by breeding the resulting heterozygous mice with C57BL/6J mice during colony expansion. Mice were genotyped by PCR analysis of DNA isolated from ear punches using primers 'a', GCCTCTACAGGATGCTCATTT; 'b', GGACAGTCATGCTAGTCTGAGG; 'c', GAGACTCTGGCTACTCATCC; and 'd', CCTTCAGCAAGAGCTGGGGAC.

To generate constitutive Pellino3-deficient mice, mice that were heterozygous for the targeted allele were bred with mice containing Cre recombinase regulated by the Rosa26 locus (C57BL/6J Gt(ROSA)26Sortm16(Cre)Arte). This results in the deletion of exon 3 and loss of function of the *Peli3* gene by generating a frame shift in all downstream exons. The Cre transgene was removed by breeding the resulting heterozygous mice with C57BL/6 mice during colony expansion. Mice were genotyped by PCR analysis of DNA isolated from ear punches using primers 'a', CCCAACATAGGTGTTTCCTCTCC; 'b', GTGCATACACATTCATGCAAGC; 'c', GACACGTGTGGAGATAATGAGG; and 'd', ACCCAGGCACAAGTCAAGC.

2.2.2 Cell biological methods

2.2.2.1 Culture of L929 for generation of MCSF (macrophage colony stimulating factor) conditioned medium

L929 cells were cultured in complete RPMI (supplemented with 10% FCS, penicillin (100 μg/ml) and streptomycin (100 μg/ml)) at 37°C and 5% CO_2. When cells reached 80% confluency, cells were passaged using a cell scraper to lift adherent cells. The cells were seeded at 5 x 10^5 cells/ml in 40 ml RPMI in a Corning T175 culture flask for 7 days to generate MCSF. After 7 days, the media was collected and centrifuged to remove debris. The supernatant was stored at -20°C for up to 6 months for use in BMDM primary cell culture. Cells were cultured to a maximum of 25 passages to minimise genetic drift.

2.2.2.2 Bone marrow derived macrophage (BMDM) culture

Age matched mice were culled by cervical dislocation and the hind legs were removed. The legs were stripped of fur and muscle and the foot was removed. The femur and tibia were separated at the joint and the fibula was discarded. The tip of the epiphyses was cut and the bone marrow was flushed out with RPMI. Once the bones were blanched, the cell suspension was centrifuged at 250 *g* for 5 min. The supernatant was discarded and the cell pellet was resuspended in 1 ml RPMI. The cells were then split between two T75 Corning flasks in complete RPMI supplemented with 15% MCSF. The cells were cultured at 37°C for 5 days with the

media being changed on day 3. For all experiments, BMDMs were seeded at 1 x 10^6 cells/ml media overnight for experiments on the following day.

2.2.2.3 ***Neutrophil culture***

Mice were culled and bone marrow from the legs was extracted as detailed in section 2.2.2.2. The cell pellet was resuspended and the cell number was determined by staining cells with trypan blue and counting using an automated cell counter (Countess). MACs Neutrophil Isolation Kit from Miltenyi Biotec was used to isolate neutrophils from bone marrow as per manufacturers instructions. Purity of the isolated neutrophil suspension was analysed by flow cytometry using Ly6G and Cd11b antibodies. Only samples above 95% purity were used for *in vitro* neutrophil experiments. Neutrophils were seeded at 1 x 10^6 cells/ml in complete RPMI for migration and assay experiments.

2.2.2.4 ***Neutrophil migration assay***

Bone marrow derived neutrophils were seeded into the upper well of a Corning 6-well transwell plate (3 μm pores) at a concentration of 1 x 10^6 cells/ml. CXCL2 (50 ng/ml) was added to the bottom well and the plate was incubated for 3 hours at 37^{o}C 5% CO_2. Neutrophil number in the bottom chamber was quantified by staining cells with trypan blue and counting using an automated cell counter (Countess).

2.2.2.5 ***PAO-1 culture***

P. aeruginosa strain PAO-1 was taken from frozen glycerol stocks. A stab of frozen stock was streaked onto an LB agar plate and cultured at 37°C for 24 hours. A single colony was then picked from the streaked agar plate and cultured in 5 ml LB (Luria broth) at 37°C agitating overnight. The bacteria were then diluted 1:5 in LB broth and incubated at 37°C agitating for a further 2 hours. A sample of the culture was then analysed by spectrometer at 600 nm using LB broth alone as a blank.

2.2.2.6 ***In vitro PAO-1 experiments***

BMDMs were seeded overnight at 1 x 10^6 cells/ml. The complete RPMI was removed and replaced with RPMI supplemented with 10% FCS only. BMDMs were treated with 1 ml PAO-1 at OD 0.5 at 600 nm and incubated at 37°C 5% CO_2 for 1 hour. After 1 hour, the supernatant was removed from the wells. The wells were washed twice with PBS and complete RPMI was added. BMDMs were cultured for a further 3 hours. The supernatant was removed and used for ELISA analysis of cytokine production.

2.2.3 Animal experiments

2.2.3.1 ***Elastase-induced emphysema***

8-12 week old mice were weighed and then anesthetised using isoflurane gas. Mice were then administered 35 μg porcine pancreatic elastase in 50 μl PBS intranasally. A

control group was administered 50 μl PBS alone. After 24 hours mice were culled by cervical dislocation and lungs removed for analysis. To induce a full course of emphysema, the above treatments were carried out on day 1, day 3, day 6, day 8, day 10 and day 13. The mice were culled by cervical dislocation on day 14 and lungs were removed for analysis.

2.2.3.2 ***P. aeruginosa acute respiratory infection model***

12-week-old C57/B6 mice were treated with PAO-1 (absorbance of 0.05 at 600 nm) intratracheally under anaesthetic. Mice were culled 10 hours later. The lungs were removed and homogenised using a handheld homogeniser in 1 ml PBS. 500 μl was taken for cytokine analysis by ELISA. The remainder of the lung homogenate was used to determine CFU. Serial log dilutions were plated on LB agar plates, incubated at 37^{o}C overnight and CFU were counted manually.

2.2.3.3 ***P. aeruginosa respiratory infection survival model***

12-week-old C57/B6 mice were treated with PAO-1 (0.5 at 600 nm) intratracheally under anaesthetic. Mice were monitored over 48 hours and were culled upon reaching humane endpoints. Hours post inoculation at which mice were culled was noted for survival curve generation.

2.2.4 Histological analysis

2.2.4.1 ***Sample preparation***

Mice were culled by cervical dislocation and lung tissue was placed in 4% formaldehyde for 24 hours in cassettes. The cassettes were then transferred to 70% ethanol for 48-72 hours. Cassettes were then transferred to an automated tissue processor and underwent sequential dehydration steps: 70% ethanol, 80% ethanol, 95% ethanol x 2, 100% ethanol x 3, 50:50 ethanol: xylene x 1, xylene x2 for 1 hour each. Tissue was embedded in paraffin wax using Shandon Histocentre. Samples were stored at 4^{o}C. 4 μm tissue sections were cut using a microtome and floated on water at 50^{o}C to flatten tissue. Tissue was applied to slides and dried overnight. Tissue could then be stored at 4^{o}C until placed at 55^{o}C for 2 hours directly before staining.

2.2.4.2 ***Haematoxylin and eosin staining***

Slides containing fixed lung tissue sections were deparaffinised by immersion in xylene for 10 min twice. Tissue was rehydrated by immersion in 100% ethanol for 10 min, 95% ethanol for 5 min and 80% ethanol for 5 min. Slides were rinsed in distilled H_2O and placed in Harris haematoxylin solution for 3 min. Slides were rinsed in running tap water for 2 min and immersed in 1% acid-alcohol for 20 sec. Slides were rinsed in tap water and immersed in Eosin Y for 3 min. Slides were rinsed under running tap water for 5 min to remove excess dye. Tissue was dehydrated through immersion in 80% ethanol for 5 min, 90% ethanol for 5 min and 100% ethanol for 5

min. Tissue was then allowed to dry and mounted using a synthetic mounting medium before imaging.

2.2.4.3 ***Periodic acid Schiff (PAS) staining***

Slides containing fixed lung tissue were deparaffinised by immersing in xylene twice for 10 min each. Tissue was rehydrated by immersing slides in 100% ethanol for 10 min, 95% ethanol for 5 min, 80% ethanol for 5 min and immersing in distilled H_2O. Slides were oxidised in 0.5% (v/v) periodic acid solution for 5 min and then rinsed in distilled H_2O. Slides were immersed in Schiff reagent for 15 min and then washed in lukewarm tap water for 5 min. Slides were counterstained in Mayer's haematoxylin for 1 min, washed in tap water for 5 min and then dipped in 1% acid alcohol for 10-20 sec. Slides were rinsed under running water before dehydration by immersion in increasing ethanol gradients: 80%, 95%, and 100% for 5 min each. Once the slides were dry they were mounted using a synthetic mounting medium before imaging.

2.2.4.4 ***Trichrome staining***

Slides containing fixed lung tissue sections were deparaffinised by immersing in xylene twice for 10 min each. The tissue was rehydrated by immersion in 100% ethanol for 10 min, 95% ethanol for 5 min, and 80% ethanol for 5 min and rinsed in distilled H_2O. The slides were incubated overnight at room temperature in Bouins solution. Slides were rinsed in running water for 5 min. Slides were then immersed in haematoxylin solution for 5 min followed by rinsing under running water. The slides

were then immersed in scarlet acid fuschin for 5 min and rinsed in water until excess stain was removed. The slides were immersed in a solution of phosphotungstic (2.5%) and phosphomolybdic (2.5%) acid for 5 min. Slides were then immersed in analine blue solution for 5 min before being directly transferred to 1% (v/v) acetic acid for 2 min. The slides were dehydrated by immersing in 80% ethanol for 5 min, 95% ethanol for 5 min and 100% ethanol for 10 min. The slides were mounted using a synthetic mounting medium before imaging.

2.2.4.5 ***Fibrosis scoring***

An entire lobe stained with trichrome was imaged at 10x magnification. The sections were scored using the Ashcroft Scale (Hübner *et al*., 2008). Briefly images taken were compared to images by Hübner *et al*. (2008) and the features identified in those images corresponded to a score: normal=0, isolated alveolar septa with minor fibrotic changes =1, fibrotic changes of alveolar septae with knot-like formation = 2, contiguous fibrotic walls of alveolar septae = 3, single fibrotic masses = 4, confluent fibrotic masses = 5, large contiguous fibrotic masses = 6, air bubbles = 7, fibrous obliteration = 8.

2.2.4.6 ***TUNEL staining***

Slides containing fixed lung tissue sections were stained by the TUNEL method where double stranded DNA breaks are labelled with a fluorescent dye using In Situ Cell Death Detection kit from Roche as per manufacturers instructions.

2.2.5 Flow cytometry

2.2.5.1 ***Isolation of total lung cells***

Mice were culled by cervical dislocation and the lungs were homogenised in 1 ml Hanks balanced salt solution containing 1 mg/ml collagenase and 20 units/ml DNAase. The homogenised lung was incubated in solution for 1 hour at 37^{o}C. The resultant cell suspension was passed through a 70 μm cell strainer using RPMI to wash through. The cell solution was brought to a total volume of 25 ml with RPMI. The cell solution was layered over 15 ml lymphoprep and centrifuged at 2400 rpm for 25 min with acceleration of 0 and brake of 1. The cell layer produced was removed into a 15 ml tube. The cells were centrifuged at 300 g for 5 min and then washed twice with PBS and centrifugation was repeated. The cell pellet was resuspended in red blood cell lysis buffer as per manufacturers instructions. The resulting cell pellet was resuspended in FACs buffer to generate a single cell suspension for flow cytometric analysis.

2.2.5.2 ***Cell staining and analysis***

For myeloid cell identification anti- CD11b, CD11c, CD45, F4/80 and Gr-1/Ly6G were used similar to methods detailed previously (Zaynagetdinov *et al*., 2013). Two panels of antibodies were used for lymphoid cell identification, which included anti-CD3, CD4, CD8, B220, CD25 in both panels and either anti-FoxP3 or isotype control (Moorman *et al*., 2012; Spagnuolo *et al*., 2016).

Cells were blocked using Fc block (anti CD16/CD32 diluted 1:50) for 10 min at room temperature. For extracellular staining, the cell suspension was incubated with antibodies for 30 min at room temperature. For myeloid cell staining (table 2.1), the cells were then fixed in 2% paraformaldehyde (PFA). For lymphoid cell staining (table 2.2), the cells were incubated with 200 µl of FoxP3 staining kit fixation/permeabilisation buffer for 1 hour at room temperature and then stained intracellularly for Fox P3 or with an isotype control for 1 hour at 4^{o}C. The lymphoid panel samples were fixed in 2% PFA. The samples were then acquired and analysed by flow cytometry.

Table 2.1 Myeloid panel of antibodies

Antibody	Fluorochrome	Dilution
CD11b	APC	1:100
CD11c	e450	1:100
CD45	FITC	1:100
F4/80	PECy7	1:50
Gr-1/Ly6G	PE	1:100

Table 2.2 Lymphoid panel of antibodies

Antibody	Fluorochrome	Dilution
B220	APCe780	1:100
CD25	PECy5	1:100
CD3	e450	1:100
CD4	FITC	1:50
CD8	e660	1:100
FoxP3 or Isotype control	PE	1:50

2.2.5.3 ***Gating strategy***

The gating strategy used was based on experiments carried out previously (Moorman *et al*., 2012; Spagnuolo *et al*., 2016; Zaynagetdinov *et al*., 2013). An example of the gating strategy for myeloid cells is shown in figure 2.1. Neutrophils were selected as CD45+CD11b+Ly6G+, macrophage were gated as CD45+CD11b+F4/80+ and myeloid dendritic cells were gated as CD45+CD11c+ excluding neutrophils and macrophages. An example of gating strategy for lymphoid cells is shown in figure 2.2. T-cells were gated as CD3+, helper T-cells were CD3+CD4+, cytotoxic T-cells were CD3+CD8+, regulatory T-cells were CD4+CD25+FoxP3+ excluding CD4+CD25+Isotype. B-cells were CD3+B220+.

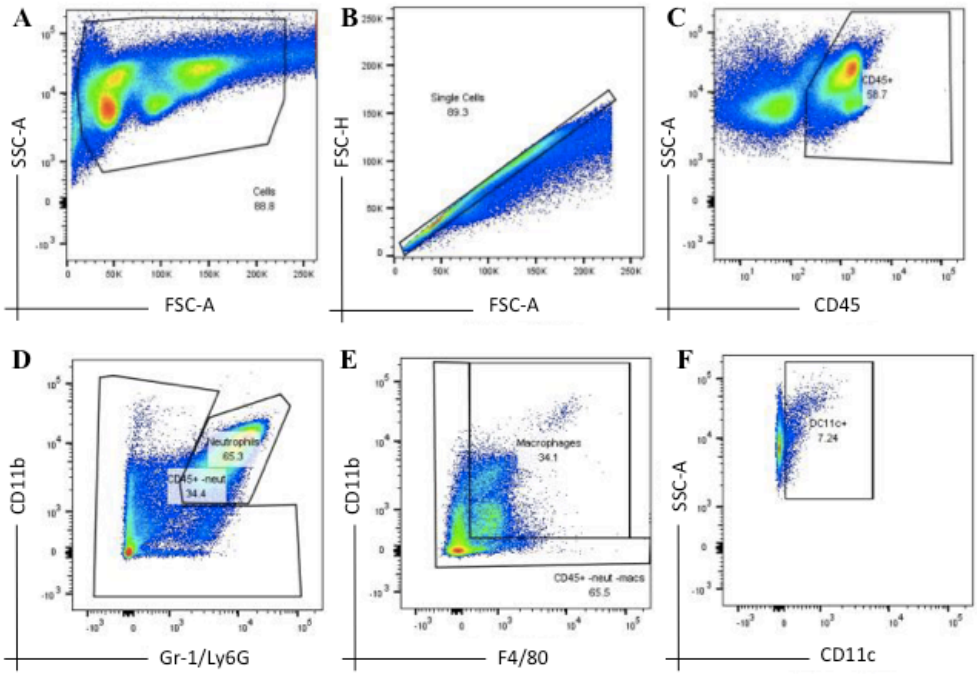

Figure 2.1 Gating strategy used for identification of neutrophils, macrophages and dendritic cells

(A) Total cells acquired by flow graphed by side scatter area (SSC-A) and forward scatter area (FSC-A). (B) Total cells are gated into single cells by graphing forward scatter height (FSC-H) against FSC-A. (C) CD45 expressing cells within the single cell population. (D) CD11b and Ly6G expressing cells within the CD45+ cell population to identify neutrophils. (E) CD11b and F4/80 expressing cells within the CD45+ cell population to identify macrophages. (F) CD11c expressing cells within the CD45+ cell population where CD11b+Ly6G+ and CD11b+F4/80+ cells have been excluded to identify dendritic cells.

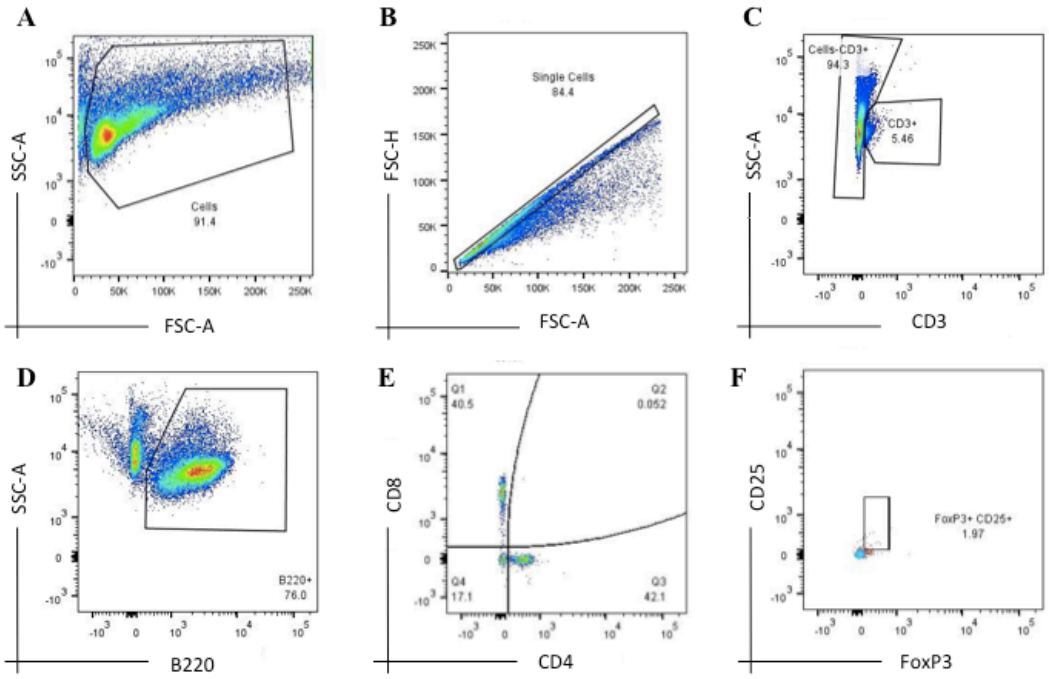

Figure 2.2 Gating strategy used for identification of helper and cytotoxic T-cells, regulatory T-cells and B-cells

(A) Total cells acquired by flow graphed by side scatter area (SSC-A) and forward scatter area (FSC-A). (B) Total cells are gated into single cells by graphing forward scatter height (FSC-H) against FSC-A. (C) CD3 expressing cells within the single cell population. (D) B220 expressing cells within the CD3+ cell population to identify B-cells. (E) CD4 and CD8 expressing cells within the CD3+ cell population to identify helper T-cells and cytotoxic T-cells respectively. (F) CD25 and FoxP3 expressing cells within the CD3+CD4+ cell population overlayed on CD25 and Isotype control positive cells within the CD3+CD4+ cell population to identify regulatory T-cells.

2.2.6 Molecular biological methods

2.2.6.1 ***Isolation of RNA***

For isolation of RNA from lung tissues, mice were culled by cervical dislocation and the left lobe was snap frozen in liquid nitrogen and stored at -80^{o}C until processing. The lobe was homogenised by sonication in 300 µl Trizol. After sonication, 700 µl Trizol was added to the tissue and RNA extraction was carried out as per manufacturer's instructions. For isolation of RNA from *in vitro* BMDM cultures, cells were seeded overnight at 1 x 10^6 cells/ml in a 12-well plate (1 ml complete RPMI per well). Cell stimulations were carried out and the supernatant was removed from the wells. RNA extraction was then carried out using Trizol as per manufacturer's instructions. RNA was quantified using Nanodrop spectrophotometer where an absorbance of 1 unit at 260 nm is ~40 µg/ml of RNA. Absorbance OD 260/280 and 260/230 values greater than 1.6 were deemed acceptable for analysis.

2.2.6.2 ***cDNA synthesis from mRNA***

0.5 µl of random primers (0.5 µg/ml) was added to 2 µg of RNA and made up to a total volume of 13 µl with DEPC-treated water. This was incubated at 72^{o}C for 5 min to allow the primers to anneal to the RNA template. 7 µl of master mix as described in table 2.3 was added to each sample.

Table 2.3 cDNA synthesis master mix

Reagent	Volume
BioScript Reverse Transcriptase (20u/µl)	0.5 µl
dNTPs (10mM)	1 µl
5x BioScript reaction buffer	4 µl
DEPC-treated water	1.5 µl

The reactions were then incubated at 42°C for 30 min followed by 5 min at 95°C to deactivate reverse transcriptase enzyme and cooled to 4°C. cDNA was stored at -20°C before analysis by real-time PCR.

*2.2.6.3 **Quantitative PCR***

cDNA generated as in section 2.2.5.2 was used as the target DNA for amplification using specific primers. Primers used for real-time PCR are detailed in section 2.1.4. The real-time PCR reaction mix is detailed in table 2.4.

Table 2.4 Real-time PCR reaction mix

Reagent	Volume
2x SensiMix™ SYBR® no-ROX	10 µl
Sense primer (4pmol/µl)	2.5 µl
Anti-sense primer (4pmol/µl)	2.5 µl
DEPC-treated water	3 µl

18 µl of the above reaction mix was added to a reaction plate and 2 µl of template cDNA was added in duplicate. The reaction was carried out in an Applied Biosystems Step one PLUS real-time PCR instrument. Samples were heated to 95^{o}C for 15 min for pre-denaturation, followed by 40 cycles of 95^{o}C for 30 sec (denaturation), 57^{o}C for 30 sec (annealing) and 72^{o}C for 45 sec (extension). Amplification of the target product was confirmed by melt curve analysis and a single melt curve peak eliminated the possibility of primer dimer formations. For melt curve analysis the samples were heated to 90^{o}C after the 40 cycles. Relative quantification of target gene mRNA expression was carried out using the crossing threshold (CT) method. The CT value is the number of cycles it takes for a pre-programmed threshold fluorescence level to be reached in the reaction well. The fewer cycles it takes for a threshold level of fluorescence to be reached, the more starting template DNA was present. To calculate delta CT, the CT value of a housekeeping gene such as HPRT was subtracted from the target gene CT value. Fold change in relative gene expression was determined by calculating $2^{-\Delta CT}$.

2.2.7 Biochemical methods

2.2.7.1 ***Western blot***

2.2.7.1.1 Sample preparation for Western blot

For Western blot analysis of lung tissue samples, homogenised protein was mixed with sample buffer. Samples were incubated at 100^{o}C for 10 min before storage at -20^{o}C until being subjected to SDS-PAGE electrophoresis.

For *in vitro* experiments, supernatants were removed from wells and cells were washed with PBS and scraped in 1 ml PBS and transferred to 1.5 ml Eppendorf tubes. The cells were centrifuged at 6,500 *g* for 10 min at 4°C. The supernatant was discarded and the cell pellet was resuspended in 90 µl lysis buffer for 20 min at 4°C with gentle agitation. Lysates were centrifuged at 10,000 *g* for 10 min at 4°C. 80 µl of the supernatant (whole cell lysate) was transferred to a fresh 1.5 ml Eppendorf tube and combined with sample buffer, incubated at 100°C for 10 min and stored at -20°C until being subjected to SDS-PAGE electrophoresis. The insoluble pellet remaining was washed with PBS and centrifuged at 10,000 *g* for 10 min. After removal of the supernatant the insoluble pellet could be treated for chemical cross-linking analysis.

2.2.7.1.2 Irreversible chemical cross-linking of insoluble protein complex

The insoluble pellets from section 2.2.6.1.1 were resuspended in 500 µl of PBS with non-cleavable protein cross-linker disuccinimydyl suberate (DSS at 4 mM). Samples were incubated with gentle agitation at room temperature for 30 min. Samples were then centrifuged at 5,000 *g* for 10 min. The cross-linked pellets were resuspended in sample buffer and incubated at 100°C for 10 min and could be stored at -20°C until being subjected to SDS-PAGE electrophoresis.

2.2.7.1.3 SDS-PAGE electrophoresis

Samples and a 10-250 kDa prestained ladder were loaded into the wells. The samples were first run through a 5% polyacrylamide stacking gel at 80 V and then at 110 V

through a 10% polyacrylamide resolving gel for 1-1.5 hours. The percentage gel and time run was chosen depending on the size of the protein being examined.

2.2.7.1.4 Immunoblotting

Following electrophoresis, protein was transferred to nitrocellulose membrane using a Hoeffman TE 70 semi-dry transfer unit. Transfer was carried out at 100 mA for 110 min. Following transfer non-specific binding was blocked by incubating the membrane with 5% milk for 30 min or 5% BSA for 30 min (when immunoblotting for phosphorylated proteins). The membrane was then washed twice for 5 min each with 1X TBST prior to incubation overnight with primary antibody in 5% milk or 5% BSA according to supplier's instruction at 4^{o}C. Optimal dilutions of primary and secondary antibodies can be seen in section 2.1.3. Membranes were washed 3 times for 5 min each in TBST before incubation with secondary antibody for 1 hour in the dark. Membranes were then washed 3 times for 10 min each with TBST. The immunoreactive bands were viewed using Odyssey infrared imaging system from Licor biosciences according to manufacturer's instructions.

2.2.7.2 ***Protein sample preparation***

Lung tissue was homogenised by sonication in RIPA buffer containing protease inhibitors, PMSF and sodium orthovanidate. The tissue was then centrifuged at 10,000 *g* for 10 min at 4^{o}C. The supernatant was used for Bradford assay to determine

protein concentration as per manufacturer's instructions. Protein was normalised to 3 μg/ml in RIPA buffer and analysed by ELISA.

2.2.7.3 ***ELISA analysis***

For analysis of *in vitro* experiments, supernatants were collected from wells and centrifuged to remove floating cells or debris. Levels of IL-1β, IL-6, IL-10, TNFα, CXCL1 (KC) and CXCL2 (MIP-2) were analysed using Duoset ELISA assays from R&D as per manufacturer's instructions.

For analysis of lung tissue homogenates, samples were prepared as in section 2.2.6.2. Levels of IL-1β, TNFα, IL-6, IL-10, IL-33, CXCL1 (KC), CXCL2 (MIP-2), RANTES, IL-4, and IL-13 were measured using Duoset ELISA kits from R&D as per manufacturer's instructions. For elastase treated tissue, samples were diluted 1 in 25 to give readings within standard range absorbance.

2.2.8 Label free LC-MS/MS analysis

2.2.8.1 ***Sample preparation***

A portion of the lung was snap frozen in liquid nitrogen and stored at -80^{o}C before use. The tissue was homogenised in lysis buffer (7 M urea, 2 M thiourea, 65 mM CHAPS, 100 mM DTT) at a ratio of a 1:10 (w/v) supplemented with protease inhibitor cocktail and DNAase, using a hand held homogeniser. Crude extracts were incubated for 2.5 hours at 4^{o}C with gentle agitation in a Thermomixer. The samples

were centrifuged at 4°C for 20 min at 14,000 *g*. The supernatant was removed and used for label-free mass spectrometry. Bradford assay was used to assess protein concentration.

2.2.8.2 ***Bradford assay***

Protein concentration in samples was assessed by Bradford assay and was carried out as per manufacturer's instructions for 96-well plate format.

2.2.8.3 ***Label-Free LC-MS/MS preparation***

Label free LC-MS/MS sample preparation was carried out as described previously (Holland *et al*., 2015). The crude homogenates were pre-treated with Ready2Prep 2D clean-up kit. The protein pellet created from the clean-up kit was re-suspended in solubilisation buffer (6 M urea, 2 M thiourea, 10 M Tris-Cl, pH 8.0 in LC-MS grade water). The samples were vortexed, sonicated and centrifuged to ensure the pellet was fully resuspended. Volumes were equalised with solubilisation buffer. The samples were reduced by incubation for 30 min with 10 mM DTT and then alkylated by incubation for 20 min in the dark with 25 mM iodoacetamide in 50 mM ammonium bicarbonate. Proteolytic digestion of samples was carried out using Lys-C at a ratio of 1:100) (protease: protein) for 4 hours at 37°C. The samples were diluted 1:5 with 50 mM ammonium bicarbonate. Further digestion was carried out using trypsin at a ratio of 1:25 (protease: protein) overnight at 37°C. The samples were diluted 3:1 (v/v) with 2% TFA in 20% ACN before vortexing and sonicating for even resuspension.

2.2.8.4 ***Label free LC-MS/MS procedure***

Label free LC-MS/MS was carried out as described previously (Holland *et al*., 2015). An Ultimate 3000 nanoLC system (Dionex) coupled to an LTQ Orbitrap XL mass spectrometer from Thermo Fisher Scientific was used for the nano LC-MS/MS analysis of lung proteins. Digested peptide mixtures (5 µl volume) were loaded onto a C18 trap column (C18 PepMap, 300 µm id × 5 mm, 5 µm particle size, 100 Å pore size; Dionex). Desalting was carried out at a flow rate of 25 µl/min in 0.1% TFA and 2% ACN for 5 min. The trap column was switched on-line with an analytical PepMap C18 column (75 µm id × 500 mm, 3 µm particle, and 100 Å pore size; Dionex). Peptides generated from lung proteins were eluted with the following binary gradients: solvent A (2% ACN and 0.1% formic acid in LC-MS grade water) and 0%–25% solvent B (80% ACN and 0.08% formic acid in LC-MS grade water) for 240 min and 25%–50% solvent B for a further 60 min. The column flow rate was set to 350 nl/min. Data was acquired with Xcalibur software, version 2.0.7 (Thermo Fisher Scientific). The MS apparatus was operated in data-dependent mode and externally calibrated. Survey MS scans were acquired in the Orbitrap in the 400–1800 m/z range with the resolution set to a value of 30,000 at m/z 400 and lock mass set to 445.120025 u. CID (collision-induced dissociation) fragmentation was carried out in the linear ion trap with up to three of the most intense ions (1+, 2+ and 3+) per scan. Within 40 sec, a dynamic exclusion window was applied. A normalised collision energy of 35%, an isolation window of 3 m/z, and one microscan were used to collect suitable tandem mass spectra.

2.2.8.5 ***Quantitative profiling by label free LC-MS/MS analysis***

Quantitative profiling by label free LC-MS/MS analysis was carried out as described previously (Holland *et al*., 2015). Progenesis label-free LC-MS software version 3.1 from Non-Linear Dynamics was used to process the raw data generated from LC-MS/MS analysis. Data alignment was based on the LC retention time of each sample, allowing for any drift in retention time given and adjusted retention time for all runs in the analysis. A reference run was established with the sample run that yielded most features (i.e. peptide ions). The retention times of all of the other runs were aligned to this reference run and peak intensities were then normalized. Prior to exporting the MS/MS output files to MASCOT (www.matrixscience.com) for protein identification, a number of criteria were used to filter the data. This data included (i) peptide features with ANOVA < 0.05 between experimental groups, (ii) mass peaks (features) with charge states of +1, +2 and +3, and (iii) greater than one isotope per peptide. A MASCOT generic file was generated from all exported MS/MS spectra from Progenesis software. The MASCOT generic file was used for peptide identification with MASCOT (version 2.2) and searched against the UniProtKB-SwissProt database with 16,638 proteins (taxonomy: Mus musculus). The following search parameters were used for protein identification: (i) MS/MS mass tolerance set at 0.5 Da; (ii) peptide mass tolerance set to 20 ppm; (iii) carbamidomethylation set as a fixed modification; (iv) up to two missed cleavages were allowed; and (v) methionine oxidation set as a variable modification. On average, 3 out of 4 peptides were identified without a missed cleavage. For further consideration and re-importation back into Progenesis LC-MS software for further analysis, only peptides with ion scores of 40 and above were chosen. The following criteria were applied to assign a

protein as differentially expressed: (i) an ANOVA score between experimental groups of ≤ 0.05, (ii) proteins with ≥ 2 peptides matched, and (iii) a MASCOT score > 40. The bioinformatics analysis of potential protein interactions was carried out with standard software programmes and applied to catalogue the clustering of molecular functions and to identify potential protein interactions of the MS-identified proteins with a changed concentration in Pellino2-deficient mice. Analyses were performed with the PANTHER (http://pantherdb.org; version 8.1) comprehensive database of protein families for the cataloguing of molecular functions.

2.2.9 Statistical analysis

Normal distribution is a probability function that describes how the values of a variable are distributed. A normal distribution refers to a symmetric distribution where most of the observations cluster around the centre/mean (McDonald, 2014). Observances near the mean are a more frequent occurrence than data far from the mean. For normal distribution 68% of observances are +/- one standard deviation from the mean, 95% are within +/- two standard deviations from the mean and 99.7% are within +/- three standard deviations from the mean. Extreme values in both tails of the distribution are similarly unlikely (McDonald, 2014).

To test if two populations of normally distributed data are significantly different, a null hypothesis and alternative hypothesis must be defined. The null hypothesis states there is no significant difference between specified populations and any observed difference is due to sampling or experimental error. The alternative hypothesis states potential or expected outcomes. In other words, the null hypothesis states that given two populations of data, the means of those two populations are equal and the

alternative hypothesis states that given two populations of data, the means of those two populations are not equal, i.e. the mean of one group sites more than two standard deviations away from the mean of the other group. Throughout the analysis in this thesis, significance is denoted as a p value or the probability an observation occurred by chance. Simply, where $p < 0.05$ there is a 95% probability that the alternative hypothesis is true and 5% probability that the differences observed are a result of chance.

Normally distributed data can be tested for significant differences by various statistical tests including Student's t-test and ANOVA (McDonald, 2014; Krzywinski and Altman, 2013). Student's t-test compares the mean of two populations and determines if they are different from one another. It also states how significant the differences are i.e. if the differences between the two populations could have occurred by chance (Krzywinski and Altman, 2013). ANOVA (Analysis of Variance) is used to compare three or more samples where more than repeated measurements have been made with a single test (McDonald, 2014). ANOVA was used to analyse data in figure 3.6.

Non-normally distributed data can also be tested for significance using Student's t-test or ANOVA but only in instances where there are over 20 observations/samples (Krzywinski and Altman, 2014). Other tests to analyse non-normal data for significance include the Mann-Whitney U test which can be used to compare two populations. In the Mann-Whitney U test the null hypothesis states that there is a probability of 50% that a randomly drawn member of the first population will exceed a member of the second population (Fagerland and Sandvik, 2009). It is a good

alterative to the t-test for non-parametric data (McDonald, 2014). Kaplan-Meier is also useful in the analysis of non-parametric data specifically in estimation of survival (Goel *et al*., 2010). The Kaplan-Meier survival curves generated in fig. 3.17 were subjected to the log-rank test (Mantel-Cox test) to test whether the difference between survival times between two groups is statistically different.

As well as being normally or non-normally distributed, data can also be paired or unpaired. Paired data can also be described as dependant data, where there are pairs of observations (Krzywinski and Altman, 2013). Unpaired data can also be described as independent data, where the observations made are not related to each other (Krzywinski and Altman, 2013). Throughout this thesis, much of the statistical analysis was carried out using a paired Student's t-test to compare the effect of treatment in wild type animals and genetically modified animals, where the genetically modified animals had a single gene knocked out as compared to the wild type animals. This analysis was used as it has been used previously in testing significance under similar experimental conditions (Humphries *et al*., 2018; Siednienko *et al*., 2012). However, as the data is not truly paired there are some limitations to this analysis. An unpaired or independent t-test had more degrees of freedom and is more likely to detect differences than a paired t-test (Xu *et al*., 2017). As such, statistical analysis in this thesis gives a lower bound estimate on statistical significance. Statistical analysis was found using Graph-Pad software by Prism.

2.2.10 Ethical approval

All procedures involving animals were performed under licenses of the Health Products Regulatory Authority (HPRA) of Ireland and the UK Home Office with all protocols being approved by Research Ethics committee of Maynooth University or Queens University Belfast.

3 Investigating the role of Pellino2 and Pellino3 in elastase-induced emphysema

3.1 Introduction

COPD is an umbrella term used to describe a group of lung diseases consisting of chronic bronchitis, chronic obstructive airway disease, chronic airflow limitation and emphysema. Patients with COPD will also have systemic inflammation where inflammation in the lungs is accompanied by inflammation of the heart, blood vessels and skeletal muscle (Chung and Adcock, 2008). Emphysema is an important pathology of COPD that is characterised by alveolar destruction and inflammation. Emphysema is typically associated with inhalation of smoke or an inherited deficiency in alpha-1 anti-trypsin that leads to an imbalance of proteases and anti-proteases in the lungs (Barnes *et al*., 2015). Neutrophils are a key element for the destruction of tissue in emphysema. Neutrophils are recruited and activated in response to cigarette smoke (Hoonhorst *et al*., 2014; van der Vaart, 2004). Upon activation, neutrophils release various proteases such as cathepsin G and elastase

(Pandey *et al*., 2017). These proteases are thought to accelerate the breakdown of alveolar walls and lead to the increased airspace seen in emphysema (Guyot *et al*., 2014). Neutrophils also contribute to the high levels of inflammatory cytokines seen in emphysema (Mortaz *et al*., 2010). To study emphysema, the disease has been modelled in mice by administration of proteases into the lungs.

Briefly, mice are given elastase in solution either intranasally or intratracheally to induce an inflammatory response and alveolar destruction in the lungs to mimic the symptoms of emphysema. Pro-inflammatory cytokines such as IL-1β TNFα and IL-6 and chemokines such as CXCL1 (KC) are produced in response to elastase administration from an early time point (Couillin *et al*., 2009; Lucey *et al*., 2002). Macrophages, dendritic cells and neutrophils are recruited and initiate further inflammatory signalling which leads to further destruction of the lung tissue. Activation of neutrophils leads to further protease production and accelerated destruction of lung tissue (Guyot *et al*., 2014).

Inflammatory mediators have previously been implicated not only in the development of inflammation but also in alveolar destruction using a single dose of elastase to induce emphysema. The NLRP3 inflammasome is important in the inflammatory response during elastase-induced emphysema (Couillin *et al*., 2009). *In vivo* studies using ASC-deficient mice showed a diminished inflammatory response to intranasal elastase, with significantly lower levels of pro-inflammatory cytokines being produced than in wild type mice (Couillin *et al*., 2009). As elastase administration in this study was associated with increased uric acid concentration in the lung, it was suggested that IL-1β production in response to elastase is mediated by the NLRP3

inflammasome. Couilin *et al*. (2009) also used IL-1R-deficient and MyD88-deficient mice to show that IL-1R signalling and MyD88 signalling is required for inflammation and alveoli destruction in response to intranasal elastase. Mice lacking IL-1R or MyD88 or mice treated with an IL-1R antagonist, developed less severe emphysema than wild type mice in response to a single dose of intranasal elastase and had a diminished pro-inflammatory profile.

Inflammasomes are also an important part of the defence against invading pathogens. Widespread activation of inflammasomes is seen in response to microbial infection. *Salmonella typhimirium* is an intracellular bacterium that can trigger NLRC4 and NLRP3 inflammasome activation through multiple motifs (Man *et al*., 2014). *Legionella pneumophila,* the pathogen responsible for Legionnaire's disease in humans, can trigger activation of NLRC4 (Cerqueira *et al*., 2015). *Mycobacterium tuberculosis* triggers activation of NLRP3 (Dorhoi *et al*., 2011). *Listeria monocytogenes* and *Fransicella tularensis* can activate AIM2 inflammasome (Rathinam *et al*., 2010). *Bacillus anthracis* can activate NLRP1 inflammasome (Levinsohn *et al*., 2012). The inflammasome function in this context is to promote host survival and bacterial clearance through the secretion of IL-1β and pyroptosis.

P. aeruginosa was used in the present study to explore the role of Pellino2 in the immune response to respiratory infection as it is known to activate the NLRP3 inflammasome (Deng *et al*., 2015). *P. aeruginosa* is a gram negative bacterial pathogen that can form biofilms (Wei and Ma, 2013). The innate immune response is crucial for the defence against *P. aeruginosa* infection. *P. aeruginosa* PAMPs can activate TLR2, TLR4 and TLR5 (Skerrett *et al*., 2007). Studies in MyD88-deficient

mice have shown that MyD88-dependant pathways are required to mount an inflammatory response to *P. aeruginosa* infection (Mijares *et al*., 2011). During respiratory infection with *P. aeruginosa*, the signalling pathways activated by epithelial cells and alveolar macrophages initiate a pro-inflammatory cytokine and chemokine cascade leading to the infiltration of phagocytes to clear the infection (Mijares *et al*. 2011). The immune response must be appropriate in response to *P. aeruginosa* infection. Studies have shown that a lack of phagocytic cells during *P. aeruginosa* respiratory infection leads to increased mortality. For example neutropenic mice will succumb to fatal lung infection following a low initial dose of bacteria (Koh *et al*., 2009). Further to this point, the absence of CXCL1 and CXCL2 impairs the ability of murine hosts to control *P. aeruginosa* replication as these chemokines are crucial for attracting immune cells to control the infection. (Bryant-Hudson and Carr, 2012). Conversely, inflammation particularly as the result of IL-1β production can be detrimental to the host. It has been shown that where IL-1β production was inhibited in alveolar macrophages through inhibition of the NLRC4 inflammasome, there was improved bacterial clearance (Cohen and Prince, 2013). This has also been demonstrated where the NLRP3 inflammasome was inhibited. NLRP3-deficient mice challenged with respiratory *P. aeruginosa* infection have lower bacterial load in the days following infection (Iannitti *et al*., 2016). IL-1β is also detected in the BAL of cystic fibrosis patients with *P. aeruginosa* infection (Bonfield *et al*., 1995; Hartl *et al*., 2012) and clearance of *P. aeruginosa* following antibiotic treatment in children is also associated with a reduction in IL-1β (Douglas *et al*., 2009).

Given the NLRP3 inflammasome is capable of responding to PAMPs and DAMPs and producing beneficial and damaging effects, there has been much interest in exploring the mechanistic basis to its activation. Activation of the NLRP3 inflammasome requires an initial priming signal and a second activating signal. These can occur sequentially or concurrently (Lin *et al*., 2014). The priming signal involves activation of NFκB-dependant pathways such as TLRs, TNFR, IL-1R or NOD2 for example by Gram negative bacteria or LPS *in vitro* (Bauernfeind *et al*., 2009). Priming increases levels of NLRP3 and induces pro-IL-β and pro-IL-18. The second signal is required for inflammasome formation and cleavage of caspase-1 into its bioactive form. The second signal can be a range of stimulus such extracellular ATP or pore forming toxins such as nigericin (Mariathasan *et al*., 2006). The second signal induces K^+ influx and intracellular Ca^{2+} signalling. (Surprenant *et al*. 1996; Rassendren *et al*. 1996; Trueblood *et al*. 2011; Chu *et al*. 2009). Caspase-1 cleaves IL-1β and IL-18 into their active forms and they are released from the cell. The priming signal was initially thought to simply cause upregulation of NLRP3 and pro-IL-1β but it has since been shown that the NLRP3 inflammasome responds quickly and caspase-1 activation can occur without new protein translation (Juliana *et al*., 2012; Schroder *et al*., 2012). It is now thought the main function of the priming signal is induction of posttranslational modifications of inflammasome components (Yang *et al*., 2017).

An important posttranslational modification that has been extensively studied in relation to the NLRP3 inflammasome is ubiquitination. E3 ubiquitin ligases such as TRIM31 (tripartite motif containing 31), FBXL2 (F-box and leucine rich repeat protein 2), MARCH7 (membrane associated ring-CH-type finger 7) and BRCC3

(BRCA1/BRCA2-containing complex subunit 3) regulate NLRP3 inflammasome activity. TRIM31, FBXL2 and MARCH7 catalyse the attachment of K48 linked polyubiquitin chains to NLRP3 and target it for degradation by the proteasome (Han *et al*., 2015; Song *et al*., 2016; Yan *et al*., 2015). BRCC3 mediates NLRP3 deubiquitination which is critical for inflammasome activation (Py *et al*., 2013). Recently, our group has shown that Pellino2, can also regulate NLRP3 inflammasome activity (Humphries *et al*., 2018). This study used Pellino2-deficient mice to demonstrate that Pellino2 promotes K63 linked ubiquitination of NLRP3 during priming. This ubiquitination step is crucial for activation of the NLRP3 inflammasome and required for mature IL-1β production. A direct interaction between Pellino2 and NLRP3 was not demonstrated, but it was shown that IRAK1 can negatively regulate ubiquitination of NLRP3 inflammasome signalling (Fernandes-Alnemri *et al*., 2013; Lin *et al*., 2014). Pellino2 was shown to ubiquitinate IRAK1 and prevent its interaction with NLRP3 (Humphries *et al*., 2018).

The activation of the NLRP3 inflammasome requires tight regulation since its dysregulation has been implicated in an array of diseases. Gain of function mutations in NLRP3 are associated with cryopyrin associated periodic syndromes (CAPS) and includes Muckle Wells syndrome, familial cold auto inflammatory syndrome and neonatal onset multisystem inflammatory disease (Aksentijevich *et al*., 2002; Hoffman *et al*., 2001). NLRP3 inflammasome dysregulation has also been well documented in other diseases including cardiovascular disease, diabetes, obesity-induced inflammation and insulin resistance and Alzheimer's disease (Grant and Dixit, 2013; Heneka *et al*., 2013; Liu *et al*., 2017; Vandanmagsar *et al*., 2011). This highlights the importance of tight regulation of the NLRP3 inflammasome, however

there are other mechanisms of IL-1β production that are independent to the inflammasomes.

Our research group has shown that Pellino3 can regulate IL-1β by regulation of HIF-1α induced expression of IL-1β (Yang *et al*., 2014). Obesity induces low-level inflammation. IL-1β is a key pro-inflammatory cytokine involved in obesity driven inflammation and promotes insulin resistance (Xu *et al*., 2003). Pellino3 was found to be reduced in adipose tissue from obese subjects and mice fed a high-fat diet. Pellino3-deficient mice also have exacerbated insulin resistance in response to a high-fat diet. It was found that Pellino3 negatively regulates TRAF6 ubiquitination and stabilisation of HIF-1α. As HIF-1α is not stabilised, there is less HIF-1α induced expression of IL-1β (Yang *et al*., 2014). Therefore, Pellino3 is a critical regulator in a new mechanism of IL-1β expression.

As Pellino2 has been shown to regulate IL-1β production by the NLRP3 inflammasome (Humphries *et al*. 2018) and the NLRP3 inflammasome has been implicated in a murine model of emphysema (Couillin *et al.,* 2009) and in responding to respiratory infection (Iannitti *et al.,* 2016), the role of Pellino2 in elastase-induced emphysema and in the inflammatory response to *P. aeruginosa* infection was examined. We were also keen to evaluate the specificity of any role for Pellino2 in respiratory inflammation by studying the role of another Pellino family member, Pellino3.

3.2 Results

3.2.1 Pellino2 deficiency results in a diminished primary inflammatory response to intranasal elastase treatment

The initial study aimed to explore the role of Pellino2 in regulating the expression of pro-inflammatory cytokines in the lungs of mice challenged with elastase. To this end the expression levels of pro-inflammatory cytokines IL-1β, TNFα, IL-6, CXCL1/KC and IL-33 were measured in lung samples from wild type and Pellino2-deficient mice that had been challenged overnight with elastase. Elastase induced the expression of IL-1β (fig. 3.1A), IL-6 (fig. 3.1B), TNFα (fig. 4.1C), CXCL1/KC (fig. 3.1D) and IL-33 (fig. 3.1E) in the lungs of wild type mice. However, the expression levels of IL-1β (fig. 3.1A), IL-6 (fig. 3.1B), TNFα (fig. 3.1C), CXCL1/KC (fig. 3.1D) and IL-33 (fig. 3.1E) were significantly reduced in the lungs of Pellino2-deficient mice following elastase treatment when compared with wild type mice. IL-33 also appears to be expressed at higher basal level in the lungs of wild type mice compared with Pellino2-deficient mice (fig. 3.1E).

It has been previously demonstrated that TGFβ can have anti-inflammatory effects on TLR signalling through crosstalk between the two signalling pathways. This crosstalk is mediated in part by Pellino1 (Choi *et al*., 2006). Excessive amounts of TGFβ or over-active signalling is also associated with fibrosis in many tissues including the lungs (Warburton, 2012). Where components of the TGFβ signalling pathway are inactivated, mice are protected against bleomycin induced lung fibrosis (Zhao *et al*., 2002). As such, it was next examined if Pellino2 played a role in regulation of TGFβ

expression in mice in response to elastase (fig. 3.1F). TGFβ is a cytokine that is synthesised in precursor or latent form and activated extracellularly by a variety of proteases (Robertson *et al*., 2015). The lung homogenate was therefore activated by heat to assess the expression of active TGFβ. Overnight elastase treatment led to expression of TGFβ to similarly high levels in the lungs of wild type and Pellino2-deficient mice (fig. 3.1F).

We next explored the role of Pellino2 in regulating the expression of type 2 cytokines. Type 2 cytokines are produced during a Th2 immune response by type 2 CD4+ T helper cells (Y. Zhang *et al*., 2014). This cell type typically responds to helminths and extracellular parasites (Artis and Spits, 2015). Type 2 cytokines promote IgE and eosinophilic responses and anti-inflammatory responses (Z. Chen *et al*., 2016). The type 2 cytokines examined here are IL-4 and IL-13. IL-4 is important for the initiation of Th2 inflammatory responses and IL-13 is a major mediator of remodelling during Th2 diseases (Richter *et al*., 2001; Saito *et al*., 2003). Both IL-4 and IL-13 are also involved in airway remodelling (Leigh *et al*., 2004). To examine if the low levels of pro-inflammatory cytokines seen in Pellino2-deficient mice in response to elastase was the result of a strong Th2 response, the levels of IL-4 and IL-13 were assessed at the protein level. Overnight treatment with elastase did not induce IL-4 (fig. 3.2A) or IL-13 (fig. 3.2B) beyond basal levels in the lungs of wild type or Pellino2-deficient mice.

We next examined the role of Pellino2 in regulating type 17 immune response. These are responses initiated by T helper 17 cells such as the production of IL-17 and IFNγ (Guglani and Khader, 2010). The isoform of IL-17 examined here was IL-17A. IL-

17A is important in protecting the body from extracellular bacteria and fungi particularly on mucosal barriers (Bayes *et al*., 2016; K. Chen *et al*., 2016; Conti *et al*., 2014). IL-17A regulated cytokines such as IL-22 are important in regulation of epithelial cell repair and regeneration after inflammatory insults (Aujla *et al*., 2008). However, overexpression or aberrant expression of IL-17 can also be detrimental and can lead to pulmonary fibrosis (Chen *et al*., 2014; Kang *et al*., 2012). IFNγ has been shown to inhibit macrophage, lymphocyte and eosinophil accumulation and can stimulate alveolar destruction in a model of emphysema in mice (Kang *et al*., 2012). It has also been shown that treatment of mice intratracheally with IFNγ alone will induce emphysema (Wang *et al*., 2000). Given the previously reported roles for IL-17A and IFNγ in the immune response of the lung, we examined the role of Pellino2 in regulating the expression of IL-17A and IFNγ in the context of elastase-induced inflammation. IL-17A was not increased beyond basal levels in response to overnight elastase treatment in the lungs of wild type or Pellino2-deficient mice (fig. 3.2C). Wild type mice had a higher level of basal expression of IFNγ which was reduced in response to overnight elastase treatment (fig. 3.2D). IFNγ was not induced in the lungs of Pellino2-deficient mice in response to overnight elastase treatment (fig. 3.2D).

We next addressed if the suppressive effects on pro-inflammatory cytokine expression was also observed at the transcriptional level. Samples were examined by quantitative RT-PCR for expression levels of mRNA encoding IL-1β, TNFα and CXCL1/KC. Overnight elastase treatment resulted in high levels of *Il1b* (fig. 3.3A), *Tnfα* (fig. 3.3B) and *Cxcl1* (fig. 3.3C) mRNA in the lungs of wild type mice. There were lower levels of mRNA for *Il1b* (fig. 3.3A), *Tnfα* (fig. 3.3B) and *Cxcl1* (fig. 3.3C) in

Pellino2-deficient mice treated with elastase when compared with wild type mice. However, the difference observed was not as striking as for pro-inflammatory cytokine expression at protein level.

We next examined if Pellino2 played a role in regulation of MMP-9 expression at mRNA level. MMP-9 is a protease produced mainly by macrophages (Atkinson and Senior, 2003; Mecham *et al*., 1997). It has long been known that MMP-9 is upregulated in the lungs of patients with COPD and emphysema (Atkinson and Senior, 2003; Betsuyaku *et al*., 1999). Other evidence also suggests MMP-9 is directly involved in development of emphysema. Mice that do not express MMP-9 are protected from emphysema induced by LPS or cigarette smoke (Atkinson *et al*., 2011; Brass *et al*., 2008). Overexpression of MMP-9 in adult mice also leads to spontaneous emphysema development (Foronjy *et al*., 2008). Recent evidence however suggests that MMP-9 may not contribute to alveolar destruction by degradation of elastic fibres (Atkinson *et al*., 2011), instead it is suggested that MMP-9 may be involved in the development small airway thickening seen in COPD (McGarry Houghton, 2015). Overnight elastase treatment led to induction of *Mmp-9* mRNA in the lungs of wild type mice but not in Pellino2-deficient mice (fig. 3.4).

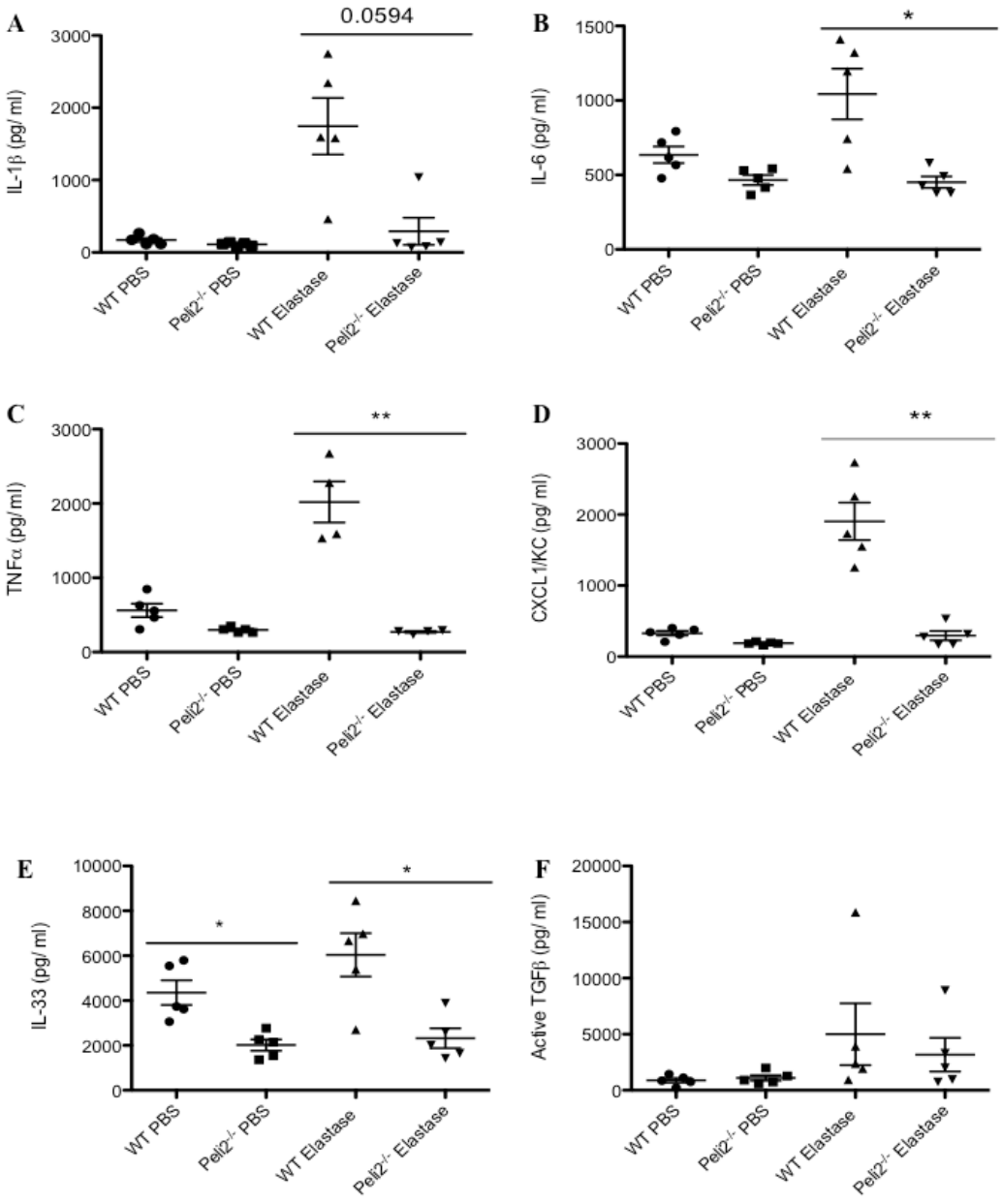

Figure 3.1 Pellino2 deficiency results in a reduced level of pro-inflammatory cytokines but not TGFβ in response to intranasal elastase treatment

Wild type and Pellino2-deficient mice were treated intranasally with 35μg elastase in 50μl PBS or 50μl PBS alone and culled 24 hours later. The lungs were removed and the left lobe was homogenized in RIPA buffer. Lung homogenates were analysed by ELISA for (A) IL-1β, (B) IL-6, (C) TNFα (D) CXCL1, (E) IL-33 and (F) active TGFβ. *$p < 0.005$, **$p < 0.001$ (paired, two-tailed Student's t-test). Each point represents data from a single mouse. Error bars, s.e.m.

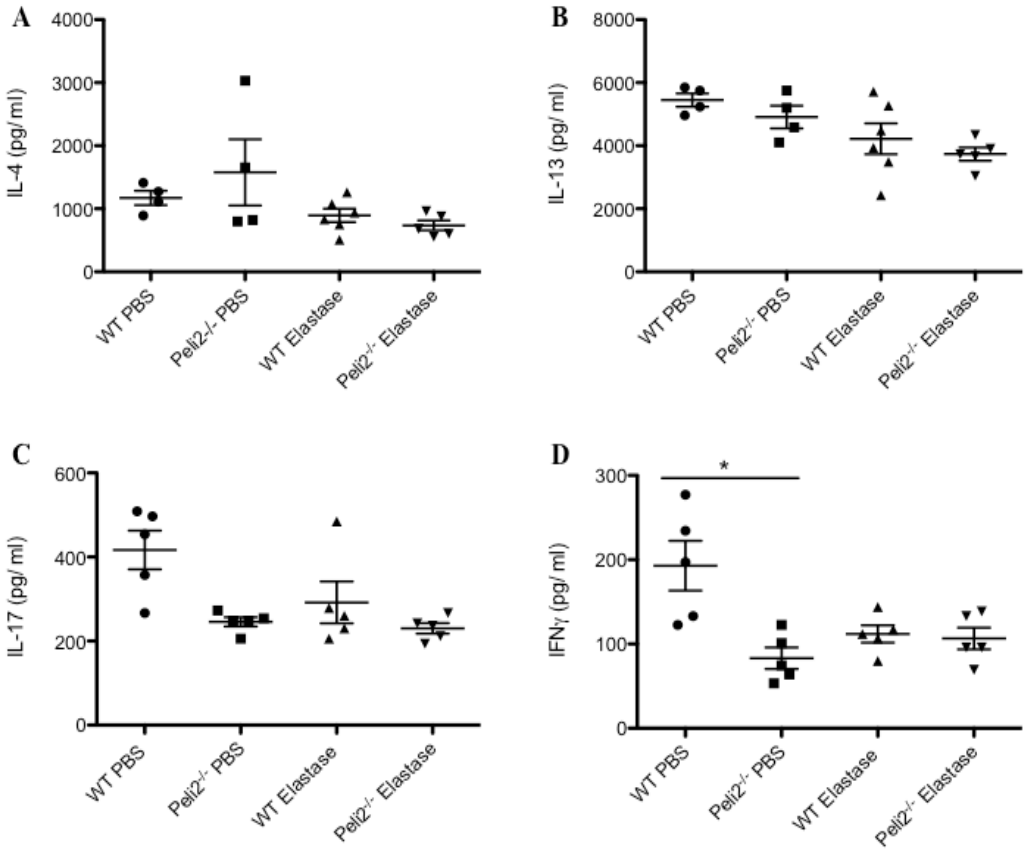

Figure 3.2 Pellino2 deficiency does not alter induction of type 2 or type 17 cytokines in response to intranasal elastase treatment

Wild type and Pellino2-deficient mice were treated intranasally with 35μg elastase in 50μl PBS or 50μl PBS alone and culled 24 hours later. The lungs were removed and the left lobe was homogenized in RIPA buffer. Lung homogenates were analysed by ELISA for type 2 cytokines, (A) IL-4 and (B) IL-13, and type 17 cytokines, (C) IL-17 and (D) IFNγ. *p < 0.005, **p < 0.001 (paired, two-tailed Student's t-test). Each point represents data from a single mouse. Error bars, s.e.m.

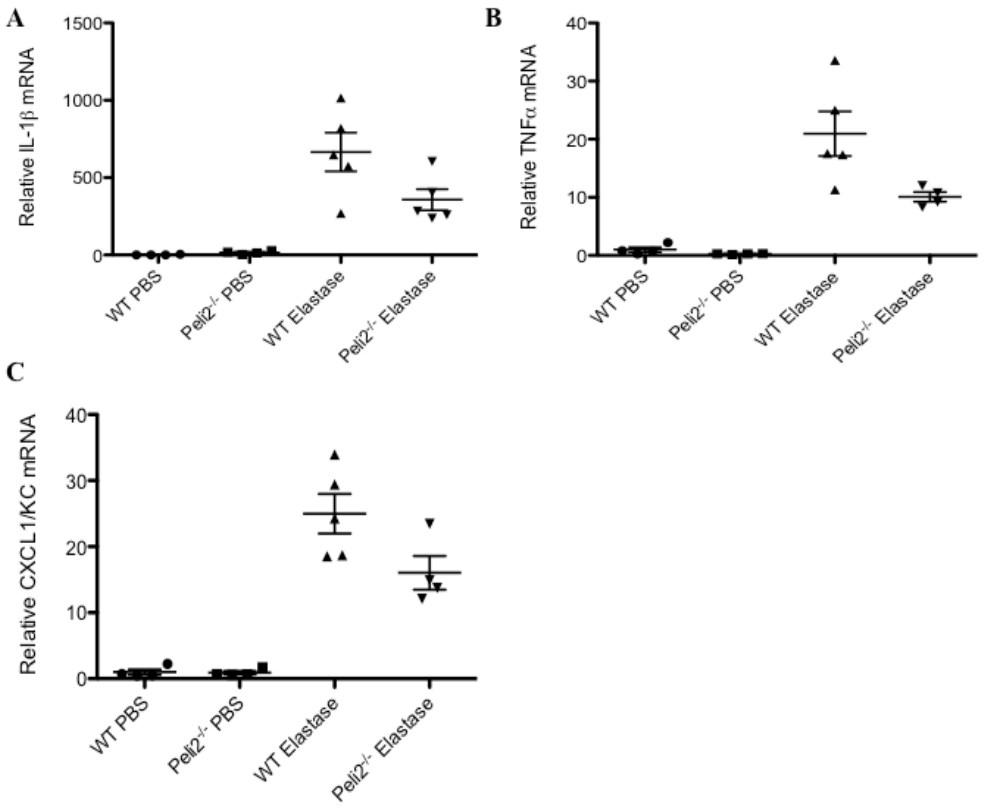

Figure 3.3 Pellino2 deficiency results in reduced expression of genes encoding IL-1β, TNFα and CXCL1 in response to intranasal elastase treatment

Wild type and Pellino2-deficient mice were treated intranasally with 35μg elastase in 50μl PBS or 50μl PBS alone and culled 24 hours later. The lungs were removed and the right lobe was homogenized in Trizol. RNA extraction and cDNA generation were carried out and samples were analysed by quantitative RT-PCR for mRNA expression of (A) *Il*-1b, (B) *Tnfa* and (C) *Cxcl1* relative to HPRT. Each data point represents a single mouse. Significance tested by paired, two-tailed Student's t test. Error bars, s.e.m.

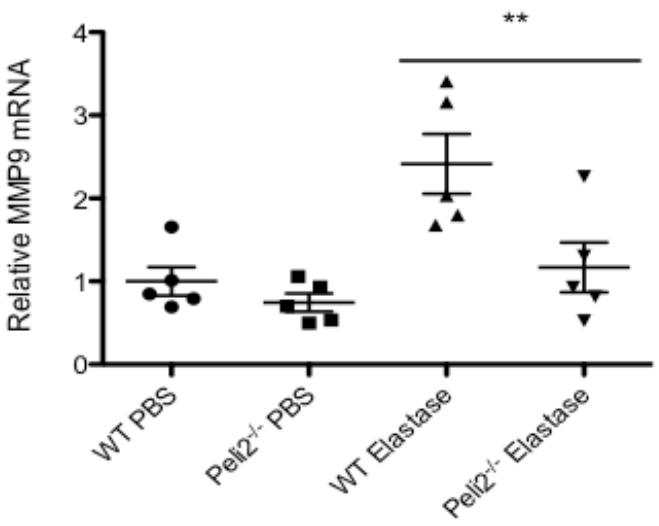

Figure 3.4 Pellino2 deficiency results in a diminished expression of genes encoding for MMP-9 in response to intranasal elastase treatment

Wild type and Pellino2-deficient mice were treated intranasally with 35μg elastase in 50μl PBS or 50μl PBS alone and culled 24 hours later. The lungs were removed and the right lobe was homogenized in Trizol. RNA extraction and cDNA generation were carried out and samples were analysed by real time PCR for mRNA expression of *Mmp9* relative to HPRT. $^{**}p < 0.001$ (paired, two-tailed Student's t-test). Each point represents a single mouse. Error bars, s.e.m.

3.2.2 Pellino2 deficiency results in altered pathology during elastase-induced emphysema

Given that Pellino2-deficient mice showed reduced responsiveness to elastase in the context of pro-inflammatory cytokine expression, we were keen to study the pathophysiological relevance of these effects. To this end, we performed a more chronic study where wild type and Pellino2-deficient mice were treated with elastase every 2-3 days for 14 days and pathology was assessed by studying alveolar destruction and increase in lung airspace.

The structure of the lungs of wild type and Pellino2-deficient mice was similar when treated with intranasal PBS alone (fig. 3.5A). Alveolar destruction occurred in both wild type and Pellino2-deficient mice when treated with intranasal elastase. However, distinct thickened areas of tissue were apparent in Pellino2-deficient mice, which is not typical of elastase-induced emphysema. To determine the relative quantity of airspace the mean linear intercept of these lung sections was calculated. Mean linear intercept is the number of times a chord drawn across a lung section intercepts with a piece of tissue. A lower mean linear intercept tends to reflect greater alveoli breakdown. Mean liner intercept calculations from the lung sections showed little difference between alveoli number in wild type and Pellino2-deficient mice following repeated elastase instillation (fig. 3.5B). This may be due to heavily thickened areas and areas with lots of airspace being counted as a single intersection. As a result of this, mean linear intersect may not accurately represent the difference in phenotype observed between wild type and Pellino2-deficient mouse lungs. A suggested

improvement on the analysis may be to carry out histological scoring as demonstrated in Oliveira *et al.* (2016), although this was not carried out in this instance.

The histological results showed a consistent thickening throughout the lung in Pellino2-deficient mice that was not seen in wild type mice and suggests a regulatory role for Pellino2 in progression of elastase-induced emphysema.

To examine if elastase-induced emphysema had systemic effects on the mice, weight change of wild type and Pellino2-deficient mice when treated with repeated doses of intranasal PBS or elastase over 14 days was recorded (fig. 3.6). Wild type and Pellino2-deficient mice treated with intranasal PBS continued to gain weight over 14 days, with an approximate increase of 2-3% on their starting weight. Both wild type and Pellino2-deficient mice treated with intranasal elastase lost weight during the course of the study. At day 3, wild type mice had lost approximately 5% of their starting body weight while Pellino2-deficient mice had lost approximately 10% of their starting body weight. For both wild type and Pellino2-deficient mice, there was some recovery of weight lost. By day 14, wild type mice had returned to their starting weight but had not gained weight to a normal level, as demonstrated by PBS treated mice. Pellino2-deficient mice did not recover to their starting weight. At day 14, Pellino2-deficient mice weighed 5% less than their starting body weight. This suggests that Pellino2 deficiency is associated with a more severe form of elastase-induced emphysema where the disease model has systemic manifestations.

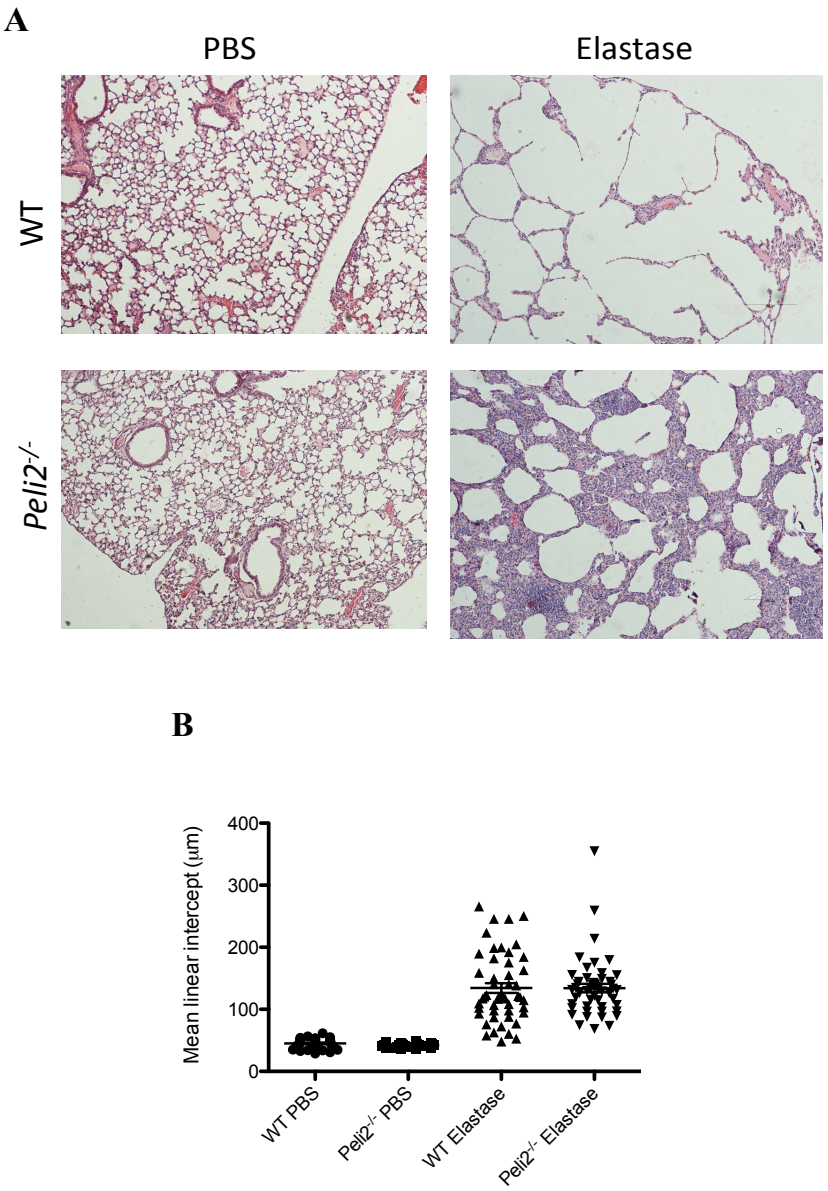

Figure 3.5 Pellino2 deficiency results in altered pathology of elastase-induced emphysema

Wild type and Pellino2-deficient mice were treated intranasally with either 35µg elastase in 50 µl PBS or 50 µl PBS alone every 2-3 days over 14 days. At day 14, mice were culled and the lungs were removed and fixed in formalin and paraffin embedded. (A) 4µm sections of the lungs were cut and stained with H&E. An entire lobe of each lung was imaged at 10x magnification. (B) Average mean linear intercept was calculated for each mouse using ImageJ. Significance tested using paired, two-tailed Student's t-test. Error bars, s.e.m.

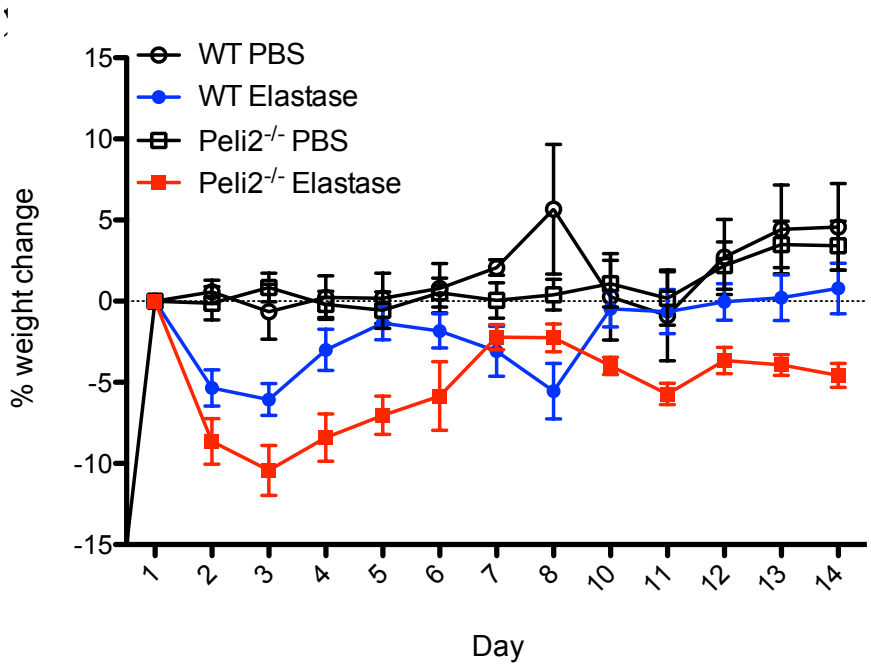

Figure 3.6 Pellino2 deficiency results in enhanced weight loss during elastase-induced emphysema

Wild type and Pellino2-deficient mice were treated intranasally with either 35μg elastase in 50 μl PBS or 50 μl PBS alone every 2-3 days over 14 days. Mice were weighed everyday and their percentage weight loss/weight gain from starting weight was calculated. Significance tested between wild type and Pellino2-deficient mice elastase treated groups using ANOVA. $p = 0.0006$. Error bars, s.e.m.

3.2.3 Pellino2 deficiency results in greater levels of fibrosis in response to elastase-induced emphysema

We next attempted to understand the basis of the histological differences between the lung tissue of wild type and Pellino2-deficient mice treated repeatedly with elastase. Given the apparent tissue thickening in Pellino2-deficient mice, trichrome staining was used to visualise areas of fibrosis in lung tissue samples and immunoblotting was used to quantify protein levels of a marker of fibrosis. Trichrome staining allows the observation of fibrotic regions by differentiating tissue components. Masson's trichrome stain was used. In this method, the three stains used are Weigert's iron haematoxylin, scarlet acid fuschin and analine blue. Nuclei stain a dark purple colour, cytoplasm is stained red and collagen (or areas of fibrosis) is stained blue.

Trichrome staining showed more frequent and larger areas of collagen deposition in Pellino2-deficient mice during elastase-induced emphysema (fig. 3.7A). This staining was typically in areas surrounding bronchioles where the tissue had become thickened. This level of collagen deposition was not apparent in the wild type mice. Areas that were stained positively in wild type lung samples were confined to small rings around bronchioles. The level of fibrosis was quantified using the Ashcroft scale as detailed previously (Ashcroft *et al*., 1988; Hübner *et al*., 2008). Briefly, sections of the lung were compared with a predetermined set of images of lungs in various stages of fibrosis with a specific score. Briefly, a higher fibrosis score relates to more severe fibrosis. For example, a score of 0 indicates a normal lung; a score of 1 indicates isolated alveolar septae with minor fibrotic changes up to a score of 8 indicating fibrotic obliteration. Pellino2-deficient mice had a higher score for fibrosis than wild

type mice following elastase-induced emphysema (fig. 3.7B). Although statistically significant, the difference observed in fibrosis score between wild type and Pellino2-deficient mice is small, with an average score of 3 for wild type mice treated with elastase and an average score of 4 for Pellino2-deficient mice. According to Hübner *et al.* (2008), a score of 3 describes fibrosis consistent with the alveolar septae whereas a score of 4 corresponds to the presence of fibrotic masses. To definitively test if this modest increase in fibrosis score affects lung function, it may be of benefit to carry out some pulmonary function tests in future.

Immunoblotting was also used to quantify levels of fibrosis. Here, the right lobe of the lung was homogenised in lysis buffer and analysed by western blotting with an anti-vimentin antibody. Vimentin is a protein that is deposited during fibrosis, which is associated with the repair process (Rogel *et al.*, 2011). Expression of vimentin is increased as epithelial cells that are damaged and undergoing epithelial-mesenchymal transition (Kalluri and Neilson, 2003). The finding of higher levels of fibrosis in Pellino2-deficient mice was further supported by immunoblot results showing higher levels of vimentin in the lungs of elastase challenged Pellino2-deficient mice relative to elastase challenged wild type mice (fig. 3.8). These various and independent indices of fibrosis are all consistent with augmented fibrosis during elastase-induced emphysema when Pellino 2 is absent.

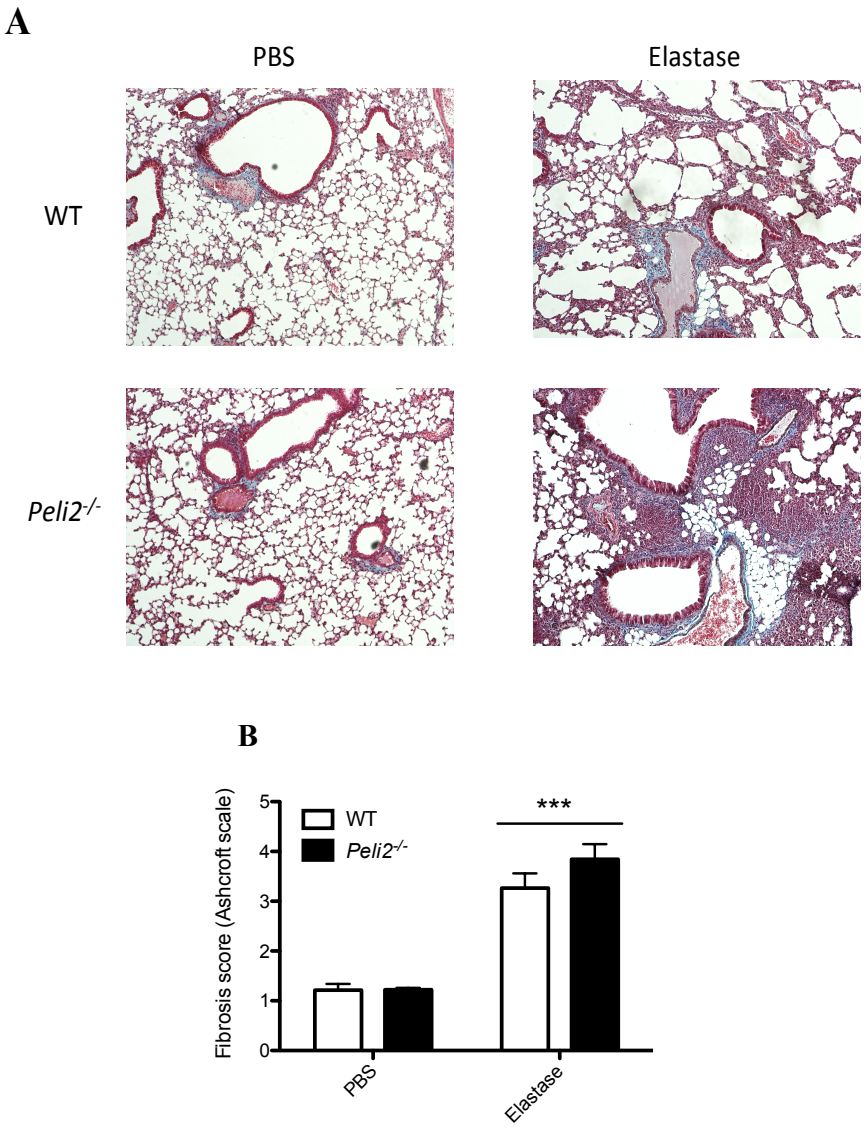

Figure 3.7 Pellino2 deficiency results in greater levels of pulmonary fibrosis in response to elastase-induced emphysema

Wild type and Pellino2-deficient mice were treated intranasally with either 35µg elastase in 50 µl PBS or PBS alone every 2-3 days over 14 days. At day 14, mice were culled and the lungs were removed and a lobe of the lung was fixed in formalin and paraffin embedded. (A) 4µm sections of the lungs were cut and stained with Trichrome. An entire lobe of each lung was imaged at 10x magnification. (B) Using these images, the level of fibrosis was scored according to the Ashcroft scale. *** $p<0.0001$ (paired, two-tailed Student's t-test). Each point represents a single mouse. Error bars, s.e.m.

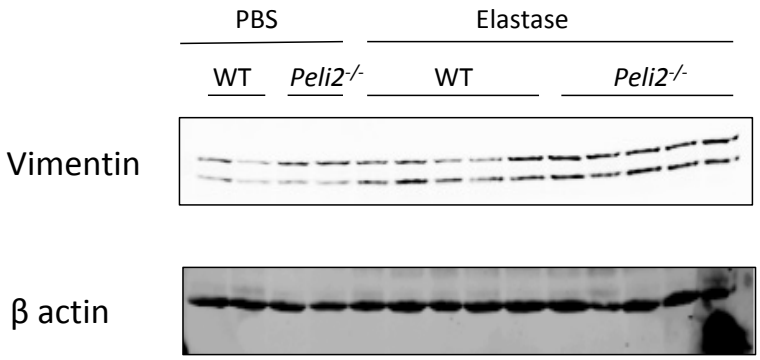

Figure 3.8 Pellino2 deficiency results in greater levels of deposition of pulmonary fibrosis marker vimentin in response to elastase-induced emphysema

Wild type and Pellino2-deficient mice were treated intranasally with either 35μg elastase in 50 μl PBS or PBS alone every 2-3 days over 14 days. At day 14, mice were culled and the right lobe of the lungs was homogenised and analysed by immunoblotting with anti-vimentin antibody. Anti-β actin antibody was used as a loading control. Each lane represents a single mouse.

3.2.4 Pellino2 deficiency affects the level of goblet cell hyperplasia in response to elastase-induced emphysema

Goblet cells line the bronchioles and produce mucus under normal circumstances. During emphysema in humans and also in the chronic elastase mouse model, these cells can undergo hyperplasia and become more numerous and larger (Chung and Adcock, 2008). Mucus hypersecretion can occur which leads to further breathing complications in the disease. In humans with emphysema, coughing and shortness of breath are exacerbated as a result of mucus hypersecretion (Jeffery, 2001). To examine if Pellino2 may play a role in goblet cell hyperplasia during emphysema, goblet cells were examined in the lungs of wild type and Pellino2-deficient mice following repeated elastase instillation over 14 days. Goblet cells were visualised by periodic acid Schiff (PAS) staining of histological lung samples. PAS stain works by staining the mucins in goblet cells bright pink and the background is stained light pink. Periodic acid oxidises the sugars in mucins, producing free aldehydes that are stained by Schiff reagent.

Using PAS stain, goblet cell hyperplasia was visualised in the lungs of wild type and Pellino2-deficient mice following repeated intranasal elastase instillation in mice over 14 days (fig. 3.9A). The proportion of positively stained goblet cells was estimated in each bronchiole. A score was given to each image depending on the proportion of positively stained cells surrounding the bronchiole: 0-10% scored 0, 10-25% scored 1, 25-50% scored 2, 50-75% scored 3 and greater than 75% scored 4. Average scores were recorded for each mouse. Goblet cell number increased in response to elastase–induced emphysema in the lungs of both wild type and Pellino2-deficient mice (fig.

3.9B). Pellino2 deficiency is associated with a reduction in PAS score. Wild type mice had an average score of 1 compared with <0.5 in Pellino2-deficient mice.

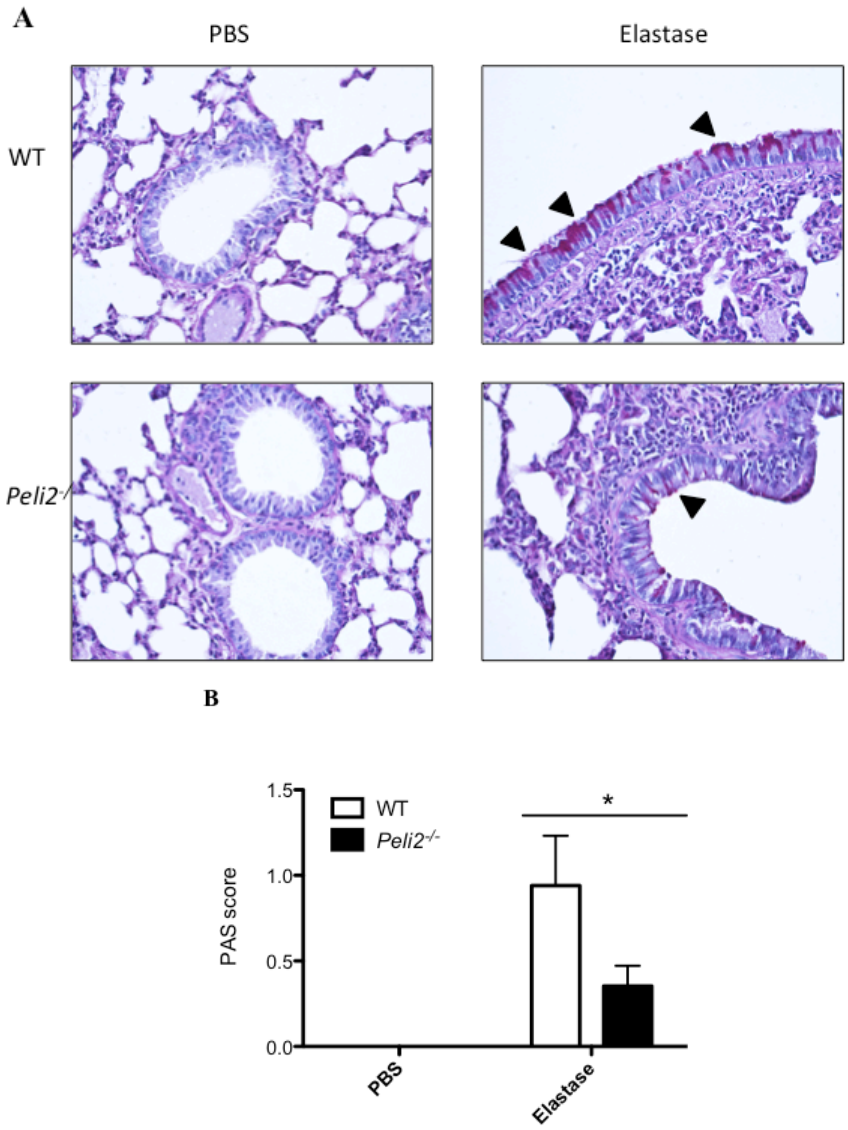

Figure 3.9 Pellino2 deficiency results in less severe alterations of goblet cells in response to elastase-induced emphysema

Wild type and Pellino2-deficient mice were treated intranasally with either 35µg elastase in PBS or PBS alone every 2-3 days over 14 days. Mice were culled and the lungs were removed, fixed in formalin and paraffin embedded. 4µm sections of the lungs were stained with PAS (A). Bronchioles throughout the lobe were imaged at 40x. Arrows denotes areas of positive staining. (B) Each imaged bronchiole was given a score depending on the percentage of cells staining positive for PAS where 0-10% scored 0, 10-25% scored 1, 25-50% scored 2, 50-75% scored 3 and >75% scored 4. An average score from all bronchioles in a lobe was taken for each mouse. * $p < 0.005$ (paired, two-tailed Student's t-test). Data presented as mean of all scores. Error bars, s.e.m.

3.2.5 Pellino3 deficiency does not alter the pathology of elastase-induced emphysema

Given the role for Pellino2 in mediating acute lung inflammation and controlling the progression of elastase-induced emphysema, we next examined the specificity of this role for Pellino2 by studying another Pellino family member, Pellino3. Wild type and Pellino3-deficient mice were treated with intranasal elastase and culled 24 hours later. The lungs were homogenised and analysed by ELISA for expression of IL-1β (fig. 3.10A), IL-6 (fig. 3.10B), TNFα (fig. 3.10C) and CXCL1 (fig. 3.10D). As before, the treatment of wild type mice with elastase induced high levels of pro-inflammatory cytokines in the lungs. The absence of Pellino3 had no affect on the ability of elastase to induce the expression of IL-1β (fig. 3.10A), IL-6 (fig. 3.10B), TNFα (fig. 3.10C) and CXCL1 (fig. 3.10D) suggesting a dispensable role for Pellino3 in this process.

Whilst Pellino3 appears to lack a role in the acute inflammatory effects of elastase, we were also keen to explore its potential involvement in pathology that is mediated by chronic administration of elastase. To examine the role of Pellino3 in induction and progression of elastase-induced emphysema, wild type and Pellino3-deficient mice were treated with elastase intranasally every 2-3 days for 14 days before examining the pathology of the lungs. Lungs were examined for alveolar destruction (fig. 3.11A) and the mean linear intercept was calculated (fig. 3.11 B)).

Alveolar wall breakdown and increased airspace was apparent in lung tissue from wild type mice repeatedly challenged with elastase and similar levels of damage were observed in lung tissue from Pellino3-deficient mice (fig. 3.11A and fig. 3.11B).

Notably, the thickening seen in Pellino2-deficient mice was not observed in wild type mice or Pellino3-deficient mice. This suggests that Pellino3 is not playing a role in the induction or progression of elastase-induced emphysema in mice and that all family members do not share the role of Pellino2 in lung inflammation and damage.

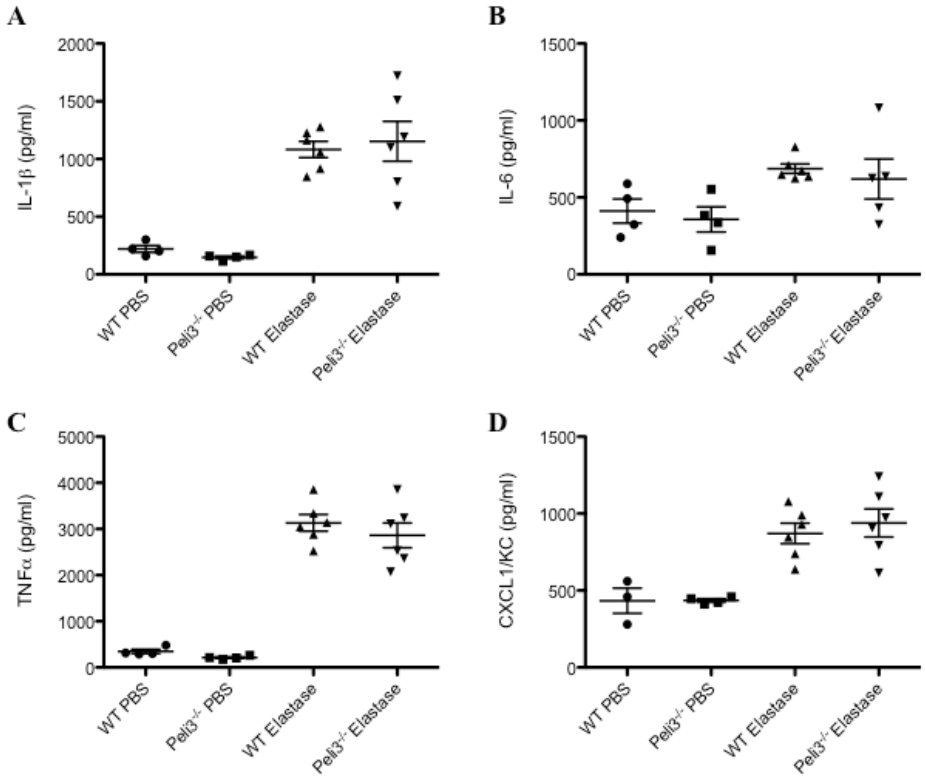

Figure 3.10 Effect of Pellino3 deficiency on the inflammatory response to intranasal elastase instillation

Wild type and Pellino3-deficient mice were given 35μg elastase in 50μl PBS or 50μl PBS alone intranasally and culled 24 hours later. The lungs were homogenised and analysed by ELISA for (A) IL-1β, (B) IL-6, (C) TNFα and (D) CXCL1. Each data point represents a single mouse. Significance using paired, two-tailed Student's t-test. Error bars, s.e.m.

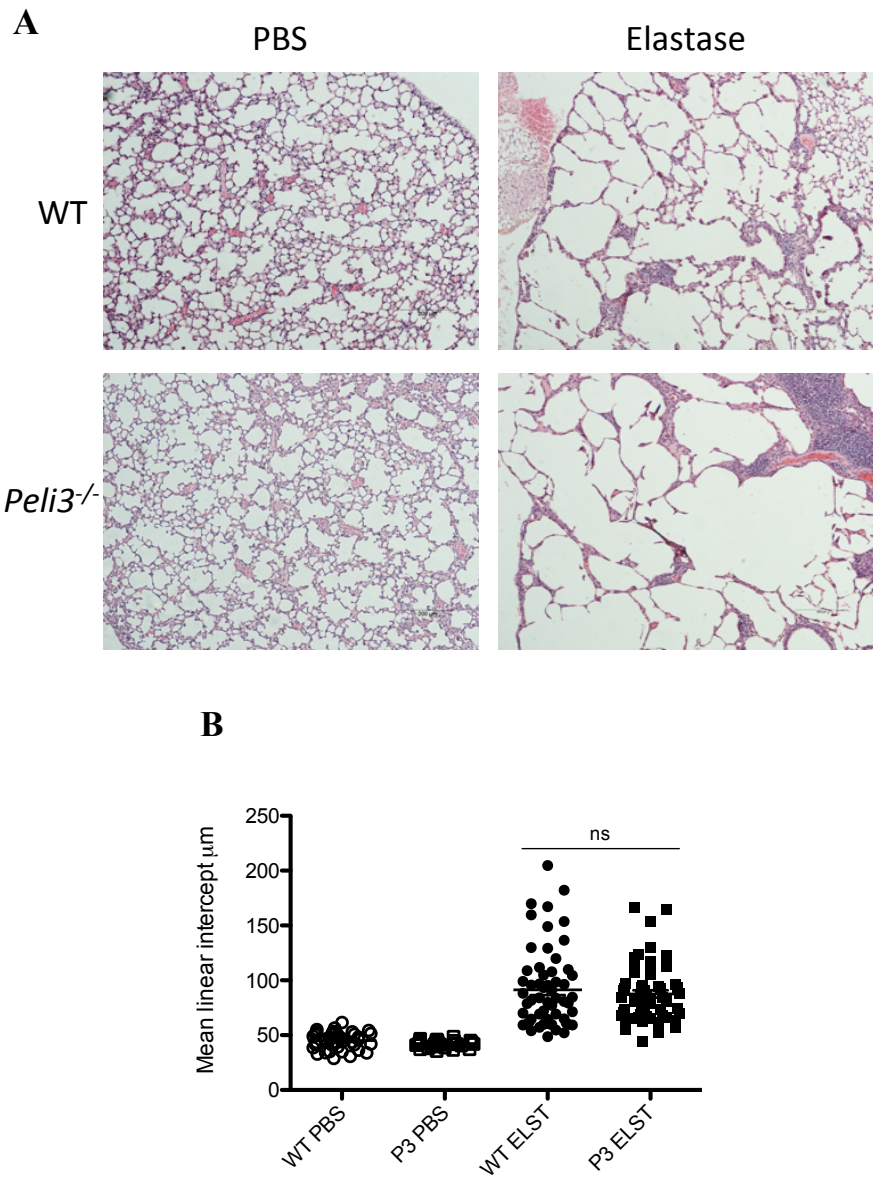

Figure 3.11 Pellino3 deficiency does not alter the pathology of elastase-induced emphysema

Wild type and Pellino3-deficient mice were treated intranasally with either 35µg elastase in 50µl PBS or 50µl PBS alone every 2-3 days over 14 days. At day 14, mice were culled and the lungs were removed and fixed in formalin and paraffin embedded. (A) 4µm sections of the lungs were generated and stained with H&E. An entire lobe of each lung was imaged at 10x magnification. (B) Average mean linear intercept was calculated for each mouse using ImageJ. Each data point represents a single mouse. Significance using paired, two-tailed Student's t-test. Error bars, s.e.m.

3.2.6 Pellino3 does not mediate NLRP3 inflammasome activation or function

In an effort to understand the differential roles for Pellino2 and Pellino3 in elastase-induced emphysema in mice, the role of Pellino3 in mediating activation of the NLRP3 inflammasome was examined. This was of interest because NLRP3 inflammasome-mediated IL-1β production has been previously implicated in the development of emphysema in mice (Couillin *et al*., 2009) and our research group has recently shown Pellino2 to mediate activation of the NLRP3 inflammasome (Humphries *et al*., 2018). The role of Pellino3 in NLRP3 inflammasome activation was assessed by employing a two-signal model of NLRP3 inflammasome activation that used LPS as a priming signal followed by ATP as a second signal. This model was used previously by our research group to study the effects of Pellino2 deficiency on NLRP3 inflammasome activation (Humphries *et al*., 2018).

Priming with LPS followed by stimulation with ATP resulted in high levels of mature IL-1β being released from wild type BMDMs as measured by ELISA (fig. 3.12). This response was reduced by approximately 50% in Pellino2-deficient BMDMs which is consistent with previous data by Humphries *et al*. (2018). The reduction, although statistically significant, was not complete which may be explained by compensation of other proteins in the absence of Pellino2 or IL-1β production via possible NLRP3-independent mechanisms as described by Netea *et al.* (2015) although these mechanisms were not examined in this thesis. The same conditions were applied to Pellino3-deficient BMDMs. Again, priming with LPS followed by treatment with ATP resulted in high levels of mature IL-1β being released from wild type BMDMs

as measured by ELISA, with a similarly strong response seen in Pellino3-deficient BMDMs (fig. 3.13). This suggests that Pellino3 does not play a role in NLRP3 inflammasome activation.

The absence of a role for Pellino3 in NLRP3 inflammasome activation is further supported by immunoblotting. LPS and ATP-induced processing of IL-1β and caspase-1 occurred to a similarly strong level in both wild type and Pellino3-deficient BMDMs (fig. 3.14). There may be slightly more pro-IL-1β induction in Pellino3-deficient BMDMs as compared to wild type BMDMs in response to both signals but levels of active IL-1β and caspase-1 p20 in the supernatant were similar. Signal 1 upregulates and stabilises NLRP3 with signal 2 likely causing NLRP3 oligomerisation and NLRP3 translocation into the insoluble complex. NLRP3 was upregulated to similar levels in wild type and Pellino3-deficient cells in response to the first signal and then reduced to similar levels in wild type and Pellino3-deficient BMDMs upon stimulation with the second signal as NLRP3 moved into the insoluble complex (fig. 3.14). These results illustrate that although Pellino2 is involved in mediating NLRP3 inflammasome activation, Pellino3 does not play a role in this pathway.

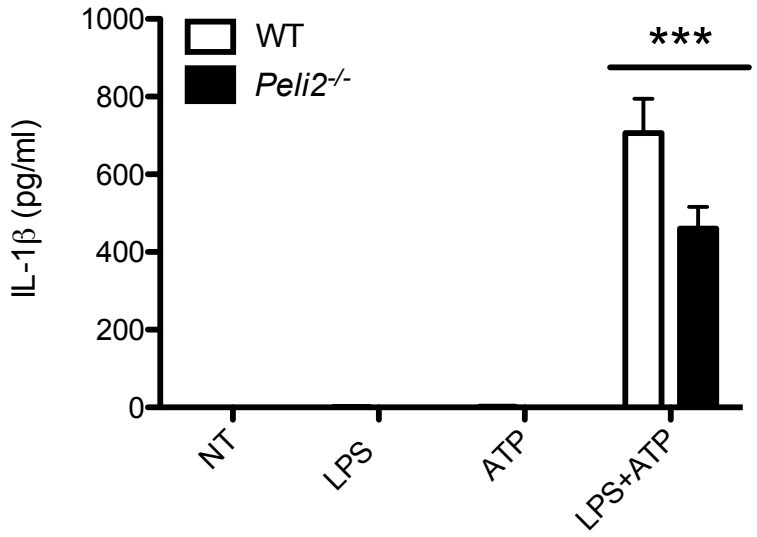

Figure 3.12 Pellino2 mediates activation of the NLRP3 inflammasome

BMDMs generated from wild type and Pellino2-deficient mice were treated with LPS (100 ng/ml) for 3 hours followed by ATP (5 mM) for 45 min. Supernatants were collected and analysed by ELISA for IL-1β. $^{***}p < 0.05$ (paired, two-tailed Student's t-test). Data are presented as the mean of three independent experiments. Error bars, s.e.m.

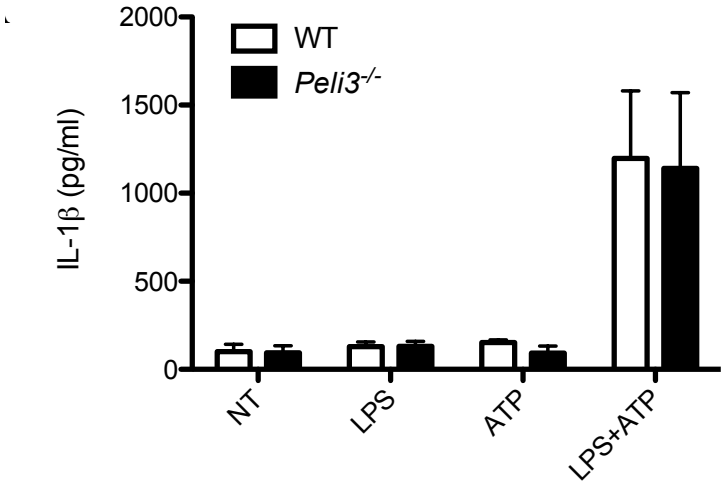

Figure 3.13 Pellino3 deficiency does not affect the secretion of IL-1β in response to NLRP3 inflammasome activation

BMDMs were generated from wild type and Pellino3-deficient mice and treated with LPS (100 ng/ml) for 3 hours followed by ATP (5 mM) for 45 minutes. Supernatants were collected and analysed for the presence of IL-1β by ELISA. Significance tested by paired, two-tailed Student's t-test. Data are presented as the mean of three independent experiments. Error bars, s.e.m.

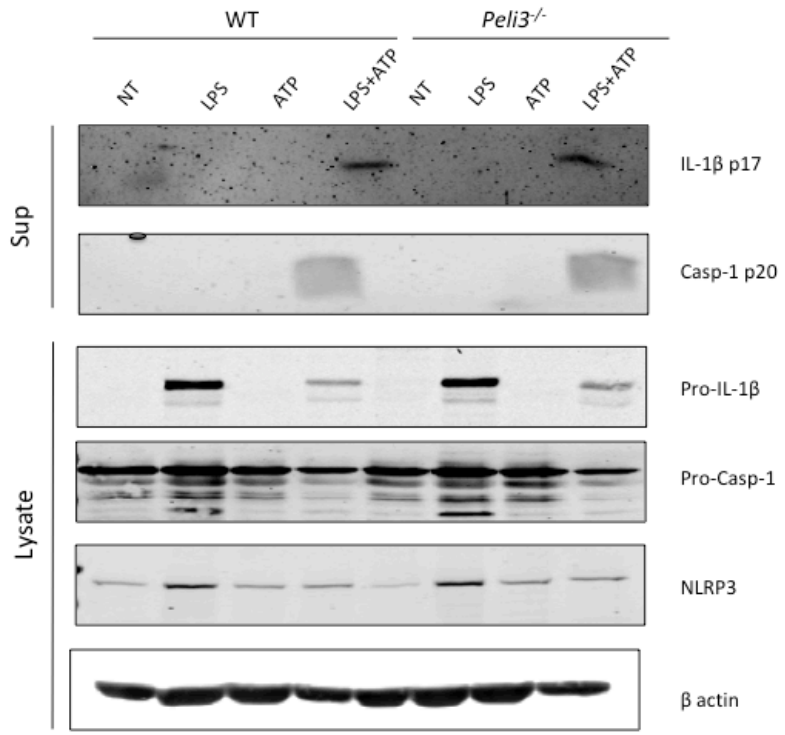

Figure 3.14 Pellino3 deficiency does not affect processing of pro caspase-1 or pro-IL-1β in response to NLRP3 activation

BMDMs generated from wild type and Pellino2-deficient mice were treated with LPS (100 ng/ml) for 3 hours followed by ATP (5 mM) for 45 min. Supernatants were collected and cells were lysed in RIPA buffer. Supernatants (Sup) and cell lysates were analysed by immunoblot using anti caspase-1 p20, anti IL-1β and anti-NLRP3 antibodies. Anti β-actin antibody was used as a loading control. Results representative of three independent experiments.

3.2.7 Pellino3 deficiency does not affect ASC oligomerisation in response to NLRP3 inflammasome activation

To confirm that Pellino3 does not play a role in NLRP3 inflammasome activation, the effect of Pellino3 deficiency on NLRP3 inflammasome assembly was next examined. NLRP3 inflammasome assembly requires the formation of ASC oligomers which group into a single ASC speck within the cell (Fernandes-Alnemri *et al*., 2007). ASC oligomers allow for binding and processing of caspase-1 into its active form (Dick *et al*., 2016). The effect of Pellino3 deficiency on ASC aggregation under conditions of NLRP3 inflammasome activation was examined. Wild type and Pellino3-deficient BMDMs were primed with LPS followed by treatment with ATP. Cell lysates were treated with the chemically cross-linking agent, disuccinimydyl suberate (DSS) and samples were analysed by immunoblotting for ASC (fig. 3.15). Similar levels of ASC oligomers, dimers and monomers were detected in cell lysates of both wild type and Pellino3-deficient BMDMs in response to LPS and ATP treatment. This correlates with the previous data, which strongly suggests that Pellino3 is not involved in mediating NLRP3 inflammasome activation.

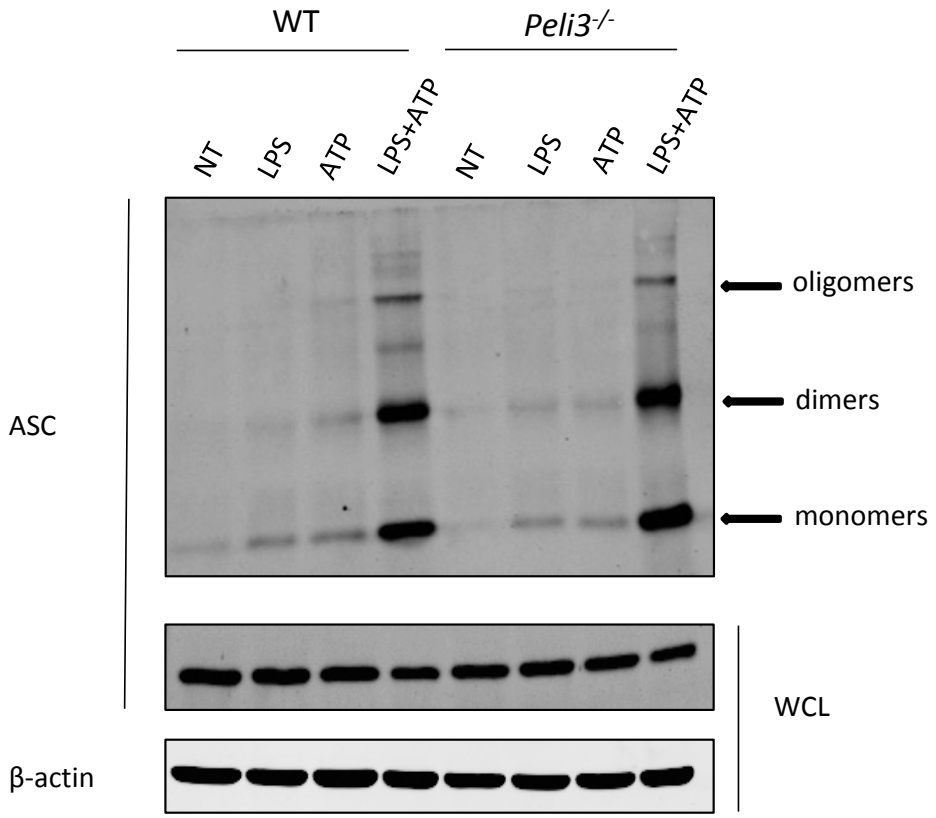

Figure 3.15 Pellino3 deficiency does not affect ASC oligomerisation in response to NLRP3 inflammasome activation

BMDMs generated from wild type and Pellino3-deficient mice were treated with LPS (100 ng/ml) for 3 hours followed by ATP (5 mM) for 45 minutes. Cells were washed with PBS and lysed. Whole cell lysate (WCL) and the insoluble pellet were separated by centrifugation. Whole cell lysates (WCL) were analysed by immunoblot using anti ASC and anti β-actin antibodies. The insoluble pellet was resuspended in PBS and proteins were cross-linked with 2mM DSS for 1 hour at room temperature. The resulting pellet was analysed by immunoblot using anti ASC antibodies. Results are representative of 2 independent experiments.

3.2.8 Pellino2 deficiency alters the proinflammatory response of macrophages to *P. aeruginosa*

As Pellino2 plays a mediatory role in NLRP3 inflammasome activation and Pellino2 deficiency suppresses early lung inflammation in response to physical insults like elastase, it was next assessed if Pellino2 also modulates the inflammatory response to respiratory infection with *P. aeruginosa.*

Initial studies focused on *in vitro* infection of BMDMs from wild type and Pellino2-deficient mice with *P. aeruginosa* (PAO-1 strain) to assess if Pellino2 deficiency affected the cellular inflammatory response to this bacterium. CXCL1 (fig. 3.16A), TNFα (fig. 3.16B), IL-6 (fig 3.16C) and IL-1β (fig. 3.16D) production in response to infection with *P. aeruginosa* were measured by ELISA. IL-6, TNFα and CXCL1 were measured to assess the specificity of the effect of Pellino2 in only regulating NLRP3 inflammasome-mediated production of IL-1β and not a broader dampening of inflammatory cytokine expression. In response to *in vitro* infection with *P. aeruginosa*, wild type BMDMs showed a strong inflammatory response and produced high levels of CXCL1 (fig. 3.16A), TNFα (fig. 3.16B), IL-6 (fig 3.16C) and IL-1β (fig. 3.16D) in response to *P. aeruginosa* infection. *P. aeruginosa* infection induced high levels of CXCL1 (fig. 3.16A), TNFα (fig. 3.16B) and IL-6 (fig 3.16C) in Pellino2-deficient BMDMs which were comparable to the response in wild type BMDMs. However, Pellino2-deficient BMDMs produced less IL-1β (fig. 3.16D) when compared with wild type BMDMs upon *P. aeruginosa* infection, with a 50% reduction in expression being apparent. This is consistent with recently published

findings from our research group of Humphries *et al*. (2018) and is consistent with Pelllino2 mediating a positive role in the priming phase of NLRP3 inflammasome activation.

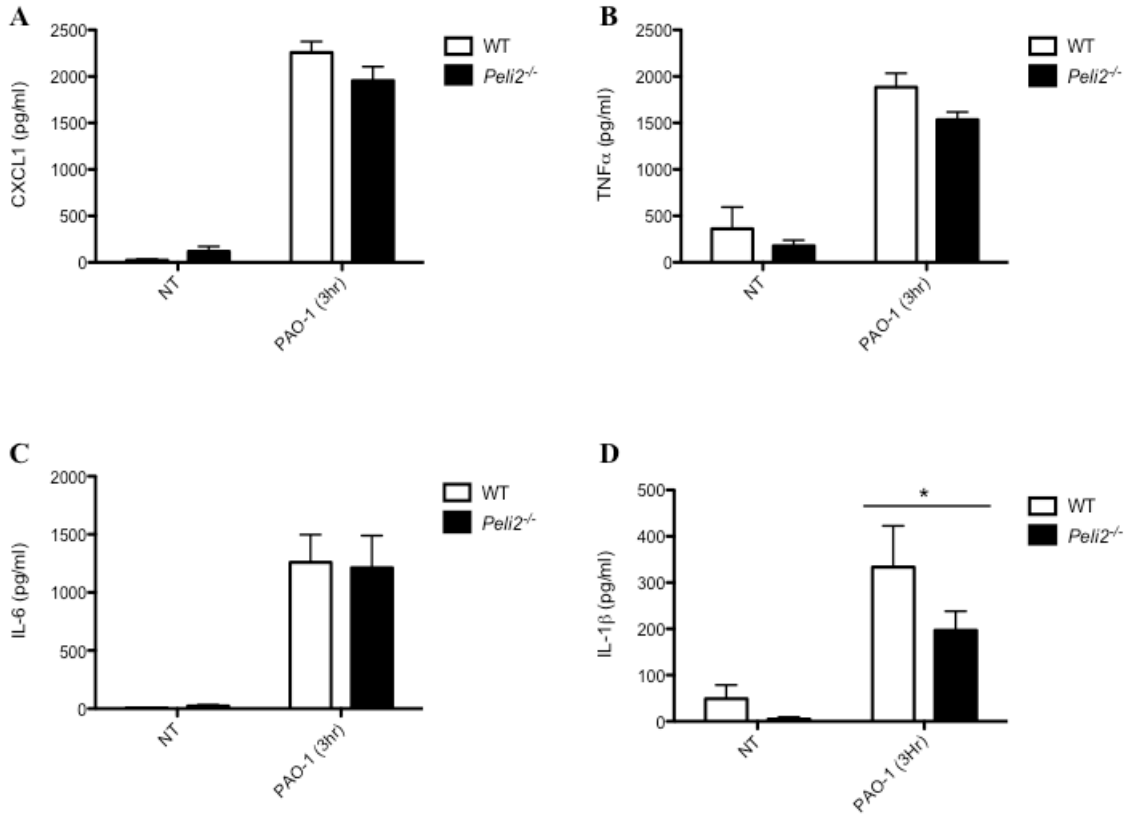

Figure 3.16 Effect of Pellino2 deficiency on pro-inflammatory cytokine induction in macrophages in response to PAO-1 infection *in vitro*

Wild type and Pellino2-deficient BMDMs were treated with 1 ml PAO-1 at OD 0.5 at 600 nm for 1 hour before application of antibiotics and cultured for a further 3 hours. Supernatants were collected and clarified and ELISA analysis was carried out for (A) CXCL1, (B) TNFα, (C) IL-6 and (D) IL-1β. $^{*}p < 0.05$ (paired, two-tailed Student's t-test). Data are presented as the mean of three independent experiments. Error bars, s.e.m.

3.2.9 Pellino2 deficiency protects mice in murine model of respiratory *P. aeruginosa* infection

P. aeruginosa is an opportunistic pathogen that frequently causes both acute and chronic respiratory infections in patients suffering from COPD and cystic fibrosis (Murphy *et al*., 2008). The innate immune response is crucial for clearance of the pathogen however it has been demonstrated that inhibition of NLRP3 inflammasome and IL-1β production improves bacterial clearance (Iannitti *et al*., 2016). Given the role for Pellino2 in positive regulation of the NLRP3 inflammasome and *in vitro* experiments showing a reduction in IL-1β production in the absence of Pellino2 in response to PAO-1 infection, it was examined if Pellino2 may play a role in regulation of the immune response to *P. aeruginosa* in a murine model of respiratory infection.

To examine the survival response, wild type and Pellino2-deficient mice were challenged with intratracheal administration of a high dose of *P. aeruginosa* (absorbance 0.5 at 600 nm). Survival was analysed based on compliance with humane end points. Survival improved significantly in the absence of Pellino2 (fig. 3.17A). All wild type mice reached a humane endpoint between 12 and 24 hours after infection but 50% of Pellino2 deficient mice survived to 48 hours post infection.

To examine bacterial load and production of inflammatory mediators, wild type and Pellino2-deficient mice were challenged with intratracheal administration of a low dose of *P. aeruginosa* (absorbance 0.05 at 600 nm). The improved survival of Pellino 2-deficient mice in response to a high dose of *P. aeruginosa* correlated with reduced

bacterial load in the lungs of Pellino2 deficient mice following a low dose infection after 24 hours (fig. 3.17B). Lung homogenates streaked on LB agar plates showed that wild type mice had log 6 CFU/ml lung homogenate whereas Pellino2-deficient mice had a 50% lower bacterial load in the lungs with log 5.5 CFU/ml lung homogenate. Samples of the same lung homogenate were then analysed by ELISA for levels of pro-inflammatory cytokines: IL-1β (fig. 3.18A), CXCL1 (fig. 3.18B), IL-6 (fig. 3.18C), CXCL2 (fig. 3.18D) and TNFα (fig. 3.18E) and type II cytokines: IL-4 (fig. 3.19A) and IL-13 (fig. 3.19B). All cytokines tested were induced to similarly high levels in both wild type and Pellino2-deficient mice in response to low dose respiratory infection with *P. aeruginosa*. These data suggest that whilst Pellino 2 deficiency protects mice and enhances survival in response to *P. aeruginosa* infection, these effects may be independent of any regulation of IL-1β.

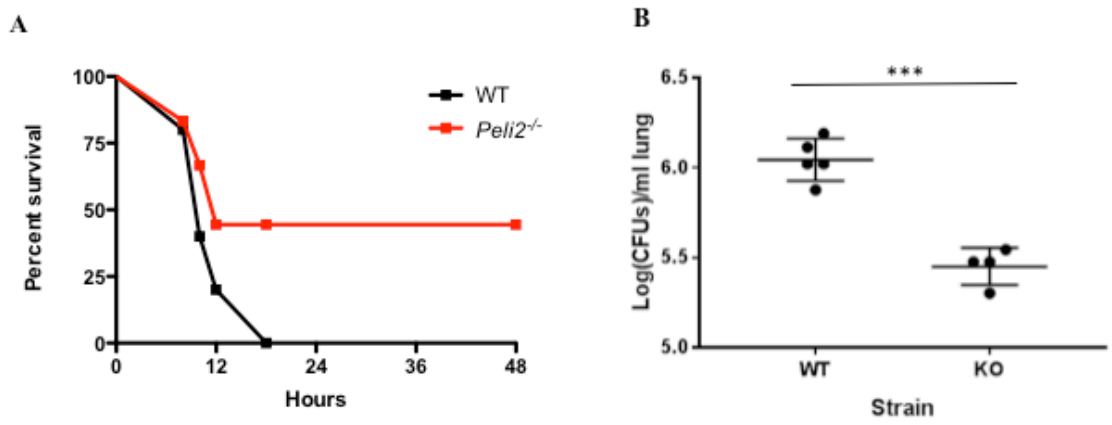

Figure 3.17 Effect of Pellino2 deficiency on survival and bacterial clearance in a murine model of *P. aeruginosa* infection

(A)Wild type (WT) and Pellino2-deficient (KO) mice were challenged with PAO-1 (OD 0.5 at 600 nm) intratracheally. Survival was assessed over a 48-hour period with humane endpoints indicating time of death at which mice were culled. A Kaplan-Meier plot was produced and significance tested using the log-rank (Mantel-Cox) test. $p = 0.08$. 5 mice were included per treatment group (B) Wild type (WT) and Pellino2-deficient (KO) mice were challenged with PAO-1 (OD 0.05 at 600 nm) intratracheally. After culling, lungs were homogenised in PBS. Lung homogenates were plated on LB agar plates and CFUs were calculated per ml of lung homogenate, graphed as Log CFU/ml. $^{***}p < 0.0001$ (paired, two-tailed Student's t-test). Data presented as the mean of 4 mice per PBS control group and 5-6 mice per PAO-1 experimental group. Error bars, s.e.m. (Data provided by Dr. Alice Dubois and Dr. Rebecca Ingram)

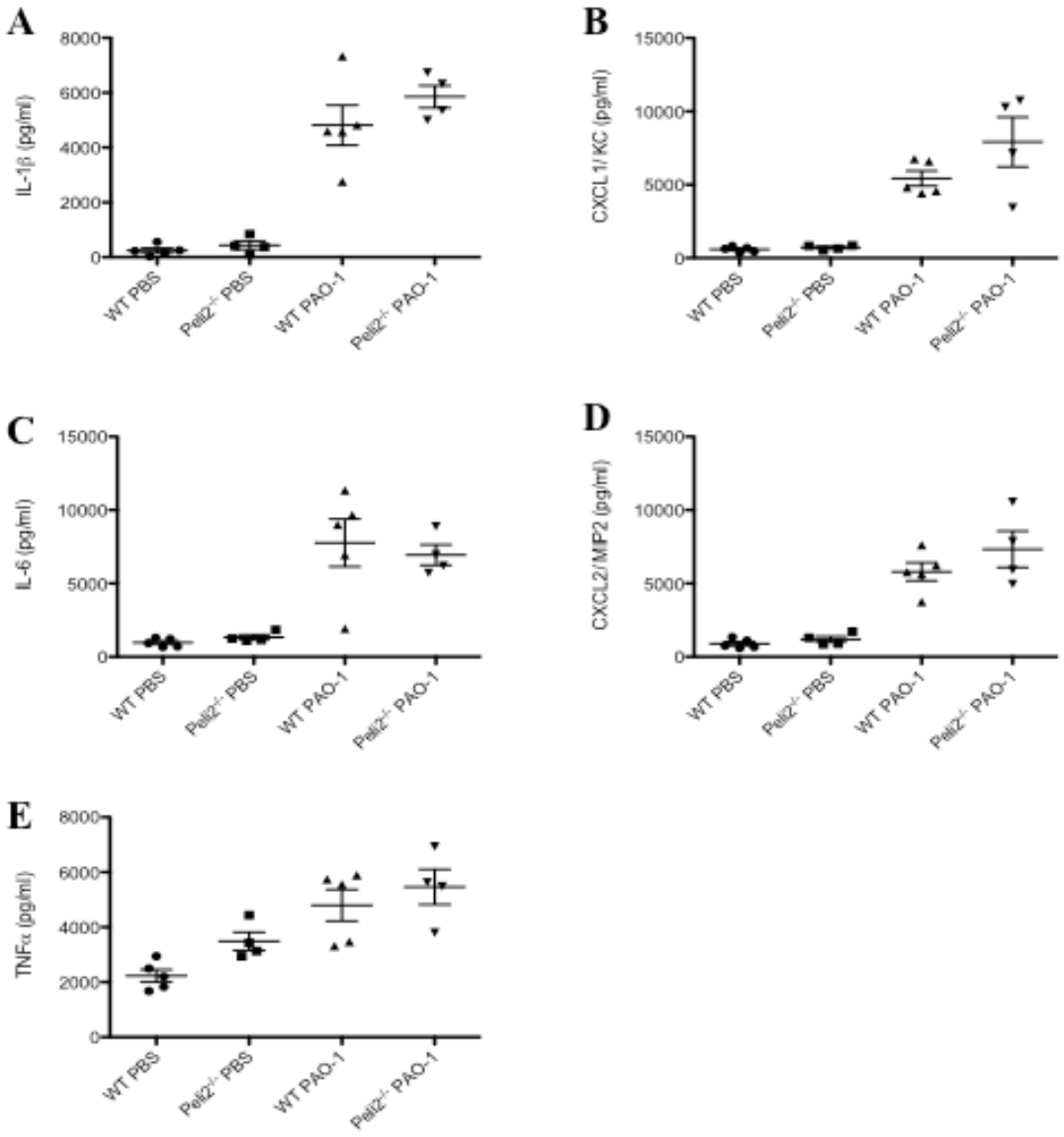

Figure 3.18 Effect of Pellino2 deficiency on proinflammatory cytokine and chemokine induction in a murine model of *P. aeruginosa* respiratory infection

Wild type and Pellino2-deficient mice were challenged with PAO-1 (OD 0.05 at 600 nm) intratracheally. After 24 hours the mice were culled and the lungs were removed and homogenised in PBS. Homogenates were analysed by ELISA for the presence of (A) IL-1β, (B) CXCL1/KC, (C) IL-6, (D) CXCL2 and (E) TNFα. Significance tested by paired, two-tailed Student's t-test. Each data point represents one mouse. Error bars, s.e.m.

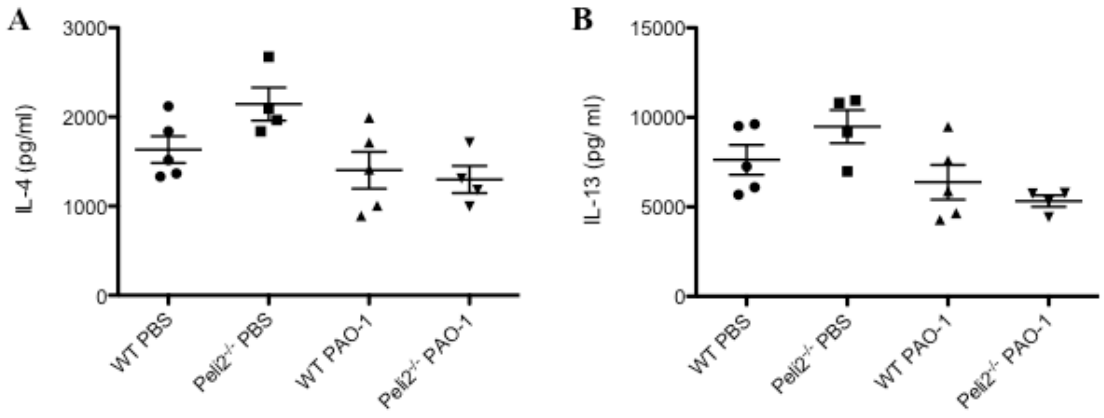

Figure 3.19 Effect of Pellino2 deficiency on induction of type 2 cytokines in a murine model of *P. aeruginosa* respiratory infection

Wild type and Pellino2-deficient mice were challenged with PAO-1 (OD 0.05 at 600 nm) intratracheally. After 24 hours the mice were culled and the lungs were removed and homogenised in PBS. Homogenates were analysed by ELISA for the presence of IL-4 and IL-13. Significance tested by paired, two-tailed Student's t-test. Each data point represents one mouse. Error bars, s.e.m.

3.3 Discussion

Emphysema is associated with an underlying chronic inflammation in the lungs and loss of airspace (Goldklang and Stockley, 2016). IL-1R signalling and the NLRP3 inflammasome have previously been implicated in the development of emphysema in mouse models of the disease (Couillin *et al*., 2009; Lucey *et al*., 2002). We wanted to examine if Pellino2, which is a mediator of NLRP3 inflammasome activation, could also be involved in mediating the immune response involved in elastase-induced emphysema. We found that Pellino2 plays a role in mediating the immune response to intranasal elastase in mice. The impairment of elastase induced expression of IL-1β, IL-6, TNFα and CXCL1 in the absence of Pellino2 manifests at the mRNA and protein levels of these cytokines and chemokines (fig. 3.1 and fig. 3.2). However the suppressive effects of Pellino2 deficiency are more pronounced when the cytokines are measured at the protein levels. This suggests that Pellino2 may regulate the expression of the genes encoding these cytokines at the transcriptional and post-transcriptional levels. Ubiquitination has been shown to be involved in regulation of mRNA decay. Specifically, TRAF6 mediates K63-ubiquitination of P-body components, a body that regulates mRNA decay (Tenekeci *et al*., 2016). It could be possible that Pellino2 serves a similar function, however this has not been tested. It should be noted that although there are published studies where levels of specific proteins and mRNA in the lungs are examined 24 hours after initial elastase instillation (Kennelly *et al*., 2016), the levels may not directly correlate with each other as mRNA for pro-inflammatory products will be present in the cell much sooner than protein.

It has been previously shown that where early markers of inflammation are reduced in elastase-induced emphysema, the final pathology of the disease is much less severe (Ishii *et al*. 2005; Lucey *et al*. 2002). This has been shown in IL-1R-deficient mice and ASC-deficient mice for example (Couillin *et al*., 2009). However, Pellino2-deficient mice have low levels of inflammation following an overnight treatment with elastase but develop worsened emphysema as measured by increased weight loss (fig. 3.6) and markers of fibrosis (fig. 3.8) after repeated doses of elastase. A higher level of collagen deposition was seen using trichrome staining (fig. 3.7A) and this was associated with a higher fibrosis/Ashcroft score (fig. 3.7B). Higher levels of fibrosis may correlate with a worsened overall pathology as seen in the form of significantly higher weight loss in Pellino2-deficient mice as compared with wild type mice (fig. 3.6). This is similar to systemic manifestation of severe COPD in humans (Lüthje *et al*., 2009). Whereas the wild type mice treated with elastase recover initial weight lost, Pellino2 deficiency results in greater weight loss that does not recover to the same level over the course of the experiment. Increased levels of fibrosis and thickening of the airway walls in Pellino2-deficient mice suggest more extensive airway remodelling is occurring and as such markers of epithelial-mesenchymal transition (EMT) and goblet cell hyperplasia was examined.

EMT is a process involved in repairing damaged tissue but has also been associated with fibrosis (Stone *et al*., 2016). To repair wounds, epithelial cells reduce expression of E-cadherin and increase expression of vimentin to become mesenchymal cells and undergo re-epithelialisation after repair has occurred (Barriere *et al*., 2015). Where mesenchymal cells do not undergo re-epithelialisation, fibrosis occurs. Vimentin is associated with fibrosis as it stabilises type I collagen (Challa and Stefanovic, 2011).

Higher levels of vimentin are estimated in lung homogenate from Pellino2-deficient mice after repeated elastase treatment (fig. 3.8). There is no previously documented role for Pellino family proteins in regulation of structural proteins such as vimentin, which suggests that investigation of Pellino2 deficiency on lung remodelling may be of interest. It should be acknowledged that the higher levels of vimentin are only estimated, as ideally densitometry should be used to confirm these higher levels from western blotting.

As well as EMT, airway remodelling during emphysema and COPD can involve goblet cell hyperplasia (Kim *et al*., 2015a). Goblet cells produce mucus. Persistent airway inflammation is associated with excessive mucus production (Kim *et al*., 2008). During increased inflammation, the epithelium can undergo remodelling leading to goblet cell metaplasia, meaning phenotypic change of the cell, or goblet cell hyperplasia, meaning an increase in goblet cell number (Williams *et al*., 2006). Goblet cell metaplasia or hyperplasia results in mucus accumulation and has long been associated with increased mortality due to COPD in humans (Prescott *et al*., 1995; Ramos *et al*., 2014). Chronic mucus production is also associated with severe exacerbations of COPD (Burgel *et al*., 2009). Looking specifically at emphysema, chronic mucus production in patients with α1-anti-trypsin-deficiency is associated with more extensive emphysema (Dowson *et al*., 2002). Our studies showed that wild type mice undergo goblet cell hyperplasia during elastase-induced emphysema, however, the level of goblet cell hyperplasia in Pellino2-deficient mice is approximately 50% less (fig. 3.9). As goblet cell hyperplasia is a hallmark of increased severity of emphysema, and also COPD in humans (Kim *et al*., 2015b), it is surprising that Pellino2-deficient mice have less severe goblet cell hyperplasia yet

worsened fibrosis and weight loss during elastase-induced emphysema. It does however correlate with other studies which show reduced pro-inflammatory cytokines at an early timepoint are associated with lower levels of goblet cell hyperplasia at a later stage of acute lung injury (Sohn *et al*., 2013). These data suggest complex and possibly multi-factorial mechanisms underlying the regulatory effects of Pellino2 in lung inflammation and fibrosis and this prompted the use of more global molecular-based approaches such as proteomics to delineate the molecular basis of the role of Pellino2 in acute lung injury. This is described in the following chapter.

Drawing on the above results, it could be hypothesised that despite the diminished inflammatory response to intranasal elastase in Pellino2-deficient mice, when the injurious insult is chronically present, diminished inflammation does not protect from alveoli destruction. This agrees with data from clinical trials where anti-inflammatory agents may not help and can be detrimental in the treatment of emphysema and COPD. For example, an anti-inflammatory agent called Regadenoson which can suppress NFκB activation and neutrophil migration, while well tolerated by COPD patients, does not improve lung function (Cazzola *et al*., 2012). The lack of effective anti-inflammatory treatments that stop the progression of emphysema and COPD correlates with the data presented here.

The specificity of the role for Pellino2 in elastase-induced emphysema was confirmed by also examining the role of Pellino3 in elastase-induced emphysema. Pellino3-deficient mice express pro-inflammatory cytokines to a similar level as wild type mice following overnight treatment with elastase and show comparable pathology to wild type mice when treated with repeated doses of elastase over 14 days (fig. 3.10 and fig.

3.11). In an effort to explain the apparent lack of a role for Pellino3 in elastase-induced emphysema, its role in mediating NLRP3 inflammasome activation was examined. This was examined as the NLRP3 inflammasome has been shown previously to be important for the development of elastase-induced emphysema in mice (Couillin *et al*., 2009) and Pellino2 has been previously shown to mediate activation of the NLRP3 inflammasome (Humphries *et al*., 2018). Studies here showed that Pellino3 does not appear to be involved in mediating activation of the NLRP3 inflammasome. Western blotting was used to assess the involvement of Pellino3 in NLRP3 inflammasome activation. It should be acknowledged that ideally data generated should have been validated by densitometry analysis to confirm protein levels. Estimation of protein levels from western blotting demonstrated similarly high levels of IL-1β secretion in Pellino3-deficient cells and wild type cells in response to NLRP3 inflammasome activation (fig. 3.13). This was further confirmed by demonstration of normal ASC oligomerisation (fig. 3.15) and caspase-1 processing (fig. 3.14) in response to NLRP3 inflammasome activation in Pellino3-deficient cells. Interestingly our research has previously shown that Pellino3 can negatively regulate the transcription of the *Il1b* gene under conditions that pertain to obesity. Pellino3 negatively regulates transcription factor HIF-1α which prevents HIF-1α from inducing expression of *Il-1b* gene and tempers obesity-induced inflammation (Yang *et al*., 2014). The role of Pellino3 in regulation of IL-1β expression may therefore be specific to hypoxia-induced IL-1β production only.

In summary, under varying circumstances Pellino2 and Pellino3 may have opposing roles in the production of IL-1β. This highlights the diversity of function of Pellino family proteins in varying physiological circumstances and may differentially regulate

the same pathway as is the case where Pellino3 negatively regulates transcription of the *Il1b* gene whereas Pellino2 mediates the processing of pro-IL-1β into the mature bioactive form of IL-1β. However, the possibility of redundancy among E3 ubiquitin ligases cannot be ignored. In order to understand how such apparently opposing roles of different members of the same family integrate at the physiological levels, it would be intriguing to perform similar studies as described in this thesis to mice that are deficient in both Pellino2 and Pellino3.

Studies were also performed to ascertain whether the role of Pellino2 in mediating the inflammatory response during acute lung injury in elastase-induced emphysema could be extended to mediation of the inflammatory response to respiratory infection. To test this, respiratory infection with *P. aeruginosa* was carried out in wild type and Pellino2-deficient mice. Pellino2 has been previously shown to alter the level of IL-1β induction *in vitro* and in a model of peritoneal injection with *P. aeruginosa* in mice (Humphries *et al*., 2018). Our studies showed that Pellino2-deficient mice had significantly improved survival and lower bacterial load than wild type mice (fig. 3.17) despite similarly high level of IL-1β induction in the lungs of wild type and Pellino2-deficient mice in response to infection (fig. 3.18). We hypothesise that although NLRP3 inflammasome activation is impaired in the absence of Pellino2, there may be other sources of IL-1β present in response to infection which compensate for the reduction NLRP3 inflammasome mediated IL-1β production. There has been suggestion by various research groups that cleavage of pro-IL-1β into its active form is caspase-1 independent in response to certain pathogens. For example, during mammary gland infection it has been shown that non-classical IL-1β activation is pathogen dependant and caspase-1 independent (Breyne *et al*., 2014).

Investigations have also shown directly that IL-1β processing during *P. aeruginosa* infection is mediated by neutrophil serine proteases and is independent of caspase-1 and NLRC4 (Karmakar *et al*., 2012). This would suggest that the improved survival and lower bacterial load seen in Pellino2-deficient mouse lungs is an effect independent of IL-1β.

Similar effects of improved survival and reduced bacterial load have been observed in NLRP3-deficient mice in response to *P. aeruginosa* infection which also express similar levels of IL-1β in BAL as their wild type counterparts (Iannitti *et al*., 2016). It has also been demonstrated that silencing of NLRP3 or ASC or caspase-1 improves *P. aeruginosa* clearance in macrophages without significantly diminished IL-1β production (Deng *et al*., 2015). Deng *et al.* (2015) suggest that the diminished pathology seen where the NLRP3-inflammasome is silenced during infection with *P. aeruginosa* is not mediated by diminished expression of IL-1β but instead by reduced levels of autophagy. They found that overexpression of NLRP3 or *P. aeruginosa* infection induce autophagy in macrophages. Induction of autophagy in macrophages results in diminished bactericidal capacity of these cells (Deng *et al*., 2015). They suggested that the ability of *P. aeruginosa* to activate the inflammasome leads to autophagy and therefore reduced bacterial killing by macrophages. An examination of the role of Pellino2 in inflammasome mediated autophagy may therefore be of interest and could help to shed light on the improved survival seen in Pellino2-deficient mice in response to respiratory infection. This is further motivated by the fact that a previous report has described Pellino3 to be degraded during autophagy (Giegerich *et al*., 2014).

In summary the studies described in this chapter indicate that Pellino2 mediates the early inflammatory response to intranasal elastase. This role is not shared with Pellino3 and this may relate to the differential roles of Pellino2 and Pellino3 in activation of the NLRP3 inflammasome. Pellino2 deficiency also results in exacerbation of elastase-induced fibrosis and improves survival in response to *P. aeruginosa* infection. This suggests important physiological and pathophysiological roles for Pellino2 in lung immunity.

4 Exploring the molecular basis to the role of Pellino2 in the pathology of elastase-induced emphysema

4.1 Introduction

The suppression of the early inflammatory response to elastase-induced emphysema in Pellino2-deficient mice coupled to the exacerbation of later fibrosis, suggests that Pellino2 may play a protective role in acute lung injury and may contribute to enhanced repair as part of the recovery process. This prompts further molecular and cellular-based characterisation of the effects of Pellino2 in acute lung injury and forms the basis of the studies in the present chapter.

Cellular infiltration of neutrophils and macrophages into the lungs is a hallmark of emphysema and COPD (Suzuki *et al*., 2017). Activation of neutrophils leads to secretion of proteases and contributes to a protease: anti-protease imbalance that leads to emphysema, chronic bronchitis and COPD. The role of neutrophils in emphysema and COPD has been well documented. Historically, many studies have shown neutrophils to be involved in development of COPD by initiating tissue destruction in

emphysema (Nadel, 1991). Neutrophil elastase levels are increased in lung tissue from emphysema patients (Damiano *et al*., 1986) and products of elastase activity being detected in the urine and blood of COPD patients (Gottlieb *et al*., 1996). Early studies on neutrophil infiltration into the lungs of COPD patients generated data on increased neutrophil number in sputum (Peleman *et al*., 1999) and airway lavage fluid (Lacoste *et al*., 1993; Thompson *et al*., 1989). Neutrophil accumulation is a feature of emphysema and COPD specifically and not simply a response to smoke inhalation (Grabcanovic-Musija *et al*., 2015; Pilette *et al*., 2007).

Macrophages are another innate immune cell that are important in the development of emphysema and produce an array of chemokines, cytokines and matrix metalloproteases (MMPs) that in combination, can degrade tissue in a similar manner to neutrophil elastase (Gharib *et al*., 2018). MMPs are important in leukocyte migration (Song *et al*., 2015). MMP12 (also known as macrophage elastase) is of particular importance in emphysema development. Mice can develop MMP12-dependant emphysema through excessive activation of alveolar macrophages in a dehydrated lung environment (Trojanek *et al*., 2014). MMP-9 is another important metalloprotease in emphysema and was discussed in the previous chapter. Alveolar macrophages have been extensively studied and implicated in the development of emphysema and COPD (Vlahos and Bozinovski, 2014). As such, it is of particular interest given the diminished inflammation seen in Pellino2-deficient mice in response to elastase to examine the levels of cellular infiltration of neutrophils and macrophages. Other immune cells that are involved in emphysema development were also examined including dendritic cells, B-cells and T-cell subsets.

As Pellino2-deficient mice show worsened pathology of elastase-induced emphysema including increased fibrosis as compared to wild type mice, the role of Pellino2 in cell death was also examined in these studies. Two forms of cell death were examined here: apoptosis and necroptosis. Both of these forms of cell death have been implicated in emphysema and COPD. Studies mainly using lung tissue sections from COPD patients have shown apoptosis in endothelial cells (Segura-Valdez *et al*., 2000), alveolar epithelial cells and mesenchymal cells (Imai *et al*., 2005). There are also high levels of pro-apoptotic active caspase-3 subunits present in emphysematous lungs (Imai *et al*., 2005). Apoptosis continues to occur in the lungs even after smoking cessation (Hodge *et al*., 2005). It is suggested that this may be a result of the rate of apoptosis outweighing the phagocytic capacity of alveolar macrophages, leading to accumulation of apoptotic cells and debris. This may cause secondary necrosis and lead to further tissue damage. It has been shown that induction of apoptosis alone is sufficient to cause emphysematous changes to the lungs of mice without cellular infiltration or inflammation (Kasahara *et al*., 2000; Tang *et al*., 2004). Induction of emphysema by induction of apoptosis alone has been achieved experimentally in mice by targeting VEGF, an important survival factor, (Tang *et al*., 2004) or inactivating the VEGF receptor (Kasahara *et al*., 2000).

Necroptosis was also examined in our studies. Necroptosis is a regulated form of necrosis that is dependant on the proteins RIP1, RIP3 and MLKL (mixed lineage kinase domain like pseudokinase) (Weinlich *et al*., 2016). This form of cell death has been linked to COPD and emphysema as it may be regulated by mitophagy. Mitophagy has been shown to regulate necroptosis and contributes to COPD (Mizumura *et al*., 2014). Mice deficient in PINK1, a protein involved in mediating

mitophagy, were protected from alveolar enlargement in cigarette smoke induced emphysema. It has been suggested that mitophagy may also control whether a cell enters senescence or necroptosis in response to injurious insults (Ito *et al*., 2015).

In an effort to define further the role of Pellino2 in emphysema, label-free mass spectrometry was also used to assess changes in protein abundance in the presence and absence of Pellino2 in normal and elastase-induced emphysematous lung tissue. Label-free mass spectrometry allows analysis of the entire proteome (Patel *et al*., 2009). Through mass spectrometry, we can gain insight into proteome alterations during disease. To illustrate the power of mass spectrometry, it has proven an invaluable tool in biomarker discovery for example in inflammatory bowel disease and Duchene muscular dystrophy (Chan *et al*., 2016; Coenen-Stass *et al*., 2015). In the present study we aimed to use label-free mass spectrometry to delineate the effects of Pellino2 deficiency on the proteome landscape in emphysema, with a view to further understanding its role in lung health and disease.

4.2 Results

4.2.1 Pellino2 deficiency results in reduced myeloid cell and B cell infiltration into the lungs in response to intranasal elastase

Tissue infiltration of neutrophils, macrophages, dendritic cells, B-cells, CD4+ T-cells, CD8+ T-cells and regulatory T-cells has been observed previously in experimental mouse models of emphysema or in emphysema development in humans (Harada *et al*., 2009; Nurwidya *et al*., 2016; Oliveira *et al*., 2016). Due to the diminished pro-inflammatory profile seen in Pellino2-deficient mice in response to elastase treatment (fig. 3.1), the level of myeloid cell infiltration (fig. 4.1) and lymphocyte infiltration (fig. 4.2) into the lungs was examined in wild type and Pellino2-deficient mice following overnight treatment with elastase. Cell populations were quantified as described in section 2.2.5.3. Studies initially focused on myeloid cells. Overnight treatment with elastase resulted in increased infiltration of neutrophils (fig. 4.1A), macrophages (fig. 4.1B) and dendritic cells (fig. 4.1C) in wild type mice. In Pellino2-deficient mice there were significantly lower levels of each myeloid population.

Lymphocyte populations were then examined. Treatment with elastase overnight resulted in high levels of lymphocyte infiltration into the lungs of wild type mice (fig 4.2A). In Pellino2-deficient mice lymphocyte infiltration occurred at much lower levels in response to overnight elastase treatment. Diminished lymphocyte recruitment in Pellino2-deficient mice in response to elastase treatment was reflected in lower levels of B-cell infiltration in Pellino2-deficient mice when compared to wild type mice in response to elastase (fig. 4.2B). Levels of CD8+ T cells (fig. 4.2D) and CD4+

T cells (fig. 4.2E) in the lungs remained relatively unchanged in wild type and Pellino2-deficient mice in response to elastase treatment. Regulatory T cell infiltration was seen in wild type mice in response to elastase but not in Pellino2-deficient mice (fig. 4.2E). However, regulatory T cell numbers were too low and may not provide meaningful analysis.

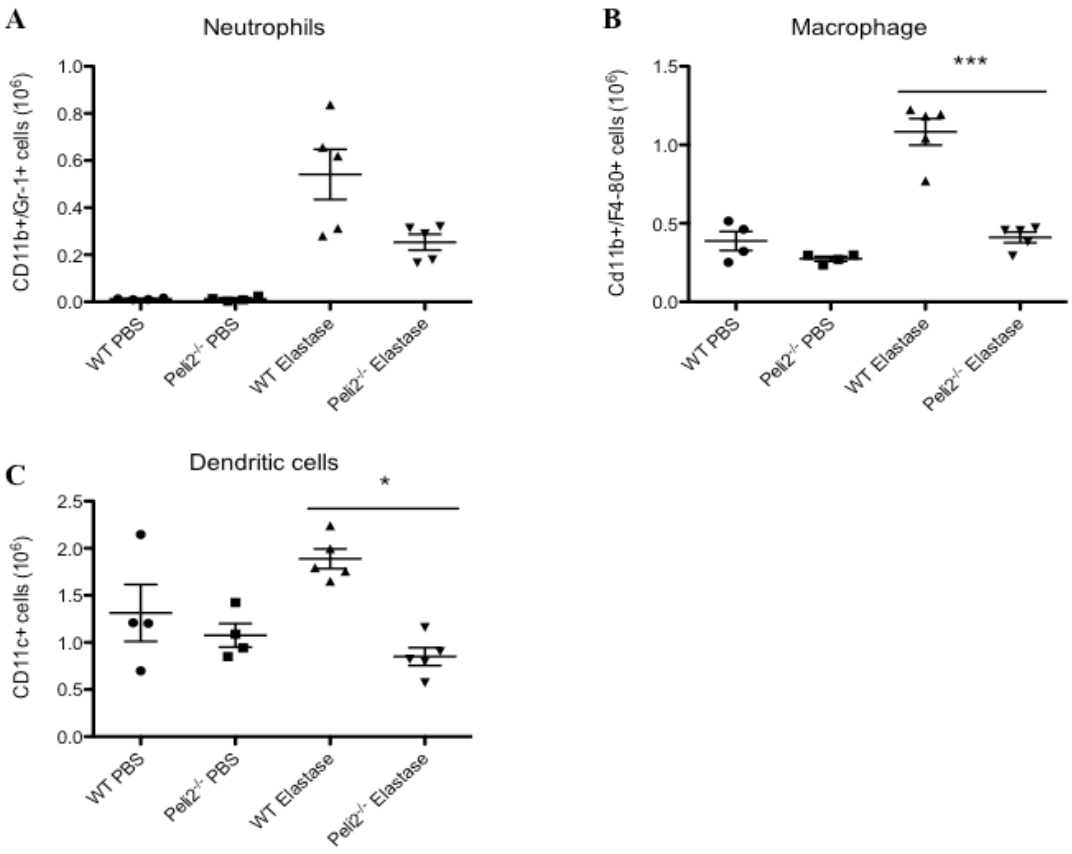

Figure 4.1 Pellino2 deficiency results in reduced myeloid cell infiltration into the lungs in response to intranasal elastase

Wild type and Pellino2-deficient mice were treated intranasally with 35 μg elastase in 50 μl PBS or 50 μl PBS alone and culled 24 hours later. Lungs were collected in PBS and homogenized. Lung homogenate was filtered through a 70 μm cell strainer and centrifuged. The pellet was treated for red blood cell lysis and resuspended in PBS. Total cells were counted using an automated cell counter. For flow cytometry Fc block was used at room temperature for 10 min. Extracellular staining was carried out for the myeloid panel with CD11b-APC and GR1/Ly6G-PE (neutrophils), F480-PECy7 (macrophage), CD45-FITC and CD11c-e450 (dendritic cells) with a gating strategy as detailed in section 2.2.5.3. (A) Neutrophil, (B) macrophage and (C) dendritic cell infiltration was quantified. * $p < 0.005$ and *** $p < 0.001$ (paired, two-tailed Student's t-test). Each point represents a single mouse. Error bars, s.e.m. (Data provided by Dr. Alice Dubois and Dr. Rebecca Ingram).

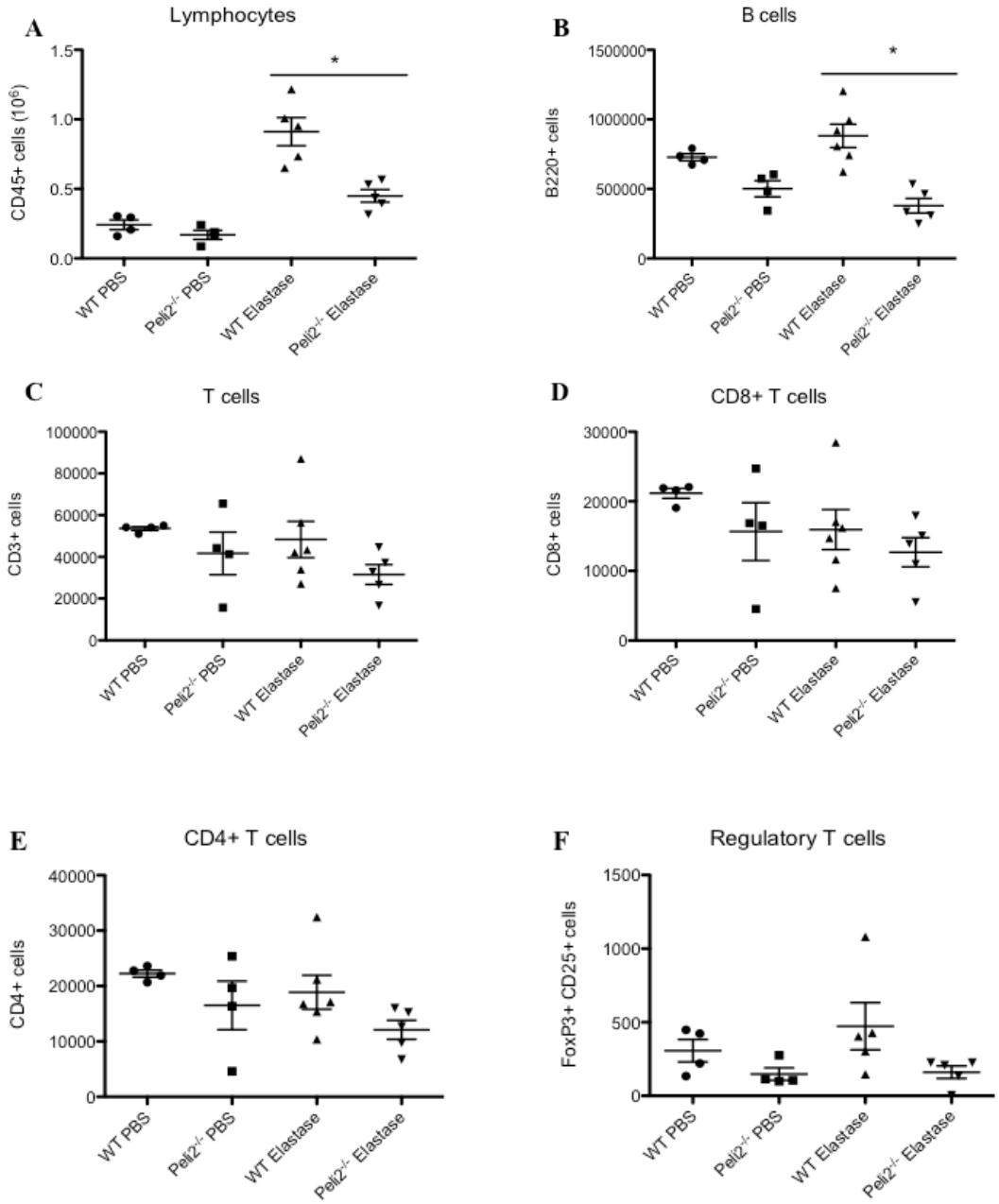

Figure 4.2 Pellino2 deficiency results in reduced B-cell infiltration into the lungs in response to intranasal elastase but does not affect T-cell infiltration

Wild type and Pellino2-deficient mice were treated intranasally with 35 μg elastase in 50 μl PBS or 50 μl PBS alone and culled 24 hours later. Lungs were collected in PBS and homogenized. Lung homogenate was filtered through a 70 μm cell strainer and centrifuged. The pellet was treated for red blood cell lysis and resuspended in PBS. Total cells were counted using an automated cell counter. For flow cytometry Fc block was used at room temperature for 10 min. Extracellular staining was carried out for the lymphoid panel with

CD3-e450 (T-cells), CD4-FITC (CD4+ T-cells), CD25-PECy5 (regulatory T-cells), B220-APCe780 (B-cells) and CD8-e660 (CD8+ T-cells) with a gating strategy as detailed in section 2.2.5.3. (A) Total lymphocytes, (B) B-cell, (C) T-cell, (D) CD8+ T-cell, (E) CD4+ T-cell and (F) regulatory T-cell infiltration was quantified. * $p < 0.005$ (paired, two-tailed Student's t-test). Each point represents a single mouse. Error bars, s.e.m. (Data provided by Dr. Alice Dubois and Dr. Rebecca Ingram).

4.2.2 Pellino2 does not mediate chemokine production by macrophages

Given that lungs from elastase-challenged Pellino2-deficient mice showed impaired recruitment of lymphocytes and lower levels of pro-inflammatory cytokines and chemokines relative to wild type mice, studies next explored the role for Pellino2 in regulating the direct production of chemokines. BMDMs were generated from wild type and Pellino2-deficient mice and treated with TNFα and IL-17. This combination of ligands drives chemokine production. Treatment with both ligands led to high levels of CXCL1 and CXCL2 production as measured by ELISA and both wild type and Pellino2-deficient BMDMs were equally responsive in terms of the production of these chemokines (fig. 4.3). These data suggest that Pellino2 does not directly regulate chemokine expression.

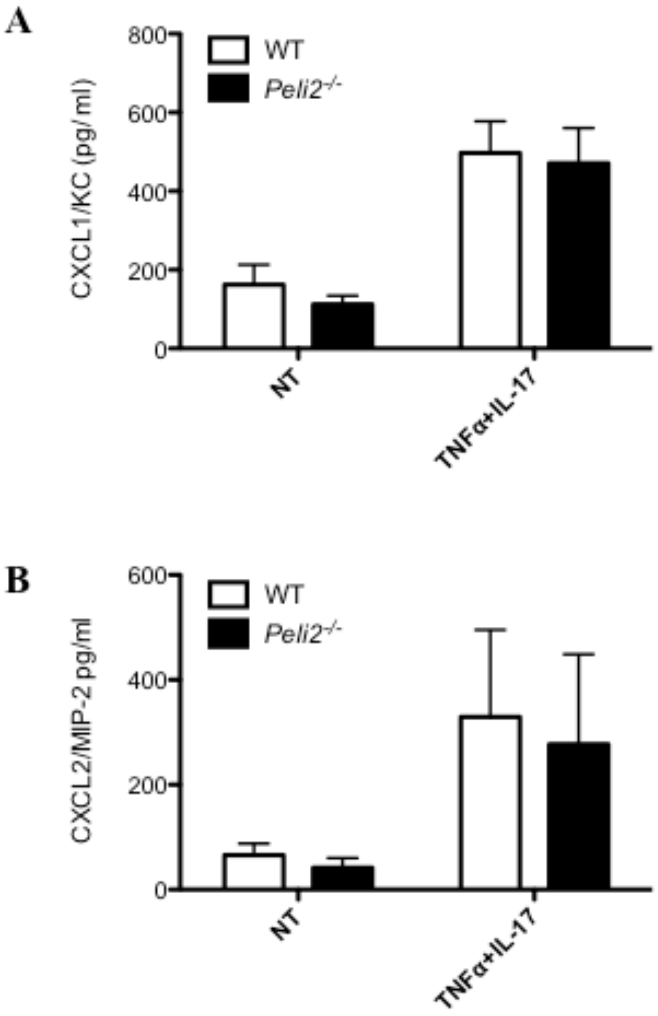

Figure 4.3 Pellino2 deficiency does not affect chemokine production by macrophages

BMDMs were generated from wild type and Pellino2-deficient mice. Cells were treated with TNFα (50 ng/ml) and IL-17 (100 ng/ml) for 2 hours. The level of CXCL1 and CXCL2 in the supernatants was measured by ELISA. Significance tested using paired, two-tailed Student's t-test. Data presented as the mean of 3 independent experiments. Error bars, s.e.m.

4.2.3 Pellino2 deficiency does not affect neutrophil migration ability in response to CXCL2 *in vitro*

Given the important role of neutrophils in the development of emphysema and their reduced recruitment in Pellino2-deficient mice, we examined if Pellino2 played a direct role in the migratory capacity of neutrophils. Neutrophils derived from the bone marrow of wild type and Pellino2-deficient mice were subjected to a transwell migration assay to study their migration along a CXCL2 chemokine gradient (fig. 4.4). In the absence of a chemokine gradient, neither wild type nor Pellino2-deficient neutrophils migrated into the lower well of the transwell. Wild type neutrophils migrated strongly along the CXCL2 chemokine gradient with approximately 2 $x10^5$ cells migrating into the lower chamber in 3 hours. A similarly high level of neutrophil migration through the transwell was observed for Pellino2-deficient mice suggesting that Pellino2 does not play a cell intrinsic role in the neutrophil migratory response to the chemoactivity of chemokines like CXCL2.

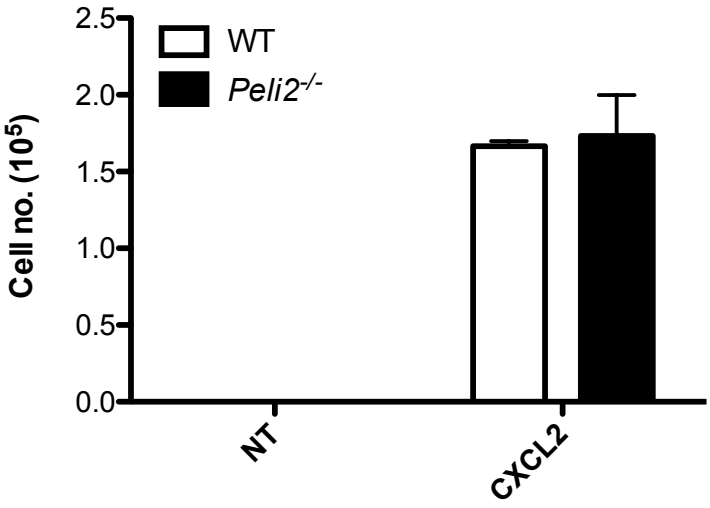

Figure 4.4 Pellino2 deficiency does not affect neutrophil migration in response to CXCL2

Neutrophils were isolated by magnetic activated cell sorting from bone marrow of wild type and Pellino2-deficient mice. Cells were plated in the upper well of a transwell plate. Cells were either non-treated (NT) or 50 ng/ml of CXCL2 was added to the lower well and after 3 hours the number of cells that had migrated from the upper well to the lower well were counted using an automated cell counter. Significance tested using paired, two-tailed Student's t-test. Data presented as the mean of 3 independent experiments. Error bars, s.e.m.

4.2.4 Pellino2 deficiency does not affect the ability of neutrophils to produce pro-inflammatory cytokines in response to classical neutrophil activators

Given that Pellino2 does not affect the migratory capacity of neutrophils the functionality of Pellino2-deficient neutrophils was next examined. Bone marrow derived neutrophils were stimulated with activating ligands namely IFNγ and zymosan, and neutrophil activation was monitored by measuring IL-6 (fig. 4.5A) and TNFα (fig. 4.5B) production by ELISA. Stimulation of wild type neutrophils with these ligands led to strong induction of IL-6 and TNFα but this response was fully intact in Pellino2-deficient neutrophils.

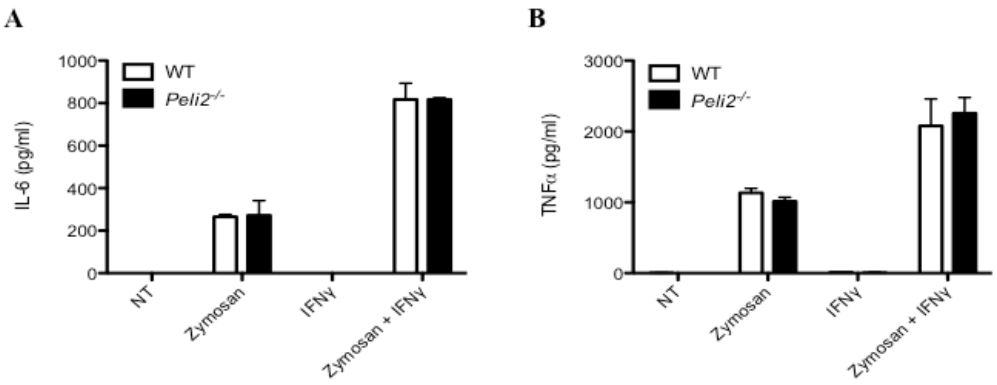

Figure 4.5 Pellino2 deficiency does not affect the ability of neutrophils to produce pro-inflammatory cytokines in response to classical activation

Neutrophils were isolated from bone marrow of wild type and Pellino2-deficient mice. Cells were primed with IFNγ (150 Ug/ml) for 2 hours followed by zymosan (200 μg/ml) for 24 hours. Supernatants were collected and analysed for the presence of pro-inflammatory cytokines (A) IL-6 and (B) TNFα and by ELISA. Significance tested by paired, two-tailed Student's t-test. Data presented as the mean of 3 independent experiments. Error bars, s.e.m.

4.2.5 Pellino2 mediates IL-1β production in response to NLRP3 inflammasome activation

Given the diminished inflammatory response of Pellino2-deficient mice to intranasal elastase, we next examined if Pellino2 deficiency affects NLRP3 inflammasome mediated IL-1β production in neutrophils. Wild type and Pellino2-deficient neutrophils stimulated with LPS and ATP lead to NLRP3 inflammasome activation and production and release of IL-1β as measured by ELISA (fig. 4.6A). The absence of Pellino2 caused a ~50% reduction in IL-1β induction compared with wild type neutrophils when the NLRP3 inflammasome was activated. This is similar to results seen for Pellino2-deficient macrophages (fig. 3.12). Importantly, following stimulation with LPS alone or LPS and ATP, wild type and Pellino2-deficient neutrophils produce similarly high levels of IL-6 and TNFα as measured by ELISA (fig. 4.6B and fig. 4.6C). This demonstrates that as seen previously, Pellino2 is mediating IL-1β production via the NLRP3 inflammasome.

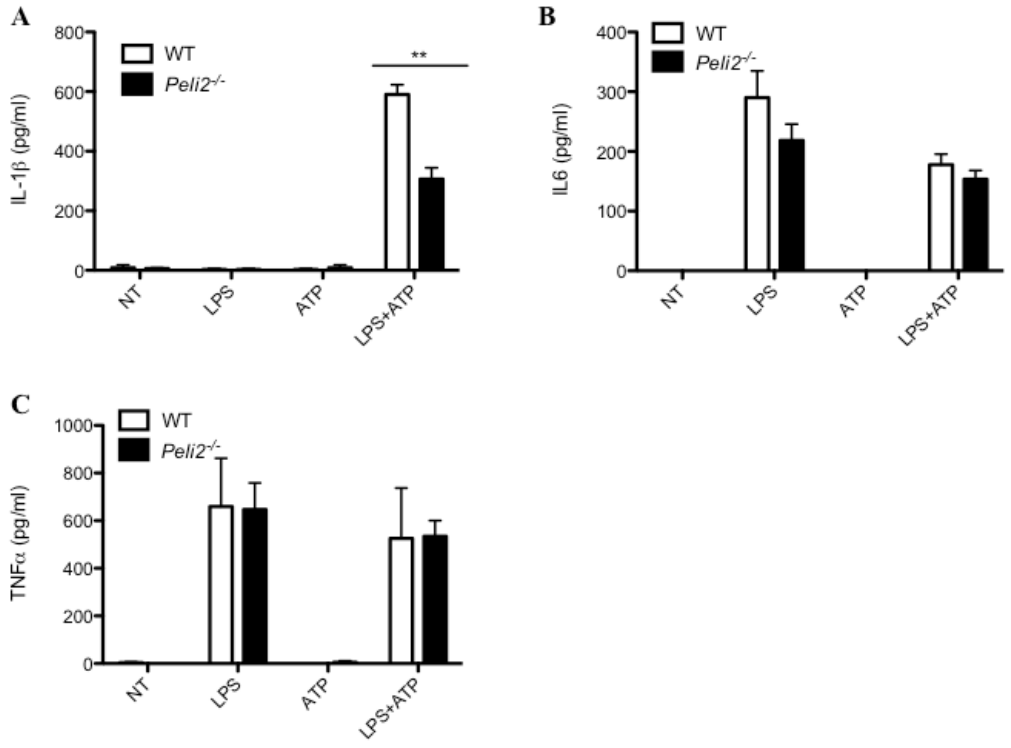

Figure 4.6 Pellino2 deficiency affects the ability of neutrophils to produce IL-1β in response to NLRP3 inflammasome activation

Neutrophils were isolated from the bone marrow of wild type and Pellino2-deficient mice. Cells were then treated with LPS (100 ng/ml) for 3 hours before treatment with ATP (5 mM) for 45 minutes to activate the NLRP3 inflammasome. Supernatants were collected and analysed for the presence of (A) IL-1β, (B) IL-6 and (C) TNFα by ELISA. ** $p < 0.001$ (paired Student's t-test). Data presented as the mean of 3 independent experiments. Error bars, s.e.m.

4.2.6 Pellino2 deficiency does not affect elastase-induced apoptosis in the lungs

Whilst the impairment of secretion of IL-1β in Pellino2-deficient mice is likely a key contributing factor to the reduced inflammation in elastase-challenged mice, we were also keen to explore other pathways that may contribute to elastase-induced pathology Apoptosis is thought to be the main cause of alveolar destruction in elastase-induced emphysema and induction of apoptosis alone can lead to emphysema in mice (Matsuyama *et al*., 2016). A member of the Pellino family, Pellino3 has been previously shown to interact with RIP1 and mediate apoptosis (Yang *et al*. 2013). It was therefore examined if Pellino2 may mediate apoptosis in response to intranasal elastase. Wild type and Pellino2-deficient mice were treated with intranasal elastase and culled after 24 hours. The lungs were fixed in formalin and terminal deoxynucleotide transferase (TdT) dUTP nick-end labelling (TUNEL) assay was carried out (fig. 4.7A). TUNEL assay identifies apoptotic cells by labelling blunt ends of double-stranded DNA breaks, which occur during apoptosis. In the assay carried out here, labelled double-stranded DNA breaks are marked by green fluorescence. A small number of apoptotic cells were present in the lungs of wild type and Pellino2-deficient mice treated with PBS. 24 hours after elastase instillation into the lungs there was a 3-4 fold increase in the number of apoptotic cells in wild type and Pellino2-deficient mice (fig. 4.7B). The level was similar in both wild type and Pellino2-deficient mice suggesting Pellino2 does not play a role in apoptosis, at least in the context of elastase instillation in the lung.

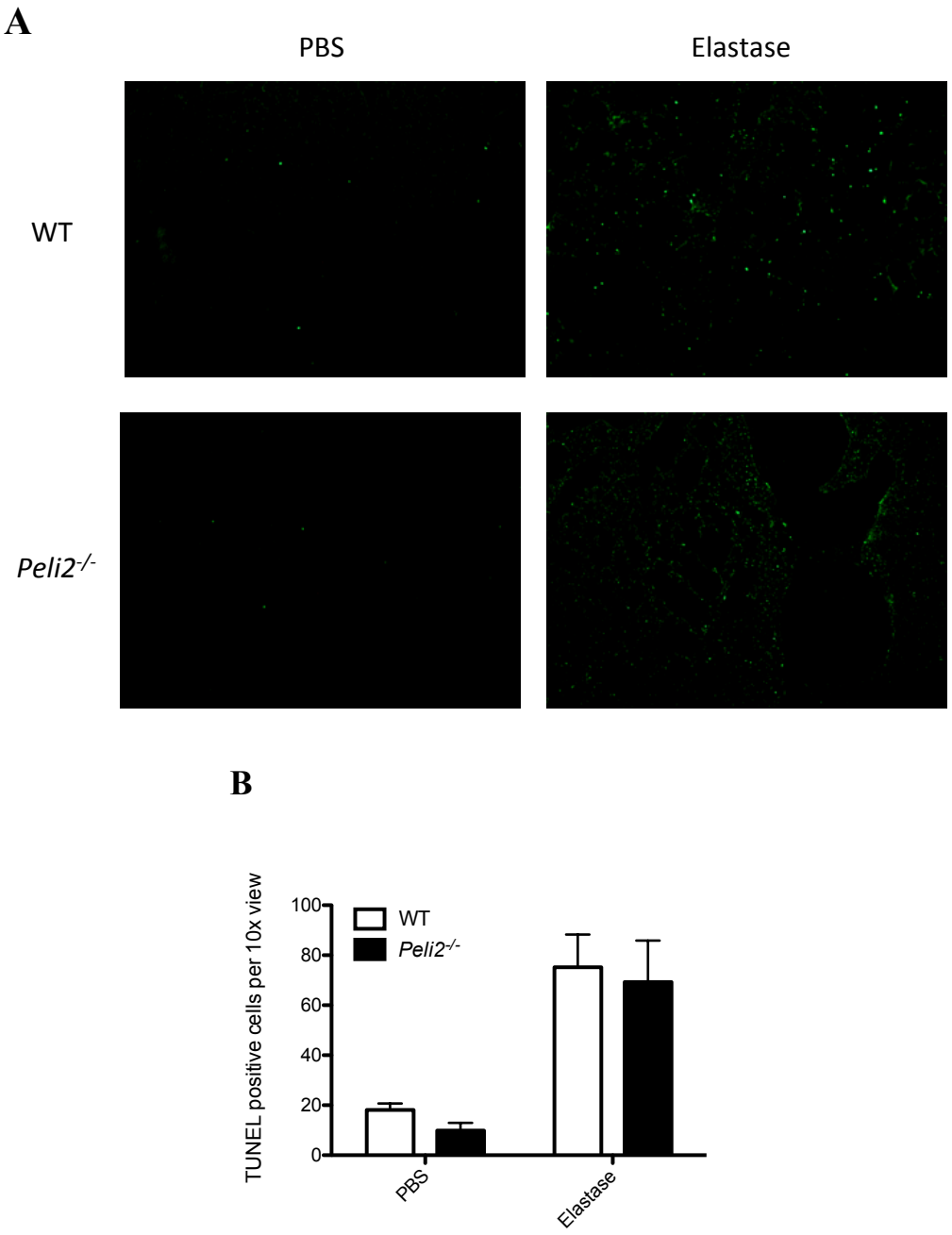

Figure 4.7 Effect of Pellino2 deficiency on apoptosis in response to intranasal elastase instillation

Wild type and Pellino2-deficient mice were treated intranasally with 35µg elastase in 50µl PBS or 50µl PBS alone and culled 24 hours later. (A) The lungs were removed and fixed in formalin before embedding in paraffin wax. 4µm sections were cut and stained using TUNEL for double stranded DNA nicks that indicate apoptotic cells. Apoptotic cells fluoresce green in and were viewed at 10x magnification by microscopy. (B) Number of positive/fluorescing

cells per 10x view was quantified. Significance tested using paired, two-tailed Student's t-test. Data representative of 4 mice per control group and 5 mice per elastase group. Error bars, s.e.m.

4.2.7 Pellino2 deficiency does not directly affect necroptosis in response to intranasal elastase

Necroptosis is another form of cell death which has been previously implicated in the development of emphysema (Mizumura *et al*., 2014). It involves the kinases RIP1, RIP3 and MLKL forming a complex called the necrosome. Since RIP1 is ubiquitinated by Pellino1 (Chang *et al*., 2009) with the latter also being recently implicated in regulating necroptosis (Choi *et al*., 2018; H. Wang *et al*., 2017) coupled with our group showing Pellino3 to ubiquitinate RIP2, another member of the RIP family of proteins (Yang *et al*. 2013) the next study investigated if Pellino2 could be involved in mediating necroptosis in the lungs in response to elastase. Wild type and Pellino2-deficient mice were treated intranasally with elastase and culled 24 hours later. Lung homogenates were analysed by immunoblotting for markers of necroptosis, phospho-MLKL and RIP3 (fig. 4.8A). Phospho-MLKL or RIP3 were not detected in wild type mice treated with PBS but were basally upregulated in Pellino2-deficient mice. Upon treatment with elastase, wild type mice showed increased levels of phospho-MLKL and RIP3 in the lungs indicative of higher levels of necroptosis. In Pellino2-deficient mice treated with elastase, both phospho-MLKL and RIP3 could be detected in the lungs but not at the same high levels as wild type mice suggesting that Pellino2 may impair the pro-necroptotic effects of elastase. This was examined in more detail since necrotic forms of cell death can promote strong inflammatory responses and so any reduced necroptosis in Pellino2-deficient mice may contribute to impaired inflammation.

In order to assess if Pellino2 has a cell intrinsic role in regulating necroptosis, studies were performed to compare the effects of necroptotic stimuli on BMDMs derived from wild type and Pellino2-deficient mice. Necroptosis is induced by combined treatment of cells with LPS, the IAP (inhibitor of apoptosis) inhibitor BV6 and the pan caspase inhibitor ZVAD. BMDMs were thus treated with ZVAD (1μM), LPS (100 ng/ml) and BV6 (1μM) for 24 hours. Cell lysates were analysed by immunoblotting for phospho-MLKL and RIP3 expression (fig. 4.8B). No basal expression of either phospho-MLKL or RIP3 was detected in wild type or Pellino2-deficient BMDMs. Upon stimulation of BMDMs with BV6, ZVAD+LPS, BV6+LPS or BV6+LPS+ZVAD, increased levels of phospho-MLKL and RIP3 were detected with their magnitude of activation being comparable in wild type and Pellino2-deficient BMDMs. This suggests that Pellino2 does not directly regulate necroptosis and that any differences in levels of necroptosis in the lungs of elastase-treated wild type and Pelllino2-deficient mice are due to indirect and secondary effects. To verify that Pellino2 does not play a role in necroptosis in the lungs however, it may be of interest to examine necroptosis in isolated epithelial or lung cells from Pellino2-deficient mice.

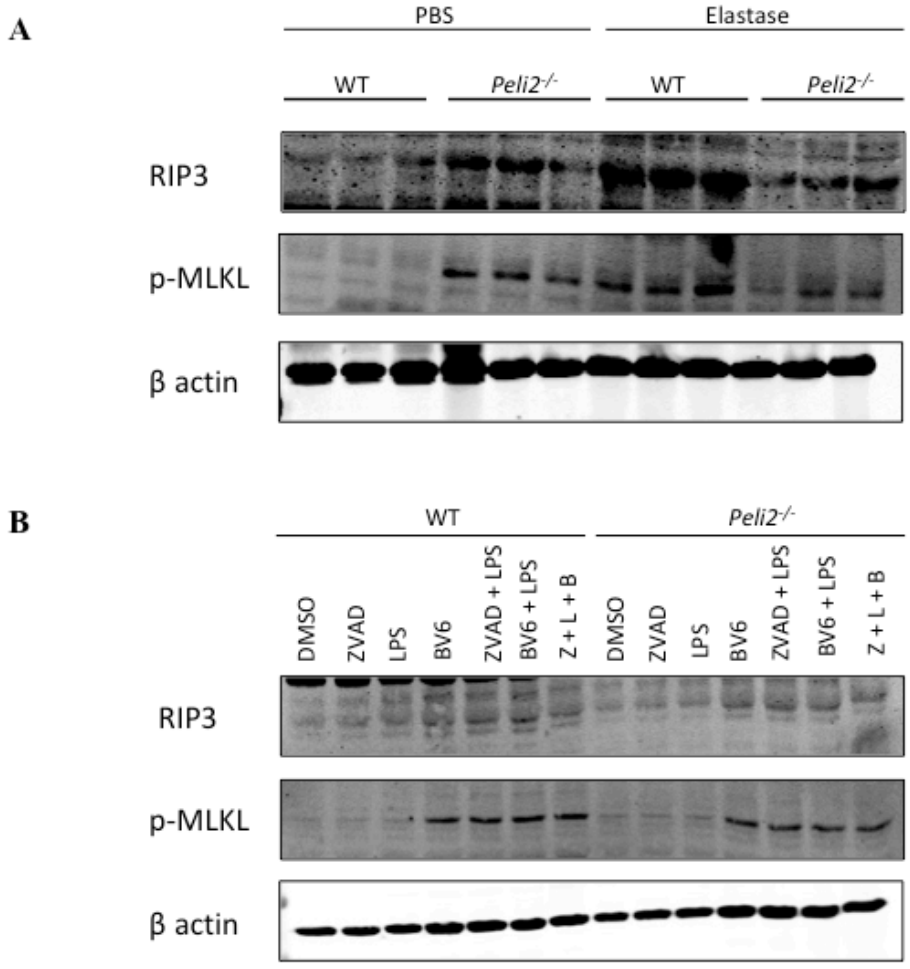

Figure 4.8 Effect of Pellino2 deficiency on induction of necroptosis

(A) Wild type and Pellino2-deficient mice were treated intranasally with 35μg elastase in 50μl PBS or 50μl PBS alone and culled 24 hours later. Lung homogenates from wild type and Pellino2-deficient mice treated with intranasal elastase for 24 hours were analysed by immunoblot using anti-phospho MLKL and anti-RIP3 antibodies. (B) BMDMs generated from wild type and Pellino2-deficient mice were pre-treated with ZVAD (1μM) for 1 hour, then LPS (100 ng/ml) for 2 hours and BV6 (1μM) for 24 hours, either alone or in combination. Cell lysates were analysed by immunoblot with anti-phospho MLKL and anti-RIP3 antibodies. For (A) and (B), anti-βactin antibody was used as a loading control. Results representative of 2 independent experiments.

4.2.8 Label-free LC-MS/MS analysis of normal wild type versus Pellino2-deficient mice lungs

In an effort to add further molecular insight into the role of Pellino2 in lung inflammation and injury, comparative proteomic profiling of the lungs of wild type and Pellino2-deficient mice was carried out using label-free mass spectrometry. Mass spectrometry analysis in the following sections was provided by Dr. Ashling Holland. Protein identification and analysis was performed using MaxQuant and Perseus. Relative protein levels in the lungs were compared between the control group (PBS treated) wild type mice and Pellino2-deficient mice. In the lungs of Pellino2-deficient mice, there was a change in abundance of 15 proteins with a fold change $\geq \pm 2$ as compared with wild type mouse lungs. Of the 15 proteins, 7 proteins were decreased in abundance and 8 were increased in abundance in Pellino2-deficient mouse lungs when compared to wild type mouse lungs (fig 4.9).

The proteins identified as having changed abundance when comparing Pellino2-deficient mouse lungs to wild type mouse lungs were next analysed using the bioinformatics database PANTHER to give a list of molecular functions (fig 4.10A). For wild type versus Pellino2-deficient mice, the functions of proteins with changed abundance in the lungs are mostly involved binding activity. These proteins included skeletal muscle isoform of myosin regulatory light chain 2, mitochondrial glutaryl-CoA dehydrogenase, reticulocalbin-3, and Ig kappa chain C region and fibrinogen beta chain. A large number of proteins of changed abundance were also involved in catalytic activity. Proteins with this function included enolase-phosphatase E1, glycylpeptide N-tetradecanoyltransferase 1 and protein AMBP. A smaller proportion

of the proteins with changed abundance had structural molecule activity, such as fibulin-1 or transporter activity, such as signal transducing adaptor molecule 1. The proteins of particular interest here that were decreased in abundance in Pellino2-deficient mouse lungs are serine protease inhibitorA3K, alpha-1-antitrypsin 1-4 and protein AMBP. These proteins have protease inhibitor functions. Since these anti-proteases were downregulated basally in Pellino2-deficient mouse lungs as compared to wild type mouse lungs, it may make Pellino2-deficient mice more susceptible to elastase-induced emphysema.

Using the PANTHER database again, we next classified the proteins of changed abundance in Pellino2-deficient mouse lungs into different protein classes (fig 4.10B). There were a broad array of protein classes represented in the proteins of changed abundance and they did not appear to cluster to any one class in particular. From the most abundant protein class to the least abundant protein class, these included: calcium-binding proteins, cytoskeletal proteins, enzyme modulators, hydrolases, membrane trafficking proteins, oxidoreductases, signalling molecules, transferases and transporters. The most abundant protein class was calcium-binding proteins which included skeletal muscle isoform of myosin regulatory light chain 2 and reticulocalbin-3. The second most abundant protein class was cytoskeletal proteins which included mitochondrial glutaryl-CoA dehydrogenase and glycylpeptide N-tetradecanoyltransferase 1. This was surprising since Pellino proteins have not previously been known to regulate the expression of any calcium-binding or cytoskeletal proteins but such changes may reflect secondary effects of Pellino2 deficiency.

Protein name	Gene name	Fold change
Myosin regulatory light chain 2, skeletal muscle isoform	Mylpf	+3.7
Enolase-phosphatase E1	Enoph1	+2.9
Protein mago nashi homolog	Magoh	+2.9
Glutaryl-CoA dehydrogenase, mitochondrial	Gcdh	+2.7
Receptor-type tyrosine-protein phosphatase C	Ptprc	+2.7
Reticulocalbin-3	Rcn3	+2.7
Signal transducing adapter molecule 1	Stam	+2.2
Glycylpeptide N-tetradecanoyltransferase 1	Nmt1	+2.2
Alanine aminotransferase 1	Gpt	-1.8
Ig mu chain C region	Ighm	-2.0
Fibrinogen beta chain	Fgb	-2.0
Ig gamma-1 chain C region secreted form	Ighg1	-2.1
Ig gamma-2A chain C region secreted form	N/A	-2.1
Ig kappa chain C region	N/A	-2.1
Ig kappa chain V-III region PC 3741/TEPC 111	N/A	-3.0
Protein AMBP	Ambp	-4.7

Figure 4.9 Differentially expressed proteins in lungs from wild type and Pellino2 – deficient mice.

Wild type and Pellino2-deficient mice were treated intranasally with PBS. After 24 hours the mice were culled and the lungs were removed. The lungs were homogenised and prepared for analysis by label-free mass spectrometry. Proteins with a greater than 2 fold change in expression when comparing Pellino2-deficient mouse lungs to wild type mouse lungs were searched and analysed with MaxQuant and Perseus. + denotes a protein with increased abundance in Pellino2-deficient mouse lungs as compared to wild type mouse lungs. – denotes a protein with decreased abundance in Pellino2-deficient mouse lungs as compared to wild type mouse lungs.

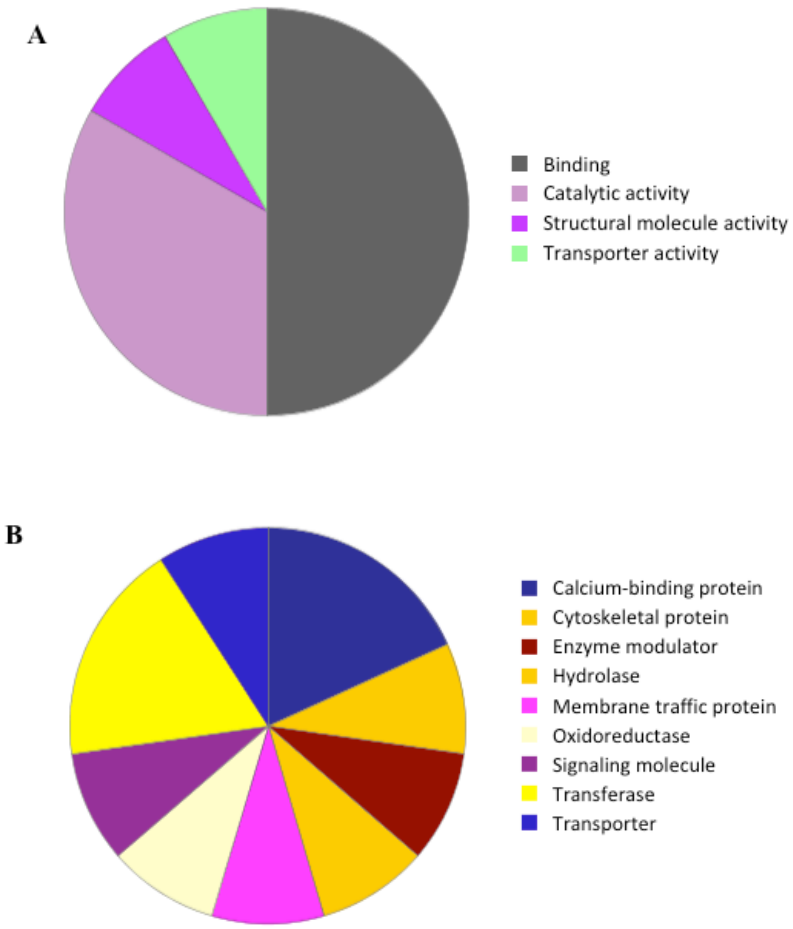

Figure 4.10 Molecular function and protein class of proteins with altered abundance in Pellino2-deficient mouse lungs as compared to wild type mouse lungs

The publicly available PANTHER database was used to cluster (A) molecular functions and (B) protein classes of MS-identified proteins with altered abundance (fig. 4.9) in the absence of Pellino2 when comparing wild type and Pellino2-deficient mouse lungs.

4.2.9 Label-free LC-MS/MS analysis of wild type versus Pellino2-deficient mouse lungs 24 hours after intranasal elastase administration

We next examined the relative proteomic profiles of the lungs of wild type and Pellino2-deficient mice 24 hours after intranasal elastase instillation. 24 hours after elastase instillation, Pellino2-deficient mouse lungs differentially expressed 60 proteins with a fold change ≥ ±2 when compared to wild type mouse lungs 24 hours after elastase instillation. Of the 60 proteins, 19 were increased in abundance (fig. 4.11) and 41 were decreased in abundance (fig. 4.12) in Pellino2-deficient mouse lungs as compared with wild type mouse lungs. The proteins of changed abundance were next analysed using the bioinformatics database PANTHER to give a list of molecular functions (fig. 4.13A). The proteins changed in abundance in Pellino2-deficient mouse lungs compared to wild type mouse lungs cover a range of molecular functions. Most of the proteins with changed abundance were involved in catalytic activity, such as cathepsin G, inter-alpha-trypsin inhibitor heavy chain 4, neutrophil elastase and myeloperoxidase. Many proteins of changed abundance were also involved in binding activity, such as neutrophil gelatinase-associated lipocalin, S100A8, S100A9 and inter-alpha-trypsin inhibitor heavy chain 3. A smaller proportion of proteins of changed abundance were involved in antioxidant activity, such as glutaredoxin-1, receptor activity, such as receptor expression enhancing protein-5 and transporter activity, such as transportin-1.

Using the PANTHER database again, we next examined proteins of changed abundance for their categorisation in protein classes (fig. 4.13B). The classes of proteins represented by the proteins of changed abundance included enzyme

modulators, hydrolases, calcium binding proteins, cell adhesion molecules, defence/immunity proteins, extracellular matrix proteins, isomerases, membrane traffic proteins, nucleic acid binding proteins, oxidoreductases, receptors, signalling molecules, storage proteins, carrier proteins transferases and transporters. The most highly represented protein classes were enzyme modulators and hydrolases. Enzyme modulators included proteins such as inter-alpha-trypsin inhibitor heavy chain 3, inter-alpha-trypsin inhibitor heavy chain 4 and serine protease inhibitor A3. Hydrolases include proteins such as cathepsin G, neutrophil elastase, myeloblastin and lactotransferrin. These results suggest that Pellino2 mediates expression the above enzymes either directly or indirectly.

Protein name	Gene name	Fold change
Zinc finger protein 638	Znf638	+9.9
GTP-binding protein SAR1a	Sar1a	+4.3
Sortilin	Sort1	+3.9
Fibulin-1	Fbln1	+3.8
ADP-ribosylation factor-like protein 1	Arl1	+3.5
60S ribosomal protein L32	Rpl32	+3.1
Carnitine O-acetyltransferase	Crat	+3.1
Histone H3.1	Hist1h3a	+2.8
Scaffold attachment factor B1	Safb	+2.8
CAAX prenyl protease 1 homolog	Zmpste24	+2.8
3-beta-hydroxysteroid-Delta(8),Delta(7)-isomerase	Ebp	+2.5
Lethal(2) giant larvae protein homolog 2	Llgl2	+2.3
Pulmonary surfactant-associated protein C	Sftpc	+2.3
Vacuolar protein sorting-associated protein 26A	Vps26a	+2.2
ATP-binding cassette sub-family A member 3	Abca3	+2.1
Prostaglandin F2 receptor negative regulator	Ptgfrn	+2.1
ADP-ribosylation factor 6	Arf6	+2.0
Regulator of microtubule dynamics protein 3	Rmdn3	+2.0
UDP-glucuronosyltransferase 1-6	Ugt1a6	+2.0

Figure 4.11 List of proteins increased in abundance in Pellino2-deficient mouse lungs after 24-hour elastase treatment as compared to wild type mouse lungs after 24-hour elastase treatment

Wild type and Pellino2-deficient mice were treated intranasally with 35μg elastase in 50μl PBS. After 24 hours the mice were culled and the lungs were removed. The lungs were homogenised and prepared for analysis by label-free mass spectrometry. Proteins with a greater than 2 fold change in expression when comparing Pellino2-deficient mouse lungs to wild type mouse lungs were searched and analysed with MaxQuant and Perseus. + denotes a protein with increased abundance in Pellino2-deficient mouse lungs as compared to wild type mouse lungs.

Protein name	Gene name	Fold change
Angiotensinogen	Agt	-2.0
Pulmonary surfactant-associated protein D	Sftpd	-2.0
Ferritin heavy chain	Fth1	-2.0
Integrin beta-2	Itgb2	-2.1
Inter alpha-trypsin inhibitor, heavy chain 4	Itih4	-2.1
Chitinase-3-like protein 1	Chi3l1	-2.1
Ras-related C3 botulinum toxin substrate 2	Rac2	-2.1
Retinol-binding protein 4	Rbp4	-2.1
Inter-alpha-trypsin inhibitor heavy chain H3	Itih3	-2.3
Rho GDP-dissociation inhibitor 2	Arhgdib	-2.3
L-amino-acid oxidase	Il4i1	-2.4
Ig gamma-1 chain C region secreted form	Ighg1	-2.5
Alpha-1-acid glycoprotein 1	Orm1	-2.6
Cathepsin G	Ctsg	-2.6
Haptoglobin	Hp	-2.7
Interferon-induced protein with tetratricopeptide repeats 3	Ifit3	-2.7
Protein phosphatase inhibitor 2	Ppp1r2	-2.8
Ig kappa chain V-III region PC 7210	N/A	-2.9
Serine protease inhibitor A3M	Serpina3m	-2.9
Serum amyloid A-1 protein	Saa1	-2.9
Mitochondrial peptide methionine sulfoxide reductase	Msra	-3.0
Serine protease inhibitor A3K	Serpina3k	-3.0
Inosine-5'-monophosphate dehydrogenase 2	Impdh2	-3.2
Chitinase-like protein 3	Chil3	-3.4
Matrix metalloproteinase-9	Mmp9	-3.4
Neutrophil cytosol factor 2	Ncf2	-3.5
Peptidoglycan recognition protein 1	Pglyrp1	-4.0
Lactotransferrin	Ltf	-4.0
Myeloperoxidase	Mpo	-4.4
Serum amyloid A-2 protein	Saa2	-4.7
Serine protease inhibitor A3N	Serpina3n	-4.8
Cathelicidin antimicrobial peptide	Camp	-4.9
CD177 antigen	Cd177	-5.0
Serum amyloid P-component	Apcs	-5.5
Integrin alpha-M	Itgam	-5.7
Neutrophil elastase	Elane	-6.0
Neutrophilic granule protein	Ngp	-6.0
Myeloblastin	Prtn3	-6.1
Neutrophil gelatinase-associated lipocalin	Lcn2	-6.1
Protein S100-A9	S100a9	-7.8
Protein S100-A8	S100a8	-8.8

Figure 4.12 List of proteins decreased in abundance in Pellino2-deficient mouse lungs after 24-hour elastase treatment as compared to wild type mouse lungs after 24-hour elastase treatment

Wild type and Pellino2-deficient mice were treated intranasally with 35μg elastase in 50μl PBS. After 24 hours the mice were culled and the lungs were removed. The lungs were homogenised and prepared for analysis by label-free mass spectrometry. Proteins with a greater than 2 fold change in expression when comparing Pellino2-deficient mouse to wild type mouse lungs were searched and analysed with MaxQuant and Perseus. – denotes a protein with decreased abundance in Pellino2-deficient mouse lungs as compared to wild type mouse lungs.

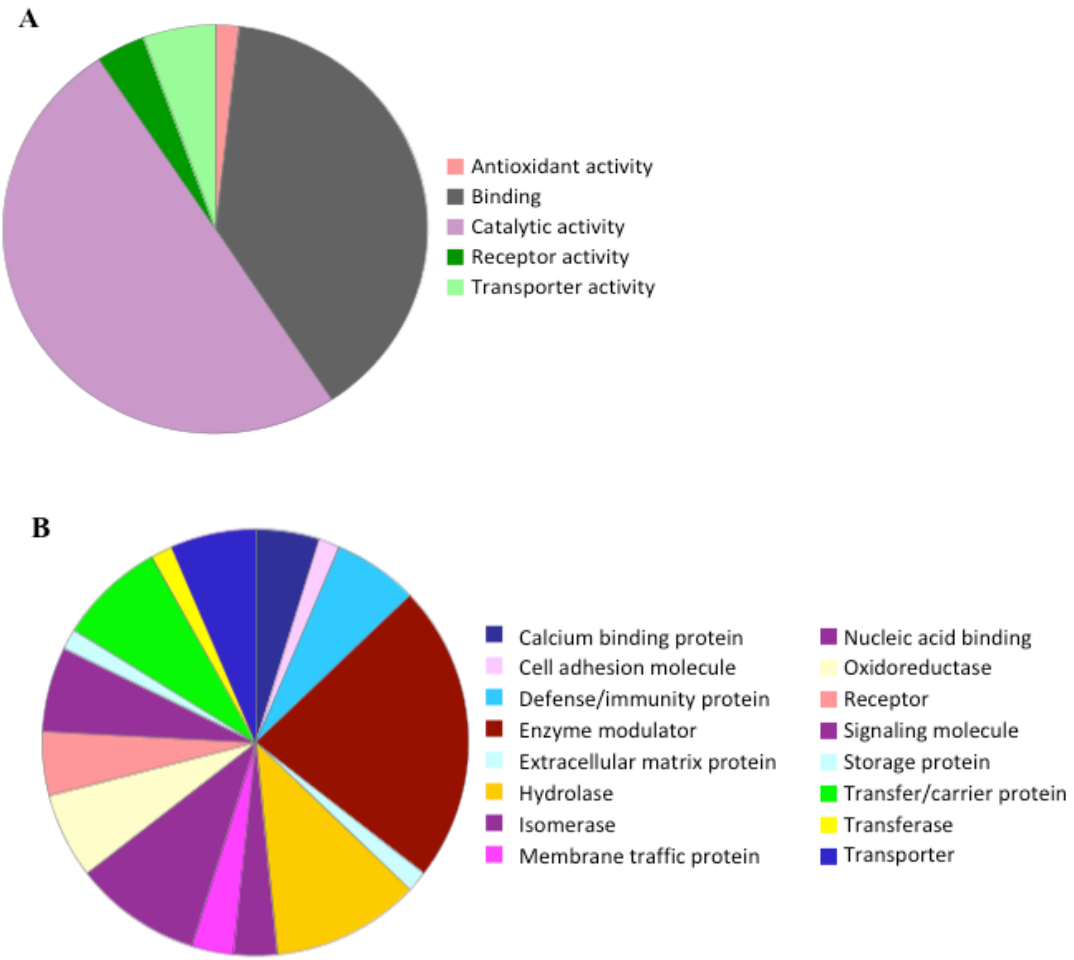

Figure 4.13 Molecular function and protein class of proteins with altered abundance in Pellino2-deficient mouse lungs as compared to wild type mouse lungs following 24-hour elastase treatment

The publicly available PANTHER database was used to cluster (A) molecular functions and (B) protein classes of MS-identified proteins with altered abundance (fig. 4.11 and fig. 4.12) in the absence of Pellino2 when comparing wild type mouse lungs after 24 hour elastase treatment and Pellino2-deficient mouse lungs after 24 hour elastase treatment.

4.2.10 Label-free LC-MS/MS analysis of wild type versus Pellino2-deficient mice lungs after 14 days of repeated intranasal PBS or elastase administration

Given our previous findings that Pellino2-deficient mice develop more fibrosis and experience greater weight loss in response to elastase-induced emphysema than wild type mice, we next compared the proteomic profile of wild type mouse lungs and Pellino2-deficient mouse lungs after 14 days of repeated intranasal elastase administration. After induction of elastase-induced emphysema, Pellino2-deficient mouse lungs differentially expressed 48 proteins with a fold change of $\geq \pm 1.5$ as compared with wild type mouse lungs after elastase-induced emphysema. Of the 48 proteins, 16 were increased (fig. 4.14) in abundance and 32 were decreased in abundance (fig. 4.15) in Pellino2-deficient mouse lungs compared with wild type mouse lungs after elastase-induced emphysema.

The proteins identified as having changed abundance when comparing Pellino2-deficient mouse lungs to wild type mouse lungs following elastase-induced emphysema were next analysed using the bioinformatics database PANTHER to give a list of molecular functions (fig 4.16). The proteins changed in abundance in Pellino2-deficient mouse lungs compared to wild type mouse lungs cover a range of molecular functions, including catalytic activity, binding activity, structural molecules activity, transporter activity, receptor activity, translation regulator activity, antioxidant activity and signal transducer activity. Most of the proteins of changed abundance were found to have catalytic activity and include MMP-9, neutrophil elastase and myeloperoxidase. There were also a high number of proteins found to have binding activity, such as neutrophil gelatinase associated lipocalin, S100A9 and

complement component 1Q subcomponent-binding protein. Many of the proteins of changed abundance are associated with neutrophils. This is consistent with our earlier studies showing diminished neutrophil infiltration in Pellino2-deficient mice in response to elastase challenge.

Protein name	Gene name	Fold change
Parvalbumin alpha	Pvalb	+8.8
Complement component 1 Q subcomponent-binding protein, mitochondrial	C1qbp	+4.1
SUMO-conjugating enzyme UBC9	Ube2i	+3.9
Receptor expression-enhancing protein 5	Reep5	+2.5
RNA-binding protein FUS	Fus	+2.3
Myc box-dependent-interacting protein 1	Bin1	+2.2
Glycogen phosphorylase, muscle form	Pygm	+2.0
Claudin-18	Cldn18	+1.7
Paralemmin-1	Palm	+1.7
Carbonic anhydrase 1	Ca1	+1.7
Adenylate kinase isoenzyme 1	Ak1	+1.6
Ganglioside GM2 activator	Gm2a	+1.6
Calmodulin	Calm1	+1.5
Eukaryotic translation initiation factor 4E	Eif4e	+1.5
Lymphocyte-specific protein 1	Lsp1	+1.5
60S ribosomal protein L38	Rpl38	+1.5

Figure 4.14 List of proteins decreased in abundance in Pellino2-deficient mouse lungs after repeated elastase instillations over 14 days as compared to wild type mouse lungs after repeated elastase instillations over 14 days.

Wild type and Pellino2-deficient mice were treated intranasally with 35μg elastase in 50μl PBS 6 times over 14 days. After 14 hours the mice were culled and the lungs were removed. The lungs were homogenised and prepared for analysis by label-free mass spectrometry. Proteins with a greater than 2 fold change in expression when comparing Pellino2-deficient mice to wild type mice were searched and analysed with MaxQuant and Perseus. + denotes a protein with increased abundance in Pellino2-deficient mouse lungs as compared to wild type mouse lungs.

Protein name	Gene name	Fold change
Complement factor B	Cfb	-1.5
Complement C4-B	C4b	-1.5
40S ribosomal protein S5	Rps5	-1.5
Glutamate--cysteine ligase regulatory subunit	Gclm	-1.5
MICOS complex subunit Mic19	Chchd3	-1.5
Fibrinogen alpha chain	Fga	-1.5
Fibrinogen gamma chain	Fgg	-1.6
NADH dehydrogenase [ubiquinone] 1 alpha subcomplex subunit 2	Ndufa2	-1.6
Inter-alpha-trypsin inhibitor heavy chain H3	Itih3	-1.7
Integrin alpha-M	Itgam	-1.7
Glia maturation factor gamma	Gmfg	-1.8
Coagulation factor XIII A chain	F13a1	-1.9
Myeloblastin	Prtn3	-1.9
Secretory carrier-associated membrane protein 3	Scamp3	-2.0
NAD-dependent malic enzyme, mitochondrial	Me2	-2.0
Protein S100-A8	S100a8	-2.5
Alpha-1-acid glycoprotein 1	Orm1	-2.5
Hexokinase-3	Hk3	-2.5
Haptoglobin	Hp	-2.7
Glycerol-3-phosphate phosphatase	Pgp	-2.8
Lactotransferrin	Ltf	-2.8
Arachidonate 12-lipoxygenase, 12S-type	Alox12	-2.8
Tax1-binding protein 3	Tax1bp3	-2.8
Matrix Gla protein	Mgp	-2.9
Neutrophilic granule protein	Ngp	-3.0
Cathelicidin antimicrobial peptide	Camp	-3.3
Neutrophil gelatinase-associated lipocalin	Lcn2	-3.5
Myeloperoxidase	Mpo	-3.8
Protein S100-A9	S100a9	-4.7
Fatty acid-binding protein, adipocyte	Fabp4	-4.9
Neutrophil elastase	Elane	-5.3
Matrix metalloproteinase-9	Mmp9	-7.7

Figure 4.15 List of proteins decreased in abundance in Pellino2-deficient mouse lungs after repeated elastase instillations over 14 days as compared to wild type mouse lungs after repeated elastase instillations over 14 days.

Wild type and Pellino2-deficient mice were treated intranasally with 35µg elastase in 50µl PBS 6 times over 14 days. After 14 hours the mice were culled and the lungs were removed. The lungs were homogenised and prepared for analysis by label-free mass spectrometry. Proteins with a greater than 2 fold change in expression when comparing Pellino2-deficient

mice to wild type mice were searched and analysed with MaxQuant and Perseus. – denotes a protein with decreased abundance in Pellino2-deficient mouse lungs as compared to wild type mouse lungs.

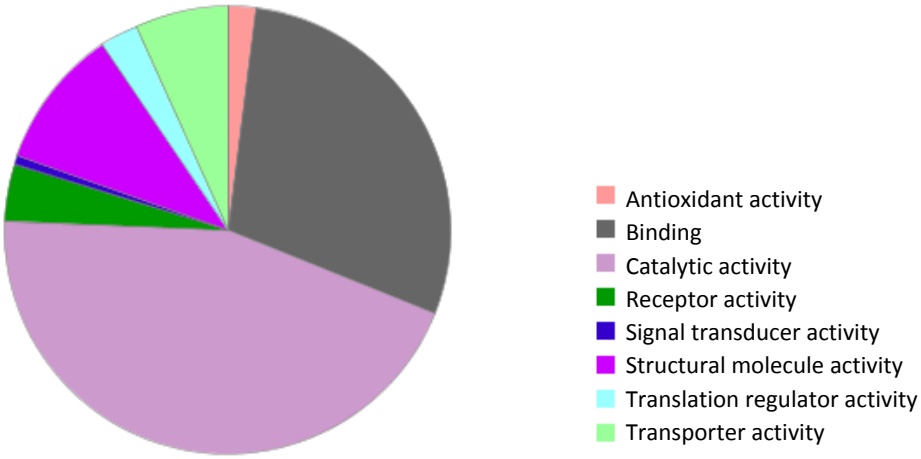

Figure 4.16 Molecular function of proteins with altered abundance in Pellino2-deficient mouse lungs as compared to wild type mouse lungs following repeated elastase instillations over 14 days

The publicly available PANTHER database was used to cluster molecular functions of MS-identified proteins with altered abundance (fig. 4.14 and fig. 4.15) in the absence of Pellino2 when comparing wild type mouse lungs after 6 elastase instillations over 14 days and Pellino2-deficient mouse lungs after 6 elastase instillations over 14 days.

4.2.11 Proteins with altered abundance in Pellino2-deficient mouse lungs at 24 hours and 14 days post initial elastase instillation compared to wild type mouse lungs at 24 hours and 14 days post initial elastase instillation

Given there were many common proteins of changed abundance when comparing Pellino2-deficient mouse lungs to wild type mouse lungs after both 24 hours elastase treatment and induction of elastase-induced emphysema at 14 days, a comparison of the proteins changed in abundance at both 24 hours and 14 days post initial elastase instillation was carried out (fig. 4.17). 27 proteins were changed in abundance in Pellino2-deficient mouse lungs compared to wild type mouse lungs after both 24 hours and 14 days post instillation elastase instillation. These proteins included acute phase proteins: S100A8, S100A9, alpha-1-acid glycoprotein and haptoglobin. These proteins are associated with inflammation and may indicate that Pellino2-deficient mouse lungs are a less inflammatory environment than wild type mouse lungs in response to single or repeated doses of elastase. Further to this end, components of the complement system such as complement factor and integrin alpha M were also decreased in abundance in Pellino2-deficient mouse lungs compared to wild type mouse lungs. The complement system is part of the immune system which is involved in orchestrating the immune response and sensing 'danger' signals (Ricklin *et al*., 2010). This further demonstrates the diminished immune response in the lungs of Pellino2-deficient mice in response to elastase.

Neutrophil associated proteins were also decreased in abundance at both 24 hours and 14 days post initial elastase instillation. These proteins included neutrophilic granule protein, neutrophil gelatinase associated lipocalin, myeloblastin- proteinase-3,

neutrophil elastase, MMP-9 and cathelicidin antimicrobial peptide. Given the flow cytometry data (fig. 4.1) that indicates there were lower levels of neutrophil infiltration into the lungs of Pellino2-deficient mice compared to wild type mice in response to elastase treatment, this would suggest that lower levels of neutrophil infiltration are sustained in Pellino2-deficient mice in response to repeated doses of elastase. Again, this favours a less inflammatory response to elastase in Pellino2-deficent mice than in wild type mice.

Interestingly, proteins involved in would repair such as fibrinogen alpha chain and fibrinogen gamma chain were decreased in abundance in Pellino2-deficient mice and this may underlie the increased fibrosis apparent in these mice 14 days after elastase challenge. The anti-inflammatory protein Annexin-1 was also decreased in abundance in Pellino2-deficient mice. Importantly, a number of anti-protease proteins were decreased in abundance in Pellino2-deficient mice. These include inter-alpha-trypsin inhibitor heavy chain H3, leukocyte elastase inhibitor A and alpha-1- antitrypsin 1-4. Given that in humans, deficiency in anti-proteases alone can lead to emphysema and a new focus for treating emphysema is on administration of anti-proteases (McElvaney *et al*., 2017), it is possible that in Pellino2-deficient mice, a combination of exogenous protease administration and a deficiency in anti-proteases and wound repair proteins could lead to the worsened emphysema phenotype seen in our studies despite a lack of inflammation.

The only proteins that were increased in abundance in Pellino2-deficient mice compared with wild type mice after both 24 hours and 14 days post initial elastase instillation are Claudin-18 and receptor expression enhancing protein-5. Claudin-18 is

a tight junction protein that is important in the maintenance of alveolar epithelial barriers (Li *et al*., 2014). Increased expression of Claudin-18 in Pellino2-deficient mouse lungs may be as a result of the increased damage seen in the lungs during elastase-induced emphysema as compared to wild type mice (fig. 3.5 and fig. 3.7). This suggests a possible role for Pellino2 in regulation of tight junctions that may warrant further investigation. The role of receptor expression enhancing protein-5 is not clear.

Alpha-1 antitrypsin 1-4 and lymphocyte specific protein-1 are two proteins of interest because they were decreased in abundance in Pellino2-deficient mouse lungs compared with wild type mouse lungs 24 hours after elastase treatment but increased in abundance after 14 days elastase treatments. Alpha-1 antitrypsin 1-4 is a protease inhibitor and lymphocyte specific protein-1 is thought to play a role in neutrophil migration (Le *et al*., 2015). Again, it is not clear whether this indicates a change towards neutrophil recruitment in Pellino2-deficient mice after 14 days of elastase treatment and may suggest Pellino2-deficient mice have a delayed inflammatory response. Given the range of inflammation-associated proteins that are consistently decreased in abundance in Pellino2-deficient mice after both 24 hours and 14 days post initial elastase instillation, it is unlikely to be the case.

	Fold change	
Protein name	**24 hours**	**14 days**
Protein S100-A9	-7.8	-4.7
Lactotransferrin	-4	-2.8
Fibrinogen gamma chain	-1.8	-1.6
Guanine deaminase	-1.7	-1.4
Neutrophil gelatinase-associated lipocalin	-6.1	-3.5
Haptoglobin	-2.7	-2.7
Myeloperoxidase	-4.4	-3.8
Protein S100-A8	-8.8	-2.5
Myeloblastin	-6.1	-1.9
Neutrophil elastase	-6	-5.3
Alpha-1-acid glycoprotein 1	-2.6	-2.5
Inter-alpha-trypsin inhibitor heavy chain H3	-2.3	-1.7
Cathelicidin antimicrobial peptide	-4.9	-3.3
Complement factor B	-1.6	-1.5
Neutrophilic granule protein	-6	-3
Fibrinogen alpha chain	-1.9	-1.5
Ribose-5-phosphate isomerase	-1.6	-1.3
Integrin alpha-M	-5.7	-1.7
Leukocyte elastase inhibitor A	-1.8	-1.4
Inosine-5'-monophosphate dehydrogenase 2	-3.2	-1.4
Matrix metalloproteinase-9	-3.4	-7.7
Alpha-1-antitrypsin 1-4	-1.8	+1.3
Annexin A1	-1.7	-1.3
Carbonic anhydrase 1	-1.7	+1.7
Lymphocyte-specific protein 1	-1.5	+1.5
Claudin-18	+1.5	+1.7
Receptor expression-enhancing protein 5	+1.7	+2.5

Figure 4.17 Proteins with altered abundance at both 24 hours and 14 days after initial elastase instillation in the absence of Pellino2

List of proteins with altered abundance at 24 hours and 14 days post initial elastase instillation in the absence of Pellino2 identified in fig. 4.11, fig. 4.12, fig. 4.14 and fig. 4.15. + denotes a protein with increased abundance in Pellino2-deficient mouse lungs as compared to wild type mouse lungs. – denotes a protein with decreased abundance in Pellino2-deficient mouse lungs as compared to wild type mouse lungs.

4.3 Discussion

The results in chapter 3 from *in vivo* experiments using the elastase induced-emphysema model in Pellino2-deficient mice suggested an important role for Pellino2 in the regulation of inflammatory processes in the lung. The molecular and cellular basis to the effects of Pellino2 was probed in this part of the study by analysis of the initial inflammatory response to *in vivo* elastase administration, *in vitro* methods and identification of proteins with changed abundance in Pellino2-deficient mouse lungs compared with wild type mouse lungs after treatment with elastase for 24 hours and 14 days.

Cellular infiltration into the lungs is a common feature of the elastase-induced emphysema model (Barnes, 2004). Given the reduction in inflammation in Pellino2-deficient mice 24 hours after intranasal elastase instillation, it was hypothesised that Pellino2-deficient mice may experience lower levels of cellular infiltration into the lungs following intranasal elastase treatment as compared to wild type mice. Cellular infiltration was examined by flow cytometry. Myeloid cell migration and B-cell migration into the lungs was significantly reduced in Pellino2-deficient mice compared to wild type mice 24 hours after elastase instillation (fig. 4.1 and fig. 4.2 (B)). This correlates with data showing that in the absence of Pellino2, mice have a diminished inflammatory response to overnight elastase treatment with a significant reduction in pro-inflammatory cytokine production (fig. 3.1). Given that the levels of the chemokine CXCL1/KC were diminished in Pellino2-deficient mice in response to elastase treatment as compared with wild type mice, studies were performed to assess

if Pellino2 is involved in mediating cellular migration directly or whether it has a cell-intrinsic role in regulating the expression of chemokines.

Neutrophil migration ability was examined using a transwell plate, where neutrophils migrate towards a chemokine source. This protocol has been previously demonstrated as an effective way of assessing neutrophil migration (Kanayama *et al*., 2015). Neutrophils from Pellino2-deficient mice showed the same migratory capacity as neutrophils from wild type mice (fig. 4.4) in response to the chemokine CXCL2. Therefore it was next examined if the reduced cellular infiltration seen in elastase-induced emphysema was due to reduced chemokine production in Pellino2-deficient cells. To examine chemokine production, CXCL1 production was driven by treatment of macrophages with TNFα and IL-17 production. The synergistic effects of IL-17 and TNFα have been shown previously to drive CXCL1 production albeit in endothelial cells (Griffin *et al*., 2012). For the purposes of this investigation both CXCL1 and CXCL2 production was assessed using this treatment. The expression levels of CXCL1 and CXCL2 (fig. 4.3) were not affected in Pellino2-deficient macrophages examined *in vitro*. Macrophages were used for chemokine investigations because although T-cells, neutrophils and airway epithelial cells are involved in production of pro-inflammatory cytokines in emphysema, macrophages are a source major source of these inflammatory mediators (Wynn and Vannella, 2016).

As Pellino2 did not appear to be involved in mediating neutrophil migration directly or regulating chemokine production, the role of Pellino2 in mediating pro-inflammatory responses in neutrophils was next examined. Stimulation of neutrophils with classically activating factors caused induction of IL-6 and TNFα to similarly

high levels in wild type and Pellino2-deficient neutrophils (fig. 4.5). However, stimulation with NLRP3 inflammasome activating factors resulted in strong expression of IL-1β in wild type neutrophils but expression was significantly reduced in Pellino2-deficient neutrophils (fig. 4.6A). Expression of IL-6 and TNFα was similar in wild type and Pellino2-deficient neutrophils (fig. 4.6B and fig. 4.6C). This led to the conclusion that similar to macrophages, Pellino2 mediates NLRP3 inflammasome induced IL-1β expression in neutrophils. We hypothesise that reduced NLRP3 inflammasome mediated IL-1β production in the absence of Pellino2 may lead to reduced pro-inflammatory cytokine expression and cellular infiltration in Pellino2-deficient mice following intranasal elastase treatment.

This is supported by studies carried out in IL-1R-deficient mice. IL-1R-deficient mice have a diminished inflammatory response to overnight elastase treatment, with low expression levels of IL-1β, TNFα, CXCL1/KC and IL-6 and reduced neutrophil infiltration as compared to wild type mice (Couillin *et al*., 2009). This study also demonstrated that the NLRP3 inflammasome is important for the production of IL-1β in response to elastase treatment in mice. This demonstrates that lower levels of IL-1β signalling can lead to reduced pro-inflammatory cytokine expression and cellular infiltration in response to elastase which may explain the diminished inflammatory response seen in Pellino2-deficient mice. To further test the role of NLRP3-mediated IL-1β in elastase-induced emphysema, experiments could be carried out where mice are treated with an IL-1R antagonist such as Anakinra or drugs which specifically block the NLRP3 inflammasome such as MCC950 following elastase instillation (Chen *et al*., 2018). Comparison of the phenotypes observed in these treatment

groups to that of Pellino2-deficient mice would further verify a role for Pellino2 in elastase-induced emphysema as a mediator of IL-1β production.

The effect of Pellino2 deficiency on other processes involved in the development of emphysema such as cell death was also examined. Apoptosis is a programmed form of cell death that is important in the development of elastase-induced emphysema (Hou *et al*., 2013). As such, it was hypothesised that Pellino2 may be playing a role in regulation of cell death which may lead to the altered phenotype of elastase-induced emphysema seen in Pellino2-deficient mice. Examination of levels of apoptosis using TUNEL assay, however, showed no difference between wild type and Pellino2-deficient mice in response to elastase (fig. 4.7). These studies gave insight into the unique functionality of the Pellino family of proteins as it appears Pellino2 does not regulate apoptosis at least in response to elastase in the lungs whilst previous studies from our research group have detailed an important regulatory role for Pellino3 in controlling TNFα-mediated apoptosis (Yang *et al*., 2013b).

Necroptosis is an inflammatory form of cell death that has also been implicated in emphysema development (Weinlich *et al*., 2016). Recent reports have described contrasting roles for Pellino1 in necroptosis (Choi *et al*., 2018; H. Wang *et al*., 2017) and Pellino3 has also been shown to interact with RIP1 and RIP2 (Yang *et al*., 2013b, 2013a). Necroptosis employs another RIP protein, RIP3. Given the similarity in structure of Pellino proteins it was examined if Pellino2 could be involved in regulation of RIP protein activation in the context of necroptosis. Lung homogenates from wild type and Pellino2-deficient mouse lungs were examined for expression of markers of necroptosis after overnight elastase treatment. Lung homogenates showed

that basally, markers of necroptosis were higher in Pellino2-deficient mice than in wild type mice. Following overnight elastase treatment, this was reversed and wild type mice expressed higher levels of necroptosis markers than Pellino2-deficient mice (fig. 4.8A). This suggested that Pellino2 may be regulating necroptosis. However, *in vitro* studies showed that Pellino2 did not have a cell intrinsic role in mediating necroptosis in macrophages (fig. 4.8B) suggesting that any differences in necroptotic markers may arise as secondary effects of Pellino2 deficiency. To further confirm that Pellino2 does not play a role in regulating necroptosis in the lungs, it would be important to carried out necroptotic studies on alveolar macrophages and epithelial cells of the lungs.

Given our studies showed that neutrophil migration, chemokine production and cell death were not affected by the absence of Pellino2, a more global approach was taken to explore the molecular basis of the reduction in inflammation and exacerbation of pathology of elastase induced emphysema in Pellino2-deficient mice. It was hypothesised that a change in protein profiles would be observed in Pellino2-deficient mice as compared to wild type mice basally and also following elastase treatment. Label free mass spectrometry was used to compare the proteomic profiles of wild type and Pellino2-deficient mouse lungs after control treatment (PBS), 24 hour elastase treatment and after induction of elastase-induced emphysema. Mass spectrometry analysis of control lungs identified a number of proteins that are changed in abundance in Pellino2-deficient mouse lungs as compared to wild type mouse lungs. Of note, fibrinogen β chain is decreased in abundance. Fibrinogen β chain is a primary component of blood clots. It is involved in wound repair as it guides cell migration during re-epithelialisation (Zuliani-Alvarez and Midwood, 2015). It may

also facilitate the immune response of innate and T-cells (Luo *et al*., 2013). As fibrinogen β is involved in both wound repair and facilitation of immune response, it is not surprising that in Pellino2-deficient mice where fibrinogen β chain is expressed at a lower basal level compared to wild type mice, that Pellino2-deficient mice appear to be more susceptible to injury and produce a reduced inflammatory response to elastase.

There are also an array of anti-proteases decreased in abundance in Pellino2-deficient mice as compared to wild type mice. The anti-proteases that are basally decreased in abundance in Pellino2-deficient mouse lungs are serine protease inhibitor A3K, alpha1 anti-trypsin 1-4 and protein AMBP, also known as inter-α-trypsin inhibitor. We hypothesise that lower expression levels of anti-proteases and protease inhibitors in Pellino2-deficient mice may leave these mice more susceptible to lung injury by proteases. Evidence to support this hypothesis is demonstrated by a genetic mutation in alpha1 anti-trypsin 1-4 being associated associated with spontaneous development of emphysema in humans and in mice (Borel *et al*., 2018; Greene *et al*., 2016). Protein AMBP has the greatest decrease in abundance in Pellino2-deficient mouse lungs compared to wild type mouse lungs. It is involved in inhibiting the action of trypsin as well as plasmin and lysosomal granulytic elastase (Atmani and Khan, 1995; Pastushkova *et al*., 2013). The comparatively lower levels of anti-protease expression seen basally in Pellino2-deficient mouse lungs are maintained following elastase-treatment. The anti-proteases with lower expression in Pellino2-deficient mice as compared to wild type mice following elastase treatment include inter-alpha-trypsin inhibitor heavy chain 3, inter-alpha trypsin inhibitor heavy chain 4 and serine protease inhibitor A3N. This further suggests that decreased expression of anti-proteases or

protease inhibitors in Pellino2-deficient mice both basally and after elastase treatment may leave Pellino2-deficient mice susceptible to more severe elastase-induced emphysema as there are less inhibitors to counteract the effects of exogenous elastase.

An analysis of proteins found to be decreased in abundance in Pellino2-deficient mouse lungs compared to wild type mouse lungs at 24 hours and 14 days post initial elastase instillation also provides some explanation as to the higher level of fibrosis associated with elastase-induced emphysema in Pellino2-deficient mice (fig. 3.7). Inter-alpha trypsin inhibitor and leukocyte elastase inhibitor A are both decreased in abundance in Pellino2-deficient mouse lungs at both timepoints. Reduced levels of these protease inhibitors, along with basally reduced levels of anti-proteases and protease inhibitors in Pellino2-deficient mouse lungs may allow for elastase to cause more damage than in wild type mouse lungs as seen in mice with a mutated alpha-1-antitrypsin gene (Borel *et al*., 2018). As the decrease in abundance of some protease inhibitors is sustained from 24 hours to 14 days after initial elastase instillation, the effects of their absence may be more pronounced despite the modest reduction in their expression in Pellino2-deficient mice.

Along with this hypothesised increased susceptibility to elastase induced damage in Pellino2-deficient mouse lungs due to lower levels of anti-protease expression, α, β and γ chains of fibrinogen are decreased in abundance in Pellino2-deficient mouse lungs at both timepoints also. As fibrinogen is involved in wound closure, repair and re-epithelialisation, lower expression levels may result in the higher levels of fibrosis (fig. 3.7) seen in Pellino2-deficient mice following elastase-induced emphysema. These data suggests that Pellino2 may directly or indirectly mediate expression

fibrinogen which has been associated with lung fibrosis using experimental animals models (Hattori *et al.,* 2000). It could be hypothesised that Pellino2 may play a role in regulation of the fibrosis in the lungs. This could be tested using a well-characterised model of lung fibrosis such as the bleomycin model (Carrington *et al*., 2018) in Pellino2-deficient mice.

24 hours after elastase treatment Pellino2-deficient mice show a number of neutrophil associated proteins also decreased in abundance as compared to wild type mice. These include MMP-9, neutrophil elastase, myeloperoxidase and neutrophil gelatinase associated lipocalin. This is most likely a direct result of lower levels of neutrophil infiltration into the lungs of Pellino2-deficient mice compared with wild type following elastase treatment (fig. 4.1 and fig. 4.2). The decreased abundance of neutrophil associated proteins seen 24 hours after elastase treatment in Pellino2-deficient mouse lungs as compared to wild type mouse lungs is sustained for up to 14 days after induction of elastase-induced emphysema. Proteins such as MMP-9, neutrophil elastase and myeloperoxidase are still decreased in abundance in Pellino2-deficient mice. Given that at 24 hours after elastase treatment, a decrease in abundance of neutrophil associated proteins in Pellino2-deficient mice correlates with decreased neutrophil infiltration as compared to wild type mice, it suggests that a reduced level of neutrophil infiltration is sustained after elastase-induced emphysema in Pellino2-deficient mice.

Some acute phase inflammatory proteins are decreased in abundance at 24 hours and 14 days post initial elastase instillation in Pellino2-deficient mouse lungs compared to wild type mouse lungs. These include S100A8 and S100A9. S100A8 and S100A9 are

constitutively expressed in the cytosol of neutrophils and expressed by macrophages in inflamed tissue (Foell *et al*., 2006). There is abundant evidence that S100A8 and S100A9 are involved in neutrophil migration. S100A8 is a chemotactic factor for neutrophils (Yano *et al*., 2010) and S100A9 promotes neutrophil adhesion (Anceriz *et al*., 2007). This has been demonstrated by injection of purified human S100A8 and S100A9 into the air pouch of mice leading to increased neutrophil recruitment to the site of injection (Ryckman *et al*., 2003). The lower levels of S100A8 and S100A9 therefore correlates with the lower levels of neutrophils seen in Pellino2-deficient mouse lungs following elastase treatment as compared to wild type mice. Pellino2 may be regulating the expression of S100A8 and S100A9 in response to elastase either directly or indirectly through reduced immune cell migration.

These data suggests a new role for Pellino proteins in regulation of anti-protease expression even at a basal level. It also suggests a role for Pellino proteins in regulation of tissue repair associated proteins such as fibrinogen. These are new regulatory roles for Pellino2 that have not been previously documented and suggest that Pellino proteins may be involved in regulating expression of proteins other than inflammatory signalling molecules. This presents important new insights into Pellino2 biology. It would be necessary to validate these mass spectrometry results by western blot to confirm fold changes in Pellino2-deficient mouse lungs however, this was not carried out due to time constraints of the study.

5 Discussion

5.1 General discussion

Pellino proteins are a family of E3 ubiquitin ligases consisting of Pellino1, Pellino2 and Pellino3. The research question posed in this thesis aimed to examine the role of Pellino2 in the innate immune response with a specific focus on lung immunology. Pellino1 has been implicated in the immune response to rhinovirus (Bennett *et al*., 2012), Pellino2 has been previously implicated in NLRP3 inflammasome function (Humphries *et al*., 2018) and Pellino3 has also been implicated in gut immunology (Yang *et al*. 2013). This thesis built upon the previous roles for Pellino proteins in giving the first physiological role for Pellino2 in lung immunology and demonstrating the non-redundant nature of Pellino2 and Pellino3 proteins.

The role of Pellino2 in regulation of lung immunology was examined using a severe damage model of elastase-induced emphysema, an important component of COPD. Pellino2-deficient mice treated with elastase have a diminished inflammatory response including lower levels of inflammatory cytokines and cell infiltration as compared to wild type mice. We hypothesise that this may be a result of reduced

NLRP3 inflammasome activation in Pellino2-deficient mice as the response seen is similar to the response seen in IL-1R-deficient or ASC-deficient mice (Couillin *et al*., 2009) and Pellino2 has been implicated in positive regulation of NLRP3 inflammasome mediated IL-1β production (Humphries *et al*., 2018). The inflammatory response to intranasal elastase is mediated primarily by macrophages and epithelial cells (Mizgerd, 2008) which in turn leads to recruitment of neutrophils. As Pellino3 has been previously implicated in the immune response of epithelial cells (Yang *et al*. 2013), it may be of relevance to examine the role of Pellino2 in regulating the immune response of epithelial cells specifically.

The data generated here may also suggest that diseases with an exaggerated inflammatory response could benefit by blocking the action of Pellino2, which may prevent excessive cellular infiltration and sterile inflammation. For example, collagen-induced rheumatoid arthritis or antibody-induced rheumatoid arthritis has been extensively modelled in mice (Caplazi *et al*., 2015). Given that Pellino2-deficient mice have normal development, rheumatoid arthritis could be easily modelled in these mice and would allow for the determination of the role for Pellino2 in cellular migration.

Pellino2 deficiency also resulted in exacerbation of pathology associated with elastase-induced emphysema. This was associated with increased weight loss and a higher fibrosis score in Pellino2-deficient mice than wild type mice, despite low levels of inflammation at early timepoints. Typically, where there is reduced inflammation at an early timepoint in response to elastase, emphysema does not develop as severely at a later timepoint. This has been shown in relation to IL-1R-

deficient, MyD88-deficient and ASC-deficient mice (Couillin *et al*., 2009; Lucey *et al*., 2002). These studies used a single dose of elastase whereas the model used here involved administration of several doses of elastase resulting in a more severe phenotype that is thought to resemble the human phenotype of emphysema more closely (Kennelly *et al*., 2016; Lüthje *et al*., 2009). Our results suggest that lack of inflammation at an early timepoint in Pellino2-deficient mice may not be sufficient to prevent development of emphysema where the injurious insult is continually present. One possible explanation for the worsened phenotype seen in the lungs of Pellino2-deficient mice may be that these mice express lower levels of anti-proteases than wild type mice. It has been well established that a protease/anti-protease imbalance leads to degradation of lung tissue (Lomas, 2016). The role of Pellino2 would need to be examined further to identify whether reduced levels of anti-proteases in Pellino2-deficient mice is the result of reduced anti-protease production or if the anti-proteases are misfolded and remain in the liver. It may therefore be of interest to examine the liver for damage in Pellino2-deficient mice before and after elastase administration as reduced alpha1 anti-trypsin in humans is typically the result of misfolded alpha1 anti-trypsin accumulating in the liver leading to autophagy and weight loss (Teckman, 2013).

The lack of inflammation followed by higher levels of fibrosis in Pellino2-deficient mice in response to repeated intranasal elastase administration could also be a result of poor repair responses. The data presented here demonstrated that Pellino2-deficient mice have diminished cellular infiltration in response to elastase at early timepoints as compared to wild type mice and there are lower levels of expression of neutrophil associated proteins in Pellino2-deficient mice after repeated elastase exposure. This

would suggest that cellular infiltration and inflammation are at lower levels in Pellino2-deficient mice in response to elastase as compared to wild type mice, which may prevent repair occurring in the lungs. Landmark studies have demonstrated that macrophage infiltration is crucial for activation of the repair process (Leibovich and Ross, 1975; Polverini *et al*., 1977; Lucas *et al*., 2013). Macrophage derived factors have been shown to promote fibroblast differentiation, regulate ECM remodelling and produce wound-associated VEGF which promotes angiogenesis at wounded sites (Lucas *et al.,* 2013). Without inflammation and infiltration in Pellino2-deficient mice in response to elastase, there is also reduced expression of Annexin A1 which has been previously demonstrated to play a positive role in promoting tissue repair (Perretti and D'Acquisto, 2009). Conditional macrophage depletion has been previously carried out (Lee *et al*., 2014) to study energy homeostasis and may provide a novel mechanism of examining elastase-induced emphysema in wild type mice where macrophage infiltration would not occur. This could provide useful insights into the role of macrophages in wound repair in the lungs and a comparison for the pathology seen in Pellino2-deficient mice following elastase-induced emphysema.

Another possible explanation for the worsened phenotype seen in Pellino2-deficient mice is alluded to by the emerging role for E3 ubiquitin ligases in fibrosis. For example, the E3 ubiquitin ligase fibrosis inducing ligase 1 (FIEL1) stimulates TGFβ signalling and is highly expressed in the lungs of patients with idiopathic pulmonary fibrosis (IPF), a fibrotic lung disease (Lear *et al*., 2016). It was found that a small molecule inhibitor of FIEL1 attenuated fibrosis in mice (Lear *et al*., 2016). This suggests that E3 ubiquitin ligases may be important in development of fibrosis in the lungs. This is further illustrated by the involvement of another E3 ubiquitin ligase

mouse double minute 2 (MDM2) in IPF. MDM2 regulates p53, a protein associated with DNA damage and apoptosis (Kuwano *et al*., 1996). Epithelial cells from IPF patients have significantly higher levels of active p53 and MDM2 expression is also significantly increased in patients with IPF (Nakashima *et al*., 2005). BRCA-1 associated RING domain 1 (BARD1) is an E3 ubiquitin ligase that has been associated with fibrosis development in mice. It was found to be upregulated in bleomycin challenged mouse lungs, a model of fibrosis in the lungs (Baer and Ludwig, 2002). BARD1 is thought to mediate pro-fibrotic functions through regulation of fibroblast proliferation and extracellular matrix deposition (André *et al*., 2015). These studies suggest a role for E3 ubiquitin ligases in regulating fibrosis, which offers a new avenue for investigation into the physiological roles of Pellino proteins. In light of data presented in this thesis, it may be of interest to examine fibrosis in bleomycin challenged Pellino2-deficient mice and ascertain definitively whether Pellino2 plays a role in regulation lung fibrosis.

To further understand the role of Pellino2 in lung immunology, respiratory infection was also examined in our studies. Chronic *P. aeruginosa* respiratory infection commonly occurs in patients with cystic fibrosis and COPD (Emerson *et al*., 2002; Murphy *et al*., 2008). *P. aeruginosa* is antibiotic resistant in nature (Zavascki *et al*., 2010). Therefore, it was examined if Pellino2 is involved in defence against respiratory infection with *P. aeruginosa* as it could act as a novel therapeutic target for treatment of infection. The research carried out here shows that Pellino2 deficiency improves survival in response to acute *P. aeruginosa* respiratory infection in mice. This correlates with reduced bacterial load in the lungs of Pellino2-deficient mice. It is possible that Pellino2 deficiency leads to impaired NLRP3 inflammasome

activation. Interestingly downregulation of NLRP3 leads to improved survival and reduced bacterial load following *P. aeruginosa* respiratory infection in mice (Deng *et al*., 2015; Iannitti *et al*., 2016). The improved survival of Pellino2-deficient mice in response to respiratory infection with *P. aeruginosa* implies that blocking or inhibiting the action of Pellino2 may be useful in the treatment of *P. aeruginosa* infection. Given the antibiotic resistant nature of *P. aeruginosa,* inhibition of Pellino2 offers a novel opportunity for controlling infection. However, the studies carried out here only offer a brief insight into the role of Pellino2 in lung defence against bacterial pathogens. Further work is needed to assess the exact mechanisms by which Pellino2 influences survival in response to respiratory infection.

The work in this thesis has also highlighted that Pellino proteins, although structurally similar carry out significantly different functions. Building on the work of Humphries *et al*. (2018), which showed Pellino2 to regulate the NLRP3 inflammasome, the work here showed that Pellino3 does not share this role. This is important as it demonstrates that Pellino proteins may not carry out redundant functions. This was further illustrated where Pellino3 does not regulate the immune response during elastase-induced emphysema in mice. The results here also further our understanding of the Pellino family of proteins in proposing roles beyond regulation of inflammation. To date, these proteins have been studied mainly in relation to regulation of the immune response. The results here suggest that Pellino2 may be regulating not only inflammation but also anti-protease production and possibly fibrosis, which are distinct cellular processes. Further analysis is needed to conclude and build upon this work regarding the role of Pellino2 in lung immunity however, this thesis has defined a new area of interest for research regarding the Pellino family of proteins.

5.2 Concluding remarks

Research regarding Pellino proteins has focused on their role in regulating the immune response. The work carried out in this thesis, demonstrates a new role for Pellino2 in regulation of the immune response in the lungs in varying capacities. Pellino2 may be important in regulating emphysema induction and progression which has suggested a role beyond inflammation in fibrotic processes, mucin and anti-protease production. These effects may be mediated by regulation of the immune response of epithelial cells but further work is needed to confirm this. Pellino2 may also be an important regulator of colonisation of *P. aeruginosa* in the lungs. As there are limited effective treatments for emphysema and *P. aeruginosa* are antibiotic resistant in nature, this highlights the importance of identifying Pellino2 as a potential novel therapeutic target. Of biochemical interest, this work has shown that Pellino2 and Pellino3 are non-redundant and may serve unique functions regarding inflammasome function and hence emphysema development.

6 Bibliography

Acuner Ozbabacan, S.E., Gursoy, A., Nussinov, R., Keskin, O., 2014. The Structural Pathway of Interleukin 1 (IL-1) Initiated Signaling Reveals Mechanisms of Oncogenic Mutations and SNPs in Inflammation and Cancer. *PLOS Comput. Biol.* **10**, e1003470.

Akira, S., Takeda, K., 2004. Toll-like receptor signalling. *Nat. Rev. Immunol.* **4**, 499–511.

Akira, S., Uematsu, S., Takeuchi, O., 2006. Pathogen recognition and innate immunity. *Cell* **124**, 783–801.

Aksentijevich, I., Nowak, M., Mallah, M., Chae, J.J., Watford, W.T., Hofmann, S.R., Stein, L., Russo, R., Goldsmith, D., Dent, P., Rosenberg, H.F., Austin, F., Remmers, E.F., Balow, J.E., Rosenzweig, S., Komarow, H., Shoham, N.G., Wood, G., Jones, J., Mangra, N., Carrero, H., Adams, B.S., Moore, T.L., Schikler, K., Hoffman, H., Lovell, D.J., Lipnick, R., Barron, K., O'Shea, J.J., Kastner, D.L., Goldbach-Mansky, R., 2002. De novo CIAS1 mutations, cytokine activation, and evidence for genetic heterogeneity in patients with neonatal-onset multisystem inflammatory disease (NOMID): A new member of the expanding family of pyrin-associated autoinflammatory diseases. *Arthritis Rheum.* **46**,

3340–3348.

Alnemri, E.S., 2010. Sensing Cytoplasmic Danger Signals by the Inflammasome. *J. Clin. Immunol.* **30**, 512–519.

Anceriz, N., Vandal, K., Tessier, P.A., 2007. S100A9 MEDIATES NEUTROPHIL ADHESION TO FIBRONECTIN THROUGH ACTIVATION OF β2 INTEGRINS. *Biochem. Biophys. Res. Commun.* **354**, 84–89.

André, P.-A., Prêle, C.M., Vierkotten, S., Carnesecchi, S., Donati, Y., Chambers, R.C., Pache, J.-C., Crestani, B., Barazzone-Argiroffo, C., Königshoff, M., Laurent, G.J., Irminger-Finger, I., 2015. BARD1 mediates TGF-β signaling in pulmonary fibrosis. *Respir. Res.* **16**, 118.

Andrews, T., Sullivan, K.E., 2003. Infections in Patients with Inherited Defects in Phagocytic Function Infections in Patients with Inherited Defects in Phagocytic Function. *Clin. Microbiol. Rev.* **16**, 597–621.

Artis, D., Spits, H., 2015. The biology of innate lymphoid cells. *Nature* **517**, 293.

Ashcroft, T., Simpson, J.M., Timbrell, V., 1988. Simple method of estimating severity of pulmonary fibrosis on a numerical scale. *J. Clin. Pathol.* **41**, 467–470.

Atkinson, J.J., Lutey, B.A., Suzuki, Y., Toennies, H.M., Kelley, D.G., Kobayashi, D.K., Ijem, W.G., Deslee, G., Moore, C.H., Jacobs, M.E., Conradi, S.H., Gierada, D.S., Pierce, R.A., Betsuyaku, T., Senior, R.M., 2011. The Role of Matrix Metalloproteinase-9 in Cigarette Smoke–induced Emphysema. *Am. J. Respir. Crit. Care Med.* **183**, 876–884.

Atkinson, J.J., Senior, R.M., 2003. Matrix Metalloproteinase-9 in Lung Remodeling. *Am. J. Respir. Cell Mol. Biol.* **28**, 12–24.

Atmani, F., Khan, S.R., 1995. Characterization of uronic-acid-rich inhibitor of calcium oxalate crystallization isolated from rat urine. *Urol. Res.* **23**, 95–101.

Aujla, S.J., Chan, Y.R., Zheng, M., Fei, M., Askew, D.J., Pociask, D.A., Reinhart, T.A., McAllister, F., Edeal, J., Gaus, K., Husain, S., Kreindler, J.L., Dubin, P.J., Pilewski, J.M., Myerburg, M.M., Mason, C.A., Iwakura, Y., Kolls, J.K., 2008. IL-22 mediates mucosal host defense against Gram-negative bacterial pneumonia. *Nat. Med.* **14**, 275–281.

Baer, R., Ludwig, T., 2002. The BRCA1/BARD1 heterodimer, a tumor suppressor complex with ubiquitin E3 ligase activity. *Curr. Opin. Genet. Dev.* **12**, 86–91.

Barnes, P., 2004. Mediators of chronic obstructive pulmonary disease. *Pharmacol. Rev.* **56**, 515–548.

Barnes, P.J., Burney, P.G.J., Silverman, E.K., Celli, B.R., Vestbo, J., Wedzicha, J.A., Wouters, E.F.M., 2015. Chronic obstructive pulmonary disease. *Nat. Rev. Dis. Prim.* **1**, 15076.

Barriere, G., Fici, P., Gallerani, G., Fabbri, F., Rigaud, M., 2015. Epithelial Mesenchymal Transition: a double-edged sword. *Clin. Transl. Med.* **4**, 14.

Bartalesi, B., Cavarra, E., Fineschi, S., Lucattelli, M., Lunghi, B., Martorana, P.A., Lungarella, G., 2005. Different lung responses to cigarette smoke in two strains of mice sensitive to oxidants. *Eur. Respir. J.* **25**, 15–22.

Bauernfeind, F.G., Horvath, G., Stutz, A., Alnemri, E.S., MacDonald, K., Speert, D., Fernandes-Alnemri, T., Wu, J., Monks, B.G., Fitzgerald, K.A., Hornung, V., Latz, E., 2009. Cutting Edge: NF-κB Activating Pattern Recognition and Cytokine Receptors License NLRP3 Inflammasome Activation by Regulating NLRP3 Expression. *J. Immunol.* **183**, 787-791.

Bayes, H.K., Ritchie, N.D., Evans, T.J., 2016. Interleukin-17 Is Required for Control of Chronic Lung Infection Caused by Pseudomonas aeruginosa. *Infect. Immun.* **84**, 3507–3516.

Bell, J.K., Askins, J., Hall, P.R., Davies, D.R., Segal, D.M., 2006. The dsRNA binding site of human Toll-like receptor 3. *Proc. Natl. Acad. Sci.* **103**, 8792–8797.

Bell, J.K., Mullen, G.E.D., Leifer, C.A., Mazzoni, A., Davies, D.R., Segal, D.M., 2003. Leucine-rich repeats and pathogen recognition in Toll-like receptors. *Trends Immunol.* **24**, 528–533.

Bennett, J. a., Prince, L.R., Parker, L.C., Stokes, C. a., de Bruin, H.G., van den Berge, M., Heijink, I.H., Whyte, M.K., Sabroe, I., 2012. Pellino-1 Selectively Regulates Epithelial Cell Responses to Rhinovirus. *J. Virol.* **86**, 6595–6604.

Bennett, J.A., Prince, L.R., Parker, L.C., Stokes, C.A., de Bruin, H.G., van den Berge, M., Heijink, I.H., Whyte, M.K., Sabroe, I., 2012. Pellino-1 Selectively Regulates Epithelial Cell Responses to Rhinovirus. *J. Virol.* **86**, 6595–6604.

Betsuyaku, T., Nishimura, M., Takeyabu, K., Tanino, M., Venge, P., Xu, S., Kawakami, Y., 1999. Neutrophil Granule Proteins in Bronchoalveolar Lavage Fluid from Subjects with Subclinical Emphysema. *Am. J. Respir. Crit. Care Med.* **159**, 1985–1991.

Beutler, B., 2000. Tlr4: central component of the sole mammalian LPS sensor. *Curr. Opin. Immunol.* **12**, 20–26.

Bhowmik, A., Seemungal, T.A.R., Sapsford, R.J., Wedzicha, J.A., 2000. Relation of sputum inflammatory markers to symptoms and lung function changes in COPD exacerbations. *Thorax* **55**, 114-120.

Boatright, K.M., Renatus, M., Scott, F.L., Sperandio, S., Shin, H., Pedersen, I.M., Ricci, J.E., Edris, W.A., Sutherlin, D.P., Green, D.R., Salvesen, G.S., 2003. A unified model for apical caspase activation. *Mol. Cell* **11**, 529–541.

Bonfield, T.L., Panuska, J.R., Konstan, M.W., Hilliard, K.A., Hilliard, J.B., Ghnaim,

H., Berger, M., 1995. Inflammatory cytokines in cystic fibrosis lungs. *Am. J. Respir. Crit. Care Med.* **152**, 2111–2118.

Borel, F., Sun, H., Zieger, M., Cox, A., Cardozo, B., Li, W., Oliveira, G., Davis, A., Gruntman, A., Flotte, T.R., Brodsky, M.H., Hoffman, A.M., Elmallah, M.K., Mueller, C., 2018. Editing out five Serpina1 paralogs to create a mouse model of genetic emphysema. *Proc. Natl. Acad. Sci.*

Brass, D.M., Hollingsworth, J.W., Cinque, M., Li, Z., Potts, E., Toloza, E., Foster, W.M., Schwartz, D.A., 2008. Chronic LPS inhalation causes emphysema-like changes in mouse lung that are associated with apoptosis. *Am. J. Respir. Cell Mol. Biol.* **39**, 584–590.

Breyne, K., Cool, S.K., Demon, D., Demeyere, K., Vandenberghe, T., Vandenabeele, P., Carlsen, H., Van Den Broeck, W., Sanders, N.N., Meyer, E., 2014. Non-classical proIL-1beta activation during mammary gland infection is pathogen-dependent but caspase-1 independent. *PLoS One* **9**.

Brown, G.D., Willment, J.A., Whitehead, L., 2018. C-type lectins in immunity and homeostasis. *Nat. Rev. Immunol.* **18**, 374–389.

Bryant-Hudson, K.M., Carr, D.J.J., 2012. CXCL1-deficient mice are highly sensitive to *Pseudomonas aeruginosa* but not Herpes Simplex Virus type 1 corneal infection. *Investigative Opthamology and Visual Science* **53**, 6785-6792.

Buist, A.S., McBurnie, M.A., Vollmer, W.M., Gillespie, S., Burney, P., Mannino, D.M., Menezes, A.M.B., Sullivan, S.D., Lee, T.A., Weiss, K.B., Jensen, R.L., Marks, G.B., Gulsvik, A., Nizankowska-Mogilnicka, E., 2007. International variation in the prevalence of COPD (The BOLD Study): a population-based prevalence study. *Lancet* **370**, 741–750.

Burgel, P.-R., Nesme-Meyer, P., Chanez, P., Caillaud, D., Carré, P., Perez, T., Roche,

N., 2009. Cough and Sputum Production Are Associated With Frequent Exacerbations and Hospitalizations in COPD Subjects. *Chest* **135**, 975–982.

Burney, P., Jithoo, A., Kato, B., Janson, C., Mannino, D., Nizankowska-Mogilnicka, E., Studnicka, M., Tan, W., Bateman, E., KoÇabas, A., Vollmer, W.M., Gislason, T., Marks, G., Koul, P.A., Harrabi, I., Gnatiuc, L., Buist, S., 2014. Chronic obstructive pulmonary disease mortality and prevalence: The associations with smoking and poverty-A bold analysis. *Thorax* **69**, 465–473.

Butler, M.P., Hanly, J.A., Moynagh, P.N., 2007. Kinase-active Interleukin-1 Receptor-associated Kinases Promote Polyubiquitination and Degradation of the Pellino Family. *J. Biol. Chem.* **282**, 29729–29737.

Caplazi, P., Baca, M., Barck, K., Carano, R.A.D., Devoss, J., 2015. Mouse Models of Rheumatoid Arthritis **52**, 819–826.

Cazzola, M., Page, C.P., Calzetta, L., Matera, M.G., 2012. Emerging anti-inflammatory strategies for COPD. *Eur. Respir. J.* **40**, 724–741.

Celhar, T., Pereira-Lopes, S., Thornhill, S.I., Lee, H.Y., Dhillon, M.K., Poidinger, M., Connolly, J.E., Lim, L.H.K., Biswas, S.K., Fairhurst, A.M., 2016. TLR7 and TLR9 ligands regulate antigen presentation by macrophages. *Int. Immunol.* **28**, 223–232.

Celli, B.R., Macnee, W., 2004. Standards for the diagnosis and treatment of patients with COPD : a summary of the ATS / ERS position paper. *Eur. Respir. J.* **23**, 932–946.

Cerceo, E., Deitelzweig, S.B., Sherman, B.M., Amin, A.N., 2016. Multidrug-Resistant Gram-Negative Bacterial Infections in the Hospital Setting: Overview, Implications for Clinical Practice, and Emerging Treatment Options. *Microb. Drug Resist.* **22**, 412–431.

Cerqueira, D.M., Pereira, M.S.F., Silva, A.L.N., Cunha, L.D., Zamboni, D.S., 2015. Caspase-1 but Not Caspase-11 Is Required for NLRC4-Mediated Pyroptosis and Restriction of Infection by Flagellated *Legionella* Species in Mouse Macrophages and In Vivo. *J. Immunol.* **195**, 2303-2311.

Challa, A.A., Stefanovic, B., 2011. A Novel Role of Vimentin Filaments: Binding and Stabilization of Collagen mRNAs. *Mol. Cell. Biol.* **31**, 3773–3789.

Chan, P.P.Y., Wasinger, V.C., Leong, R.W., 2016. Current application of proteomics in biomarker discovery for inflammatory bowel disease. *World J. Gastrointest. Pathophysiol.* **7**, 27–37.

Chang, M., Jin, W., Chang, J.-H., Xiao, Y., Brittain, G., Yu, J., Zhou, X., Wang, Y.-H., Cheng, X., Li, P., Rabinovich, B.A., Hwu, P., Sun, S.-C., 2011. Peli1 negatively regulates T-cell activation and prevents autoimmunity. *Nat. Immunol.* **12**, 1002–1009.

Chang, M., Jin, W., Sun, S.-C., 2009. Peli1 facilitates TRIF-dependent Toll-like receptor signaling and proinflammatory cytokine production. *Nat. Immunol.* **10**, 1089.

Chavarría-Smith, J., Vance, R.E., 2015. The NLRP1 inflammasomes. *Immunol. Rev.* **265**, 22–34.

Chen, K., Eddens, T., Trevejo-Nunez, G., Way, E.E., Elsegeiny, W., Ricks, D.M., Garg, A. V, Erb, C.J., Bo, M., Wang, T., Chen, W., Lee, J.S., Gaffen, S.L., Kolls, J.K., 2016. IL-17 receptor signaling in the lung epithelium is required for mucosal chemokine gradients and pulmonary host defense against K. pneumoniae. *Cell Host Microbe* **20**, 596–605.

Chen, L., Huang, C.F., Li, Y.C., Deng, W.W., Mao, L., Wu, L., Zhang, W.F., Zhang, L., Sun, Z.J., 2018. Blockage of the NLRP3 inflammasome by MCC950

improves anti-tumor immune responses in head and neck squamous cell carcinoma. *Cellular and Molecular Life Sciences* **75**, 2045-2058.

Chen, Y., Li, C., Weng, D., Song, L., Tang, W., Dai, W., Yu, Y., Liu, F., Zhao, M., Lu, C., Chen, J., 2014. Neutralization of interleukin-17A delays progression of silica-induced lung inflammation and fibrosis in C57BL/6 mice. *Toxicol. Appl. Pharmacol.* **275**, 62–72.

Chen, Z., Andreev, D., Oeser, K., Krljanac, B., Hueber, A., Kleyer, A., Voehringer, D., Schett, G., Bozec, A., 2016. Th2 and eosinophil responses suppress inflammatory arthritis. *Nat. Commun.* **7**, 11596.

Chmiel, J.F., Berger, M., Konstan, M.W., 2002. The role of inflammation in the pathophysiology of CF lung disease. *Clin. Rev. Allergy Immunol.* **23**, 5–27.

Cho, M.H., McDonald, M.-L.N., Zhou, X., Mattheisen, M., Castaldi, P.J., Hersh, C.P., DeMeo, D.L., Sylvia, J.S., Ziniti, J., Laird, N.M., Lange, C., Litonjua, A.A., Sparrow, D., Casaburi, R., Barr, R.G., Regan, E.A., Make, B.J., Hokanson, J.E., Lutz, S., Dudenkov, T.M., Farzadegan, H., Hetmanski, J.B., Tal-Singer, R., Lomas, D.A., Bakke, P., Gulsvik, A., Crapo, J.D., Silverman, E.K., Beaty, T.H., 2014. Risk loci for chronic obstructive pulmonary disease: a genome-wide association study and meta-analysis. *Lancet Respir. Med.* **2**, 214–225.

Choi, K., Lee, Y.S., Lim, S., Choi, H.K., Lee, C., Lee, E., Hong, S., Kim, I., Kim, S., Park, S.H., 2006. Smad6 negatively regulates interleukin 1-receptor – Toll-like receptor signaling through direct interaction with the adaptor Pellino-1. *Nat. Immunol.* **7**, 1057–1065.

Choi, S.-W., Park, H.-H., Kim, S., Chung, J.M., Noh, H.-J., Kim, S.K., Song, H.K., Lee, C.-W., Morgan, M.J., Kang, H.C., Kim, Y.-S., 2018. PELI1 Selectively Targets Kinase-Active RIP3 for Ubiquitylation-Dependent Proteasomal

Degradation. *Mol. Cell* **70**, 920–935.

Choteau, L., Parny, M., François, N., Bertin, B., Fumery, M., Dubuquoy, L., Takahashi, K., Colombel, J.F., Jouault, T., Poulain, D., Sendid, B., Jawhara, S., 2016. Role of mannose-binding lectin in intestinal homeostasis and fungal elimination. *Mucosal Immunol.* **9**, 767–776.

Chu, J., Thomas, L.M., Watkins, S.C., Franchi, L., Nunez, G., Salter, R.D., 2009. Cholesterol-dependent cytolysins induce rapid release of mature IL-1 from murine macrophages in a NLRP3 inflammasome and cathepsin B-dependent manner. *J. Leukoc. Biol.* **86**, 1227–1238.

Chung, K.F., 2001. Cytokines in chronic obstructive pulmonary disease. *Eur. Respir. J.* **18**, 50–59.

Chung, K.F., Adcock, I.M., 2008. Multifaceted mechanisms in COPD: inflammation, immunity, and tissue repair and destruction. *Eur. Respir. J.* **31**, 1334-1356.

Cleynen, I., Boucher, G., Jostins, L., Schumm, L.P., Zeissig, S., Ahmad, T., Andersen, V., Andrews, J.M., Annese, V., Brand, S., Brant, S.R., Cho, J.H., Daly, M.J., Dubinsky, M., Duerr, R.H., Ferguson, L.R., Franke, A., Gearry, R.B., Goyette, P., Hakonarson, H., Halfvarson, J., Hov, J.R., Huang, H., Kennedy, N.A., Kupcinskas, L., Lawrance, I.C., Lee, J.C., Satsangi, J., Schreiber, S., Théâtre, E., van der Meulen-de Jong, A.E., Weersma, R.K., Wilson, D.C., Parkes, M., Vermeire, S., Rioux, J.D., Mansfield, J., Silverberg, M.S., Radford-Smith, G., McGovern, D.P.B., Barrett, J.C., Lees, C.W., 2016. Inherited determinants of Crohn's disease and ulcerative colitis phenotypes: a genetic association study. *Lancet* **387**, 156–167.

Coenen-Stass, A.M.L., Mcclorey, G., Manzano, R., Betts, C.A., Blain, A., Saleh, A.F., Gait, M.J., Lochmüller, H., Wood, M.J.A., Roberts, T.C., 2015.

Identification of novel, therapy-responsive protein biomarkers in a mouse model of Duchenne muscular dystrophy by aptamer-based serum proteomics. *Sci. Rep.* **5**, 1–11.

Cohen, T.S., Prince, A.S., 2013. Activation of inflammasome signaling mediates pathology of acute P. aeruginosa pneumonia. *J. Clin. Invest.* **123**, 1630–1637.

Conti, H.R., Peterson, A.C., Brane, L., Huppler, A.R., Hernández-Santos, N., Whibley, N., Garg, A. V, Simpson-Abelson, M.R., Gibson, G.A., Mamo, A.J., Osborne, L.C., Bishu, S., Ghilardi, N., Siebenlist, U., Watkins, S.C., Artis, D., McGeachy, M.J., Gaffen, S.L., 2014. Oral-resident natural Th17 cells and γδ T cells control opportunistic *Candida albicans* infections. *J. Exp. Med.* **211**, 2075-2084.

Couillin, I., Vasseur, V., Charron, S., Gasse, P., Tavernier, M., Guillet, J., Lagente, V., Fick, L., Jacobs, M., Coelho, F.R., Moser, R., Ryffel, B., 2009. IL-1R1/MyD88 signaling is critical for elastase-induced lung inflammation and emphysema. *J. Immunol.* **183**, 8195–8202.

Couillin, I., Vasseur, V., Charron, S., Tavernier, M., Guillet, J., Lagente, V., Fick, L., Jacobs, M., Coelho, F.R., Couillin, I., Vasseur, V., Charron, S., Gasse, P., Tavernier, M., Guillet, J., Lagente, V., Fick, L., Jacobs, M., Coelho, F.R., 2015. IL-1R1/MyD88 Signaling Is Critical for Elastase-Induced Lung Inflammation and Emphysema.

Crotty, S., 2015. A brief history of T cell help to B cells. *Nat. Rev. Immunol.* **15**, 185–189.

Cruz, F.F., Antunes, M.A., Abreu, S.C., Fujisaki, L.C., Silva, J.D., Xisto, D.G., Maron-Gutierrez, T., Ornellas, D.S., Sá, V.K., Rocha, N.N., Capelozzi, V.L., Morales, M.M., Rocco, P.R.M., 2012. Protective effects of bone marrow

mononuclear cell therapy on lung and heart in an elastase-induced emphysema model. *Respir. Physiol. Neurobiol.* **182**, 26–36.

Cutting, G.R., 2015. Cystic fibrosis genetics: from molecular understanding to clinical application. *Nat Rev Genet* **16**, 45–56.

Da Silva Correia, J., Soldau, K., Christen, U., Tobias, P.S., Ulevitch, R.J., 2001. Lipopolysaccharide is in close proximity to each of the proteins in its membrane receptor complex. Transfer from CD14 to TLR4 and MD-2. *J. Biol. Chem.* **276**, 21129–21135.

Damiano, V. V., Tsang, A., Kucich, U., Abrams, W.R., Rosenbloom, J., Kimbel, P., Fallahnejad, M., Weinbaum, G., 1986. Immunolocalization of elastase in human emphysematous lungs. *J. Clin. Invest.* **78**, 482–493.

David, A., Sarah, H., Kris, J., Gillian, N., Rosemary, C., John, C., Colin, R., Keith, G., 2005. Lower Airway Inflammation in Infants with Cystic Fibrosis Detected by Newborn Screening. *Pediatr. Pulmonol.* **40**, 500–510.

de Duve, C., 2005. The lysosome turns fifty. *Nat. Cell Biol.* **7**, 847.

de Duve, C., Pressman, B.C., Gianetto, R., Wattiaux, R., Appelmans, F., 1955. Tissue fractionation studies. 6. Intracellular distribution patterns of enzymes in rat-liver tissue. *Biochem. J.* **60**, 604–617.

de Marco, R., Accordini, S., Marcon, A., Cerveri, I., Antó, J.M., Gislason, T., Heinrich, J., Janson, C., Jarvis, D., Kuenzli, N., Leynaert, B., Sunyer, J., Svanes, C., Wjst, M., Burney, P., 2011. Risk Factors for Chronic Obstructive Pulmonary Disease in a European Cohort of Young Adults. *Am. J. Respir. Crit. Care Med.* **183**, 891–897.

Deguine, J., Barton, G.M., 2014. MyD88: a central player in innate immune signaling. *F1000Prime Rep.* **6**, 97.

DeMeo, D.L., Sandhaus, R.A., Barker, A.F., Brantly, M.L., Eden, E., McElvaney, N.G., Rennard, S., Burchard, E., Stocks, J.M., Stoller, J.K., Strange, C., Turino, G.M., Campbell, E.J., Silverman, E.K., 2007. Determinants of airflow obstruction in severe alpha-1-antitrypsin deficiency. *Thorax* **62**, 805–812.

Deng, Q., Wang, Y., Zhang, Y., Li, M., Li, D., Huang, X., Wu, Y., Pu, J., Wu, M., 2015. Pseudomonas aeruginosa triggers macrophage autophagy to escape intracellular killing by activation of the NLRP3 inflammasome. *Infect. Immun.* **84**, 56–66.

Dick, M.S., Sborgi, L., Rühl, S., Hiller, S., Broz, P., 2016. ASC filament formation serves as a signal amplification mechanism for inflammasomes. *Nat. Commun.* **7**.

Dinarello, C.A., 2009. Immunological and Inflammatory Functions of the Interleukin-1 Family. *Annu. Rev. Immunol.* **27**, 519–550.

Dinarello, C.A., 2011. Interleukin-1 in the pathogenesis and treatment of inflammatory diseases. *Blood* **117**, 3720–3732.

Donaldson, S.H., Boucher, R.C., 2007. Sodium Channels and Cystic Fibrosis. *Chest* **132**, 1631–1636.

Dorhoi, A., Nouailles, G., Jörg, S., Hagens, K., Heinemann, E., Pradl, L., Oberbeck-Müller, D., Duque-Correa, M.A., Reece, S.T., Ruland, J., Brosch, R., Tschopp, J., Gross, O., Kaufmann, S.H.E., 2011. Activation of the NLRP3 inflammasome by Mycobacterium tuberculosis is uncoupled from susceptibility to active tuberculosis. *Eur. J. Immunol.* **42**, 374–384.

Dossang, A.C.G., Motshwene, P.G., Yang, Y., Symmons, M.F., Bryant, C.E., Borman, S., George, J., Weber, A.N.R., Gay, N.J., 2016. The N-terminal loop of IRAK-4 death domain regulates ordered assembly of the Myddosome signalling scaffold. *Sci. Rep.* **6**, 1–12.

Douglas, T.A., Brennan, S., Gard, S., Berry, L., Gangell, C., Stick, S.M., Clements, B.S., Sly, P.D., 2009. Acquisition and eradication of P. aeruginosa in young children with cystic fibrosis. *Eur. Respir. J.* **33**, 305–311.

Dowson, L.J., Guest, P.J., Stockley, R.A., 2002. The Relationship of Chronic Sputum Expectoration to Physiologic, Radiologic, and Health Status Characteristics in α_1-Antitrypsin Deficiency (PiZ). *Chest* **122**, 1247–1255.

Emerson, J., Rosenfeld, M., McNamara, S., Ramsey, B., Gibson, R.L., 2002. Pseudomonas aeruginosa and other predictors of mortality and morbidity in young children with cystic fibrosis. *Pediatr. Pulmonol.* **34**, 91–100.

Enesa, K., Ordureau, A., Smith, H., Barford, D., Cheung, P.C.F., Patterson-Kane, J., Arthur, J.S., Cohen, P., 2012. Pellino1 is required for interferon production by viral double-stranded RNA. *J. Biol. Chem.* **287**, 34825-34835.

Evavold, C.L., Ruan, J., Tan, Y., Xia, S., Wu, H., Kagan, J.C., 2018. The Pore-Forming Protein Gasdermin D Regulates Interleukin-1 Secretion from Living Macrophages. *Immunity* **48**, 35–44.e6.

Ewald, S.E., Chavarria-Smith, J., Boothroyd, J.C., 2014. NLRP1 is an inflammasome sensor for Toxoplasma gondii. *Infect. Immun.* **82**, 460–468.

Fagerland, M.W., and L. Sandvik. 2009. The Wilcoxon-Mann-Whitney test under scrutiny. *Statistics in Medicine* **28**, 1487-1497

Farhat, K., Riekenberg, S., Heine, H., Debarry, J., Lang, R., Mages, J., Buwitt-Beckmann, U., Roschmann, K., Jung, G., Wiesmuller, K.-H., Ulmer, A.J., 2007. Heterodimerization of TLR2 with TLR1 or TLR6 expands the ligand spectrum but does not lead to differential signaling. *J. Leukoc. Biol.* **83**, 692–701.

Fernandes-Alnemri, T., Kang, S., Anderson, C., Sagara, J., Fitzgerald, K. a, Alnemri, E.S., 2013. Cutting edge: TLR signaling licenses IRAK1 for rapid activation of

the NLRP3 inflammasome. *J. Immunol.* **191**, 3995–9.

Fernandes-Alnemri, T., Wu, J., Yu, J.W., Datta, P., Miller, B., Jankowski, W., Rosenberg, S., Zhang, J., Alnemri, E.S., 2007. The pyroptosome: A supramolecular assembly of ASC dimers mediating inflammatory cell death via caspase-1 activation. *Cell Death Differ.* **14**, 1590–1604.

Finger, J.N., Lich, J.D., Dare, L.C., Cook, M.N., Brown, K.K., Duraiswamis, C., Bertin, J.J., Gough, P.J., 2012. Autolytic proteolysis within the function to find domain (FIIND) is required for NLRP1 inflammasome activity. *J. Biol. Chem.* **287**, 25030–25037.

Fink, S.L., Cookson, B.T., 2006. Caspase-1-dependent pore formation during pyroptosis leads to osmotic lysis of infected host macrophages. *Cell. Microbiol.* **8**, 1812–1825.

Fitzgerald, K.A., McWhirter, S.M., Faia, K.L., Rowe, D.C., Latz, E., Golenbock, D.T., Coyle, A.J., Liao, S.-M., Maniatis, T., 2003. IKKε and TBK1 are essential components of the IRF3 signaling pathway. *Nat. Immunol.* **4**, 491.

Foell, D., Wittkowski, H., Vogl, T., Roth, J., 2006. S100 proteins expressed in phagocytes: a novel group of damage-associated molecular pattern molecules. *J. Leukoc. Biol.* **81**, 28–37.

Foronjy, R., Nkyimbeng, T., Wallace, A., Thankachen, J., Okada, Y., Lemaitre, V., D'Armiento, J., 2008. Transgenic expression of matrix metalloproteinase-9 causes adult-onset emphysema in mice associated with the loss of alveolar elastin. *Am. J. Physiol. Cell. Mol. Physiol.* **294**, L1149–L1157.

Franchi, L., Amer, A., Body-Malapel, M., Kanneganti, T.D., Özören, N., Jagirdar, R., Inohara, N., Vandenabeele, P., Bertin, J., Coyle, A., Grant, E.P., Núñez, G., 2006. Cytosolic flagellin requires Ipaf for activation of caspase-1 and interleukin

1β in salmonella-infected macrophages. *Nat. Immunol.* **7**, 576–582.

Fredericksen, B.L., Keller, B.C., Fornek, J., Katze, M.G., Gale, M., 2008. Establishment and Maintenance of the Innate Antiviral Response to West Nile Virus Involves both RIG-I and MDA5 Signaling through IPS-1. *J. Virol.* **82**, 609–616.

Frew, B.C., Joag, V.R., Mogridge, J., 2012. Proteolytic processing of Nlrp1b is required for inflammasome activity. *PLoS Pathog.* **8**, e1002659.

Ge, B., Gram, H., Di Padova, F., Huang, B., New, L., Ulevitch, R.J., Luo, Y., Han, J., 2002. MAPKK-Independent Activation of p38α Mediated by TAB1-Dependent Autophosphorylation of p38α. *Science (80-.).* **295**, 1291-1294.

Gershon, A.S., Warner, L., Cascagnette, P., Victor, J.C., To, T., 2011. Lifetime risk of developing chronic obstructive pulmonary disease: a longitudinal population study. *Lancet* **378**, 991–996.

Geuking, P., Narasimamurthy, R., Lemaitre, B., Basler, K., Leulier, F., 2009. A non-redundant role for Drosophila Mkk4 and hemipterous/Mkk7 in TAK1-mediated activation of JNK. *PLoS One* **4**, 1–8.

Gharib, S.A., Manicone, A.M., Parks, W.C., 2018. Matrix metalloproteinases in emphysema. *Matrix Biol.*

Giegerich, A.K., Kuchler, L., Sha, L.K., Knape, T., Heide, H., Wittig, I., Behrends, C., Brüne, B., Von Knethen, A., 2014. Autophagy-dependent PELI3 degradation inhibits proinflammatory IL1B expression. *Autophagy* **10**, 1937–1952.

Girardin, S.E., Boneca, I.G., Viala, J., Chamaillard, M., Labigne, A., Thomas, G., Philpott, D.J., Sansonetti, P.J., 2003. Nod2 is a general sensor of peptidoglycan through muramyl dipeptide (MDP) detection. *J. Biol. Chem.* **278**, 8869–8872.

Goel, M.K., Khanna, P., Kishore, J. (2010) Understanding survival analysis: Kaplan-

Meier estimate. *Int J Ayurveda Res*. **4**, 274-278.

Goldklang, M., Stockley, R., 2016. Pathophysiology of Emphysema and Implications . *Chronic Obstr. Pulm. Dis.* **3**, 454–458.

Gorfu, G., Cirelli, K.M., Melo, M.B., Mayer-Barber, K., Crown, D., Koller, B.H., Masters, S., Sher, A., Leppla, S.H., Moayeri, M., Saeij, J.P.J., Grigg, M.E., 2014. Dual role for inflammasome sensors NLRP1 and NLRP3 in murine resistance to Toxoplasma gondii. *MBio* **5**, 1–12.

Gottlieb, D.J., Stone, P.J., Sparrow, D., Gale, M.E., Weiss, S.T., Snider, G.L., O'Connor, G.T., 1996. Urinary desmosine excretion in smokers with and without rapid decline of lung function: the Normative Aging Study. *Am. J. Respir. Crit. Care Med.* **154**, 1290–1295.

Grabcanovic-Musija, F., Obermayer, A., Stoiber, W., Krautgartner, W.-D., Steinbacher, P., Winterberg, N., Bathke, A.C., Klappacher, M., Studnicka, M., 2015. Neutrophil extracellular trap (NET) formation characterises stable and exacerbated COPD and correlates with airflow limitation. *Respir. Res.* **16**, 59.

Grant, R.W., Dixit, V.D., 2013. Mechanisms of disease: Inflammasome activation and the development of type 2 diabetes. *Front. Immunol.* **4**, 1–10.

Greene, C.M., Marciniak, S.J., Teckman, J., Ferrarotti, I., Brantly, M.L., Lomas, D.A., Stoller, J.K., McElvaney, N.G., 2016. α1-Antitrypsin deficiency. *Nat. Rev. Dis. Prim.* **2**, 16051.

Gregor, M.F., Hotamisligil, G.S., 2011. Inflammatory Mechanisms in Obesity. *Annu. Rev. Immunol.* **29**, 415–445.

Griffin, G.K., Newton, G., Tarrio, M.L., Bu, D.X., Maganto-Garcia, E., Azcutia, V., Alcaide, P., Grabie, N., Luscinskas, F.W., Croce, K.J., Lichtman, A.H., 2012. IL-17 and TNF-alpha sustain neutrophil recruitment during inflammation through

synergistic effects on endothelial activation. *J Immunol* **188**, 6287–6299.

Grimes, C.L., Ariyananda, L.D.Z., Melnyk, J.E., O'Shea, E.K., 2012. The Innate Immune Protein Nod2 Binds Directly to MDP, a Bacterial Cell Wall Fragment. *J. Am. Chem. Soc.* **134**, 13535–13537.

Grobans, J., Schnorrer, F., Nu, C., 1999. Oligomerisation of Tube and Pelle leads to nuclear localisation of Dorsal. *Mech. Dev.* **81**, 127–138.

Groenewegen, K.H., Postma, D.S., Hop, W.C.J., Wielders, P.L.M.L., Schlösser, N.J.J., Wouters, E.F.M., 2008. Increased Systemic Inflammation Is a Risk Factor for COPD Exacerbations. *Chest* **133**, 350–357.

Gross, P., Pfitzer, E.A., Tolker, E., Babyak, M.A., Kaschak, M., 1965. Experimental Emphysema. *Arch. Environ. Heal. An Int. J.* **11**, 50–58.

Guglani, L., Khader, S.A., 2010. Th17 cytokines in mucosal immunity and inflammation. *Curr. Opin. HIV AIDS* **5**, 120–127.

Guyot, N., Wartelle, J., Malleret, L., Todorov, A.A., Devouassoux, G., Pacheco, Y., Jenne, D.E., Belaaouaj, A., 2014. Unopposed Cathepsin G, Neutrophil Elastase, and Proteinase 3 Cause Severe Lung Damage and Emphysema. *Am. J. Pathol.* **184**, 2197–2210.

Haley, C.L., Colmer-Hamood, J.A., Hamood, A.N., 2012. Characterization of biofilm-like structures formed by Pseudomonas aeruginosa in a synthetic mucus medium. *BMC Microbiol.* **12**, 181.

Han, S.H., Lear, T.B., Jerome, J.A., Rajbhandari, S., Snavely, C.A., Gulick, D.L., Gibson, K.F., Zou, C., Chen, B.B., Mallampalli, R.K., 2015. Lipopolysaccharide primes the NALP3 inflammasome by inhibiting its ubiquitination and degradation mediated by the SC^{FFBXL2} E3 ligase. *J. Biol. Chem.* **290**, 18124–18133.

Harada, H., Imamura, M., Okunishi, K., Nakagome, K., Matsumoto, T., Sasaki, O., Tanaka, R., Yamamoto, K., Dohi, M., 2009. Upregulation of Lung Dendritic Cell Functions in Elastase-Induced Emphysema, International archives of allergy and immunology.

Hartl, D., Gaggar, A., Bruscia, E., Hector, A., Marcos, V., Jung, A., Greene, C., McElvaney, G., Mall, M., Döring, G., 2012. Innate immunity in cystic fibrosis lung disease. *J. Cyst. Fibros.* **11**, 363–382.

Hatai, H., Lepelley, A., Zeng, W., Hayden, M.S., Ghosh, S., 2016. Toll-like receptor 11 (TLR11) Interacts with flagellin and profilin through disparate mechanisms. *PLoS One* **11**, 1–13.

Hattori, N., Degen, J.L., Sisson, T.H., Liu, H., Moore, B.B., Pandrangi, R.G., Simon, R.H., Drew, A.F., 2000. Bleomycin-induced pulmonary fibrosis in fibrinogen-null mice. *J. Clin. Invest.* **106**, 1341-1350.

Hayashi, F., Smith, K.D., Ozinsky, A., Hawn, T.R., Yi, E.C., Goodlett, D.R., Eng, J.K., Akira, S., Underhill, D.M., Aderem, A., 2001. The innate immune response to bacterial flagellin is mediated by Toll-like receptor 5. *Nature* **410**, 1099.

Heil, F., Ahmad-Nejad, P., Hemmi, H., Hochrein, H., Ampenberger, F., Gellert, T., Dietrich, H., Lipford, G., Takeda, K., Akira, S., Wagner, H., Bauer, S., 2003. The Toll-like receptor 7 (TLR7)-specific stimulus loxoribine uncovers a strong relationship within the TLR7, 8 and 9 subfamily. *Eur. J. Immunol.* **33**, 2987–2997.

Heilig, R., Dick, M.S., Sborgi, L., Meunier, E., Hiller, S., Broz, P., 2017. The Gasdermin-D pore acts as a conduit for IL-1β secretion in mice. *Eur. J. Immunol.* **48**, 584–592.

Hemmi, H., Takeuchi, O., Kawai, T., Kaisho, T., Sato, S., Sanjo, H., Matsumoto, M.,

Hoshino, K., Wagner, H., Takeda, K., Akira, S., 2000. A Toll-like receptor recognizes bacterial DNA. *Nature* **408**, 740.

Heneka, M.T., Kummer, M.P., Stutz, A., Delekate, A., Schwartz, S., Vieira-Saecker, A., Griep, A., Axt, D., Remus, A., Tzeng, T.-C., Gelpi, E., Halle, A., Korte, M., Latz, E., Golenbock, D.T., 2013. NLRP3 is activated in Alzheimer's disease and contributes to pathology in APP/PS1 mice. *Nature* **493**, 674–8.

Hiroshima, Y., Hsu, K., Tedla, N., Wong, S.W., Chow, S., Kawaguchi, N., Geczy, C.L., 2017. S100A8/A9 and S100A9 reduce acute lung injury. *Immunol. Cell Biol.* **95**, 461–472.

Hodge, S., Hodge, G., Holmes, M., Reynolds, P.N., 2005. Increased airway epithelial and T-cell apoptosis in COPD remains despite smoking cessation. *Eur. Respir. J.* **25**, 447–454.

Hoffman, H.M., Mueller, J.L., Broide, D.H., Wanderer, A.A., Kolodner, R.D., 2001. Mutation of a new gene encoding a putative pyrin-like protein causes familial cold autoinflammatory syndrome and Muckle–Wells syndrome. *Nat. Genet.* **29**, 301.

Holland, A., Henry, M., Meleady, P., Winkler, C.K., Krautwald, M., Brinkmeier, H., Ohlendieck, K., 2015. Comparative label-free mass spectrometric analysis of mildly versus severely affected mdx mouse skeletal muscles identifies annexin, lamin, and vimentin as universal dystrophic markers. *Molecules* **20**, 11317–11344.

Homer, C.R., Richmond, A.L., Rebert, N.A., Achkar, J., McDonald, C., 2010. ATG16L1 and NOD2 interact in an autophagy-dependent antibacterial pathway implicated in crohn's disease pathogenesis. *Gastroenterology* **139**, 1630–1641.e2.

Hoonhorst, S.J.M., Timens, W., Koenderman, L., Lo Tam Loi, A.T., Lammers, J.-W.J., Boezen, H.M., van Oosterhout, A.J.M., Postma, D.S., ten Hacken, N.H.T., 2014. Increased activation of blood neutrophils after cigarette smoking in young individuals susceptible to COPD. *Respir. Res.* **15**, 121.

Hornung, V., Bauernfeind, F., Halle, A., Samstad, E.O., Kono, H., Rock, K.L., Fitzgerald, K.A., Latz, E., 2008. Silica crystals and aluminum salts mediate NALP-3 inflammasome activation via phagosomal destabilization. *Nat. Immunol.* **9**, 847–856.

Hou, H., Cheng, S., Liu, H., Yang, F., Wang, H., Yu, C., 2013. Elastase induced lung epithelial cell apoptosis and emphysema through placenta growth factor 1–9.

Hübner, R., Gitter, W., Eddine, N., Mokhtari, E., Mathiak, M., Both, M., Bolte, H., Freitag-wolf, S., Bewig, B., 2008. Standardized quantification of pulmonary fibrosis in histological samples **44**.

Humphries, F., Bergin, R., Jackson, R., Delagic, N., Wang, B., Yang, S., Dubois, A. V, Ingram, R.J., Moynagh, P.N., 2018. The E3 ubiquitin ligase Pellino2 mediates priming of the NLRP3 inflammasome. *Nat. Commun.* **9**, 1560.

Hurd, S., 2000. The Impact of COPD on Lung Health Worldwide. *Chest* **117**, 1S–4S.

Iannitti, R.G., Napolioni, V., Oikonomou, V., De Luca, A., Galosi, C., Pariano, M., Massi-Benedetti, C., Borghi, M., Puccetti, M., Lucidi, V., Colombo, C., Fiscarelli, E., Lass-Flörl, C., Majo, F., Cariani, L., Russo, M., Porcaro, L., Ricciotti, G., Ellemunter, H., Ratclif, L., De Benedictis, F.M., Talesa, V.N., Dinarello, C.A., Van De Veerdonk, F.L., Romani, L., 2016. IL-1 receptor antagonist ameliorates inflammasome-dependent inflammation in murine and human cystic fibrosis. *Nat. Commun.* **7**.

Imai, K., Mercer, B.A., Schulman, L.L., Sonett, J.R., D'Armiento, J.M., 2005.

Correlation of lung surface area to apoptosis and proliferation in human emphysema. *Eur. Respir. J.* **25**, 250–258.

Imaizumi, T., Kumagai, M., Taima, K., Fujita, T., Yoshida, H., Satoh, K., 2005. Involvement of retinoic acid-inducible gene-I in the IFN-γ/STAT1 signalling pathway in BEAS-2B cells. *Eur. Respir. J.* **25**, 1077-1083.

Inohara, N., Ogura, Y., Chen, F.F., Muto, A., Nuñez, G., 2001. Human Nod1 Confers Responsiveness to Bacterial Lipopolysaccharides. *J. Biol. Chem.* **276**, 2551–2554.

Inohara, N., Ogura, Y., Fontalba, A., Gutierrez, O., Pons, F., Crespo, J., Fukase, K., Inamura, S., Kusumoto, S., Hashimoto, M., Foster, S.J., Moran, A.P., Fernandez-Luna, J.L., Nuñez, G., 2003. Host recognition of bacterial muramyl dipeptide mediated through NOD2: Implications for Crohn's disease. *J. Biol. Chem.* **278**, 5509–5512.

Ishii, Y., Itoh, K., Morishima, Y., Kimura, T., Kiwamoto, T., IIzuka, T., Hegab, A.E., Hosoya, T., Nomura, A., Sakamoto, T., Yamamoto, M., Sekizawa, K., 2005. Transcription Factor Nrf2 Plays a Pivotal Role in Protection against Elastase-Induced Pulmonary Inflammation and Emphysema. *J. Immunol.* **175**, 6968-6975.

Ito, S., Araya, J., Kurita, Y., Kobayashi, K., Takasaka, N., Yoshida, M., Hara, H., Minagawa, S., Wakui, H., Fujii, S., Kojima, J., Shimizu, K., Numata, T., Kawaishi, M., Odaka, M., Morikawa, T., Harada, T., Nishimura, S.L., Kaneko, Y., Nakayama, K., Kuwano, K., 2015. PARK2-mediated mitophagy is involved in regulation of HBEC senescence in COPD pathogenesis. *Autophagy* **11**, 547–559.

Iwasaki, A., Medzhitov, R., 2010. Regulation of Adaptive Immunity by the Innate Immune System. *Science (80-.).* **327**, 291-295.

Janeway, C.A., 2013. Pillars Article: Approaching the Asymptote? Evolution and Revolution in Immunology. Cold Spring Harb Symp Quant Biol. 1989. 54: 1–13. *J. Immunol.* **191**, 4475-4487.

Jeffery, P.K., 2001. Remodeling in asthma and chronic obstructive lung disease. *Am.J.Respir.Crit Care Med.* **164**, S28–S38.

Jeon, Y.K., Kim, C.K., Hwang, K.R., Park, H.Y., Koh, J., Chung, D.H., Lee, C.W., Ha, G.H., 2017. Pellino-1 promotes lung carcinogenesis via the stabilization of Slug and Snail through K63-mediated polyubiquitination. *Cell Death Differ.* **24**, 469–480.

Jiang, Z., Johnson, H.J., Nie, H., Qin, J., Bird, T.A., Li, X., 2003. Pellino 1 is required for interleukin-1 (IL-1)-mediated signaling through its interaction with the IL-1 receptor-associated kinase 4 (IRAK4)-IRAK-tumor necrosis factor receptor-associated factor 6 (TRAF6) complex. *J. Biol. Chem.* **278**, 10952–10956.

Jin, Y., Mailloux, C.M., Gowan, K., Riccardi, S.L., LaBerge, G., Bennett, D.C., Fain, P.R., Spritz, R.A., 2007. NALP1 in Vitiligo-Associated Multiple Autoimmune Disease. *N. Engl. J. Med.* **356**, 1216–1225.

Johansen, H., Gøtzsche, P., 2015. Vaccines for preventing infection with Pseudomonas aeruginosa in cystic fibrosis (Review). *Cochrane Libr.*

Juliana, C., Fernandes-Alnemri, T., Kang, S., Farias, A., Qin, F., Alnemri, E.S., 2012. Non-transcriptional priming and deubiquitination regulate NLRP3 inflammasome activation. *J. Biol. Chem.* **287**, 36617–36622.

Kalluri, R., Neilson, E.G., 2003. Epithelial-mesenchymal transition and its implications for fibrosis **112**.

Kanayama, A., Seth, R.B., Sun, L., Ea, C.K., Hong, M., Shaito, A., Chiu, Y.H., Deng, L., Chen, Z.J., 2004. TAB2 and TAB3 activate the NF-κB pathway through

binding to polyubiquitin chains. *Mol. Cell* **15**, 535–548.

Kanayama, M., Inoue, M., Danzaki, K., Hammer, G., He, Y.-W., Shinohara, M.L., 2015. Autophagy enhances NFκB activity in specific tissue macrophages by sequestering A20 to boost antifungal immunity. *Nat. Commun.* **6**, 5779.

Kang, D.C., Gopalkrishnan, R. V., Lin, L., Randolph, A., Valerie, K., Pestka, S., Fisher, P.B., 2004. Expression analysis and genomic characterization of human melanoma differentiation associated gene-5, mda-5: A novel type I interferon-responsive apoptosis-inducing gene. *Oncogene* **23**, 1789–1800.

Kang, M.-J., Choi, J.-M., Kim, B.H., Lee, C.-M., Cho, W.-K., Choe, G., Kim, D.-H., Lee, C.G., Elias, J.A., 2012. IL-18 Induces Emphysema and Airway and Vascular Remodeling via IFN-γ, IL-17A, and IL-13. *Am. J. Respir. Crit. Care Med.* **185**, 1205–1217.

Kanneganti, T.D., Lamkanfi, M., Núñez, G., 2007. Intracellular NOD-like Receptors in Host Defense and Disease. *Immunity* **27**, 549–559.

Karmakar, M., Sun, Y., Hise, A.G., Rietsch, A., Pearlman, E., 2012. IL-1β processing during Pseudomonas aeruginosa infection is mediated by neutrophil serine proteases and is independent of NLRC4 and Caspase-1. *J. Immunol.* **189**, 4231–4235.

Kasahara, Y., Tuder, R.M., Taraseviciene-Stewart, L., Le Cras, T.D., Abman, S., Hirth, P.K., Waltenberger, J., Voelkel, N.F., 2000. Inhibition of VEGF receptors causes lung cell apoptosis and emphysema. *J. Clin. Invest.* **106**, 1311–1319.

Kato, H., Takeuchi, O., Sato, S., Yoneyama, M., Yamamoto, M., Matsui, K., Uematsu, S., Jung, A., Kawai, T., Ishii, K.J., Yamaguchi, O., Otsu, K., Tsujimura, T., Koh, C.-S., Reis e Sousa, C., Matsuura, Y., Fujita, T., Akira, S., 2006. Differential roles of MDA5 and RIG-I helicases in the recognition of RNA

viruses. *Nature* **441**, 101.

Kawasaki, K., Akashi, S., Miyake, K., Nishijima, M., 2000. Signal Transduction by Taxol. *Biochemistry* **275**, 2251–2254.

Kawasaki, T., Kawai, T., 2014. Toll-like receptor signaling pathways. *Front. Immunol.* **5**, 461–468.

Kaye, K.S., Pogue, J.M., 2015. Infections Caused by Resistant Gram-Negative Bacteria: Epidemiology and Management. *Pharmacother. J. Hum. Pharmacol. Drug Ther.* **35**, 949–962.

Kennelly, H., Mahon, B.P., English, K., 2016. Human mesenchymal stromal cells exert HGF dependent cytoprotective effects in a human relevant pre-clinical model of COPD. *Nat. Publ. Gr.* 1–11.

Kim, H.M., Park, B.S., Kim, J.I., Kim, S.E., Lee, J., Oh, S.C., Enkhbayar, P., Matsushima, N., Lee, H., Yoo, O.J., Lee, J.O., 2007. Crystal Structure of the TLR4-MD-2 Complex with Bound Endotoxin Antagonist Eritoran. *Cell* **130**, 906–917.

Kim, T.W., Yu, M., Zhou, H., Cui, W., Wang, J., DiCorleto, P., Fox, P., Xiao, H., Li, X., 2012. Pellino 2 is critical for toll-like receptor/interleukin-1 receptor (TLR/IL-1R)-mediated post-transcriptional control. *J. Biol. Chem.* **287**, 25686–25695.

Kim, V., Cornwell, W.D., Oros, M., Durra, H., Criner, G.J., Rogers, T.J., 2015a. Plasma Chemokine signature correlates with lung goblet cell hyperplasia in smokers with and without chronic obstructive pulmonary disease. *BMC Pulm. Med.* **15**, 111.

Kim, V., Oros, M., Durra, H., Kelsen, S., Aksoy, M., Cornwell, W.D., Rogers, T.J., Criner, G.J., 2015b. Chronic Bronchitis and Current Smoking Are Associated

with More Goblet Cells in Moderate to Severe COPD and Smokers without Airflow Obstruction. *PLoS One* **10**, e0116108.

Kim, V., Rogers, T.J., Criner, G.J., 2008. New Concepts in the Pathobiology of Chronic Obstructive Pulmonary Disease. *Proc. Am. Thorac. Soc.* **5**, 478–485.

Ko, F.W.S., Hui, D.S.C., Lai, C.K.W., 2008. Chronic obstructive pulmonary disease in high- and low-income countries Worldwide burden of COPD in high- and low-income countries . Part III . Asia-Pacifi c studies. *Int. J. Tuberc. Lung Dis.* **12**, 713–717.

Kobayashi, S., Fujinawa, R., Ota, F., Kobayashi, S., Angata, T., Ueno, M., Maeno, T., Kitazume, S., Yoshida, K., Ishii, T., Gao, C., Ohtsubo, K., Yamaguchi, Y., Betsuyaku, T., Kida, K., Taniguchi, N., 2013. A single dose of lipopolysaccharide into mice with emphysema mimics human Chronic obstructive pulmonary disease exacerbation as assessed by micro-computed tomography. *Am. J. Respir. Cell Mol. Biol.* **49**, 971–977.

Koblansky, A.A., Jankovic, D., Oh, H., Hieny, S., Sungnak, W., Mathur, R., Hayden, M.S., Akira, S., Sher, A., Ghosh, S., 2013. Recognition of Profilin by Toll-like Receptor 12 Is Critical for Host Resistance to Toxoplasma gondii. *Immunity* **38**, 119–130.

Koh, A.Y., Priebe, G.P., Ray, C., Van Rooijen, N., Pier, G.B., 2009. Inescapable need for neutrophils as mediators of cellular innate immunity to acute Pseudomonas aeruginosa pneumonia. *Infect. Immun.* **77**, 5300–5310.

Kooguchi, K., Hashimoto, S., Kobayashi, A., Kitamura, Y., Kudoh, I., Wiener-Kronish, J., Sawa, T., 1998. Role of alveolar macrophages in initiation and regulation of inflammation in *Pseudomonas aeruginosa* pneumonia. *Infect Immun* **66**, 3164–3169.

Krieg, A.M., 2002. CpG Motifs in Bacterial DNA and Their Immune Effects. *Annu. Rev. Immunol.* **20**, 709–760.

Krzywinski, M., Altman, N., 2013. Significance, *P* values and *t*-tests. *Nat. Methods* **10**, 1041-1042.

Krzywinski, M., Altman, N., 2014. Nonparametric tests. *Nat. Methods* **11**, 467-468.

Kumar, H., Kawai, T., Akira, S., 2009. Pathogen recognition in the innate immune response. *Biochem. J.* **420**, 1-16.

Kurtz, J., 2005. Specific memory within innate immune systems. *Trends Immunol.* **26**, 186–192.

Kuwano, K., Kunitake, R., Kawasaki, M., Nomoto, Y., Hagimoto, N., Nakanishi, Y., Hara, N., 1996. P21Waf1/Cip1/Sdi1 and p53 expression in association with DNA strand breaks in idiopathic pulmonary fibrosis. *Am. J. Respir. Crit. Care Med.* **154**, 477–483.

Labarca, J.A., Salles, M.J.C., Seas, C., Guzmán-Blanco, M., 2016. Carbapenem resistance in Pseudomonas aeruginosa and Acinetobacter baumannii in the nosocomial setting in Latin America. *Crit. Rev. Microbiol.* **42**, 276–292.

Lacoste, J.Y., Bousquet, J., Chanez, P., Van Vyve, T., Simony-Lafontaine, J., Lequeu, N., Vic, P., Enander, I., Godard, P., Michel, F.B., 1993. Eosinophilic and neutrophilic inflammation in asthma, chronic bronchitis, and chronic obstructive pulmonary disease. *J. Allergy Clin. Immunol.* **92**, 537–48.

Lamkanfi, M., Dixit, V.M., 2012. Inflammasomes and Their Roles in Health and Disease. *Annu. Rev. Cell Dev. Biol.* **28**, 137–161.

Lamkanfi, M., Kanneganti, T.-D., Franchi, L., Nunez, G., 2007. Caspase-1 inflammasomes in infection and inflammation. *J. Leukoc. Biol.* **82**, 220–225.

Lanier, L.L., Sun, J.C., 2009. Do the terms innate and adaptive immunity create

artificial conceptual barriers? *Nat. Rev. Immunol.* **9**, 302–303.

Latz, E., Xiao, T.S., Stutz, A., 2013. Activation and regulation of the inflammasomes. *Nat. Rev. Immunol.* **13**, 397.

Le, N.P.K., Channabasappa, S., Hossain, M., Liu, L., Singh, B., 2015. Leukocyte-specific protein 1 regulates neutrophil recruitment in acute lung inflammation. *Am. J. Physiol. - Lung Cell. Mol. Physiol.* **309**, L995–L1008.

Lear, T., Mckelvey, A.C., Rajbhandari, S., Dunn, S.R., Coon, T.A., Connelly, W., Zhao, J.Y., Kass, D.J., Zhang, Y., Liu, Y., Chen, B.B., 2016. Ubiquitin E3 ligase FIEL1 regulates fibrotic lung injury through SUMO-E3 ligase PIAS4 1–18.

Lee, B., Qiao, L., Kinney, B., Feng, G.S., Shaw, J., 2014. Macrophage depletion disrupts immune balance and energy homeostasis. *PLoS ONE* **9**, e99575.

Lee, K.-H., Jang, A.-H., Jeong, J., Lee, C.-H., Yoo, C.-G., 2016. Cigarette smoke extracts enhance neutrophil elastase-induced IL-8 production via up-regulation of proteinase-activated receptor-2 in human bronchial epithelial cells. *J. Immunol.* **196**, 124.46-124.46.

Leid, J.G., Willson, C.J., Shirtliff, M.E., Hassett, D.J., Parsek, M.R., Jeffers, A.K., 2005. The Exopolysaccharide Alginate Protects *Pseudomonas aeruginosa* Biofilm Bacteria from IFN-γ-Mediated Macrophage Killing. *J. Immunol.* **175**, 7512-7518.

Leibovich, S.J., Ross, R., 1975. The role of the macrophage in wound repair. A study with hydrocortisone and antimacrophage serum. *Am J Pathol* **78**, 71- 100

Leigh, R., Ellis, R., Wattie, J.N., Hirota, J.A., Matthaei, K.I., Foster, P.S., O'Byrne, P.M., Inman, M.D., 2004. Type 2 Cytokines in the Pathogenesis of Sustained Airway Dysfunction and Airway Remodeling in Mice. *Am. J. Respir. Crit. Care Med.* **169**, 860–867.

Lemaitre, B., Nicolas, E., Michaut, L., Reichhart, J., Hoffmann, J.A., 1996. The Dorsoventral Regulatory Gene Cassette ¨ tzle / Toll / cactus Controls the spa Potent Antifungal Response in Drosophila Adults **86**, 973–983.

Levinsohn, J.L., Newman, Z.L., Hellmich, K.A., Fattah, R., Getz, M.A., Liu, S., Sastalla, I., Leppla, S.H., Moayeri, M., 2012. Anthrax Lethal Factor Cleavage of Nlrp1 Is Required for Activation of the Inflammasome. *PLOS Pathog.* **8**, e1002638.

Li, G., Flodby, P., Luo, J., Kage, H., Sipos, A., Gao, D., Ji, Y., Beard, L.L., Marconett, C.N., DeMaio, L., Kim, Y.H., Kim, K.-J., Laird-Offringa, I.A., Minoo, P., Liebler, J.M., Zhou, B., Crandall, E.D., Borok, Z., 2014. Knockout Mice Reveal Key Roles for Claudin 18 in Alveolar Barrier Properties and Fluid Homeostasis. *Am. J. Respir. Cell Mol. Biol.* **51**, 210–222.

Li, X.-D., Chen, Z.J., 2012. Sequence specific detection of bacterial 23S ribosomal RNA by TLR13. *Elife* **1**, 1–14.

Li, Z., Kosorok, M.R., Farrell, P.M., Laxova, A., West, S.E.H., Green, C.G., Rock, M.J., Splaingard, M.L., 2017. Infection and Lung Disease Progression in Children With Cystic Fibrosis **293**, 581–588.

Liao, K.C., Mogridge, J., 2013. Activation of the Nlrp1b inflammasome by reduction of cytosolic ATP. *Infect. Immun.* **81**, 570–579.

Limjunyawong, N., Craig, J.M., Lagassé, H.A.D., Scott, A.L., Mitzner, W., 2017. Biomarkers in Lung Diseases : from Pathogenesis to Prediction to New Therapies Experimental progressive emphysema in BALB / cJ mice as a model for chronic alveolar destruction in humans. *Am J Physiol Lung Cell Mol Physiol* **309**, 662–676.

Lin, K.-M., Hu, W., Troutman, T.D., Jennings, M., Brewer, T., Li, X., Nanda, S.,

Cohen, P., Thomas, J.A., Pasare, C., 2014. IRAK-1 bypasses priming and directly links TLRs to rapid NLRP3 inflammasome activation. *Proc. Natl. Acad. Sci. U. S. A.* **111**, 775–80.

Liselotte, J.E., Whitehead, A.S., 2003. Pellino2 activates the mitogen activated protein kinase pathway. *FEBS Lett.* **545**, 199–202.

Liu, D., Zeng, X., Li, X., Mehta, J.L., Wang, X., 2017. Role of NLRP3 inflammasome in the pathogenesis of cardiovascular diseases. *Basic Res. Cardiol.* **113**, 5.

Liu, L., Botos, I., Wang, Y., Leonard, J.N., Shiloach, J., Segal, D.M., Davies, D.R., 2009. Structural basis of Toll-Like Receptor 3 signaling with double-stranded DNA. *Science (80-.).* **320**, 379–381.

Loiarro, M., Gallo, G., Fantò, N., De Santis, R., Carminati, P., Ruggiero, V., Sette, C., 2009. Identification of critical residues of the MyD88 death domain involved in the recruitment of downstream kinases. *J. Biol. Chem.* **284**, 28093–28103.

Lomas, D.A., 2016. Does Protease–Antiprotease Imbalance Explain Chronic Obstructive Pulmonary Disease? *Ann. Am. Thorac. Soc.* **13**, S130–S137.

Loo, Y.-M., Gale, M., 2011. Immune Signaling by RIG-I-like Receptors.pdf. *Immunity* **34**, 680–692.

Lopez-Castejon, G., Luheshi, N.M., Compan, V., High, S., Whitehead, R.C., Flitsch, S., Kirov, A., Prudovsky, I., Swanton, E., Brough, D., 2013. Deubiquitinases Regulate the Activity of Caspase-1 and Interleukin-1β Secretion via Assembly of the Inflammasome. *J. Biol. Chem.* **288**, 2721–2733.

Lucas, T., Waisman, A., Ranjan, R., Roes, J., Krieg, T., Muller, W., Roers, A., Eming, S.A., 2010. Differential roles of macrophages in diverse phases of skin repair. *J. Immunol.* **184**, 3964-3977

Lucey, E.C., Keane, J., Kuang, P.-P., Snider, G.L., Goldstein, R.H., 2002. Severity of Elastase-Induced Emphysema Is Decreased in Tumor Necrosis Factor-α and Interleukin-1β Receptor-Deficient Mice. *Lab. Investig.* **82**, 79–85.

Lugrin, J., Martinon, F., 2017. The AIM2 inflammasome: Sensor of pathogens and cellular perturbations. *Immunol. Rev.* **281**, 99–114.

Luo, D., Lin, S., Parent, M.A., Kanevsky, I.M., Szaba, F.M., Kummer, L.W., Duso, D.K., Tighe, M., Hill, J., Gruber, A., Mackman, N., Gailani, D., Smiley, S.T., 2013. Fibrin facilitates both innate and T cell-mediated defense against Yersinia pestis. *J. Immunol.* **190**, 4149–4161.

Lüthje, L., Raupach, T., Michels, H., Unsöld, B., Hasenfuss, G., Kögler, H., Andreas, S., 2009. Exercise intolerance and systemic manifestations of pulmonary emphysema in a mouse model. *Respir. Res.* **10**.

Lyczak, J.B., Cannon, C.L., Pier, G.B., 2000. Establishment of Pseudomonas aeruginosa infection: lessons from a versatile opportunist1*Address for correspondence: Channing Laboratory, 181 Longwood Avenue, Boston, MA 02115, USA. *Microbes Infect.* **2**, 1051–1060.

MacNee, W., Wiggs, B., Belzberg, A.S., Hogg, J.C., 1989. The Effect of Cigarette Smoking on Neutrophil Kinetics in Human Lungs. *N. Engl. J. Med.* **321**, 924–928.

Malynn, B.A., Ma, A., 2010. Review Ubiquitin Makes Its Mark on Immune Regulation. *Immunity* **33**, 843–852.

Man, S.M., Hopkins, L.J., Nugent, E., Cox, S., Gluck, I.M., Tourlomousis, P., Wright, J.A., Cicuta, P., Monie, T.P., Bryant, C.E., 2014. Inflammasome activation causes dual recruitment of NLRC4 and NLRP3 to the same macromolecular complex. *Proc. Natl. Acad. Sci.* **111**, 7403–7408.

Margaret, R., Julia, E., Frank, A., David, A., Robert, C., Keith, G., Peter, H., Karen, M., Sharon, M., Bonnie, R., Jeffrey, W., 1999. Diagnostic accuracy of oropharyngeal cultures in infants and young children with cystic fibrosis. *Pediatr. Pulmonol.* **28**, 321–328.

Mariathasan, S., Weiss, D.S., Newton, K., McBride, J., O'Rourke, K., Roose-Girma, M., Lee, W.P., Weinrauch, Y., Monack, D.M., Dixit, V.M., 2006. Cryopyrin activates the inflammasome in response to toxins and ATP. *Nature* **440**, 228–232.

Martín-Sánchez, F., Diamond, C., Zeitler, M., Gomez, A.I., Baroja-Mazo, A., Bagnall, J., Spiller, D., White, M., Daniels, M.J.D., Mortellaro, A., Peñalver, M., Paszek, P., Steringer, J.P., Nickel, W., Brough, D., Pelegrín, P., 2016. Inflammasome-dependent IL-1β release depends upon membrane permeabilisation. *Cell Death Differ.* **23**, 1219.

Martin, M., Böl, G.F., Eriksson, A., Resch, K., Brigelius-Flohé, R., 1994. Interleukin-1-induced activation of a protein kinase co-precipitating with the type I interleukin-1 receptor in T cells. *Eur. J. Immunol.* **24**, 1566–1571.

Martinon, F., Burns, K., Tschopp, J., 2002. The Inflammasome: A molecular platform triggering activation of inflammatory caspases and processing of proIL-β. *Mol. Cell* **10**, 417–426.

Martinon, F., Mayor, A., Tschopp, J., 2009. The Inflammasomes: Guardians of the Body. *Annu. Rev. Immunol.* **27**, 229–265.

Masubuchi, T., Koyama, S., Sato, E., Takamizawa, A., Kubo, K., Sekiguchi, M., Nagai, S., Izumi, T., 1998. Smoke extract stimulates lung epithelial cells to release neutrophil and monocyte chemotactic activity. *Am.J.Pathol.* **153**, 1903–1912.

Matsushima, N., Tanaka, T., Enkhbayar, P., Mikami, T., Taga, M., Yamada, K., Kuroki, Y., 2007. Comparative sequence analysis of leucine-rich repeats (LRRs) within vertebrate toll-like receptors. *BMC Genomics* **8**, 1–20.

Matsuyama, S., Palmer, J., Bates, A., Poventud-Fuentes, I., Wong, K., Ngo, J., Matsuyama, M., 2016. Bax-induced apoptosis shortens the life span of DNA repair defect Ku70-knockout mice by inducing emphysema. *Exp. Biol. Med.* **241**, 1265–1271.

Matzinger, P., 2002. The Danger Model: A Renewed Sense of Self. *Science (80-.).* **296**, 301-305.

McAuley, J.B., 2014. Congenital toxoplasmosis. *J. Pediatric Infect. Dis. Soc.* **3**, 30–35.

McCartney, S., Marco, C., 2008. Viral sensors: diversity in pathogen recognition. *Immunol. Rev.* **227**, 87–94.

McDonald, J.H., 2014. *Handbook of biological statistics*, **3rd Ed.** Sparky House Publishing, Maryland.

McElvaney, N.G., Burdon, J., Holmes, M., Glanville, A., Wark, P.A.B., Thompson, P.J., Hernandez, P., Chlumsky, J., Teschler, H., Ficker, J.H., Seersholm, N., Altraja, A., Mäkitaro, R., Chorostowska-Wynimko, J., Sanak, M., Stoicescu, P.I., Piitulainen, E., Vit, O., Wencker, M., Tortorici, M.A., Fries, M., Edelman, J.M., Chapman, K.R., 2017. Long-term efficacy and safety of α1 proteinase inhibitor treatment for emphysema caused by severe α1 antitrypsin deficiency: an open-label extension trial (RAPID-OLE). *Lancet Respir. Med.* **5**, 51–60.

McGarry Houghton, A., 2015. Matrix metalloproteinases in destructive lung disease. *Matrix Biol.* **44–46**, 167–174.

Mecham, R.P., Broekelmann, T.J., Fliszar, C.J., Shapiro, S.D., Welgus, H.G., Senior, R.M., 1997. Elastin Degradation by Matrix Metalloproteinases: CLEAVAGE SITE SPECIFICITY AND MECHANISMS OF ELASTOLYSIS . *J. Biol. Chem.* **272**, 18071–18076.

Medici, D., Hay, E.D., Olsen, B.R., 2008. Snail and Slug Promote Epithelial-Mesenchymal Transition through β-Catenin–T-Cell Factor-4-dependent Expression of Transforming Growth Factor-β3. *Mol. Biol. Cell* **19**, 4875–4887.

Medzhitov, R., Janeway, C., 2000. Innate Immunity. *N. Engl. J. Med.* **343**, 338–344.

Miao, E.A., Andersen-Nissen, E., Warren, S.E., Aderem, A., 2007. TLR5 and Ipaf: dual sensors of bacterial flagellin in the innate immune system. *Semin. Immunopathol.* **29**, 275–288.

Michael, K., Lan, Z., Susan, W., Michael, R., Mark, S., Anita, L., Christopher, G., Jannette, C., Philip, F., 2003. Acceleration of lung disease in children with cystic fibrosis after Pseudomonas aeruginosa acquisition. *Pediatr. Pulmonol.* **32**, 277–287.

Mijares, L.A., Wangdi, T., Sokol, C., Homer, R., Medzhitov, R., Kazmierczak, B.I., 2011. Airway Epithelial MyD88 Restores Control of Pseudomonas aeruginosa Murine Infection via an IL-1-Dependent Pathway. *J. Immunol.* **186**, 7080–7088.

Mio, T., Romberger, D.J., Thompson, A.B., Robbins, R.A., Heires, A., Rennard, S.I., 1997. Cigarette smoke induces interleukin-8 release from human bronchial epithelial cells. *Am. J. Respir. Crit. Care Med.* **155**, 1770–1776.

Mizgerd, J.P., 2008. Acute Lower Respiratory Tract Infection. *N. Engl. J. Med.* **358**, 716–727.

Mizumura, K., Cloonan, S.M., Nakahira, K., Bhashyam, A.R., Cervo, M., Owen, C.A., Mahmood, A., Washko, G.R., Hashimoto, S., Ryter, S., Choi, A.M.K.,

2014. Mitophagy-regulated necroptosis contributes to the pathogenesis of chronic obstructive pulmonary disease. *Am. J. Respir. Crit. Care Med. Conf. Am. Thorac. Soc. Int. Conf. ATS* **189**, 3987–4004.

Moorman, J.P., Wang, J.M., Zhang, Y., Ji, X.J., Ma, C.J., Wu, X.Y., Jia, Z.S., Wang, K.S., Yao, Z.Q., 2012. Tim-3 Pathway Controls Regulatory and Effector T Cell Balance during Hepatitis C Virus Infection. *J. Immunol.* **189**, 755–766.

Mortaz, E., Adcock, I.M., Ito, K., Kraneveld, A.D., Nijkamp, F.P., Folkerts, G., 2010. Cigarette smoke induces CXCL8 production by human neutrophils via activation of TLR9 receptor. *Eur. Respir. J.* **36**, 1143–1154.

Moynagh, P.N., 2014. The roles of Pellino E3 ubiquitin ligases in immunity. *Nat Rev Immunol* **14**, 122–131.

Muñoz-Planillo, R., Kuffa, P., Martínez-Colón, G., Smith, B.L., Rajendiran, T.M., Núñez, G., 2013. K(+) efflux is the Common Trigger of NLRP3 inflammasome Activation by Bacterial Toxins and Particulate Matter. *Immunity* **38**, 1142–1153.

Murphy, T.F., 2009. Pseudomonas aeruginosa in adults with chronic obstructive pulmonary disease. *Curr. Opin. Pulm. Med.* **15**.

Murphy, T.F., Brauer, A.L., Eschberger, K., Lobbins, P., Grove, L., Cai, X., Sethi, S., 2008. Pseudomonas aeruginosa in Chronic Obstructive Pulmonary Disease. *Am. J. Respir. Crit. Care Med.* **177**, 853–860.

Nadel, J.A., 1991. Role of Mast Cell and Neutrophil Proteases in Airway Secretion. *Am. Rev. Respir. Dis.* **144**, S48–S51.

Nakahira, K., Haspel, J.A., Rathinam, V.A.K., Lee, S.-J., Dolinay, T., Lam, H.C., Englert, J.A., Rabinovitch, M., Cernadas, M., Kim, H.P., Fitzgerald, K.A., Ryter, S.W., Choi, A.M.K., 2011. Autophagy proteins regulate innate immune response by inhibiting NALP3 inflammasome-mediated mitochondrial DNA release. *Nat.*

Immunol. **12**, 222–230.

Nakashima, N., Kuwano, K., Maeyama, T., Hagimoto, N., Yoshimi, M., Hamada, N., Yamada, M., Nakanishi, Y., 2005. The p53–Mdm2 association in epithelial cells in idiopathic pulmonary fibrosis and non-specific interstitial pneumonia. *J. Clin. Pathol.* **58**, 583–589.

Netea, M., van der Veerdonk, F., van der Meer, J., Dinarello, C., Joosten, L., 2015. Inflammasome-independent regulation of IL-1-family cytokines. *Annual Review of Immunology* **33**, 49-77.

Neumann, D., Kollewe, C., Resch, K., Martin, M.U., 2007. The death domain of IRAK-1: An oligomerization domain mediating interactions with MyD88, Tollip, IRAK-1, and IRAK-4. *Biochem. Biophys. Res. Commun.* **354**, 1089–1094.

Nixon, G.M., Armstrong, D.S., Carzino, R., Carlin, J.B., Olinsky, A., Robertson, C.F., Grimwood, K., 2001. Clinical outcome after early Pseudomonas aeruginosa infection in cystic fibrosis. *J. Pediatr.* **138**, 699–704.

Noguera, A., Batle, S., Miralles, C., Iglesias, J., Busquets, X., Macnee, W., Agustí, A.G.N., 2001. Enhanced neutrophil response in chronic obstructive pulmonary disease **67**, 432–437.

Nurwidya, F., Damayanti, T., Yunus, F., 2016. The Role of Innate and Adaptive Immune Cells in the Immunopathogenesis of Chronic Obstructive Pulmonary Disease. *Tuberc. Respir. Dis. (Seoul).* **79**, 5–13.

O'Neill, L.A.J., Bowie, A.G., 2007. The family of five: TIR-domain-containing adaptors in Toll-like receptor signalling. *Nat. Rev. Immunol.* **7**, 353.

Oldenburg, M., Krüger, A., Ferstl, R., Kaufmann, A., Nees, G., Sigmund, A., Bathke, B., Lauterbach, H., Suter, M., Dreher, S., Koedel, U., Akira, S., Kawai, T., Buer, J., Wagner, H., Bauer, S., Hochrein, H., Kirschning, C.J., 2012. TLR13

Recognizes Bacterial 23s rRNA Devoid of Erythromycin Resistance–Forming Modification. *Science (80-.).* **337**, 1111-1115.

Oliveira-Nascimento, L., Massari, P., Wetzler, L.M., 2012. The role of TLR2 ininfection and immunity. *Front. Immunol.* **3**, 1–17.

Oliveira, M. V., Abreu, S.C., Padilha, G.A., Rocha, N.N., Maia, L.A., Takiya, C.M., Xisto, D.G., Suki, B., Silva, P.L., Rocco, P.R.M., 2016. Characterization of a mouse model of emphysema induced by multiple instillations of low-dose elastase. *Front. Physiol.* **7**, 1–12.

Oosting, M., Cheng, S.-C., Bolscher, J.M., Vestering-Stenger, R., Plantinga, T.S., Verschueren, I.C., Arts, P., Garritsen, A., van Eenennaam, H., Sturm, P., Kullberg, B.-J., Hoischen, A., Adema, G.J., van der Meer, J.W.M., Netea, M.G., Joosten, L.A.B., 2014. Human TLR10 is an anti-inflammatory pattern-recognition receptor. *Proc. Natl. Acad. Sci.* **111**, E4478–E4484.

Oroz, J., Barrera-Vilarmau, S., Alfonso, C., Rivas, G., De Alba, E., 2016. ASC pyrin domain self-associates and binds NLRP3 protein using equivalent binding interfaces. *J. Biol. Chem.* **291**, 19487–19501.

Oshiumi, H., Matsumoto, M., Funami, K., Akazawa, T., Seya, T., 2003. TICAM-1, an adaptor molecule that participates in Toll-like receptor 3–mediated interferon-β induction. *Nat. Immunol.* **4**, 161.

Overbeek, S.A., Braber, S., Koelink, P.J., Henricks, P.A.J., Mortaz, E., LoTam Loi, A.T., Jackson, P.L., Garssen, J., Wagenaar, G.T.M., Timens, W., Koenderman, L., Blalock, J.E., Kraneveld, A.D., Folkerts, G., 2013. Cigarette Smoke-Induced Collagen Destruction; Key to Chronic Neutrophilic Airway Inflammation? *PLoS One* **8**, e55612.

Pandey, K.C., De, S., Mishra, P.K., 2017. Role of proteases in chronic obstructive

pulmonary disease. *Front. Pharmacol.* **8**, 1–9.

Pastushkova, Lk., Valeeva, O.A., Kononikhin, A.S., Nikolaev, E.N., Larina, I.M., Dobrokhotov, I. V, Popov, I.A., Pochuev, V.I., Kireev, K.S., 2013. Changes of protein profile of human urine after long-term orbital flights. *Bull Exp Biol Med* **156**, 201–204.

Patel, V.J., Thalassinos, K., Slade, S.E., Connolly, J.B., Crombie, A., Murrell, J.C., Scrivens, J.H., 2009. A Comparison of Labeling and Label-Free Mass Spectrometry-Based Proteomics Approaches. *J. Proteome Res.* **8**, 3752–3759.

PAUWELS, R.A., BUIST, A.S., CALVERLEY, P.M.A., JENKINS, C.R., HURD, S.S., 2001. Global Strategy for the Diagnosis, Management, and Prevention of Chronic Obstructive Pulmonary Disease. *Am. J. Respir. Crit. Care Med.* **163**, 1256–1276.

Peleman, R. a, Rytilä, P.H., Kips, J.C., Joos, G.F., Pauwels, R. a, 1999. The cellular composition of induced sputum in chronic obstructive pulmonary disease. *Eur. Respir. J.* **13**, 839–43.

Perretti, M., D'Acquisto, F., 2009. Annexin A1 and glucocorticoids as effectors of the resolution of inflammation. *Nat. Rev. Immunol.* **9**, 62-70

Piao, W., Ru, L.W., Piepenbrink, K.H., Sundberg, E.J., Vogel, S.N., Toshchakov, V.Y., 2013. Recruitment of TLR adapter TRIF to TLR4 signaling complex is mediated by the second helical region of TRIF TIR domain. *Proc. Natl. Acad. Sci. U. S. A.* **110**, 19036–19041.

Pichlmair, A., Schulz, O., Tan, C.-P., Rehwinkel, J., Kato, H., Takeuchi, O., Akira, S., Way, M., Schiavo, G., Reis e Sousa, C., 2009. Activation of MDA5 Requires Higher-Order RNA Structures Generated during Virus Infection. *J. Virol.* **83**, 10761–10769.

Pilette, C., Colinet, B., Kiss, R., André, S., Kaltner, H., Gabius, H.-J., Delos, M., Vaerman, J.-P., Decramer, M., Sibille, Y., 2007. Increased galectin-3 expression and intra-epithelial neutrophils in small airways in severe COPD. *Eur. Respir. J.* **29**, 914-922.

Pinkerton, K.E., Van Winkle, L.S., Plopper, C.G., Smiley-Jewell, S., Covarrubias, E.C., McBride, J.T., 2015. Chapter 4 - Architecture of the Tracheobronchial Tree A2 - Parent, Richard A. BT - Comparative Biology of the Normal Lung **2nd Ed.** Academic Press, San Diego, pp. 33–51.

Pizzirani, C., Ferrari, D., Chiozzi, P., Adinolfi, E., Sandonà, D., Savaglio, E., Di Virgilio, F., 2007. Stimulation of P2 receptors causes release of IL-1β–loaded microvesicles from human dendritic cells. *Blood* **109**, 3856-3864.

Plumet, S., Herschke, F., Bourhis, J.M., Valentin, H., Longhl, S., Gerlier, D., 2007. Cytosolic 5′-triphosphate ended viral leader transcript of measles virus as activator of the RIG I-mediated interferon response. *PLoS One* **2**, 1–11.

Poltorak, A., Smirnova, I., He, X., Liu, M., Huffel, C. Van, Birdwell, D., Alejos, E., Silva, M., Du, X., Thompson, P., Chan, E.K.L., Ledesma, J., Roe, B., Clifton, S., Vogel, S.N., Beutler, B., 1998. Genetic and Physical Mapping of the Lps Locus : Identification of the Toll-4 Receptor as a Candidate Gene in the Critical Region **240**, 340–355.

Polverini, P.J., Cotran, P.S., Gimbrone, M.A., Urnanue, E.R., 1977. Activated macrophages induce vascular proliferation. *Nature* **269**, 804-806

Prescott, E., Lange, P., Vestbo, J., 1995. Chronic mucus hypersecretion in COPD and death from pulmonary infection. *Eur. Respir. J.* **8**, 1333–1338.

Price, D., Yawn, B., Brusselle, G., Rossi, A., 2012. Risk-to-benefit ratio of inhaled corticosteroids in patients with COPD. *Prim. Care Respir. J.* **22**, 92.

Proell, M., Riedl, S.J., Fritz, J.H., Rojas, A.M., Schwarzenbacher, R., 2008. The Nod-Like Receptor (NLR) family: A tale of similarities and differences. *PLoS One* **3**, 1–11.

Py, B.F., Kim, M.S., Vakifahmetoglu-Norberg, H., Yuan, J., 2013. Deubiquitination of NLRP3 by BRCC3 Critically Regulates Inflammasome Activity. *Mol. Cell* **49**, 331–338.

Qu, Y., Franchi, L., Nunez, G., Dubyak, G.R., 2007. Nonclassical IL-1 Secretion Stimulated by P2X7 Receptors Is Dependent on Inflammasome Activation and Correlated with Exosome Release in Murine Macrophages. *J. Immunol.* **179**, 1913–1925.

Ramos, F.L., Krahnke, J.S., Kim, V., 2014. Clinical issues of mucus accumulation in COPD. *Int. J. COPD* **9**, 139–150.

Rathinam, V.A.K., Jiang, Z., Waggoner, S.N., Sharma, S., Cole, L.E., Waggoner, L., Vanaja, S.K., Monks, B.G., Ganesan, S., Latz, E., Hornung, V., Vogel, S.N., Szomolanyi-Tsuda, E., Fitzgerald., K.A., 2010. The AIM2 inflammasome is essential for host-defense against cytosolic bacteria and DNA viruses. *Nat. Immunol.* **11**, 395–402.

Rawlings, W., Kreiss, P., Levy, D., Cohen, B., Menkes, H., Brashears, S., Permutt, S., 1976. Clinical, Epidemiologic, and Pulmonary Function Studies in Alpha1-Antitrypsin-Deficient Subjects of Pi Z Type. *Am. Rev. Respir. Dis.* **114**, 945–953.

Reuven, E.M., Fink, A., Shai, Y., 2014. Regulation of innate immune responses by transmembrane interactions: Lessons from the TLR family. *Biochim. Biophys. Acta - Biomembr.* **1838**, 1586–1593.

Richter, A., Puddicombe, S.M., Lordan, J.L., Bucchieri, F., Wilson, S.J., Djukanović,

R., Dent, G., Holgate, S.T., Davies, D.E., 2001. The Contribution of Interleukin (IL)-4 and IL-13 to the Epithelial–Mesenchymal Trophic Unit in Asthma. *Am. J. Respir. Cell Mol. Biol.* **25**, 385–391.

Ricklin, D., Hajishengallis, G., Yang, K., Lambris, J.D., 2010. Complement: a key system for immune surveillance and homeostasis. *Nat. Immunol.* **11**, 785.

Robertson, I.B., Horiguchi, M., Zilberberg, L., Dabovic, B., Hadjiolova, K., Rifkin, D.B., 2015. Latent TGF-β-binding proteins. *Matrix Biol.* **47**, 44–53.

Rogel, M.R., Soni, P.N., Troken, J.R., Sitikov, A., Trejo, H.E., Ridge, K.M., 2011. Vimentin is sufficient and required for wound repair and remodeling in alveolar epithelial cells. *FASEB J.* **25**, 3873–3883.

Romieu, I., Riojas-Rodríguez, H., Marrón-Mares, A.T., Schilmann, A., Perez-Padilla, R., Masera, O., 2009. Improved biomass stove intervention in rural Mexico: Impact on the respiratory health of women. *Am. J. Respir. Crit. Care Med.* **180**, 649–656.

Russo, R.C., Garcia, C.C., Teixeira, M.M., Amaral, F.A., 2014. The CXCL8/IL-8 chemokine family and its receptors in inflammatory diseases. *Expert Rev. Clin. Immunol.* **10**, 593–619.

Ryckman, C., Vandal, K., Rouleau, P., Talbot, M., Tessier, P.A., 2003. Proinflammatory Activities of S100: Proteins S100A8, S100A9, and S100A8/A9 Induce Neutrophil Chemotaxis and Adhesion. *J. Immunol.* **170**, 3233–3242.

Saito, A., Okazaki, H., Sugawara, I., Yamamoto, K., Takizawa, H., 2003. Potential Action of IL-4 and IL-13 as Fibrogenic Factors on Lung Fibroblasts in vitro. *Int. Arch. Allergy Immunol.* **132**, 168–176.

Salvi, S.S., Barnes, P.J., 2009. Chronic obstructive pulmonary disease in non-smokers. *Lancet* **374**, 733–743.

Sathyanarayana, P., Barthwal, M.K., Lane, M.E., Acevedo, S.F., Skoulakis, E.M.C., Bergmann, A., Rana, A., 2003. Drosophila mixed lineage kinase/slipper, a missing biochemical link in Drosophila JNK signaling. *Biochim. Biophys. Acta - Mol. Cell Res.* **1640**, 77–84.

Sauer, J.-D., Witte, C.E., Zemansky, J., Hanson, B., Lauer, P., Portnoy, D.A., 2010. Listeria monocytogenes that lyse in the macrophage cytosol trigger AIM2-mediated pyroptosis. *Cell Host Microbe* **7**, 412–419.

Schauvliege, R., Janssens, S., Beyaert, R., 2006. Pellino proteins are more than scaffold proteins in TLR / IL-1R signalling : A role as novel RING E3 – ubiquitin-ligases. *FEBS Lett.* **580**, 4697–4702.

Schroder, K., Sagulenko, V., Zamoshnikova, A., Richards, A.A., Cridland, J.A., Irvine, K.M., Stacey, K.J., Sweet, M.J., 2012. Acute lipopolysaccharide priming boosts inflammasome activation independently of inflammasome sensor induction. *Immunobiology* **217**, 1325–1329.

Schroder, K., Tschopp, J., 2010. The Inflammasomes. *Cell* **140**, 821–832.

Sebastian, A., Pehrson, C., Larsson, L., 2006. Elevated concentrations of endotoxin in indoor air due to cigarette smoking. *J. Environ. Monit.* **8**, 519–522.

Segura-Valdez, L., Pardo, A., Gaxiola, M., Uhal, B.D., Becerril, C., Selman, M., 2000. Upregulation of Gelatinases A and B, Collagenases 1 and 2, and Increased Parenchymal Cell Death in COPD. *Chest* **117**, 684–694.

Selby, C., Drost, E., Lannan, S., Wraith, P.K., Macnee, W., 1991. Neutrophil Retention in the Lungs of Patients with Chronic Obstructive Pulmonary Disease. *Am. Rev. Respir. Dis.* **143**, 1359–1364.

Sharma, S., tenOever, B.R., Grandvaux, N., Zhou, G.-P., Lin, R., Hiscott, J., 2003. Triggering the Interferon Antiviral Response Through an IKK-Related Pathway.

Science (80-.). **300**, 1148-1151.

Shoji, S., Ertl, R.F., Koyama, S., Robbins, R., Leikauf, G., Von Essen, S., Rennard, S.I., 1995. Cigarette Smoke Stimulates Release of Neutrophil Chemotactic Activity from Cultured Bovine Bronchial Epithelial Cells. *Clin. Sci.* **88**, 337-344.

Shrimpton, R.E., Butler, M., Morel, A.S., Eren, E., Hue, S.S., Ritter, M.A., 2009. CD205 (DEC-205): A recognition receptor for apoptotic and necrotic self. *Mol. Immunol.* **46**, 1229–1239.

Siednienko, J., Jackson, R., Mellett, M., Delagic, N., Yang, S., Wang, B., Tang, L.S., Callanan, J.J., Mahon, B.P., Moynagh, P.N., 2012a. Pellino3 targets the IRF7 pathway and facilitates autoregulation of TLR3- and viral-induced expression of type I interferons. *Nat. Immunol.* **13**, 1055.

Siednienko, J., Jackson, R., Mellett, M., Delagic, N., Yang, S., Wang, B., Tang, L.S., Callanan, J.J., Mahon, B.P., Moynagh, P.N., 2012b. Pellino3 targets the IRF7 pathway and facilitates autoregulation of TLR3- and viral-induced expression of type I interferons. *Nat. Immunol.* **13**, 1055–62.

Sinden, N.J., Baker, M.J., Smith, D.J., Kreft, J.-U., Dafforn, T.R., Stockley, R.A., 2014. α-1-Antitrypsin variants and the proteinase/antiproteinase imbalance in chronic obstructive pulmonary disease. *Am. J. Physiol. Cell. Mol. Physiol.* **308**, L179–L190.

Skerrett, S.J., Wilson, C.B., Liggitt, H.D., Hajjar, A.M., 2007. Redundant Toll-like receptor signaling in the pulmonary host response to Pseudomonas aeruginosa. *Am. J. Physiol. Cell. Mol. Physiol.* **292**, L312–L322.

Sly, P.D., Brennan, S., Gangell, C., De Klerk, N., Murray, C., Mott, L., Stick, S.M., Robinson, P.J., Robertson, C.F., Ranganathan, S.C., 2009. Lung disease at diagnosis in infants with cystic fibrosis detected by newborn screening. *Am. J.*

Respir. Crit. Care Med. **180**, 146–152.

Sohn, S.-H., Jang, H., Kim, Y., Jang, Y.P., Cho, S.-H., Jung, H., Jung, S., Bae, H., 2013. The effects of Gamijinhae-tang on elastase/lipopolysaccharide-induced lung inflammation in an animal model of acute lung injury. *BMC Complement. Altern. Med.* **13**, 176.

Song, H., Liu, B., Huai, W., Yu, Z., Wang, W., Zhao, J., Han, L., Jiang, G., Zhang, L., Gao, C., Zhao, W., 2016. The E3 ubiquitin ligase TRIM31 attenuates NLRP3 inflammasome activation by promoting proteasomal degradation of NLRP3. *Nat. Commun.* **7**, 1–11.

Song, J., Wu, C., Korpos, E., Zhang, X., Agrawal, S.M., Wang, Y., Faber, C., Schäfers, M., Körner, H., Opdenakker, G., Hallmann, R., Sorokin, L., 2015. Focal MMP-2 and MMP-9 Activity at the Blood-Brain Barrier Promotes Chemokine-Induced Leukocyte Migration. *Cell Rep.* **10**, 1040–1054.

Spagnuolo, L., Simone, M. De, Lorè, N.I., Fino, I. De, Basso, V., Mondino, A., Cigana, C., Bragonzi, A., 2016. The host genetic background defines diverse immune-reactivity and susceptibility to chronic Pseudomonas aeruginosa respiratory infection. *Sci. Rep.* **6**, 1–10.

Srinivasula, S.M., Poyet, J.L., Razmara, M., Datta, P., Zhang, Z., Alnemri, E.S., 2002. The PYRIN-CARD protein ASC is an activating adaptor for caspase-1. *J. Biol. Chem.* **277**, 21119–21122.

Stockley, R.A., 2002. Neutrophils and the Pathogenesis of COPD. *Chest* **121**, 151S–155S.

Stone, R.C., Pastar, I., Ojeh, N., Chen, V., Liu, S., Garzon, K.I., Tomic-Canic, M., 2016. Epithelial-mesenchymal transition in tissue repair and fibrosis. *Cell Tissue Res.*

Subramanian, N., Natarajan, K., Clatworthy, M.R., Wang, Z., Germain, R.N., 2013. The adapter MAVS promotes NLRP3 mitochondrial localization and inflammasome activation. *Cell* **153**, 348–361.

Suzuki, M., Sze, M.A., Campbell, J.D., Brothers, J.F., Lenburg, M.E., McDonough, J.E., Elliott, W.M., Cooper, J.D., Spira, A., Hogg, J.C., 2017. The cellular and molecular determinants of emphysematous destruction in COPD. *Sci. Rep.* **7**, 9562.

Suzuki, T., Franchi, L., Toma, C., Ashida, H., Ogawa, M., Yoshikawa, Y., Mimuro, H., Inohara, N., Sasakawa, C., Nuñez, G., 2007. Differential regulation of caspase-1 activation, pyroptosis, and autophagy via Ipaf and ASC in Shigella-infected macrophages. *PLoS Pathog.* **3**, 1082–1091.

Tack, C.J., Stienstra, R., Joosten, L.A.B., Netea, M.G., 2012. Inflammation links excess fat to insulin resistance: the role of the interleukin-1 family. *Immunol. Rev.* **249**, 239–252.

Tanash, H.A., Ekström, M., Rönmark, E., Lindberg, A., Piitulainen, E., 2017. Survival in individuals with severe alpha 1-antitrypsin deficiency (PiZZ) in comparison to a general population with known smoking habits. *Eur. Respir. J.* **50**.

Tang, K., Rossiter, H.B., Wagner, P.D., Breen, E.C., 2004. Lung-targeted VEGF inactivation leads to an emphysema phenotype in mice. *J. Appl. Physiol.* **97**, 1559–66; discussion 1549.

Teckman, J.H., 2013. Liver Disease in Alpha-1 Antitrypsin Deficiency: Current Understanding and Future Therapy. *COPD J. Chronic Obstr. Pulm. Dis.* **10**, 35–43.

Tenekeci, U., Poppe, M., Beuerlein, K., Buro, C., Müller, H., Weiser, H., Kettner-

Buhrow, D., Porada, K., Newel, D., Xu, M., Chen, Z.J., Busch, J., Schmitz, M.L., Kracht, M., 2016. Erratum: K63-Ubiquitylation and TRAF6 Pathways Regulate Mammalian P-Body Formation and mRNA Decapping (Molecular Cell (2016) 63(3) (540) (S1097276516301800) (10.1016/j.molcel.2016.05.017)). *Mol. Cell* **63**, 540.

Thompson, A.B., Daughton, D., Robbins, R.A., Ghafouri, M.A., Oehlerking, M., Rennard, S.I., 1989. Intraluminal Airway Inflammation in Chronic Bronchitis: Characterization and Correlation with Clinical Parameters. *Am. Rev. Respir. Dis.* **140**, 1527–1537.

Ting, J.P.-Y., Davis, B.K., 2004. CATERPILLER: A Novel Gene Family Important in Immunity, Cell Death, and Diseases. *Annu. Rev. Immunol.* **23**, 387–414.

Toward, T.J., Broadley, K.J., 2000. Airway reactivity, inflammatory cell influx and nitric oxide in guinea-pig airways after lipopolysaccharide inhalation. *Br. J. Pharmacol.* **131**, 271–281.

Trojanek, J.B., Cobos-Correa, A., Diemer, S., Kormann, M., Schubert, S.C., Zhou-Suckow, Z., Agrawal, R., Duerr, J., Wagner, C.J., Schatterny, J., Hirtz, S., Sommerburg, O., Hartl, D., Schultz, C., Mall, M.A., 2014. Airway Mucus Obstruction Triggers Macrophage Activation and Matrix Metalloproteinase 12–Dependent Emphysema. *Am. J. Respir. Cell Mol. Biol.* **51**, 709–720.

van der Vaart, H., 2004. Acute effects of cigarette smoke on inflammation and oxidative stress: a review. *Thorax* **59**, 713–721.

Van Eerd, E., Van Der Meer, R.M., Van Schayck, O., Kotz, D., 2016. Smoking cessation for people with chronic obstructive pulmonary disease, Cochrane Database of Systemic Reviews.

Vandanmagsar, B., Youm, Y.-H., Ravussin, A., Galgani, J.E., Stadler, K., Mynatt,

R.L., Ravussin, E., Stephens, J.M., Dixit, V.D., 2011. The NLRP3 inflammasome instigates obesity-induced inflammation and insulin resistance. *Nat. Med.* **17**, 179.

Vandivier, R.W., Ghosh, M., 2017. Understanding the relevance of the mouse cigarette smoke model of COPD: Peering through the smoke. *Am. J. Respir. Cell Mol. Biol.* **57**, 3–4.

Ve, T., Gay, N.J., Mansell, A., Kellie, B.K. and S., 2012. Adaptors in Toll-Like Receptor Signaling and their Potential as Therapeutic Targets. *Curr. Drug Targets*.

Ventola, C.L., 2015. The Antibiotic Resistance Crisis: Part 1: Causes and Threats. *Pharm. Ther.* **40**, 277–283.

Vernooy, J.H.J., Dentener, M. a, van Suylen, R.J., Buurman, W. a, Wouters, E.M.F., 2002. Long-term intratracheal lipopolysaccharde exposure in mice results in chronic lung inflammation and persistent pathology. *Am. J. Respir. Cell Mol. Biol.* **26**, 152–159.

Vestbo, J., Hurd, S.S., Agustí, A.G., Jones, P.W., Vogelmeier, C., Anzueto, A., Barnes, P.J., Fabbri, L.M., Martinez, F.J., Nishimura, M., Stockley, R.A., Sin, D.D., Rodriguez-Roisin, R., 2013. Global strategy for the diagnosis, management, and prevention of chronic obstructive pulmonary disease GOLD executive summary. *Am. J. Respir. Crit. Care Med.* **187**, 347–365.

Vlahos, R., Bozinovski, S., 2014. Role of Alveolar Macrophages in Chronic Obstructive Pulmonary Disease . *Front. Immunol.* .

Vogelmeier, C.L.F., Criner, G.E.J., Martinez, F.E.J., Anzueto, A.N., Barnes, P.E.J., Bourbeau, J.E.A.N., Celli, B.A.R., Chen, R.O., Decramer, M.A.R.C., Fabbri, L.E.M., Frith, P.E., Halpin, D.A.M.G., Varela, M.V.I.L., 2017. Global Strategy

for the Diagnosis , Management and Prevention of Chronic Obstructive Lung Disease 2017 Report GOLD Executive Summary. *Respirology* **22**, 575–601.

Wang, H., Meng, H., Li, X., Zhu, K., Dong, K., Mookhtiar, A.K., Wei, H., Li, Y., Sun, S.-C., Yuan, J., 2017. PELI1 functions as a dual modulator of necroptosis and apoptosis by regulating ubiquitination of RIPK1 and mRNA levels of c-FLIP. *Proc. Natl. Acad. Sci.* **114**, 11944–11949.

Wang, Z.-D., Liu, H.-H., Ma, Z.-X., Ma, H.-Y., Li, Z.-Y., Yang, Z.-B., Zhu, X.-Q., Xu, B., Wei, F., Liu, Q., 2017. Toxoplasma gondii Infection in Immunocompromised Patients: A Systematic Review and Meta-Analysis. *Front. Microbiol.* **8**, 1–12.

Wang, Z., Zheng, T., Zhu, Z., Homer, R.J., Riese, R.J., Chapman, H.A., Shapiro, S.D., Elias, J.A., 2000. Interferon γ Induction of Pulmonary Emphysema in the Adult Murine Lung. *J. Exp. Med.* **192**, 1587-1600.

Warburton, D., 2012. Developmental responses to lung injury: repair or fibrosis. *Fibrogenesis Tissue Repair* **5**, S2.

Weber, A., Wasiliew, P., Kracht, M., 2010. Interleukin-1 (IL-1) Pathway. *Sci. Signal.* **3**, cm1-cm1.

Wei, Q., Ma, L.Z., 2013. Biofilm matrix and its regulation in Pseudomonas aeruginosa. *Int. J. Mol. Sci.* **14**, 20983–21005.

Weinlich, R., Oberst, A., Beere, H.M., Green, D.R., 2016. Necroptosis in development, inflammation and disease. *Nat. Rev. Mol. Cell Biol.* **18**, 127.

Williams, O.W., Sharafkhaneh, A., Kim, V., Dickey, B.F., Evans, C.M., 2006. Airway mucus: From production to secretion. *Am. J. Respir. Cell Mol. Biol.* **34**, 527–536.

Witola, W.H., Mui, E., Hargrave, A., Liu, S., Hypolite, M., Montpetit, A., Cavailles,

P., Bisanz, C., Cesbron-Delauw, M.F., Fournié, G.J., McLeod, R., 2011. NALP1 influences susceptibility to human congenital toxoplasmosis, proinflammatory cytokine response, and fate of Toxoplasma gondii-infected monocytic cells. *Infect. Immun.* **79**, 756–766.

Wu, Y., Zheng, Z., Jiang, Y., Chess, L., Jiang, H., 2009. The specificity of T cell regulation that enables self-nonself discrimination in the periphery. *Proc. Natl. Acad. Sci. U. S. A.* **106**, 534–539.

Wynn, T.A., Vannella, K.M., 2016. Macrophages in Tissue Repair, Regeneration, and Fibrosis. *Immunity* **44**, 450–462.

Xiao, Y., Jin, J., Chang, M., Chang, J.-H., Hu, H., Zhou, X., Brittain, G.C., Stansberg, C., Torkildsen, Ø., Wang, X., Brink, R., Cheng, X., Sun, S.-C., 2013. Peli1 promotes microglia-mediated CNS inflammation by regulating Traf3 degradation. *Nat. Med.* **19**, 595.

Xu, H., Barnes, G.T., Yang, Q., Tan, G., Yang, D., Chou, C.J., Sole, J., Nichols, A., Ross, J.S., Tartaglia, L. a., Others, 2003. Chronic inflammation in fat plays a crucial role in the development of obesity-related insulin resistance. *J. Clin. Invest.* **112**, 1821–1830.

Xu, M., Fralick, D., Zheng, J.Z., Wang, B., Tu, X.M., Feng, C., 2017. The differences and similarities between two-sample t-test and paired t-test. *Shanghai Arch Psychiatry* **29**, 184-188

Yamamoto, M., Sato, S., Hemmi, H., Sanjo, H., Uematsu, S., Kaisho, T., Hoshino, K., Takeuchi, O., Kobayashi, M., Fujita, T., Takeda, K., Akira, S., 2002. Essential role for TIRAP in activation of the signalling cascade shared by TLR2 and TLR4. *Nature* **420**, 324.

Yamamoto, Y., Gaynor, R.B., 2004. IκB kinases: key regulators of the NFκB

pathway. *Trends Biochem. Sci.* **29**, 72–79.

Yan, Y., Jiang, W., Liu, L., Wang, X., Ding, C., Tian, Z., Zhou, R., 2015. Dopamine controls systemic inflammation through inhibition of NLRP3 inflammasome. *Cell* **160**, 62–73.

Yang, J., Liu, Z., Xiao, T.S., 2017. Post-translational regulation of inflammasomes. *Cell. Mol. Immunol.* **14**, 65–79.

Yang, S., Wang, B., Humphries, F., Hogan, A.E., Shea, D.O., Moynagh, P.N., 2014. The E3 Ubiquitin Ligase Pellino3 Protects against Obesity-Induced Inflammation and Insulin Resistance. *Immunity* **41**, 973–987.

Yang, S., Wang, B., Humphries, F., Jackson, R., Healy, M.E., Bergin, R., Aviello, G., Hall, B., McNamara, D., Darby, T., Quinlan, A., Shanahan, F., Melgar, S., Fallon, P.G., Moynagh, P.N., 2013a. Pellino3 ubiquitinates RIP2 and mediates Nod2-induced signaling and protective effects in colitis. *Nat. Immunol.* **14**, 927–36.

Yang, S., Wang, B., Tang, L.S., Siednienko, J., Callanan, J.J., Moynagh, P.N., 2013b. Pellino3 targets RIP1 and regulates the pro-apoptotic effects of TNF-α. *Nat. Commun.* **4**, 1–19.

Yano, J., Lilly, E., Barousse, M., Fidel, P.L., 2010. Epithelial cell-derived S100 calcium-binding proteins as key mediators in the hallmark acute neutrophil response during Candida vaginitis. *Infect. Immun.* **78**, 5126–5137.

Yarovinsky, F., 2014. Innate immunity to Toxoplasma gondii infection. *Nat. Rev. Immunol.* **14**, 109.

Yarovinsky, F., Hieny, S., Sher, A., 2008. Recognition of Toxoplasma gondii by TLR11 Prevents Parasite-Induced Immunopathology. *J. Immunol.* **181**, 8478–8484.

Yoneyama, M., Kikuchi, M., Matsumoto, K., Imaizumi, T., Miyagishi, M., Taira, K., Foy, E., Loo, Y.-M., Gale, M., Akira, S., Yonehara, S., Kato, A., Fujita, T., 2005. Shared and Unique Functions of the DExD/H-Box Helicases RIG-I, MDA5, and LGP2 in Antiviral Innate Immunity. *J. Immunol.* **175**, 2851–2858.

Zavascki, A.P., Carvalhaes, C.G., Picão, R.C., Gales, A.C., 2010. Multidrug-resistant Pseudomonas aeruginosa and Acinetobacter baumannii: resistance mechanisms and implications for therapy. *Expert Rev. Anti. Infect. Ther.* **8**, 71–93.

Zaynagetdinov, R., Sherrill, T.P., Kendall, P.L., Segal, B.H., Weller, K.P., Tighe, R.M., Blackwell, T.S., 2013. Identification of myeloid cell subsets in murine lungs using flow cytometry. *Am. J. Respir. Cell Mol. Biol.* **49**, 180–189.

Zhang, D., Zhang, G., Hayden, M.S., Greenblatt, M.B., Bussey, C., Flavell, R.A., Ghosh, S., 2004. A Toll-like Receptor That Prevents Infection by Uropathogenic Bacteria. *Science (80-.).* **303**, 1522-1526.

Zhang, J., Clark, K., Lawrence, T., Peggie, M.W., Cohen, P., 2014. An unexpected twist to the activation of IKKβ: TAK1 primes IKKβ for activation by autophosphorylation. *Biochem. J.* **461**, 531–537.

Zhang, Y., Zhang, Y., Gu, W., He, L., Sun, B., 2014. Th1/Th2 Cell's Function in Immune System BT - T Helper Cell Differentiation and Their Function. In: Sun, B. (Ed.), . Springer Netherlands, Dordrecht, pp. 45–65.

Zhang, Z., Ohto, U., Shibata, T., Krayukhina, E., Taoka, M., Yamauchi, Y., Tanji, H., Isobe, T., Uchiyama, S., Miyake, K., Shimizu, T., 2016. Structural Analysis Reveals that Toll-like Receptor 7 Is a Dual Receptor for Guanosine and Single-Stranded RNA. *Immunity* **45**, 737–748.

Zhao, J., Shi, W., Wang, Y.-L., Chen, H., Bringas, P., Datto, M.B., Frederick, J.P., Wang, X.-F., Warburton, D., 2002. Smad3 deficiency attenuates bleomycin-

induced pulmonary fibrosis in mice. *Am. J. Physiol. - Lung Cell. Mol. Physiol.* **282**, L585–L593.

Zhou, R., Yazdi, A.S., Menu, P., Tschopp, J., 2011. A role for mitochondria in NLRP3 inflammasome activation. *Nature* **469**, 221–226.

Zhou, Y., Zou, Y., Li, X., Chen, S., Zhao, Z., He, F., Zou, W., Luo, Q., Li, W., Pan, Y., Deng, X., Wang, X., Qiu, R., Liu, S., Zheng, J., Zhong, N., Ran, P., 2014. Lung Function and Incidence of Chronic Obstructive Pulmonary Disease after Improved Cooking Fuels and Kitchen Ventilation: A 9-Year Prospective Cohort Study. *PLoS Med.* **11**.

Zuliani-Alvarez, L., Midwood, K.S., 2015. Fibrinogen-Related Proteins in Tissue Repair: How a Unique Domain with a Common Structure Controls Diverse Aspects of Wound Healing. *Adv. Wound Care* **4**, 273–285.